UNIVERSITY OF SOUTHAMPTON

MHV Lagrangians for Yang–Mills and QCD

by

James Ettle

A thesis submitted in partial fulfillment for the degree of Doctor of Philosophy

in the
Faculty of Engineering, Science and Mathematics
School of Physics and Astronomy

August 2008

UNIVERSITY OF SOUTHAMPTON

Abstract

Faculty of Engineering, Science and Mathematics
School of Physics and Astronomy

Doctor of Philosophy

by James Ettle

Over the past few decades, it has been realised that gauge theory scattering amplitudes have structures much simpler than the traditional Feynman graph driven approach would suggest. In particular, Parke and Taylor found a particularly simple expression for the tree-level amplitudes with two gluons of different helicity than the others (the so-called MHV amplitudes). Cachazo, Svrček and Witten (CSW) devised rules for constructing tree-level amplitudes by sewing lower-valence MHV amplitudes together with scalar propagators. It was shown by Mansfield in 2005 that a canonical change of the field variables could be constructed that resulted in a lagrangian whose vertices were proportional to MHV amplitudes, continued off-shell by CSW's prescription, the so-called Canonical MHV Lagrangian. We derive the explicit form of this transformation and use this to show that the vertices are indeed the Parke–Taylor amplitudes for up to five gluons. Noting that CSW's MHV rules cannot be used to construct the tree-level $(--++)$ or one-loop $(++++)$ amplitudes, we extend our work to augment the MHV rules with so-called completion vertices. These permit construction of these missing amplitudes by means of evasion of the S-matrix equivalence theorem. Indeed, together they reconstruct off-shell light-cone Yang-Mills amplitudes algebraically. We also give a prescription for dimensional regularisation of the Canonical MHV Lagrangian. Finally, we construct a canonical MHV lagrangian with massless fermions in the fundamental representation using a similar methodology.

Contents

List of Figures

Acknowledgements

I would like to start by thanking my supervisor, Tim Morris, for his support and wisdom throughout this project. It has also been an absolute pleasure to work in collaboration with Chih-Hao Fu, Jonathan Fudger, Zhiguang Xiao, and of course Paul Mansfield and I would like to extend the greatest gratitude to them all.

I would like to thank the following individuals, who have provided interesting discussions on the subject and/or helped in an indirect manner: Rutger Boels, Andreas Brandhuber, Jacques Distler (for putting MHV lagrangians on the Blog-o-Sphere), Nick Evans, Nigel Glover, Simon McNamara, Doug Ross, Bill Spence, Gabriele Travaglini and Konstantinos Zubos. I also thank the STFC (né PPARC) for financial support throughout.

The many years I have spent at the University of Southampton would not have been so joyful were it not for the help, support, encouragement, good humour, and out-and-out tolerance of the staff, post-docs and my fellow students. In particular, I'd like to thank Michael Donnellan, Jonathan Flynn, Chris Sachrajda, Andrew Tedder, and Martin Wiebusch.

Finally, I would like to thank my family for their patience and support.

Chapter 1

Introduction

The Standard Model[1] of Particle Physics is a quantum field theory with an $SU(3)_C \times SU(2)_I \times U(1)_Y$ gauge symmetry which gives rise to three of the four fundamental forces: electromagnetism, the Weak interaction and the Strong force. The quantisation of gravity is, at time of writing, an open question and it is omitted from the Standard Model framework.

The $SU(2)_I \times U(1)_Y$ factor of the Standard Model gauge symmetry provides the *electroweak* interaction, a union of electromagnetism and the Weak interaction. The $SU(2)_I$ component acts on representations classified by *weak isospin* I, and the U(1) on *weak hypercharge* Y. Below energies of around 100 GeV this is spontaneously broken to the Weak interaction and electromagnetism via the Higgs mechanism. This endows the Weak interaction gauge bosons $W^{\pm}$ and Z^0 (discovered in 1983 at the UA1 and UA2 experiments at CERN) with masses 80 GeV and 91 GeV, respectively.

The Strong force is governed by the $SU(3)_C$ component of the gauge group. It acts only on quark matter, generations of which live in its fundamental representation called *colour*, hence the choice of name 'Quantum Chromodynamics' (QCD) for the underlying theory. This force is seen to exhibit two properties of particular phenomenological interest. The first is *confinement*: physical states are only ever in the colour singlet representation, and free individual quarks and gluons are never observed. This property has never been proved analytically for QCD[2]. The second interesting property of QCD is that it demonstrates *asymptotic freedom* [3,4] in the ultraviolet: its coupling α_s runs with energy scale Q according to (see *e.g.* section 17.2 of [1])

$$\alpha_s(Q) = \frac{2\pi}{(11 - 2n_f/3)\ln(Q/\Lambda_{QCD})}$$

to one-loop order in perturbation theory for n_f quark flavours. Clearly the coupling becomes smaller as the energy scale increases. Λ_{QCD} characterises the energy scale around which α_s transitions between strong and weak, and is determined experimentally

[1]The purpose of this discussion is to give an overview of the Standard Model that provides sufficient context for the rest of the thesis. Further details can be found in many textbooks, *e.g.* that of ref. [1]

[2]Studies with lattice gauge theory have yielded an analytical proof for confinement and the linear form of quark-antiquark potential [2], but it is not known how this behaves in the continuum limit.

to be around 200 MeV. At energies below Λ_{QCD} the Strong force coupling is larger than unity so we cannot expect perturbation theory to work. Instead one must resort to lattice techniques (see *e.g.* [5, 6]) or strong-weak dualities such as the AdS/CFT correspondence [7]. But at energy scales further above Λ_{QCD} (of the order 1 GeV or more), the running coupling is less than unity, so we may attempt to use perturbation theory with increasing confidence as the energy scale rises. For high-energy processes, QCD exhibits a factorisation property which allows us to split cross-sections into a non-perturbative hadronic part and a perturbative partonic piece. This is a core concept in perturbative QCD phenomenology, a rich subject in itself and we refer the interested reader to *e.g.* refs. [8, 9], but the important idea in this is that long- and short-distance physics can be decoupled. The perturbative piece is computed as if the partons were free physical states, 'weighted' by form factors computed from hadronic physics.

The Standard Model has been tested extensively and found to be a remarkably robust theory. Nevertheless, it suffers from a number of limitations. First, there is the Higgs mechanism. The $W^{\pm}$ and Z^0 particles acquire mass through *spontaneous symmetry breaking* — the scalar Higgs field acquires a non-zero vacuum expectation value. Yet its particle the Higgs boson, believed to have a mass somewhere between 115 GeV and 180 GeV (see *e.g.* 'Higgs Boson Theory and Searches' in [10]), has yet to be observed. Furthermore, there are indications of the presence of physics beyond the Standard Model arising from questions concerning the origin of neutrino masses, the observed matter/antimatter asymmetry in the universe, the nature of dark matter, and the so-called 'hierarchy problem' of the vastly different energy scales in physics.

It is hoped that the Large Hadron Collider (LHC) at CERN will help resolve (at least some of) these issues from the experimental end. This machine is a 14 TeV proton-proton collider and, assuming that the current bounds on the Higgs mass are correct, Higgs production should be well within its reach. Furthermore it is believed that it is at the TeV energy scales at which the first signals of trans-Standard Model 'New Physics' should emerge. There are a number of candidate models for this, amongst which the most phenomenologically promising are rooted in supersymmetric[3] and/or extra dimensional[4] extensions of the Standard Model. But being a hadronic collider, the signal from any collision event it generates will be dominated by the QCD background — processes involving quarks and gluons, often with many being involved in any given process. Furthermore, experimentalists have published a next-to-leading order 'LHC "priority" wish list' [12] of processes important to both Higgs production and New Physics discovery, some of which involve sub-processes with potentially large numbers of gluons and quark-antiquark pairs. These background effects are all Standard Model physics, and we know how to compute perturbative quantities with the Standard Model using Feynman graphs. Putting this into practice is where we come unstuck: computing amplitudes for many-particle processes quickly becomes prohibitively complicated; for

[3]For an introduction, see *e.g.* [11]; a more technical review can be found in the 'Supersymmetry' sections of [10].

[4]Such as those of the section 'Extra Dimensions' of ref. [10].

example, even at tree-level, a six gluon amplitude has 216 Feynman diagrams, a figure which grows faster than the factorial of the number of gluons involved.

Thankfully, a number of methods for quickly computing tree-level amplitudes have been developed. First is the realisation that much of the complexity associated with non-abelian gauge theories, the colour structure, can be separated from the kinematical part of the dynamics leaving one to consider just 'partial' amplitudes. Famously, Parke and Taylor in [13] conjectured a compact formula for the tree-level maximally helicity-violating (MHV) partial amplitudes containing only gluons, with no more than two having a different helicity than the others:

$$\begin{aligned} A(1^+,\ldots,n^+) &= 0, \\ A(1^-,2^+,\ldots,n^+) &= 0, \\ A(1^-,2^+,\ldots,j^-,\ldots,n^+) &= \frac{\langle 1\,j\rangle^4}{\langle 1\,2\rangle\langle 2\,3\rangle\cdots\langle n-1,n\rangle\langle n\,1\rangle}. \end{aligned}$$

(Note that in the last line only gluons 1 and j have negative helicity; the notation is explained in section 2.1.) This was later proved by Berends and Giele [14]. More recently, Cachazo, Svrček and Witten developed the CSW rules for connecting MHV vertices with scalar propagators (using a particular prescription for off-shell spinors) [15, 16] that can be used to compute tree-level amplitudes with arbitrary helicity configurations, using a *polynomial* number of diagrams. We will consider these in some detail. Additionally, Britto, Cachazo and Feng discovered (in ref. [17]) the BCF recursion relations between tree-level amplitudes, which were proved with the help of Witten in ref. [17, 18]. These arise from general considerations on the pole structure and analytic properties of tree-level scattering amplitudes, rather than relying on particular details of the theory under consideration; correspondingly, recursion relations have been found for theories involving non-gluonic matter [19–23] and even for perturbative gravity [24–26]. The CSW rules have been extended likewise [19, 27, 28], and indeed it has come to be understood that the CSW rules arise from a particular adaptation of the BCF relations.

Work has also been done to search for labour-saving devices for the one-loop contributions, although no satisfactorily complete systematic method has been found to date. A variety of techniques have been shown to reproduce known results both in QCD and Supersymmetric Yang-Mills (SYM) theories, and have even been used to predict results for all helicity configurations for up to six gluons and particular configurations at higher orders. These methods include:

- the twistor-string inspired holomorphic anomaly [29–32];
- (generalised) unitarity [33–36], whereby cuts in the complex plane of the momentum invariants are matched to those of functions known to arise in one-loop amplitudes, thereby recovering the *cut constructible* parts. The $\mathcal{N}=1$ and $\mathcal{N}=4$ supersymmetric Yang–Mills theories are completely cut constructible since their

rational terms are inextricably linked to the cut-containing pieces. In QCD, however, the rational terms cannot be correctly recovered by cut construction (indeed, some classes of loop amplitudes are purely rational) and these must be determined *e.g.* by extracting the cut-free parts from the Feynman integrals [37–39] or using:

- 'bootstrap' methods [40–42], which exploit recursion relations between amplitudes at one-loop to extract the rational parts given the cut-constructible pieces; and
- one-loop MHV diagrams [43–45], essentially the application of the CSW rules at one-loop to recover the cut-constructible parts of QCD amplitudes.

A feature common to all these techniques is that they have taken place outside the usual Lagrangian framework, drawing inspiration from the twistor-string dual theories in the cases of the CSW rules and holomorphic anomaly computations, or studies of the analytic structure of scattering amplitudes. The Lagrangian formulation underpins a large body of our understanding of quantum field theory, in particular making manifest the symmetries and guiding us towards a systematic application of regularisation structure, something which these techniques currently lack. This brings us neatly to the motivation of the work documented in this thesis: to formulate the modern techniques, in particular the CSW rules, from a field theory viewpoint. We construct the rules in terms of the Lagrangian formalism, and begin a study of the consequences thereof.

1.1 Outline

The rest of this thesis is organised as follows. In chapter 2, we establish the necessary background materials and preliminaries from perturbative gauge theory that provide the tools and the context for the work presented in chapters 3–5. In particular, we review gauge theory itself; the important techniques of colour-ordered decomposition, the spinor helicity formalism, the Parke–Taylor MHV amplitudes, and the use of supersymmetry to extract information about scattering amplitudes. We describe the BCFW construction of recurrence relations between on-shell amplitudes, and the CSW rules at tree-level. Although loop-level techniques are not the main focus of this thesis, we will also review the most successful developments in this area, in particular unitarity and generalised unitarity.

Chapter 3 introduces and develops the Canonical MHV Lagrangian. In ref. [46][5], Mansfield gave a canonical (in the sense of classical mechanics) field transformation that re-wrote the lagrangian of light-cone gauge Yang–Mills theory as one in terms of an infinite series of Parke–Taylor MHV vertices connected by scalar propagators and continued off-shell in a manner that follows the CSW rules. Following the construction set out in [46], we proceed to solve for this transformation explicitly as a power series. We demonstrate explicitly that the transformation results in vertices of the Parke–Taylor form for up to five gluons. This work was originally published in ref. [48].

[5]We note that a similar transformation was proposed by Gorsky and Rosly in ref. [47].

Next, chapter 4 addresses some of the issues identified at the end of the previous chapter. We follow the research published in ref. [49], where we use the transformation discovered previously to define *MHV completion* vertices. We use these to reconstruct amplitudes which could not be obtained from MHV vertices alone, such as $(--++)$ at tree-level and $(++++)$ at one loop. We apply the transformation to dimensionally regulated light-cone Yang–Mills and obtain D-dimensional MHV vertices. We find strong evidence that MHV vertices and completion vertices together algebraically reconstruct the original LCYM theory, even off shell.

Chapter 5 extends the construction of chapter 3 to include massless quarks in the fundamental representation, and follows the work published in ref. [50]. By considering a similarly specified canonical transformation which results in a lagrangian consisting of an infinite series of vertices with an MHV helicity content, we construct a series solution from which we define completion vertices and test the resulting lagrangian vertices against known QCD MHV amplitudes.

Finally, in chapter 6, we review this work and consider it in the context laid out in this introduction, considering its value as a computational tool and as a means of gaining insight into the structure of gauge theories. We also outline what is left to be understood in the techniques developed herein, and what routes for further research this implies. Finally, we take the opportunity to consider similar developments.

Chapter 2

Modern Perturbative Gauge Theory

The Strong Interaction is described by QCD, a non-Abelian gauge theory with the following action:

$$S_{\mathrm{QCD}} = \int d^4x \left\{ \bar{\psi}(i\not{D} - m)\psi - \frac{1}{4} \operatorname{tr} F_{\mu\nu} F^{\mu\nu} \right\}. \tag{2.1}$$

The phenomenologically relevant implementation of QCD has an SU(3) gauge group with the quark field ψ transforming in the fundamental representation. It also features (from QCD's point of view) six different flavours of quark, each with a different mass. However, for the purposes of the studies conducted in this thesis, we will be concerned with the case of just one flavour with $m = 0$ when we come to consider quarks. We will also generalise the gauge group slightly and work with $\mathrm{SU}(N_{\mathrm{C}})$ (and sometimes $\mathrm{U}(N_{\mathrm{C}})$ where convenient) where N_{C} is the number of colours of quark (*i.e.* the dimension of the fundamental representation).

Let us make (2.1) more concrete by making some further definitions. First, the gauge covariant derivative is

$$D_\mu = \partial_\mu - \frac{ig}{\sqrt{2}} A_\mu, \tag{2.2}$$

where $A_\mu = A_\mu^a T^a$ is the gluon field, living in the adjoint representation of the gauge group. The $N_{\mathrm{C}}^2 - 1$ generators of the $\mathfrak{su}(N_{\mathrm{C}})$ Lie algebra are normalised according to $\operatorname{tr}(T^a T^b) = \delta^{ab}$, giving the factor of $2^{-1/2}$ in (2.2)[1], and the structure constants f^{abc} defined according to

$$[T^a, T^b] = i\sqrt{2} f^{abc} T^c. \tag{2.3}$$

The field strength $F_{\mu\nu}$ is an algebra-valued 2-form, defined here by

$$F_{\mu\nu} = [D_\mu, D_\nu] = \partial_\mu A_\nu - \partial_\nu A_\mu + [A_\mu, A_\nu]. \tag{2.4}$$

[1]This factor would be absent had we chosen the 'textbook' normalisation $\operatorname{tr}(T^a T^b) = \frac{1}{2}\delta^{ab}$, but this would lead to a proliferation of factors of $\sqrt{2}$ elsewhere.

Note that in this thesis, we will use the term 'QCD' to refer to the massless, quark-containing $\mathrm{SU}(N_\mathrm{C})$ gauge theory. In absence of quarks, the non-Abelian nature of the gauge group (*i.e.* $f^{abc} \neq 0$) means that the gauge field still interacts with itself, and so what is left over is still interesting. We will refer to this theory as '(pure) Yang–Mills'.

As noted in chapter 1, QCD is asymptotically free, and its running coupling constant decreases with increasing energy scale Q like $(\ln Q)^{-1}$. From a phenomenological point of view, it will be the perturbatively amenable, high-energy regime on which we focus our studies. Alternatively, noting that in the absence of an experimental impetus the theory described continues to exhibit UV asymptotic freedom, we can simply *presume* to work at *some* energy scale at which the coupling constant is much smaller than 1.

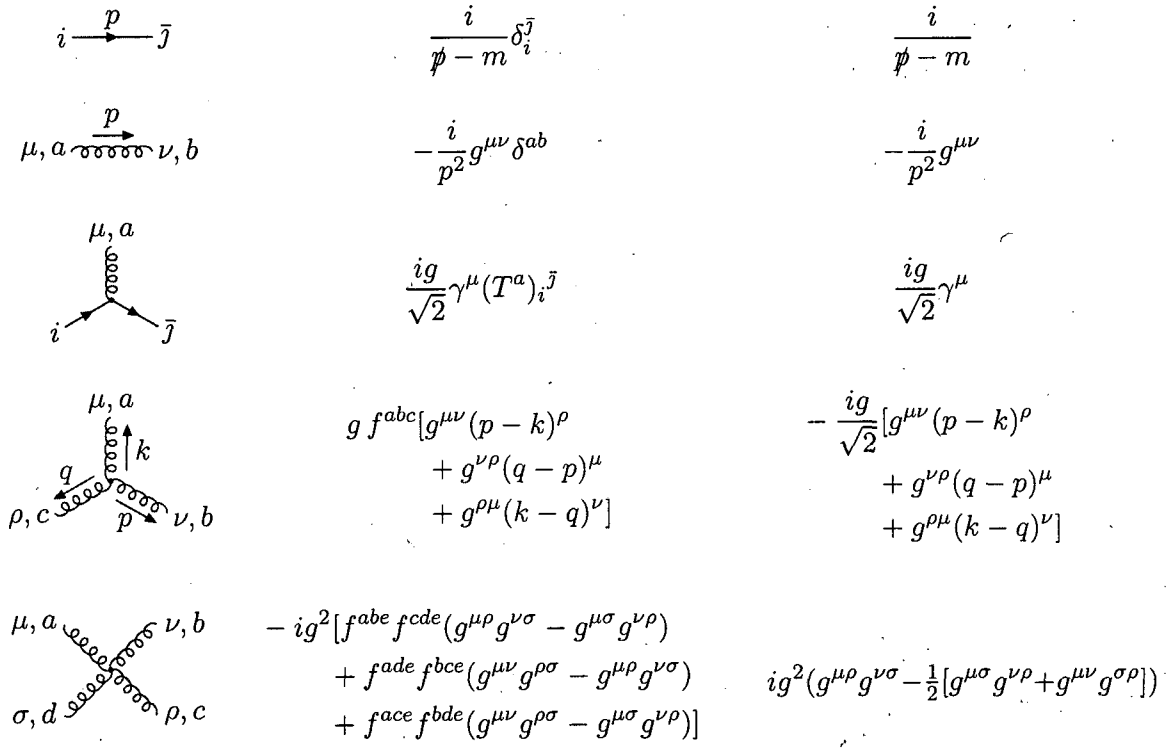

FIGURE 2.1: Feynman rules for QCD, excluding Faddeev–Popov ghosts. The expressions in the second column are for the traditional formulation that includes colour explicitly. The third column gives the colour-ordered Feynman rules. All momenta are out-going.

The textbook treatment of the theory of (2.1) is to expand the expression for the action in terms of its component fields, and then gauge fix in order to define the path integral. This is conventionally carried out by the Faddeev–Popov procedure working in Feynman gauge. The procedure introduces extra 'ghost' fields which may be understood as 'anti-degrees-of-freedom' that eliminate the non-physical degrees of freedom that arise from gauge invariance. Ghosts couple to gluons but are not physical particles (which may be understood by considering the BRST transformation properties of the theory [51]), so they only show up in loop diagrams. Nevertheless, the Feynman gauge is not the only

possible gauge and a judicious choice (such as an axial gauge, $n \cdot A^a = 0$) decouples the ghosts entirely (albeit often at the cost of increased computational difficulties).

With a gauge-fixed action, we can construct Feynman rules and thence Feynman graphs. The Feynman rules (minus ghost vertices) for the theory (2.1) in Feynman gauge are shown in fig. 2.1. Calculating perturbative gauge theory amplitudes is from then on a straightforward procedure: one draws all the relevant diagrams contributing to an amplitude at a desired order in g, contracts with external polarisation vectors and spinors and adds them up.

Unfortunately, in practise this turns out to be a computationally intensive task as the number of particles in the amplitude grows. Consider the multi-gluon amplitudes, which have a phenomenological relevance to the computation of the LHC background (amongst other things): just at tree level, the number of diagrams and the complexity of their expressions grows incredibly rapidly. Indeed, for n gluons the number of Feynman graphs increases faster than $n!$ [52]: 220 diagrams for 6 gluons, increasing (from 7 gluons) as $2\,485, 34\,300, 589\,405, 10\,525\,900, \ldots$, and any attempt to calculate these amplitudes soon encounters the limitations of time or memory. It is, therefore, surprising to find that the final expressions for these amplitudes often take a very simple form (when expressed in the right framework), even at the loop level. Computational techniques have also been discovered that have a great computational advantage over Feynman graphs. All this hints that gauge theories have a structure much simpler than we would otherwise expect.

The remainder of this chapter aims to establish some of the formalism that makes these simplifications manifest, and illustrate some of the modern techniques that exploit this. Sections 2.1, 2.2 and 2.3 introduce the spinor-helicity formalism, the concept of colour ordered amplitudes and the Parke–Taylor MHV amplitude, and explain the role of supersymmetry in dealing with a non-supersymmetric theory. Sections 2.4 and 2.5 discuss two important modern tools for computing tree-level amplitudes, the CSW rules and BCF recursion relations, and finally in section 2.6, we review the techniques that have been applied at the loop level.

2.1 The spinor formalism

Much development in modern perturbative gauge theory uses the spinor framework to represent momenta and helicity. Ref. [53] has a particularly clear exposition of this, and we will follow closely the formalism therein.

It is well-known that the complexified Lorentz group $\mathrm{SO}(1,3;\mathbb{C})$ is locally isomorphic to $\mathrm{SL}(2;\mathbb{C}) \times \mathrm{SL}(2;\mathbb{C})$, so its representations may be classified as (m,n) where m and n are half-integers giving the spin of the representation. $(\frac{1}{2},0)$ and $(0,\frac{1}{2})$ are the left- and right-handed chiral Weyl spinors, respectively, whose direct sum gives the Dirac spinor. $(\frac{1}{2},\frac{1}{2})$ is the 4-vector, so it can be represented as a bispinor $p_{\alpha\dot{\alpha}}$, and we can map from

Minkowski co-ordinates (p^t, p^1, p^2, p^3) into this representation using

$$p_{\alpha\dot{\alpha}} = p_\mu (\bar{\sigma}^\mu)_{\dot{\alpha}\alpha} = \begin{pmatrix} p^t + p^3 & p^1 - ip^2 \\ p^1 + ip^2 & p^t - p^3 \end{pmatrix}, \tag{2.5}$$

where the 4-vectors of Pauli matrices are

$$(\sigma^\mu)^{\dot{\alpha}\alpha} = (1, \boldsymbol{\sigma}) \quad \text{and} \quad (\bar{\sigma}^\mu)_{\alpha\dot{\alpha}} = (1, -\boldsymbol{\sigma})$$

and $\boldsymbol{\sigma}$ is the usual 3-vector of Pauli matrices. (The spinor indices are printed here to show their 'natural' position, *i.e.* as they dereference the elements of the matrices on the RHS.) From this, it is clear that $\det p = p^2$. If p is null then $p_{\alpha\dot{\alpha}}$ may be factorised into two Weyl spinors as

$$p_{\alpha\dot{\alpha}} = \lambda_\alpha \tilde{\lambda}_{\dot{\alpha}}.$$

λ_α is commonly termed the *holomorphic* spinor, transforming in the $(0, \frac{1}{2})$ representation, and $\tilde{\lambda}_{\dot{\alpha}}$ the *antiholomorphic* spinor in the $(\frac{1}{2}, 0)$ representation[2].

We define raising (and hence lowering) of spinor indices as follows:

$$\lambda^\alpha = \epsilon^{\alpha\beta}\lambda_\beta \quad \Leftrightarrow \quad \lambda_\alpha = \epsilon_{\alpha\beta}\lambda^\beta, \tag{2.6}$$

and likewise with dotted indices. In our convention, the invariant antisymmetric bispinor has $\epsilon^{12} = \epsilon^{\dot{1}\dot{2}} = 1$. We define the downstairs-indexed ϵ to be just the inverse of the one with indices raised: $\epsilon^{\alpha\beta}\epsilon_{\beta\gamma} = \delta^\alpha_\gamma$. Thus,

$$p^{\alpha\dot{\alpha}} q_{\alpha\dot{\alpha}} = 2p \cdot q, \tag{2.7}$$

which can be seen either by direct application of (2.5) and (2.6), or by noticing that $(\sigma^\mu)^{\dot{\alpha}\alpha} = (\bar{\sigma}^\mu)^{\alpha\dot{\alpha}}$, and hence

$$(\bar{\sigma}^\mu)_{\alpha\dot{\alpha}}(\bar{\sigma}^\nu)^{\alpha\dot{\alpha}} = \operatorname{tr} \bar{\sigma}^\mu \sigma^\nu = 2g^{\mu\nu}.$$

Since the ϵ bispinor is an $\mathrm{SL}(2;\mathbb{C})$ invariant, the following products of spinors are Lorentz invariants:

$$\langle \lambda\, \mu \rangle := \epsilon^{\alpha\beta}\lambda_\alpha \mu_\beta \quad \text{and} \quad [\lambda\, \mu] := \epsilon^{\dot{\alpha}\dot{\beta}}\tilde{\lambda}_{\dot{\alpha}}\tilde{\mu}_{\dot{\beta}} \tag{2.8}$$

In what follows, for null momenta we will often simply use that momentum's symbol or its number directly in the $\langle\,\rangle$ and $[\,]$ brackets, using its (anti)holomorphic spinor as the context above suggests. Clearly these brackets are antisymmetric in their arguments. Combining (2.8) with (2.7), we have for any two null momenta $p = \lambda\tilde{\lambda}$ and $q = \mu\tilde{\mu}$

$$2p \cdot q = \langle \lambda\, \mu \rangle [\lambda\, \mu]. \tag{2.9}$$

[2]While we are following the discussion of [53], this is closer to the convention of [15].

2.1.1 Spinor helicity

For massless vector particles, we choose the following polarisation vectors, written as bispinors [53]:

$$\epsilon^{+}_{\alpha\dot{\alpha}}(p,\mu) = \sqrt{2}\frac{\nu_\alpha \tilde{\lambda}_{\dot{\alpha}}}{\langle \nu\, \lambda\rangle} \quad \text{and} \quad \epsilon^{-}_{\alpha\dot{\alpha}}(p,\mu) = \sqrt{2}\frac{\lambda_\alpha \tilde{\nu}_{\dot{\alpha}}}{[\nu\, \lambda]} \tag{2.10}$$

for a gluon with momentum $p_{\alpha\dot{\alpha}} = \lambda_\alpha \tilde{\lambda}_{\dot{\alpha}}$. The spinors ν and $\tilde{\nu}$ correspond to a null *reference vector* $\mu_{\alpha\dot{\alpha}} = \nu_\alpha \tilde{\nu}_{\dot{\alpha}}$. It is easy to verify (*e.g.* using (2.7) and the antisymmetry of $\epsilon^{\alpha\beta}$) that these polarisation vectors satisfy the following:

$$p \cdot \epsilon^{\pm}(p,\mu) = p^{\alpha\dot{\alpha}} \epsilon^{+}_{\alpha\dot{\alpha}}(p,\mu) = 0,$$

$$\epsilon^{+}(p,\mu) \cdot \epsilon^{+}(q,\mu) = 0, \tag{2.11}$$

$$\epsilon^{+}(p,q) \cdot \epsilon^{-}(q,\mu) = 0. \tag{2.12}$$

The choice of μ is arbitrary (so long as its respective spinors are not proportional to those of p), and this is due to residual gauge invariance. We can add to $\epsilon^{\pm}$ any multiple of p and still preserve the Lorentz gauge condition, and clearly any change of ν and $\tilde{\nu}$ effects precisely that: since they are not parallel, ν and λ (and their conjugates) form a basis for the Weyl spinors. Any change along the ν direction cancels in (2.10), whereas the component of λ leaves a piece proportional to $\lambda\tilde{\lambda}$ — that is, p.

Last but not least, we state the Schouten identity,

$$\langle i\, j\rangle\langle k\, l\rangle = \langle i\, k\rangle\langle j\, l\rangle + \langle i\, l\rangle\langle k\, j\rangle \tag{2.13}$$

and its conjugate under $\langle\,\rangle \leftrightarrow [\,]$. This may be derived by noting Fierz-type identity for Weyl spinors $\epsilon_{\alpha\beta}\epsilon_{\gamma\delta} = \epsilon_{\alpha\gamma}\epsilon_{\beta\delta} + \epsilon_{\alpha\delta}\epsilon_{\gamma\beta}$.

2.2 Colour ordered decomposition

The first significant simplification of the process of computing QCD scattering amplitudes comes from the observation that we can separate the management of the colour information from the kinematics, and this gives rise to *colour ordering* and *colour ordered partial amplitudes.*

Now consider the Feynman rules of the Yang–Mills theory. We see that the vertices have group theory factors that are either linear or quadratic in the gauge theory structure constants f^{abc}. We can re-write these as traces:

$$f^{abc} = \frac{i}{\sqrt{2}}\,\mathrm{tr}(T^a T^b T^c - T^c T^b T^a).$$

Internal $\mathrm{SU}(N_\mathrm{C})$ colour lines in the adjoint representation make contractions between indices of these structure constants, but by definition, $i\sqrt{2}T^c f^{cde} = [T^d, T^e]$, so inserting this into the above simply unrolls the further permutations of gauge generator matrices.

Thus for a purely gluonic tree-level amplitude, the entire colour content can be moved out into a trace. A n-gluon tree-level amplitude with all particles out-going, where the gluon label i subsumes a momentum p_i and helicity state h_i, and a_i is an adjoint index, can be decomposed as[3]:

$$\mathcal{A}(1\cdots n) = (2\pi)^4\delta(\textstyle\sum_{i=1}^n p_i) \sum_{\sigma\in S_n/\mathbb{Z}_n} \mathrm{tr}(T^{a_{\sigma(1)}}\cdots T^{a_{\sigma(n)}})\, A(\sigma(1)\cdots\sigma(n)), \qquad (2.14)$$

where $S_n/\mathbb{Z}_n$ is the group of all permutations of n objects, modulo cycles (under which the trace is invariant). The colour-stripped object $A(1\cdots n)$ is a *partial amplitude.*

When a single quark-antiquark pair is present in an amplitude, carrying fundamental indices $\bar{\imath}$ and j, respectively, we obtain colour structures with exposed fundamental indices of the form

$$(X_0 T^{a_1} T^{a_2} Y_0)_i{}^{\bar{\jmath}}\,\mathrm{tr}(X_1 T^{a_1} Y_1)\,\mathrm{tr}(X_2 T^{a_2} Y_2)\cdots$$

where the ellipsis on the extreme right denotes further omitted traces, and X_i and Y_i are products of gauge generators. We can use the $\mathrm{SU}(N_\mathrm{C})$ Fierz identity

$$(T^a)_i{}^{\bar{\jmath}}(T^a)_k{}^{\bar{l}} = \delta_i^{\bar{l}}\delta_k^{\bar{\jmath}} - \frac{1}{N_\mathrm{C}}\delta_i^{\bar{\jmath}}\delta_k^{\bar{l}} \qquad (2.15)$$

to break up these products into a product of all the gauge generators, plus a product of traces suppressed by $1/N_\mathrm{C}$ of the form

$$(X_0 Y_1 X_1 Y_2 X_2 \cdots Y_0)_i{}^{\bar{\jmath}} + \frac{1}{N_\mathrm{C}}(\text{products of traces})\delta_i^{\bar{\jmath}}.$$

Now for one quark line, we can ignore the $\mathcal{O}(1/N_\mathrm{C})$ piece: to see this, consider that it is just the statement that the $\mathfrak{su}(N_\mathrm{C})$ generators are traceless. Had we considered the $\mathrm{U}(N_\mathrm{C})$ gauge group instead, the $\mathcal{O}(1/N_\mathrm{C})$ term would be absent from (2.15). Now, $\mathrm{U}(N_\mathrm{C}) = \mathrm{SU}(N_\mathrm{C})\times\mathrm{U}(1)$ so in this case the theory has an extra gauge boson (a photon); its corresponding gauge generator is proportional to the identity and so commutes with the $\mathrm{SU}(N_\mathrm{C})$ generators and decouples from the gluons. Thus, *with one quark line at tree level,* the $\mathrm{U}(N_\mathrm{C})$ and $\mathrm{SU}(N_\mathrm{C})$ amplitudes are the same and we may discard terms $\mathcal{O}(1/N_\mathrm{C})$. The colour decomposition for an amplitude with one quark-antiquark pair is therefore

$$\mathcal{A}(1_\mathrm{q}, 2, \ldots, n-1, n_{\bar{\mathrm{q}}}) = (2\pi)^4\delta(\textstyle\sum_{i=1}^n p_i) \sum_{\sigma\in S_{n-2}} (T^{a_{\sigma(2)}}\cdots T^{a_{\sigma(n-1)}})_{i_1}{}^{\bar{\imath}_n} \times A(1_\mathrm{q}, \sigma(2), \ldots, \sigma(n-1), n_{\bar{\mathrm{q}}}). \qquad (2.16)$$

With more than one quark line, the extra photon from the $\mathrm{U}(N_\mathrm{C})$ theory can couple between the quark lines. Thus, in this situation we do have to consider terms $\mathcal{O}(1/N_\mathrm{C})$

[3]Note that it will be our convention to absorb the factors of i and g into the partial amplitude.

in the decomposition of the colour structures. This is explained in detail in [28,54]. We will not reproduce the full construction here for the purposes of this thesis, since we will only encounter this in section 5.3.3 for four-quark amplitudes with no gluons; these are simple enough to permit us to work out the colour structures on-the fly. However, we note below that for an amplitude with two quark-antiquark pairs and an arbitrary number of positive-helicity gluons, the *leading* partial amplitude is

$$A(1_{\mathrm{q}}^{h_1}, 2, \ldots, j-2, (j-1)_{\bar{\mathrm{q}}}^{-h_j}; j_{\mathrm{q}}^{h_j}, j+1, \ldots, n-1, n_{\bar{\mathrm{q}}}^{-h_1}), \tag{2.17}$$

which is associated with the colour factor

$$(T^{a_2} \ldots T^{a_{j-2}})_{i_1}{}^{\bar{\imath}_{j-1}} (T^{a_{j+1}} \ldots T^{a_{n-1}})_{i_j}{}^{\bar{\imath}_n}. \tag{2.18}$$

There are also sub-leading partial amplitudes associated with the colour structure

$$-\frac{1}{N_{\mathrm{C}}} (T^{a_2} \ldots T^{a_{j-2}})_{i_1}{}^{\bar{\imath}_n} (T^{a_{j+1}} \ldots T^{a_{n-1}})_{i_j}{}^{\bar{\imath}_{j-1}}. \tag{2.19}$$

The full amplitude is obtained by summing over the permutations of the gluon labels $\{2, \ldots, j-2, j+1, \ldots, n-1\}$, over permutations of the quarks $\{1, j\}$ and antiquarks $\{j-1, n\}$ so as not to over-count and remembering a Fermi statistics factor of -1 for an odd permutation; and finally over j, interpreted as the *position* of the second quark in (2.18) and (2.19) (or equivalently as a parametrisation of the length of T-strings).

't Hooft double-line diagrams and colour-ordered Feynman rules

In [55], 't Hooft described a novel way of analysing the colour structure of an amplitude. One assigns a directed line to each line in the graph that carries a charge in the fundamental representation. In our convention where all particles are out-going, lines start on fundamental indices i and end on antifundamental indices $\bar{\jmath}$, such as with the gluon vertex of fig. 2.2(a). A trace of gauge matrices, such as at a three-gluon vertex, joins up fundamental lines cyclically as shown in fig. 2.2(b). Gluon lines contract fundamental indices, and may be dealt with using the SU(N_{C}) Fierz identity. This manifests itself as two possible ways of connecting lines to the fundamental indices of the matrices on which the gluons end, and so connections between vertices in double-line diagrams are made using the right-hand side of in fig. 2.2(c).

The third column of fig. 2.1 shows the *colour ordered Feynman rules* for QCD, which are derived from the normal Feynman rules by taking their colour factors and writing them in terms of [traces of] the various T^a matrices, and one then simply extracts the term bearing the leading colour order (*e.g.* $\mathrm{tr}(T^a T^b T^c T^d)$ for the four gluon vertex). These rules are used to compute colour-ordered partial amplitudes, which we obtain by summing all planar graphs whose external legs' labels (into which we remind the reader we have subsumed both colour and helicity information) are ordered so as to match the colour factor with which the partial amplitude is associated. That these graphs must

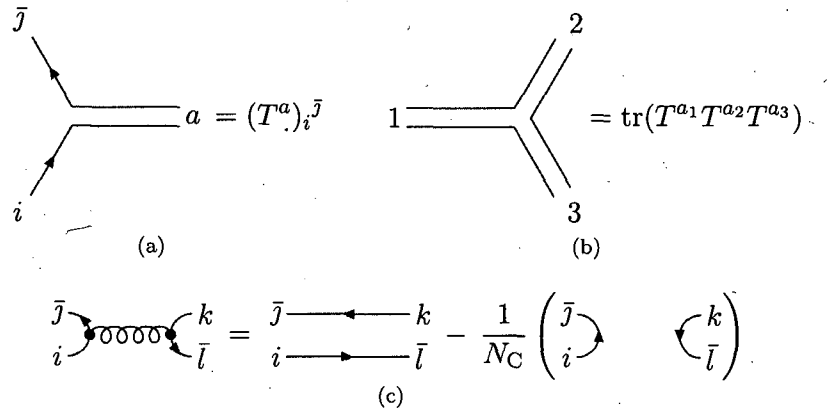

FIGURE 2.2: 't Hooft double line diagrams for (a) the quark-gluon vertex, (b) a three-gluon vertex, and (c) the SU(N_C) Fierz identity (2.15).

be planar and ordered in this fashion is clear upon considering the associated 't Hooft diagrams: non-planar graphs contribute to other colour orders' partial amplitudes.

Symmetries of gluonic partial amplitudes

The pure-gluon partial amplitude is gauge invariant (inasmuch as it does not change under redefinitions of polarisation $\epsilon_i \to \epsilon_i + \alpha p_i$), and satisfies a number of useful symmetry properties.

- The argument list is only defined up to cycles, so $A(1\cdots n) = A(2\cdots n1) = \cdots = A(n, 1, \ldots, n-1)$.
- Under complete reversal of the arguments, $A(1\cdots n) = (-1)^n A(n\cdots 1)$. To see this, note that under *complete reversal* of a planar diagram, the three-point Feynman rule changes sign but the four point rule does not. An n-gluon tree with m 4-point vertices has $n-2-2m$ 3-point vertices, so the overall sign change is $(-1)^{n-2-2m} = (-1)^n$.
- The *dual Ward identity* links cycles of $n-1$ consecutive arguments:

$$A(1\cdots n) + A(23\cdots 1n) + A(34\cdots 12n)\cdots + A(n-1, \ldots, n-2, n) = 0.$$

  This can be seen from the construction of the amplitudes in terms of colour-ordered Feynman rules: one can always pair up each graph from one term with another graph in another term of the opposite sign. Alternatively, one works with the the gauge group U(N_C) and lets particle n be the photon in (2.14). Carry out the sum noting now that T^{a_n} is proportional to the identity, and by collecting terms of the same trace structure we arrive at the expression above.

Already, we can see that these symmetries cut down on the amount of work we have to do to assemble amplitudes. For example, for five gluons, we first note that parity invariance means that we only need to consider partial amplitudes with up to two

negative helicity gluons, since for more we can flip the helicities by complex conjugation. Furthermore, we note (as seen in section 2.2.1), the partial amplitudes with fewer than two negative helicity gluons vanish. Thus, applying the rotational symmetry, we are left with just two independent partial amplitudes:

$$A(1^-2^-3^+4^+5^+) \quad \text{and} \quad A(1^-2^+3^-4^+5^+).$$

2.2.1 The Parke–Taylor amplitudes

Some of the most important colour-ordered amplitudes were first given in ref. [13] by Parke and Taylor. The following expressions are for tree-level colour-ordered gluon amplitudes with an arbitrary number of particles with positive helicity, and up to two with negative helicity:

$$A(1^+ \cdots n^+) = 0, \tag{2.20}$$

$$A(1^-2^+ \cdots n^+) = 0, \tag{2.21}$$

$$A(1^-2^+ \cdots j^- \cdots n^+) = ig^{n-2} \frac{\langle 1\, j\rangle^4}{\langle 1\, 2\rangle\langle 2\, 3\rangle \cdots \langle n-1, n\rangle\langle n\, 1\rangle}. \tag{2.22}$$

(The amplitudes with the opposite helicity follow by parity symmetry upon exchanging $\langle\,\rangle \leftrightarrow [\,]$.) The last amplitude above is the first one which is non-vanishing at tree-level for the largest difference between the number of positive- and negative-helicity gluons, and hence is referred to as *maximally helicity-violating*, or MHV for short. When the helicities are flipped, we refer to this as an $\overline{\text{MHV}}$ amplitude. An amplitude with three negative-helicity gluons is termed a next-to-MHV or NMHV amplitude, with four a NNMHV and so-on so that an N^nMHV amplitude has $n+2$ negative-helicity gluons.

It is fairly straightforward to prove the first two expressions (2.20) and (2.21) by considering the (colour-ordered) Feynman graphs that contribute to them. For the all-+ amplitude with n gluons, first consider the gluon vertices of fig. 2.1: each one can contribute at the most one external momentum p_i^μ, and there are at the most $n-2$ vertices. Now contract the polarisation vectors $\epsilon_i^+ = \epsilon_\mu^+(p_i, k_i)$ into this expression. There are n of these, so each term must contain a factor of the form $\epsilon_i^+ \cdot \epsilon_j^+$, which vanishes by (2.11) if we choose all the reference momenta to be the same; the amplitude therefore vanishes by gauge invariance. When one gluon has negative helicity, the same thing happens: we obtain factors $\epsilon_i^- \cdot \epsilon_j^+$, $j \geq 2$, which vanish by (2.12) if we pick reference momenta $k_j = p_1$ for $j \geq 2$.

Berends and Giele proved (2.22) in [56] using a recursive technique that connected together off-shell gluon currents. We will not reproduce this here; instead, we refer the reader to the proof obtained by Britto, Cachazo and Feng in [17], and shown in section 2.5.1, using on-shell recursion relations.

Now, it is clear these are remarkably simple expressions: even for tree-level amplitudes, given what we remarked earlier about the growth in the complexity of the expressions arising in conventional perturbation theory. What might not be so clear is

precisely why. They hint that gauge theories have a much simpler structure than implied by traditional Feynman diagrams — and as such we might well ask how this simplicity extends to higher order computations, and moreover wherein lie its origins.

2.2.2 Colour ordering at one loop

At one loop, the colour ordered decomposition is more complicated due to the presence of non-planar diagrams. For the planar pieces, the leading colour structure is still of the form $\mathrm{tr}(T^{a_1}\cdots T^{a_n})$, but is amplified by a factor of N_C arising from the trace of the identity of the $SU(N_C)$'s fundamental representation. The non-planar graphs contribute structures of the form $\mathrm{tr}(T^{a_1}\cdots T^{a_{c-1}})\,\mathrm{tr}(T^{a_c}\cdots T^{a_n})$, which are correspondingly suppressed relative to the planar terms. The one-loop colour ordered decomposition for gluon amplitudes was obtained in [57] as

$$\mathcal{A}^{1\text{ loop}}(1\cdots n) = \sum_{\sigma\in S_n/\mathbb{Z}_n} N_C\,\mathrm{tr}(T^{a_1}\cdots T^{a_n})A_{n;1}(\sigma(1)\cdots\sigma(n))$$
$$+\sum_{c=2}^{\lfloor n/2\rfloor+1}\sum_{\sigma\in S_n/S_{n;c}}\mathrm{tr}(T^{a_{\sigma(1)}}\cdots T^{a_{\sigma(c-1)}})\,\mathrm{tr}(T^{a_{\sigma(c-1)}}\cdots T^{a_{\sigma(n)}})A_{n;c}(\sigma(1)\cdots\sigma(n)). \quad (2.23)$$

$S_{n;c}$ is the subset of S_n that leaves the traces invariant. Amazingly, it turns out [58] that the non-planar partial amplitudes $A_{n;c}(\sigma(1)\cdots\sigma(n))$, $c>1$, can be computed as sums of permutations of the *primitive* amplitudes $A_{n;1}(\sigma(1)\cdots\sigma(n))$, which are obtained from planar graphs. As such, the majority of the literature is devoted to the computation of the latter.

2.3 Techniques from Supersymmetry

While QCD is not itself a supersymmetric theory, we can use prototypical unbroken supersymmetric theories as elements in the calculation of QCD amplitudes, and thereby leverage the cancellations and simplifications the supersymmetry produces.

2.3.1 Supersymmetric Ward identities

SUSY transformations mix fermions and bosons in a supermultiplet, and so construct relationships between pure-gluon amplitudes and those also containing gluinos. This is useful for QCD since *at tree level* the theory is effectively supersymmetric (once we have removed the colour information) by virtue of sharing its kinematic structure with unbroken SUSY theories. (Because SUSY multiplets have a different field content to QCD, this breaks at loop level; however, this turns out to be a blessing in disguise as discussed in section 2.3.2.) We can map the gluon–gluino amplitudes back to gluon–quark amplitudes (albeit with a few caveats for certain configurations of pure-quark amplitudes).

Consider a 'parallel' theory with $\mathcal{N} = 1$ supersymmetry and a vector supermultiplet consisting of a gauge field A_μ, with two bosonic physical degrees of freedom, and the Majorana spinor Λ (also in the adjoint representation) with its two fermionic degrees of freedom. The theory has the lagrangian density

$$\mathcal{L} = \mathrm{tr}\left(-\frac{1}{4}F^{\mu\nu}F_{\mu\nu} + i\bar{\Lambda}\not{D}\Lambda + \frac{D^2}{2}\right), \tag{2.24}$$

where D is the auxiliary field. Now let q be a null vector with corresponding chiral Weyl polarisation spinors $\varphi(q)$ and $\bar{\varphi}(q)$ (defined, *e.g.* in (3.5) upon identifying $\varphi = \lambda$, $\bar{\varphi} = \tilde{\lambda}$), from which we define $\eta_\alpha(q) = \theta\varphi_\alpha(q)/\sqrt{2}$ and $\bar{\eta}^{\dot{\alpha}}(q) = \theta\bar{\varphi}^{\dot{\alpha}}(q)/\sqrt{2}$ where θ is a Grassman number. Then for on-shell fields in the asymptotic (free) limit, one can show that the commutators of the SUSY generator $Q(\eta) = \eta^\alpha Q_\alpha + \bar{\eta}_{\dot{\alpha}}\bar{Q}^{\dot{\alpha}}$ with the gluon and gluino helicity–momentum annihilation operators, $A^\pm(k)$ and $\Lambda^\pm(k)$ respectively, are as follows[4]:

$$[Q(\eta), A^\pm(k)] = i\Gamma^\pm(k,\eta)\Lambda^\pm(k), \tag{2.25}$$

$$[Q(\eta), \Lambda^\pm(k)] = i\Gamma^\mp(k,\eta)A^\pm(k), \tag{2.26}$$

with

$$\Gamma^+(k,\eta) = -\theta[k\,q] \quad \text{and} \quad \Gamma^-(k,\eta) = \theta\langle k\,q\rangle. \tag{2.27}$$

Applying the commutation relations (2.25)–(2.27) to strings of annihilation operators gives relationships known as *supersymmetric Ward identities* [59, 61] that link different amplitudes. Let us study some examples of this in action to see how it is useful for obtaining QCD amplitudes.

First, let us use these ideas to derive the gluon–gluino MHV amplitude. We define $|\mathrm{vac}\rangle = S|0\rangle$, where the S-matrix S evolves asymptotic 'in' states (defined in the infinite past) to 'out' states (defined in the infinite future), and $|0\rangle$ is the free vacuum state. $Q(\eta)$ annihilates the vacuum, so

$$0 = \langle 0|[Q(\eta), A_1^- A_2^+ \cdots A_j^- \cdots A_{n-1}^+\Lambda_n^+]|\mathrm{vac}\rangle.$$

We expand the commutator, and choose η, $\bar{\eta}$ to be the spinors associated with the null momentum p_j to obtain (noting, of course, that the terms with two Λ^+ operators vanish by helicity conservation)

$$\begin{aligned}\langle 0|\Lambda_1^- A_2^+ \cdots A_j^- \cdots A_{n-1}^+\Lambda_n^+|\mathrm{vac}\rangle &= -\frac{\langle n\,j\rangle}{\langle 1\,j\rangle}\langle 0|A_1^- A_2^+ \cdots A_j^- \cdots A_n^+|\mathrm{vac}\rangle \\ \Rightarrow A(\Lambda_1^- A_2^+ \cdots A_j^- \cdots A_{n-1}^+\Lambda_n^+) &= ig^{n-2}\frac{\langle 1\,j\rangle^3\langle j\,n\rangle}{\langle 1\,2\rangle\langle 2\,3\rangle\cdots\langle n-1,n\rangle\langle n\,1\rangle}.\end{aligned} \tag{2.28}$$

[4]These may be obtained directly by considering the effect of SUSY transformations acting on the annihilation operators expressed in terms of the asymptotic (free) fields [59]. We note that the convention used here differs slightly from that found in [60], which results in a sign difference for every fermion-antifermion pair in the amplitudes.

Similarly,

$$\langle 0|\Lambda_1^+ A_2^+ \cdots A_j^- \cdots A_{n-1}^+ \Lambda_n^-|\text{vac}\rangle = \frac{\langle 1\, j\rangle}{\langle n\, j\rangle}\langle 0|A_1^+ A_2^+ \cdots A_j^- \cdots A_{n-1}^+ A_n^-|\text{vac}\rangle$$
$$\Rightarrow A(\Lambda_1^+ A_2^+ \cdots A_j^- \cdots A_{n-1}^+ \Lambda_n^-) = ig^{n-2}\frac{\langle 1\, j\rangle\langle n\, j\rangle^3}{\langle 1\, 2\rangle\langle 2\, 3\rangle\cdots\langle n-1, n\rangle\langle n\, 1\rangle}. \tag{2.29}$$

Extracting a QCD amplitude from this is straightforward. For example, when $n = 4$,

$$\langle 0|\Lambda_1^- A_2^+ A_3^- \Lambda_4^+|\text{vac}\rangle = -\frac{\langle 4\, 3\rangle}{\langle 1\, 3\rangle}\langle 0|A_1^- A_2^+ A_3^- A_4^+|\text{vac}\rangle. \tag{2.30}$$

Now since everything is in the adjoint representation, we can interpret both sides as *partial* amplitudes associated with $\text{tr}(T^{a_1}T^{a_2}T^{a_3}T^{a_4})$. Conversely, we can interpret the LHS of (2.30) as $A(1_{\text{q}}^-2^+3^-4_{\bar{\text{q}}}^+)$, to be associated with the $(T^{a_2}T^{a_3})_{i_1}{}^{\bar{\imath}_4}$ colour structure, as follows. We draw the 't Hooft double-line diagram for the QCD colour structure such that the quark lines run on the outside, shown for this case in fig. 2.3. To lift to the SUSY side, we add an extra line alongside each quark line. Note that in the case of up to one quark-antiquark pair, there is a unique way to do this, hence we can map these QCD partial amplitudes directly onto SUSY partial amplitudes with the associated gluinos *adjacent* to each other.

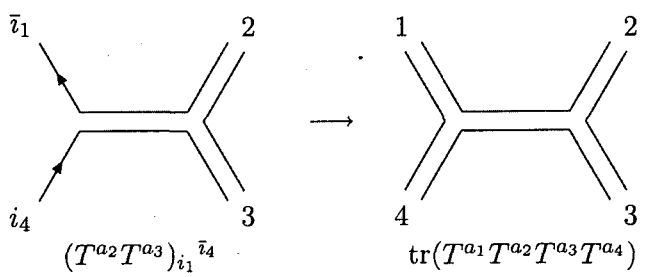

FIGURE 2.3: 't Hooft double-line diagrams relating QCD to SUSY colour structures with one quark-antiquark pair. On the left is the QCD structure with the fundamental indices, the quark line running on the outside. It is lifted to the colour trace on the right by adding an extra line.

Correspondingly, we can define the MHV amplitudes with a quark-antiquark pair and a single gluon of negative helicity by

$$A(1_{\text{q}}^-2^+\cdots j^-\cdots(n-1)^+n_{\bar{\text{q}}}^+) = ig^{n-2}\frac{\langle 1\, j\rangle^3\langle j\, n\rangle}{\langle 1\, 2\rangle\langle 2\, 3\rangle\cdots\langle n-1, n\rangle\langle n\, 1\rangle} \tag{2.31}$$

and

$$A(1_{\text{q}}^+2^+\cdots j^-\cdots(n-1)^+n_{\bar{\text{q}}}^-) = ig^{n-2}\frac{\langle 1\, j\rangle\langle n\, j\rangle^3}{\langle 1\, 2\rangle\langle 2\, 3\rangle\cdots\langle n-1, n\rangle\langle n\, 1\rangle}, \tag{2.32}$$

both of which are associated with the $(T^{a_2}\cdots T^{a_{n-1}})_{i_1}{}^{\bar{\imath}_n}$ colour structure.

To add more gluino pairs, we continue the process. For example, to obtain four gluino amplitudes, start from

$$\begin{aligned} 0 &= \langle 0|[Q(\eta), \Lambda_1^- \Lambda_2^+ A_3^- \Lambda_4^+]|\text{vac}\rangle \\ &= \langle 0|\Gamma^+(1,\eta) A_1^- \Lambda_2^+ A_3^- \Lambda_4^+ - \Gamma^-(2,\eta)\Lambda_1^- A_2^+ A_3^- \Lambda_4^+ \\ &\quad + \Gamma^-(3,\eta)\Lambda_1^- \Lambda_2^+ \Lambda_3^- \Lambda_4^+ + \Gamma^-(4,\eta)\Lambda_1^- \Lambda_2^+ A_3^- A_4^+|\text{vac}\rangle. \end{aligned} \tag{2.33}$$

If we choose η and $\bar{\eta}$ to be the spinors associated with the momentum p_4, then

$$A(\Lambda_1^- \Lambda_2^+ \Lambda_3^- \Lambda_4^+) = -\frac{\langle 4\,2\rangle}{\langle 4\,3\rangle} A(\Lambda_1^- A_2^+ A_3^- \Lambda_4^+) = ig^2 \frac{\langle 2\,4\rangle \langle 1\,3\rangle^3}{\langle 1\,2\rangle\langle 2\,3\rangle\langle 3\,4\rangle\langle 4\,1\rangle}. \tag{2.34}$$

Similarly

$$A(\Lambda_1^+ \Lambda_2^- \Lambda_3^+ \Lambda_4^-) = \frac{\langle 3\,1\rangle}{\langle 4\,1\rangle} A(\Lambda_2^- A_3^+ A_4^- \Lambda_1^+) = ig^2 \frac{\langle 2\,4\rangle^3 \langle 1\,3\rangle}{\langle 1\,2\rangle\langle 2\,3\rangle\langle 3\,4\rangle\langle 4\,1\rangle}, \tag{2.35}$$

and

$$A(\Lambda_1^+ \Lambda_2^+ \Lambda_3^- \Lambda_4^-) = -\frac{\langle 1\,2\rangle}{\langle 2\,4\rangle} A(\Lambda_3^- A_4^- A_1^+ \Lambda_2^+) = -ig^2 \frac{\langle 3\,4\rangle^2}{\langle 2\,3\rangle\langle 4\,1\rangle}. \tag{2.36}$$

There is one caveat to note when mapping between QCD and the parallel SUSY theory. Certain pure quark amplitudes with the alternating $+-+-\ldots$ helicity configuration contain colour structures whereby the (anti)fundamental indices of adjacent quarks are connected by Kronecker δs, such as shown for $n = 4$ in fig. 2.4. In this particular example, we see that two separate QCD amplitudes bear colour structures that lift to the same trace on the SUSY side upon adding additional lines to the 't Hooft diagram. Indeed, the quarks' charges are flipped between the left and centre diagrams, necessary because the gluinos are in the adjoint representation. As such, we expect both QCD partial amplitudes to contribute to the SUSY partial amplitude (something which we demonstrate explicitly in section 5.A).

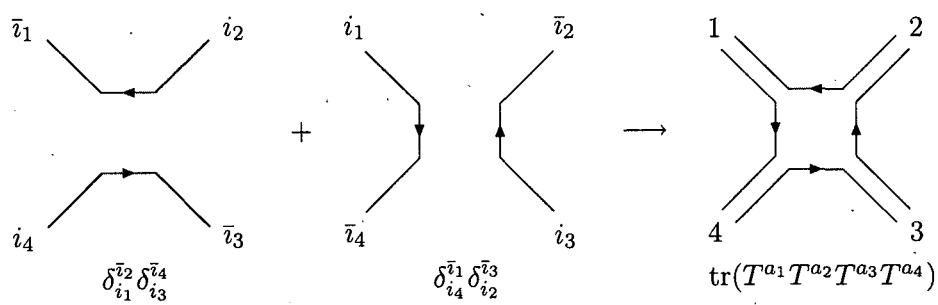

FIGURE 2.4: Certain amplitudes with two or more quark-antiquark pairs in QCD have multiple colour structures lifting to the same trace on the SUSY side.

We end this section by noting that this programme can be extended to include scalar particles by considering a $\mathcal{N} = 2$ extended supersymmetric theory with a vector supermultiplet (which has four bosonic degrees of freedom, from the two gluon states, the

scalar and anti-scalar, and four fermionic degrees of freedom). From this we obtain the result

$$A(1^-2_P^-3_P^+4^+\cdots n^+) = \left(\frac{\langle 1\,2\rangle}{[1\,2]}\right)^{2s_P} A(1^-2_\phi^-3_\phi^+4^+\cdots n^+)$$

where P is one of $\{A, \Lambda, \phi\}$ for gluon, gluino and scalar, respectively. s_P is the spin of particle species P. (For a scalar, $+$ and $-$ 'helicity' refer to particle and antiparticle, respectively). Whence,

$$A(1^\pm 2^+\cdots n^+) = 0$$

for any spin content.

It is important to point out here that *for supersymmetric theories*, the SWIs were derived without resorting to any particular perturbative expansion. Therefore they hold to all orders of perturbation theory.

2.3.2 Supersymmetric decomposition of loop amplitudes

The properties (such as those above) endowed upon SUSY theories by their extra symmetries can be exploited at the loop level to make Yang–Mills and QCD calculations easier. By counting the respective degrees of freedom, a gluon amplitude with a gluon running around the loop

$$A^{\text{gluon}} = A^{\mathcal{N}=4} - 4A^{\mathcal{N}=1,\chi} + A^{\text{scalar}}. \tag{2.37}$$

Here,

- $A^{\mathcal{N}=4}$ is the same amplitude but with a $\mathcal{N} = 4$ supermultiplet running around the loop, which contains a gluon (one bosonic d.o.f. for each helicity), four gluinos (each contributing one fermionic d.o.f. for each helicity) and six complex scalars (two bosonic d.o.f.s each);
- $A^{\mathcal{N}=1,\chi}$ has an $\mathcal{N} = 1$ supermultiplet in its loop, consisting of a Weyl fermion and a complex scalar; and
- A^{scalar} has just a complex scalar in its loop.

Similarly for a fermion in the loop,

$$A^{\text{fermion}} = A^{\mathcal{N}=1,\chi} - A^{\text{scalar}}. \tag{2.38}$$

Why is this helpful? Well firstly, we saw that the supersymmetric Ward identities tell us that a significant number of amplitudes vanish exactly. This means that gluon amplitudes with a $(\pm + \cdots +)$ helicity content receive contributions only from the scalar loop. These have an algebraically simpler form, and as a result much of the recent effort in computing multi-gluon loop amplitudes has focused on obtaining scalar loop amplitudes. For cases where the supersymmetric contributions do not vanish, the supersymmetry provides useful cancellations that simplify the calculation. In particular,

the SUSY amplitudes are 'cut-constructible' (see section 2.6.1) — a knowledge of its unitarity cuts is sufficient to reconstruct the amplitude itself. At one-loop level, these cuts can be computed from the tree graphs, which are much easier to obtain.

2.4 The CSW construction

Motivated by the observation [53] that MHV amplitudes (2.22) localise on complex lines in twistor space[5], and that lines in twistor space correspond to points in space-time, Cachazo, Svrček and Witten proposed [15] a framework for computing tree-level colour-ordered partial amplitudes for gluons by sewing together MHV amplitudes according to the following rules:

1. Use MHV amplitudes as vertices.
2. Join the vertices together, helicities + to −, using a scalar propagator i/P^2, where P is the momentum flowing between the vertices.
3. For each leg of a vertex that joins to a propagator carrying momentum P, define its corresponding holomorphic spinor as $(\lambda_P)_{\dot\alpha} = P_{\alpha\dot\alpha}\tilde\eta^{\dot\alpha}$, where $\tilde\eta$ is some arbitrary spinor.

On the last point, we note that if we supplement $\tilde\eta$ with a holomorphic spinor η and use it define a null vector $\mu = \eta\tilde\eta$, then we can construct the null projection of an arbitrary four vector p by

$$p_{\text{null}} = p - \frac{p^2}{2\mu\cdot p}\mu. \tag{2.39}$$

Then if $(p_{\text{null}})_{\alpha\dot\alpha} = \lambda_\alpha\tilde\lambda_{\dot\alpha}$, $\lambda_\alpha = p_{\alpha\dot\alpha}\tilde\eta^{\dot\alpha}/[\lambda\,\eta]$. This is coincident with point 3 above: a propagator links a + line on one vertex to a − line on another, so under a scaling $\lambda \to c\lambda$ the diagram will scale like $c^{-2}\cdot(c^4\cdot c^{-2}) = 1$. Hence we can discard the $[\lambda\,\eta]$ denominator.

Adding all the so-called CSW diagrams constructed this way returns the desired scattering amplitude. Given the unbounded positive-helicity valence of the vertices, an amplitude with n_- negative helicity gluons has $n_- - 1$ vertices; for n gluons overall, the number of diagrams grows no faster than n^2, so this method clearly presents a significant computational advantage over Feynman diagrams.

2.4.1 An example: $A(1^+2^-3^-4^-)$

In [15], the authors give examples of calculations for the tree-level amplitudes $A(1^+2^-3^-4^-)$ as well as for the five-gluon amplitudes. They also note verification of the technique for certain configurations of higher-valence tree amplitudes, and even apply it to obtain the n-gluon amplitude with three consecutive gluons of negative helicity. We refer the interested reader to the literature for these examples; here, we will repeat the calculation

[5] Specifically, copies of $\mathbb{CP}^1$ embedded in $\mathbb{CP}^3$.

of vanishing amplitude $A(1^+2^-3^-4^-)$, since this not only illustrates the construction in action, but also forms a consistency check.

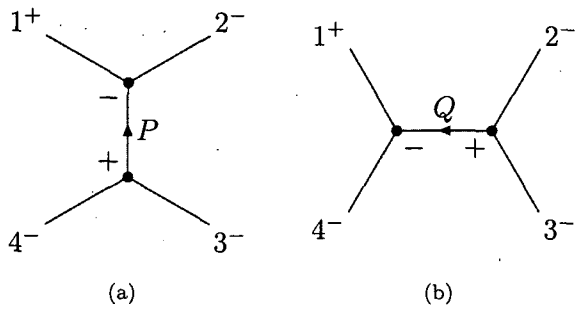

FIGURE 2.5: CSW diagrams contributing to the $A(1^+2^-3^-4^-)$ amplitude.

The contributing CSW rules diagrams are shown in fig. 2.5. Since the final result vanishes anyway, we will drop any phase and coupling factors from propagators and the formula (2.22) for the MHV amplitudes. The first diagram, fig. 2.5(a), has a contribution

$$\frac{\langle 2\,\lambda_P\rangle^3}{\langle 1\,3\rangle\langle\lambda_P\,1\rangle}\frac{1}{P^2}\frac{\langle 3\,4\rangle^3}{\langle 4\,\lambda_{-P}\rangle\langle\lambda_{-P}\,3\rangle} \tag{2.40}$$

where $P = p_1 + p_2$. We pick a reference spinor $\tilde{\eta}$ (whose specific value will not be needed). Then according to the CSW prescription,

$$(\lambda_P)_\alpha = [(\lambda_1)_\alpha(\tilde{\lambda}_1)_{\dot{\alpha}} + (\lambda_2)_\alpha(\tilde{\lambda}_2)_{\dot{\alpha}}]\tilde{\eta}^{\dot{\alpha}},$$
$$(\lambda_{-P})_\alpha = [(\lambda_3)_\alpha(\tilde{\lambda}_3)_{\dot{\alpha}} + (\lambda_4)_\alpha(\tilde{\lambda}_4)_{\dot{\alpha}}]\tilde{\eta}^{\dot{\alpha}},$$

so that $\langle 2\lambda_P\rangle = \langle 21\rangle\alpha_1$, $\langle\lambda_P 1\rangle = \langle 21\rangle\alpha_2$, $\langle 4\lambda_{-P}\rangle = \langle 43\rangle\alpha_3$ and $\langle\lambda_{-P}3\rangle = \langle 43\rangle\alpha_4$, where $\alpha_i := [i\,\eta]$. Substituting, and using (2.9) to deal with the propagator, (2.40) becomes

$$\frac{\langle 3\,4\rangle}{[1\,2]}\frac{\alpha_1^3}{\alpha_2\alpha_3\alpha_4}. \tag{2.41}$$

Repeating the exercise for the graph of fig. 2.5(b) gives, similarly,

$$\frac{\langle 3\,2\rangle}{[1\,4]}\frac{\alpha_1^3}{\alpha_2\alpha_3\alpha_4}.$$

Adding this to (2.41) results in an expression with a numerator proportional to

$$\langle 3\,4\rangle[4\,1] + \langle 3\,2\rangle[2\,1] = \sum_{i=1}^{4}\langle 3\,i\rangle[i\,1] = 0$$

by conservation of momentum. Thus, the amplitude vanishes.

2.4.2 Proving the CSW rules

In the latter part of ref. [18], the authors gave a neat proof of the validity of the CSW construction by considering Lorentz invariance and the singularity structure of tree-level scattering amplitudes. It proceeds as follows.

It turns out that upon analytic continuation to complex momenta, a tree amplitude can be determined entirely by its physical singularities — something which gives rise to recursion relations between on-shell amplitudes (see section 2.5). Now suppose we calculate a particular amplitude in two ways: by colour-ordered Feynman graphs, to give A_{Feyn}, and A_{CSW} by the CSW construction. Both are clearly rational functions of the external momenta's spinors. In ref. [15], the authors argue that A_{CSW} contains the same physical singularities as A_{Feyn} (individual graphs in A_{CSW} might contain outstanding singularities of the form $1/\lambda^\alpha P_{\alpha\dot{\alpha}}\tilde{\eta}^{\dot{\alpha}}$, but in their sum these must vanish by Lorentz invariance) so $A_{\text{CSW}} - A_{\text{Feyn}}$ must be a polynomial. For n gluons, we can check directly that this polynomial vanishes when $n = 3, 4$, and for $n > 4$, such a polynomial cannot exist on dimensional grounds. Therefore $A_{\text{CSW}} = A_{\text{Feyn}}$.

2.4.3 CSW rules for fermions

One extension of the CSW rules that will have relevance to the work in chapter 5 is that of ref. [28] which adds massless quarks in the fundamental representation. This extension works as one might expect: the propagator and off-shell prescription are as in the purely gluonic case above, but one adds two new classes of vertices (using the expressions for the corresponding amplitudes found in ref. [54]) to the fold.

The first has either the quark or antiquark carrying a negative helicity (by conservation of helicity) and one gluon of negative helicity. Thus these vertices are

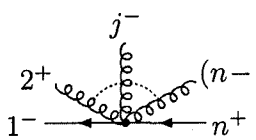

$$= A(1_{\text{q}}^-, 2^+, \ldots, j^-, \ldots, (n-1)^+, n_{\bar{\text{q}}}^+) \tag{2.42}$$

$$= ig^{n-2}\frac{\langle 1\, j\rangle^3\langle j\, n\rangle}{\langle 1\, 2\rangle\langle 2\, 3\rangle\cdots\langle n-1, n\rangle\langle n\, 1\rangle},$$

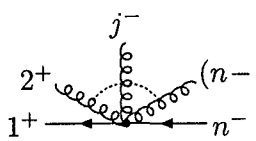

$$= A(1_{\text{q}}^+, 2^+, \ldots, j^-, \ldots, (n-1)^+, n_{\bar{\text{q}}}^-) \tag{2.43}$$

$$= ig^{n-2}\frac{\langle 1\, j\rangle\langle n\, j\rangle^3}{\langle 1\, 2\rangle\langle 2\, 3\rangle\cdots\langle n-1, n\rangle\langle n\, 1\rangle},$$

associated with the colour structure of (2.16).[6] The second has two quark-antiquark pairs. For this to be an MHV vertex, all the gluons have positive helicity, and it is

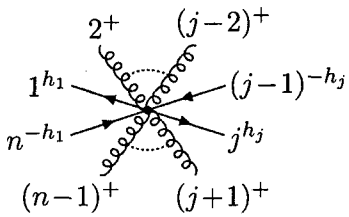

$$= A(1_{\rm q}^{h_1}, 2^+, \ldots, (j-2)^+, (j-1)_{\bar{\rm q}}^{-h_j}; \\ j_{\rm q}^{h_j}, (j+1)^+, \ldots, (n-1)^+, n_{\bar{\rm q}}^{-h_1})$$

$$= ig^{n-2} \frac{F(h_1, h_j)}{\langle 1\, n\rangle\langle j, j-1\rangle} \frac{\langle 1, j-1\rangle}{\langle 1\, 2\rangle \cdots \langle j-2, j-1\rangle} \frac{\langle j\, n\rangle}{\langle j, j+1\rangle \cdots \langle n-1, n\rangle} \tag{2.44}$$

with

$$F(+,+) = \langle n, j-1\rangle^2 \qquad F(+,-) = -\langle n\, j\rangle^2,$$
$$F(-,+) = -\langle 1, j-1\rangle^2, \qquad F(-,-) = \langle 1\, j\rangle^2,$$

and associated with the colour structure of (2.18). The sub-leading amplitude associated with (2.19) is

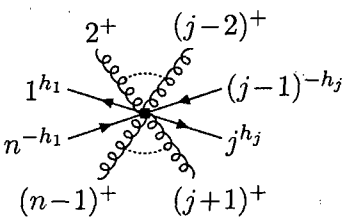

$$= A_{(1)}(1_{\rm q}^{h_1}, 2^+, \ldots, (j-2)^+, n_{\bar{\rm q}}^{-h_1}; \\ j_{\rm q}^{h_j}, (j+1)^+, \ldots, (n-1)^+, (j-1)_{\bar{\rm q}}^{-h_j})$$

$$= ig^{n-2} \frac{F(h_1, h_j)}{\langle 1\, n\rangle\langle j, j-1\rangle} \frac{\langle 1\, n\rangle}{\langle 1\, 2\rangle \cdots \langle j-3, j-2\rangle\langle j-2, n\rangle} \frac{\langle j, j-1\rangle}{\langle j, j+1\rangle \cdots \langle n-2, n-1\rangle\langle n-1, j-1\rangle}. \tag{2.45}$$

There are no MHV vertices with more quark-antiquark lines. We notice that in both cases the gluons lie to the *right* of the quark lines as one travels along them in the direction of the arrows. This can be seen from the 't Hooft diagram construction, where in planar graphs the external fermion lines can always be arranged to run on the outside.

2.5 BCF recursion relations

Britto, Cachazo and Feng discovered a recursion relation that shows one how to construct tree-level amplitudes in terms of lower-valence, on-shell amplitudes and a scalar propagator. This works by shifting the external momenta by an amount parametrised by a complex number z; the amplitude sought is therefore a rational function of z, and

[6] We note that our expressions have a sign difference with those of [28] due to a different choice of external state fermion ordering.

we can use knowledge of its pole structure to reconstruct it. Ultimately, every amplitude reduces to sums of products of MHV and $\overline{\text{MHV}}$ amplitudes.

Concretely, suppose we are to compute the amplitude $A(1\cdots n)$ for some helicity configuration. We pick external lines k and l which without loss of generality we may assume to have helicities $-,+$, $-,-$ or $+,+$, respectively[7]. We then shift these null momenta $p_k = \lambda_k\tilde{\lambda}_k \to \hat{p}_k(z)$ and $p_l = \lambda_l\tilde{\lambda}_l \to \hat{p}_l(z)$ by shifting their spinors according to

$$\tilde{\lambda}_k \to \tilde{\lambda}_k - z\tilde{\lambda}_l, \quad \lambda_l \to \lambda_l + z\lambda_k, \tag{2.46}$$

which defines the amplitude $A(z) \equiv A(1,\ldots,\hat{k}(z),\ldots,\hat{l}(z),\ldots,n)$. Now let us choose a partition[8] of the external lines, $i,\ldots,j$ such that this range includes l. Since we are dealing with tree diagrams, there is (for general momenta) a unique propagator carrying momentum $P_{ij} := p_i + \cdots + p_j$, and all propagators can be found this way by choosing an appropriate range. P_{ij} becomes shifted to

$$\hat{P}_{ij}(z) = P_{ij} + z\lambda_k\tilde{\lambda}_l. \tag{2.47}$$

Now $A(z)$ will have poles whenever the $\hat{P}_{ij}(z)^2 = 0$, *i.e.* when the shifted propagators go on shell. As

$$\begin{aligned}\hat{P}_{ij}(z)^2 &= \tfrac{1}{2}\hat{P}_{ij}(z)_{\alpha\dot{\alpha}}\hat{P}_{ij}(z)^{\alpha\dot{\alpha}}\\ &= \tfrac{1}{2}\{(P_{ij})_{\alpha\dot{\alpha}}(P_{ij})^{\alpha\dot{\alpha}} + 2z(P_{ij})_{\alpha\dot{\alpha}}\lambda_k^\alpha\tilde{\lambda}_l^{\dot{\alpha}}\}\\ &= P_{ij}^2 - z\langle k|P_{ij}|l],\end{aligned}$$

these poles are located at

$$z = z_{ij} := \frac{P^2}{\langle k|P_{ij}|l]}, \tag{2.48}$$

using the notation

$$\langle k|P_{ij}|l] \equiv -\lambda_k^\alpha P_{\alpha\dot{\alpha}}\tilde{\lambda}_l^{\dot{\alpha}}. \tag{2.49}$$

Since $A(z)$ is a rational function, these are its only poles[9].

Let us now assume that $A(z) \to 0$ as $|z| \to \infty$, so that

$$0 = \frac{1}{2\pi i}\oint_C \frac{A(z)}{z} = A(0) + \sum_{z\in\{z_{ij}\}} \frac{1}{z_{ij}} \operatorname*{Res}_{z=z_{ij}} A(z), \tag{2.50}$$

where C is a contour at infinity. Since the residues in the sum above are taken at points where we know propagators to go on shell, each term in the sum must be product of the amplitudes to either side of that propagator multiplied by the residue of the shifted

[7]The $+,-$ case can be dealt with by re-labelling the external momenta using the cyclic symmetry of partial amplitudes.

[8]We defined 'partition' here and hereafter to mean a choice of contiguous, non-intersecting, sequential subsets.

[9]There may be poles in z arising from the action of the shifts (2.46) on the denominators of the polarisation vectors (2.10), but these may always be removed by an appropriate choice of reference spinor and as such are gauge artifacts that do not contribute to the final amplitude.

propagator, so

$$\begin{aligned}\frac{1}{z_{ij}}\operatorname*{Res}_{z=z_{ij}} A(z) &= \frac{\langle k|P_{ij}|n]}{P_{ij}^2}\sum_{\pm} A_{\mathrm{L}}^{\pm}(z_{ij})\operatorname*{Res}_{z=z_{ij}}\frac{1}{P_{ij}^2 - z\langle k|P_{ij}|n]}A_{\mathrm{R}}^{\mp}(z_{ij}) \\ &= -\sum_{\pm} A_{\mathrm{L}}^{\pm}(z_{ij})\frac{1}{P_{ij}^2}A_{\mathrm{R}}^{\mp}(z_{ij}),\end{aligned}$$

where the sub-amplitudes

$$A_{\mathrm{L}}^{\pm}(z_{ij}) = A(\hat{P}_{ij}^{\pm}(z_{ij}), j+1, \ldots, k(z_{ij}), \ldots, i-1), \tag{2.51}$$

$$A_{\mathrm{R}}^{\mp}(z_{ij}) = A(-\hat{P}_{ij}^{\mp}(z_{ij}), i, \ldots, l(z_{ij}), \ldots, j), \tag{2.52}$$

and all index arithmetic should be carried out cyclically. Thus we obtain the recursion relation

$$\begin{aligned}A(1\cdots n) = \sum_{(i,j)\in\mathcal{P}}\sum_{\pm} & A(\hat{P}_{ij}^{\pm}(z_{ij}), j+1, \ldots, k(z_{ij}), \ldots, i-1) \\ & \times \frac{1}{P_{ij}^2}A(-\hat{P}_{ij}^{\pm}(z_{ij}), i, \ldots, l(z_{ij}), \ldots, j),\end{aligned} \tag{2.53}$$

where $\mathcal{P}$ is the set of all partitions into two of ranges of external lines that include line l. This may be described schematically by the diagram of fig. 2.6.

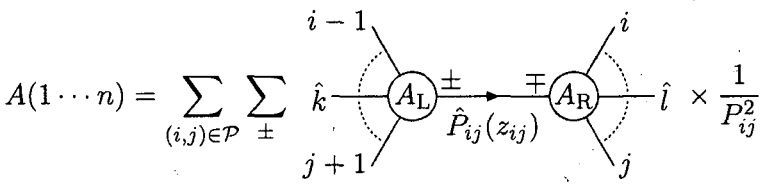

FIGURE 2.6: Mnemonic diagram illustrating the terms of the BCF construction. Index arithmetic should be carried out cyclically. All external momenta are out-going.

What remains is to prove that for Yang–Mills theory $A(z)$ vanishes as $|z| \to 0$. In ref. [18], the authors use the CSW construction (discussed in section 2.4) to prove this, and we reproduce this reasoning here. First, we recall the possible choices of helicity for the gluons k and l as outline above. We can restrict the analysis to the case where gluon l has $+$ helicity; the case where gluon k is of $-$ helicity can be treated by the same reasoning but using the conjugate CSW construction with $\overline{\mathrm{MHV}}$ vertices.

Now a general CSW tree graph consists of a number of MHV vertices continued off shell by the CSW prescription, multiplied by a number of propagators. Under the momentum shifts, a subset of these propagators may be shifted such that they vanish as $|z| \to \infty$. Now in the CSW prescription, one defines the holomorphic spinor of a propagator's momentum by $(\lambda_P)_\alpha = (\hat{P}_{ij})_{\alpha\dot{\alpha}}\tilde{\eta}^{\dot{\alpha}}$, where $\tilde{\eta}$ is some arbitrary spinor. But we know that $\hat{P}_{ij} = P_{ij} + z\lambda_k\tilde{\lambda}_l$, so if we pick $\tilde{\eta} = \tilde{\lambda}_l$, λ_P will be independent of z. Thus, all MHV vertices that connect to it will be z independent, *except* for the vertex

connected to gluon l. By postulation, l has + helicity, so its shifted spinor $\lambda_l + z\lambda_k$ shows up in the vertex's denominator. Hence, the contribution for the vertices vanishes as $|z| \to \infty$, and the rest of the amplitude along with it.

2.5.1 An example: the Parke–Taylor MHV amplitude

The BCF recursion relations provide a very neat, quick proof of the expression (2.22)

$$A(1^-2^+\cdots m^-\cdots n^+) = ig^{n-2}\frac{\langle 1\, m\rangle^4}{\langle 1\, 2\rangle\cdots\langle n-1, n\rangle\langle n\, 1\rangle}$$

for the MHV amplitude. We choose to shift momenta 1 and 2 according to

$$\tilde{\lambda}_1 \to \tilde{\lambda}_1 - z\tilde{\lambda}_2, \quad \lambda_2 \to \lambda_2 + z\lambda_1$$

For the purposes of this example, we will take $m > 3$; the cases of $m \leq 3$ may be treated similarly. In this case, there is only one choice of partition and intermediate helicity for the propagator, specifically $i = 2$ and $j = 3$, for which neither of the amplitudes in (2.53) vanish. This is illustrated in fig. 2.7. The momentum flowing across this split is $P_{23} = p_2 + p_3$, so under the shift $\hat{P}_{23}(z)^2$ vanishes when $z = P_{23}^2/\langle 1|P|2]$. Let us denote by $\hat{P}$ the value $\hat{P}_{23}(z)$ takes for this choice of z.

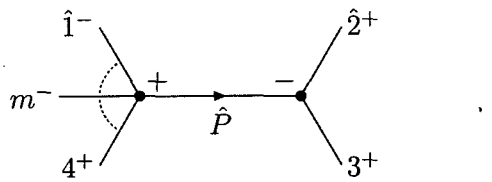

FIGURE 2.7: The only term contributing to the BCF recursion computation of the $A(1^-2^+\cdots m^-\cdots n^+)$ MHV amplitude. The vertex on the left is an MHV amplitude, obtained by a lower-valence Parke–Taylor expression. The vertex on the right is a three-gluon $\overline{\text{MHV}}$ amplitude. Missing lines are for +-helicity gluons. All external momenta are out-going.

Assume that the Parke–Taylor expression is valid for MHV amplitudes with up to $n-1$ gluons. If we drop the coupling constant factors, the BCF recursion relations give

$$\frac{\langle \hat{1}\, m\rangle^4}{\langle 4\, 5\rangle\cdots\langle n\, \hat{1}\rangle\langle \hat{1}\, \hat{P}\rangle\langle \hat{P}\, 4\rangle}\frac{1}{P_{23}^2}\frac{[\hat{2}\, 3]^3}{[3\, \hat{P}][\hat{P}\, 2]}, \tag{2.54}$$

where we remind the reader that the hats above the numbers denote a shifted momentum. First, $P_{23}^2 = 2p_2\cdot p_3 = \langle 23\rangle[23]$. Next, we remove the shifted pieces of the momenta. Since we have only shifted the antiholomorphic part of p_1, we can drop the hat from any 1 that occurs in a $\langle\,\rangle$, and likewise for any 2 in a pair of $[\,]$ brackets. Next, we note that

since $\hat{P}_{ij}(z) = P_{ij} + z\lambda_k\tilde{\lambda}_l$, for general spinors x and y

$$\langle x\, \hat{P}_{ij}(z)\rangle[\hat{P}_{ij}(z)\, l] = -\langle x|\hat{P}_{ij}(z)|l] = -\langle x|P_{ij}|l], \tag{2.55}$$

$$\langle k\, \hat{P}_{ij}(z)\rangle[\hat{P}_{ij}(z)\, y] = -\langle k|\hat{P}_{ij}(z)|y] = -\langle k|P_{ij}|y], \tag{2.56}$$

$$\tag{2.57}$$

whence

$$\langle \hat{1}\, \hat{P}\rangle = -\frac{\langle 1|2+3|2]}{[\hat{P}\, 2]} = \frac{\langle 1\, 3\rangle[3\, 2]}{[\hat{P}\, 2]},$$

and similarly

$$\langle \hat{P}\, 4\rangle = -\frac{\langle 4\, 3\rangle[3\, 2]}{[\hat{P}\, 2]}, \quad [3\, \hat{P}] = \frac{\langle 1\, 2\rangle[3\, 2]}{\langle 1\, \hat{P}\rangle}, \quad \text{and} \quad [\hat{P}\, 2] = \frac{\langle 1\, 3\rangle[3\, 2]}{\langle 1\, \hat{P}\rangle}.$$

Inserting into (2.54), we find we readily obtain the Parke–Taylor expression for the MHV amplitude.

2.5.2 A direct proof of the CSW rules

By a modification of the BCF recursion relations (studied in section 2.5), Risager obtained a direct proof of the CSW rules of section 2.4, and we refer the interested reader to ref. [16] wherein is documented the exact reasoning. The essence of Risager's proof is to construct a shift of the momenta such that each propagator that occurs in a CSW rules graph is shifted. This will occur if the antiholomorphic spinor of the momentum of *every* negative helicity gluon is shifted and the shift is crafted such that no proper subset of them vanishes. With this shift, any possible $\overline{\text{MHV}}$ sub-amplitude vanishes, and so one reasons inductively that the CSW construction must give the correct amplitude if the lower-valence sub-amplitudes to either side of partition do as well.

2.5.3 Application to other field theories

Although the BCF recursion relations were introduced in the context of Yang–Mills theory and multi-gluon scattering, their derivation only makes use of the fact that shifted amplitudes are vanishing in the complex infinity limit, and that at tree-level they contain only simple, physical poles. From a knowledge of these poles, the BCF recursion relations provide a mechanism to determine tree-level amplitudes.

There is much literature on the application of BCF recursion relations to amplitudes of other particle content. CSW rules and BCF recursion relations for QED were derived in [19]. Ref. [20] adds massless fermions to the QCD relations, with massive fermions in [21]. Recursion relations for amplitudes involving massive propagating scalars can be found in [22] (which is of particular use in the cut construction of loop amplitudes, *cf.* (2.37) and section 2.6), and with massive vector bosons and fermions in ref. [23]. BCF relations for gravity were found in [24, 25] with the proof that the amplitudes vanish as $|z| \to \infty$ appearing in ref. [26].

2.6 Loop level techniques

In this section we discuss two techniques that are important for the calculation of one-loop amplitudes. The first is (generalised) unitarity and cut construction, and the second is the application of the CSW rules in one-loop diagrams. Of course, these are not the only techniques on the market for loop amplitudes. Two others worth mentioning are the twistor-space studies of Cachazo *et al.* [29–32]; and so-called 'bootstrapping' approaches [40–42, 62], which combine unitarity with on-shell recursion relations to obtain the rational parts of non-cut-constructible amplitudes. We refer the interested reader to the literature for further details on these approaches.

2.6.1 Unitarity, generalised unitarity, and cut construction

The so-called 'cut construction' of loop amplitudes stems from the observation that, on general grounds, a gauge theory loop amplitude can be written as a rational function of kinematical invariants, plus some linear combination with rational coefficients over a basis of loop integrals that contain branch cuts in their kinematic invariants. By studying an amplitude's cuts, one can (in certain circumstances) deduce the loop integrals' coefficients; the advantage of this is that, at one loop, these discontinuities can be computed from a knowledge of on-shell tree-level amplitudes.

Although *in general* the rational pieces cannot be determined this way, in a number of theories *all* the rational terms are associated to functions that do contain cuts. Such theories are termed *cut-constructible*, and in [34] Bern, Dixon, Dunbar and Kosower found a power-counting criterion that is satisfied by these theories. For an amplitude in a massless theory, this criterion is that its n-point loop integrals have in their numerators not more than one power of the loop momentum for $n = 2$, and not more than $n - 2$ powers of the loop momentum for $n > 2$, *i.e.* given the n-point loop integral with momentum p_i flowing out of the i^{th} point

$$I_n[P] := \int \frac{d^{4-2\epsilon}L}{(2\pi)^{4-2\epsilon}} \frac{P(L)}{L^2(L-p_1)^2(L-p_1-p_2)^2\cdots(L+p_n)^2} \tag{2.58}$$

where P is a polynomial, then

$$\deg P(L) \leq \begin{cases} 1 & (n=2) \\ n-2 & (n>2) \end{cases}. \tag{2.59}$$

A key result of [34] was showing that supersymmetric Yang–Mills amplitudes satisfy this criterion.

If the external momenta are all four dimensional, integrals satisfying this criterion can be processed using a variety of reduction techniques [63–72] through which it can be shown [34] that they can be reduced to linear combinations of scalar box, triangle and bubble functions (*i.e.* those of the form $I_4[1]$ $I_3[1]$ and $I_2[1]$ in (2.58)). These are all one-loop integrals for diagrams with a massless scalar running between each of the external

points; the external momenta are partitioned amongst these points, the momentum flowing from each point being the sum of those in its partition. For $n \geq 4$ gluons, this set is listed with diagrams in section 2.A and summarised here as:

- the box functions $I^{\text{4m}}_{4:jkl;i}$, $I^{\text{3m}}_{4:jk,i}$, $I^{\text{2me}}_{4:j;i}$, $I^{\text{2mh}}_{4:j;i}$, $I^{\text{1m}}_{4:i}$ and $I^{\text{0m}}_{4:i}$;
- the triangle functions $I^{\text{3m}}_{3:jk;i}$, $I^{\text{2m}}_{3:j;i}$, $I^{\text{1m}}_{3:i}$; and
- the bubble function $I^{\text{2m}}_{2:i}$.

The subscripts denote how the external momenta are partitioned, starting at i and put into partitions of length j, k and l. The external momenta are taken to be on-shell, but when there is more than one in a particular partition, their sum will in general not be null. A m-mass function (noted in the superscripts of the functions above) has m such points. For box functions when $m = 2$, there are two possible (cyclically) distinct configurations: when the two null legs are opposing, the so-called 'two-mass easy' function $I^{\text{2me}}_{4:j;i}$ (shown in fig. 2.12(c)); and the 'two-mass hard' function $I^{\text{2mh}}_{4:j;i}$ when they are adjacent (as in fig. 2.12(d)).

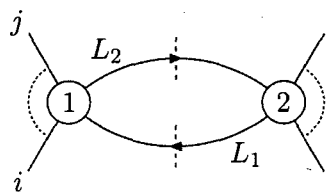

FIGURE 2.8: Schematic diagram of the two-particle cut in the plane of the $(p_i + \cdots + p_j)^2$ invariant. The blobs represent the tree amplitudes A_1^{tree} and A_2^{tree} in the text.

The procedure used by BDDK to extract the rational coefficients may be summarised as follows:

1. For the amplitude being constructed, consider a particular kinematical channel (characterised by a partition into two of the external momenta), and draw all planar cut diagrams that contribute in this channel. (Remember from section 2.2.2 that we only need the leading one-loop partial amplitude.) These are constructed by connecting tree amplitudes either side of the cut, A_1^{tree} and A_2^{tree}, together with propagators as shown in fig. 2.8. The propagators connect to adjacent lines in the amplitudes, whose remaining lines connect to external states according to colour order and helicity configuration. The discontinuity in the branch cut of this channel's kinematic invariant is obtained by integrating over the two-particle *phase space* of the internal particles instead of over the propagators *viz.* the Cutkosky rules [73–75]:

$$\sum_{\text{spin}} \int d^4L \, \delta^{+4}(L_1^2) \delta^{+4}(L_2^2) A_1^{\text{tree}} A_2^{\text{tree}},$$

where $L_1 \equiv L$ and $L_2 = L_1 - p_i - \cdots - p_j$, and $\delta^{+4}(p^2) \equiv \theta(p^t)\delta^4(p^2)$. The sum here is over the admissible spin configurations of the internal particles, as determined by the helicity configuration of the particles on either side of the cut.

2. Reconstruct the Feynman integral. To do this, promote the $\delta^{+4}(p^2)$ functions to propagators i/p^2.

$$\sum_{\text{spin}} \int d^4L \, \frac{i}{L_1^2} \frac{i}{L_2^2} A_1^{\text{tree}} A_2^{\text{tree}}.$$

The resulting Feynman integral has the same cut in the channel under consideration as the amplitude. One may use $L_1^2 = L_2^2 = 0$ in the numerator above. Now the Passarino–Veltman procedure is applied to the reconstructed integral to express it in terms of the basis of scalar integrals with rational coefficients.

3. By considering the reconstructed integrals of the cuts in all kinematic channels without over-counting each scalar integral's contribution, one deduces the rational coefficients and obtains the full amplitude.

Note that by reconstructing the integral algebraically in step 2, one avoids having to explicitly calculate the channel's discontinuity.

QCD is a theory that does not satisfy the BDDK criterion (2.59) and so cannot be reconstructed from knowledge of the four-dimensional cuts alone. However, we have the supersymmetric decompositions (2.37) and (2.38), so many terms in QCD amplitudes *are* cut-constructible. This leaves the scalar loops as the source of the BDDK violation. (Indeed, in situations where (2.59) is not satisfied, the reduction procedure can result in additional tensor functions (*i.e.* those of the form $I_n[L^\mu L^\nu \cdots]$ in (2.58)). In this case, as [34] notes, one can construct linear combinations of these and the scalar functions with rational coefficients that are rational functions in four dimensions.) Nevertheless, the cut-containing terms in the scalar loop amplitudes can be obtained through unitarity. The rational pieces left over must be obtained by other means, such as on-shell recursion relations [40–42, 62] which use the cut-constructible pieces as inputs, or more direct methods that extract the rational terms from the original Feynman integrals [37–39].

Quadruple cuts

$\mathcal{N} = 4$ amplitudes have a particularly special decomposition: they can be constructed purely from scalar box integrals [34] *i.e.*

$$A_{n;1}^{\mathcal{N}=4} = \sum_i b_i I_{4:i}^{\text{1m}} + \sum_{ij} (c_{ij} I_{4:j;i}^{\text{2me}} + d_{ij} I_{4:j;i}^{\text{2mh}}) + \sum_{ijk} g_{ijk} I_{4:jk;i}^{\text{3m}} + \sum_{ijkl} f_{ijkl} I_{4:jkl;i}^{\text{4m}}. \quad (2.60)$$

b, c, d, g and f are rational coefficients and in [36], Britto, Cachazo and Feng use *generalised unitarity* to deduce the rational coefficients of these functions. In this approach, one cuts two *or more* lines by replacing their propagators $i/p^2 \to \delta^{+4}(p^2)$. By choosing

different sets of lines to cut, we can isolate the discontinuities of different cuts in the kinematic variables.[10]

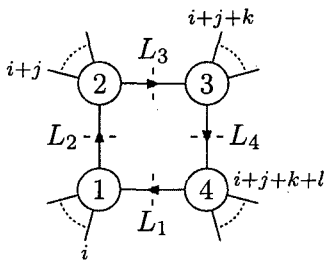

FIGURE 2.9: Quadruple cut of an amplitude that contributes the coefficient of the box function $I^{4m}_{4;jkl;i}$ (see fig. 2.12(a)). The circular blobs represent the tree-level amplitudes $A^{tree}_{1,2,3,4}$ in the text.

Britto, Cachazo and Feng compute the quadruple cuts of the LHS of (2.60), and there are a number of such cuts parametrised by the partitioning of the gluon labels into four. An example is shown in fig. 2.9: this particular cut is given by an expression proportional to

$$\sum_{\text{spin}} \int d^4L\, \delta^{+4}(L_1)\delta^{+4}(L_2)\delta^{+4}(L_3)\delta^{+4}(L_4)\, A_1^{\text{tree}} A_2^{\text{tree}} A_3^{\text{tree}} A_4^{\text{tree}} \tag{2.61}$$

where $L_1 \equiv L$, $L_2 = L_i - p_i - \cdots - p_{j-1}$, *etc.* and the sum is over the permissible spin configurations of the internal particles. (Since all internal lines are put on shell by the cut, one must take care to deal with the vanishing of the three-particle tree amplitudes for partitions containing just one external gluon. In [36] this is handled by working in $(2,2)$ signature; alternatively, one can use complex momenta.) In four dimensions a quadruple cut freezes the momentum integral so that L has discrete set of solutions $\mathcal{S}$ to leave us with an expression proportional to

$$\sum_{\text{spin},\mathcal{S}} A_1^{\text{tree}} A_2^{\text{tree}} A_3^{\text{tree}} A_4^{\text{tree}}.$$

On the other hand, the quadruple cut of a box function is unique to that box function; that is, there is only one box function on the RHS of (2.60) with the cut computed in (2.61) — namely, the one with the corresponding external momentum configuration. As such, its coefficient must be proportional to the product of tree amplitudes computed as given above.

(Generalised) unitarity in $4-2\epsilon$ dimensions

While only the supersymmetric Yang–Mills theories are cut-constructible in four dimensions, by analytically continuing to $4-2\epsilon$ dimensions BDDK-violating theories also

[10] Generalised unitarity is a rich topic, and we refer the reader to chapter 2 of [33] for a thorough treatment.

become so [76]. This can be understood on dimensional grounds: terms in the amplitudes must contain factors of the form $(-K^2)^{-\epsilon}$ for some kinematic invariant K^2 and so have have cuts in the complex plane that allow us to deduce the presence of terms that are rational in the four-dimensional limit. This was used in [77] to obtain the $(++++)$ amplitude with a scalar in the loop by considering unitarity cuts, and later in [35] with generalised unitarity (using triple and quadruple cuts) to re-derive the one-loop $(++++)$, $(-+++)$, four-gluon MHV and $(+++++)$ amplitudes in QCD. These amplitudes vanish for supersymmetric theories, and so are equal to those with just a complex scalar in the loop — thereby avoiding the complications of $4-2\epsilon$-dimensional polarisations in the internal states. In particular, we reproduce here the result [77]

$$A_{4;1}(1^+2^+3^+4^+) = A_{4;1}^{\text{scalar}}(1^+2^+3^+4^+) = \frac{2ig^4}{(4\pi)^{2-\epsilon}} K_4 \frac{[1\,2][3\,4]}{\langle 1\,2\rangle\langle 3\,4\rangle} \tag{2.62}$$

where K_4 is the $4-2\epsilon$-dimensional box function,

$$K_4 = -\frac{i}{(4\pi)^{\epsilon-2}} \int \frac{d^{4-2\epsilon}L}{(2\pi)^{4-2\epsilon}} \frac{\nu^4}{L^2(L-p_1)^2(L-p_1-p_2)^2(L+p_4)^2}. \tag{2.63}$$

As $\epsilon \to 0$, $K_4 \to -1/6$, leaving a rational expression.

The scalar's D-dimensional loop momentum L_D is split into two parts, L in four dimensions and ν in a -2ϵ-dimensional orthogonal spacelike subspace, and so the loop integration can be expressed as two over these subspaces:

$$\int \frac{d^D L_D}{(2\pi)^D} = \int \frac{d^4 L}{(2\pi)^4} \frac{d^{-2\epsilon}\nu}{(2\pi)^{-2\epsilon}}. \tag{2.64}$$

Since L_D is the only $4-2\epsilon$-dimensional quantity present (all external momenta are kept four-dimensional), the -2ϵ-dimensional parts only show up as ν^2 the integrand[11] so the integration over ν above can be traded for one over ν^2 when it comes to actually evaluating or analysing the integral. Since $L_D^2 = L^2 - \nu^2$, the *massless* scalar in D dimensions may be treated in the four dimensional tree amplitudes used to obtain unitarity cuts as a *massive* scalar of mass ν.

2.6.2 MHV amplitudes and loops

Following the success of the CSW rules at computing tree-level gluon scattering, one might consider applying them at one loop (and beyond). Brandhuber, Spence and Travaglini (BST) developed a method for applying the CSW rules at one loop, initially in the context of $\mathcal{N}=4$ scattering amplitudes in [43]. In that paper, their procedure was used to obtain an expression for $A_{n;1}^{\text{MHV}}$ (the leading one-loop partial amplitude), in exact agreement with the result obtained by cut construction in ref. [58]. To compute partial amplitudes using the BST construction:

[11] We take ν^2 to be the scalar product with respect to a $(+\cdots+)$-signature metric on the subspace.

1. Draw all planar graphs with a scalar loop and the external lines matching the specified configuration. Use the MHV amplitudes as vertices, and connect legs of opposing helicities with scalar propagators.

2. Continue the internal lines off-shell as per the CSW prescription using a null reference momentum $\mu = \eta\tilde{\eta}$.

3. Integrate over the loop momentum using a measure that splits the loop integral into one over phase space and a dispersive integral.

The momenta L_i carried on each internal line in the loop can be written using (2.39) as

$$L_i = l_i + z_i\mu,$$

where $z_i = L^2/2l_i \cdot \mu$, and l_i is the null momentum whose spinors feature in the MHV vertices. The integral over d^4L_i is traded for one over phase-space and z_i by using [43,78]

$$\frac{d^4L_i}{L_i^2 + i\epsilon} = \frac{dz_i}{z_i + i\epsilon}\frac{d^3l_i}{2l_i^0},$$

where to regulate the IR divergences, the phase-space integral over l is continued to $4-2\epsilon$ dimensions. However, without a full extension of the vertices to $4-2\epsilon$ dimensions, this process can only be expected to return the correct cut-constructible parts of non-supersymmetric amplitudes [44].

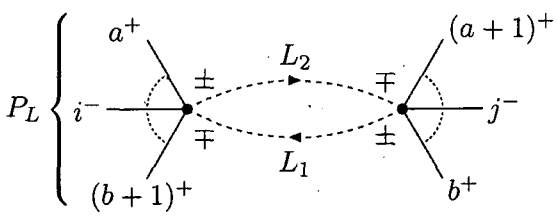

FIGURE 2.10: Contribution to the multi-gluon one-loop MHV amplitude with a scalar running in the loop, constructed using MHV diagrams.

With this in mind, in [44] the technique was applied to the scalar loop contributions to the pure Yang–Mills MHV amplitude with the two negative-helicity gluons adjacent, and for five gluons in both of the two independent helicity configurations. The generic graph for the MHV amplitude, with gluons i and j of negative helicity, is shown in fig. 2.10; note that for complex scalar, helicity should be understood as charge. The measure for this, incorporating propagators and momentum-conserving δ function, is

$$\frac{d^4L_1}{L_1^2 + i\epsilon}\frac{d^4L_2}{L_2^2 + i\epsilon}\delta^4(L_1 - L_2 - P_L).$$

Now define $P_{L;z}$ such that $L_1 - L_2 - P_L = l_1 - l_2 - P_{L;z}$, so the full integral is re-written as one over $P_{L;z}$ [43]:

$$2\pi i \frac{dP^2_{L;z}}{P^2_{L;z} - P^2_L - i\epsilon} \theta(P^2_{L;z}) d\text{LIPS}(l_2, -l_1; P_{L;z}),$$

where the last differential is the two-particle phase space measure that enforces $l_1 - l_2 = P_{L;z}$. Note that the phase space integral computes the unitarity cut in the $P^2_{L;z}$ channel, and the dispersion integral reconstructs the terms in the amplitude that have that cut (see *e.g.* [33]); the sum over all diagrams of fig. 2.10 computes the sum of these integrals over all kinematic channels. The phase-space integration is extended to $4-2\epsilon$ dimensions and both integrals are then evaluated, the details of which may be found in [44], wherein the cut-constructible parts of the MHV loop amplitudes specified above are recovered.

The articles of refs. [79, 80] apply this method to $\mathcal{N} = 1$ supersymmetric Yang–Mills theory to calculate its one-loop MHV amplitude. In ref. [45], the authors make arguments for the validity of their method (for supersymmetric theories), demonstrating its covariance by using the Feynman Tree Theorem [81], and that all the discontinuities and soft and collinear singularities are the same as those computed using traditional methods.

Yang–Mills inspired approach

In [82], the authors take a different approach to integrating over the loop momentum which in many ways makes contact with the field theory-driven approach to the CSW rules we will explore in detail in chapters 3 and 4 . Again, they compute the scalar loop part of non-supersymmetric amplitudes using the integral measure of (2.64) and the protocol described thereunder to split the loop momentum across the four- and -2ϵ-dimensional subspaces. The vertices used are taken from the light-cone gauge Yang–Mills theory coupled to a complex scalar, and they depend on the null vector $\mu = \eta\tilde{\eta}$ that defines the gauge. They also contract the D-dimensional loop momentum with 4-dimensional spinors corresponding to an external momentum and $\tilde{\eta}$, and this has two important effects. First, it means that -2ϵ-dimensional part of the loop momentum can be discarded in the vertices. Secondly, the scalar's off-shell momentum is projected down to a null vector in the vertex according to (2.39). As a result, one obtains precisely the scalar-gluon vertex one would have by applying the CSW prescription with η as the reference spinor to the associated amplitude. This is something we will come across in more detail in our studies in section 3.2.2.

Using this method, Brandhuber *et al.* were able to obtain the correct expression for the one-loop $(----)$ amplitude. This amplitude vanishes in supersymmetric theories (see *e.g.* supersymmetric Ward identities, section 2.3.1) and being rational in four dimensions is not cut constructible. By considering the diagrams of fig. 2.11 and their rotations, it was found that this method leads, after performing Passarino–Veltman reduction — a purely *algebraic* manipulation — to an expression in terms of $4 - 2\epsilon$-dimensional box,

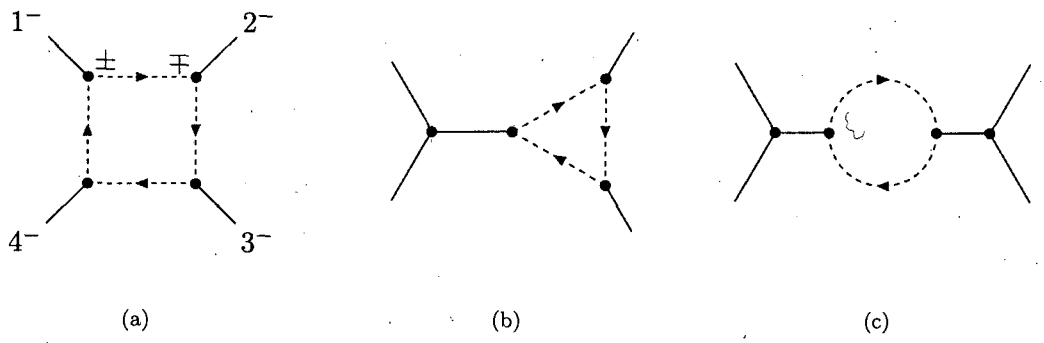

FIGURE 2.11: The box and typical triangle and bubble contributions to the one-loop ($--$) amplitude with a scalar running in the loop, constructed using MHV diagrams. Dashed lines are scalars, solid lines gluons, and all momenta are out-going.

triangle and bubble integrals. The triangle and bubble functions' contributions cancel to leave the known answer

$$\frac{2ig^4}{(4\pi)^{2-\epsilon}} K_4 \frac{\langle 1\,2\rangle\langle 3\,4\rangle}{[1\,2][3\,4]}. \tag{2.65}$$

As the authors of [82] note, the survival of this piece arises from a cancellation between the ϵ^{-1} supplied by the underlying $4-2\epsilon$-dimensional integration over the propagators, and the factor of ϵ provided by keeping track of the factors of ν^2 in the numerator.

2.7 A summary of the state of the art up to one loop

The methods described in sections 2.4 and 2.5 (the latter in particular) for the analytic computation of tree-level amplitudes involving many external gluons have lead to considerable advancement in our ability to compute new results. From an automation standpoint, the discovery of algorithms with complexity growing no faster than the square of the number of external partons has lead many to consider the tree-level problem 'solved'. Numerical techniques useful to builders of Monte Carlo simulations should not be overlooked, either. A recent analysis in [83] concluded that for numerical calculations of tree-level amplitudes, the Berends–Giele *off*-shell recursion relations [56] were fastest for nine or more external partons, whereas on-shell recursion relations offered better performance in cases with fewer.

Table 2.7 shows the current state-of-the-art for one-loop gluon amplitudes. As can be seen, analytic expressions for gluon loop amplitudes have been obtained via a number of methods and there is extensive literature on the subject. The highest valence with analytic results for all helicity configurations is six gluons. The higher-point amplitudes are, at time of writing, still awaiting the various other components required for assembly. On the other hand, numerical programmes have been forging ahead and for the more demanding phenomenologist, results in ref. [84] have been published for up to twenty gluons evaluated using **Rocket**, a program which implements the algorithms and techniques given in refs. [85, 86].

Amplitude(s)	**Methodology**
5 gluons	String based calculation [87]
6 gluons	$\mathcal{N} = 4$ part via unitarity [34]; $\mathcal{N} = 1$ MHV in [34], NMHV in [88, 89]; scalar by unitarity [90], rational terms by Feynman integrals [39]
$(--++++)$	Bootstrap [42]
Up to 20 gluons	Numerical, selected regions of phase space [84]
$\mathcal{N} = 1$ n gluons MHV	Unitarity [34]
$\mathcal{N} = 4$ n gluons MHV	Unitarity [58]
$\mathcal{N} = 4$ n gluons NMHV	Unitarity [91]
$(\pm + \cdots +)$	Recursive techniques [92]
n gluon MHV	Cuts of scalar pieces by MHV diagrams in [44], rational terms by on-shell recursion relations in [93]
$(---+\cdots+)$	Unitarity [89]
$(----+\cdots+)$	Bootstrap leading to recursive solution in [94] (with numerical results given for 7 and 8 gluon cases)

TABLE 2.1: Summary of the current state-of-the-art in gluon loop amplitudes and when and how they were first derived.

2.8 Closing statement: From the CSW rules to field theory

We are now in a position to make more concrete the context and spirit of the remainder of this thesis. The CSW rules described in section 2.4 were originally derived based on observations in twistor string theory. As the foregoing bears witness, a lot of work has been undertaken to develop these ideas at tree and loop level, powered mostly by applied understanding of the analytic structure of scattering amplitudes and twistor-space geometry.

While highly inspired, this is perhaps not so satisfying from a field theorist's point of view. The CSW rules look *qualitatively* like the end product of quantising some kind of field theory, albeit one with an infinite series of vertices of increasing valence joined together by a scalar propagator. One might therefore ask: Is it possible to construct the *field theory* QCD in such a way that the CSW rules are made manifest? In other words, can we write down an action for QCD with a scalar propagator and an infinite series of vertices that take the form of MHV amplitudes? Such a formulation would make the construction accessible to the well-established framework of quantum field theory, as well as indicate how to incorporate (the as-yet missing) regulation structure needed for quantum corrections. For a start, the formalisms we have seen so far are fundamentally tied to four dimensions. Might deriving the CSW rules from an action viewpoint lead

to a dimensionally regulated version of the construction?[12,13]

It turns out that these suspicions are well-founded. Without wishing to give away too much at this stage one can construct a transformation of light-cone gauge Yang–Mills that re-writes the usual action in precisely the 'MHV lagrangian' form we desire. The bulk of this thesis, chapters 3–5, is devoted to obtaining this transformation and studying the lagrangians it constructs. As well as deriving the CSW rules at the action level from a field theoretic point of view, we will see that this approach provides extra structure that can answer certain questions concerning the apparent incompleteness of the CSW rules. In particular, we note here that with MHV vertices alone, one simply cannot assemble a graph for the one-loop $(+\cdots+)$ amplitudes.

2.A 4D cut-constructible loop integrals

Here we list the set of functions that can appear in cut-constructible amplitudes satisfying the BDDK criteria with four or more external particles. These are also given in Figures 1–3 of [34], along with explicit expressions in Appendix I of the same reference.

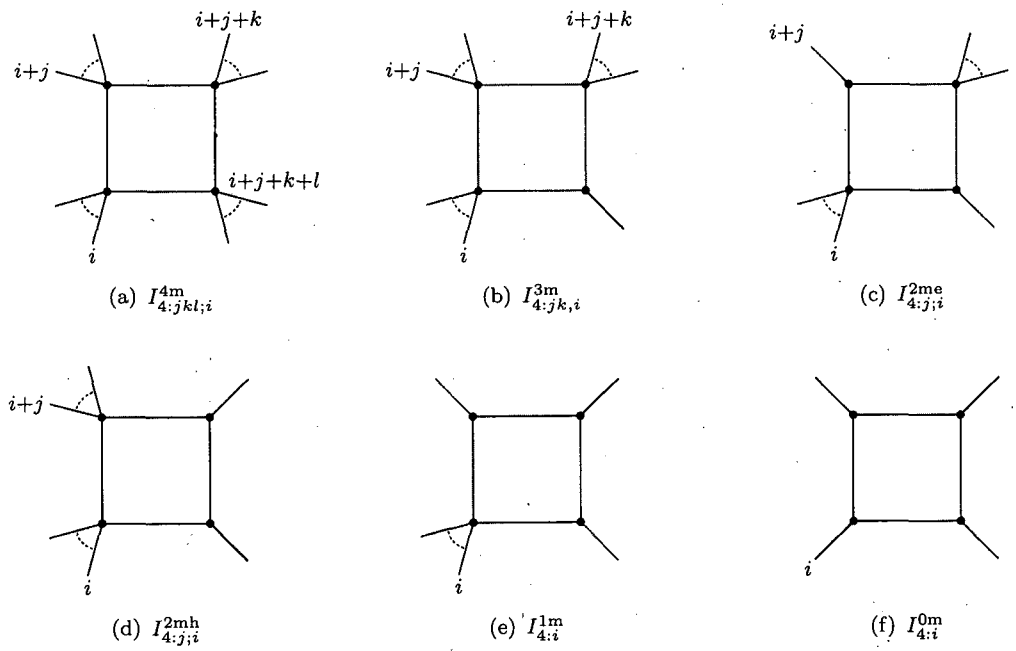

FIGURE 2.12: Cut-constructible box integral contributions, $n \geq 4$.

[12]Here we are talking about a *full* dimensional regularisation of amplitudes consisting of purely gluonic components, *i.e.* accounting for the changing number of degrees of freedom this introduces. This is in contrast to the calculations mentioned in the foregoing (such as MHV amplitudes in loop diagrams and $4-2\epsilon$-dimensional cut construction) with a complex *scalar* in the loop.

[13]We note that there are other regulators that work within four dimensions, such as that of ref. [95], but thanks largely to its Lorentz and gauge invariance (ignoring chiral anomalies) dimensional regularisation has emerged as the phenomenologists' favourite.

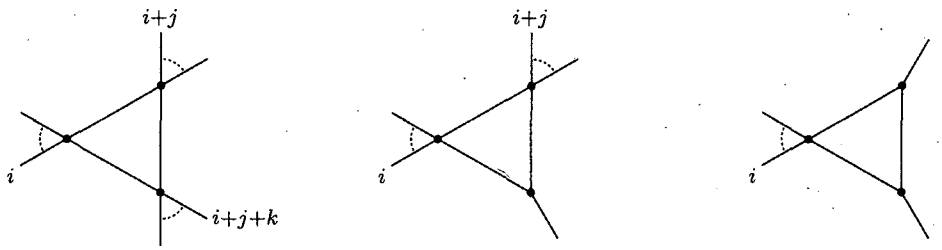

(a) $I^{\text{3m}}_{3:jk;i}$ (b) $I^{\text{2m}}_{3:j;i}$ (c) $I^{\text{1m}}_{3:i}$

FIGURE 2.13: Cut-constructible triangle integral contributions, $n \geq 4$.

FIGURE 2.14: Cut-constructible bubble integral contribution $I^{\text{2m}}_{2:i}$.

Chapter 3

An MHV Lagrangian for Pure Yang–Mills

In the previous chapter, we studied the MHV rules of Cachazo, Svrček and Witten and how they are applied to the calculation of multi-gluonic scattering amplitudes. There, we hinted that the construction is reminiscent of a field theory with an infinite set of MHV vertices connected by scalar propagators. However, the CSW construction lies outside the framework of Lagrangian mechanics as usually applied to quantum field theory and the well understood machinery thereof.

In this chapter, we will show how to put the MHV rules within the Lagrangian framework by means of a canonical transformation of the field variables of light-cone gauge Yang–Mills theory. The result is the Canonical MHV Lagrangian, consisting of an infinite series of MHV-like vertices in the new field variables. The structure of the rest of this chapter is as follows. In section 3.1, we derive the action for light-cone Yang–Mills, and in sections 3.2–3.3 we specify and solve the field transformation that gives us an MHV lagrangian. Next, in section 3.4 we compute explicitly terms in our MHV lagrangian for up to 5 gluons and demonstrate that (up to polarisation factors) these are the Parke–Taylor amplitudes of (2.22). Finally we draw our conclusions on this work in section 3.5.

This work was published in [48].

3.1 Light-cone gauge Yang–Mills Theory

In this section, we detail the preliminaries underlying the construction of the Canonical MHV Lagrangian, specifically our choice of co-ordinates and normalisation, and derive the Yang–Mills action fixed to the light-cone gauge.

3.1.1 Light-cone co-ordinates

The forthcoming analysis is adapted to a light-cone co-ordinate system, which is defined by

$$x^0 = \tfrac{1}{\sqrt{2}}(t - x^3), \quad x^{\bar{0}} = \tfrac{1}{\sqrt{2}}(t + x^3), \quad z = \tfrac{1}{\sqrt{2}}(x^1 + ix^2), \quad \bar{z} = \tfrac{1}{\sqrt{2}}(x^1 - ix^2). \tag{3.1}$$

Here, t and x^i are the usual Minkowski co-ordinates. Note here the presence of the $1/\sqrt{2}$ factors that preserve the normalisation of the volume form. Since we will frequently be dealing with specific components of momenta, we will make use of the short-hand $(p_0, p_{\bar{0}}, p_z, p_{\bar{z}}) \equiv (\check{p}, \hat{p}, p, \bar{p})$ for the components of 1-forms. For the n^{th} external momentum, we write the number with the embellishments so that the momentum's components are $(\check{n}, \hat{n}, \tilde{n}, \bar{n})$. In these co-ordinates, the Lorentz invariant is

$$A \cdot B = \check{A}\hat{B} + \hat{A}\check{B} - A\bar{B} - \bar{A}B. \tag{3.2}$$

It will also turn out to be useful to define the following quantities which are bilinear in their momentum arguments:

$$(1\,2) := \hat{1}\tilde{2} - \hat{2}\tilde{1}, \quad \{1\,2\} := \hat{1}\bar{2} - \hat{2}\bar{1}. \tag{3.3}$$

These quantities have a simple relationship with the $\langle\cdots\rangle$ and $[\cdots]$ spinor brackets of (2.8). We will not make much use of the latter in the forthcoming, but it will be necessary to understand this relationship in order to compare the techniques we have developed with established results. First, we begin by writing the bispinor representation of a 4-vector p of (2.5) in light-cone co-ordinates:

$$p \cdot \bar{\sigma} = \sqrt{2} \begin{pmatrix} \check{p} & -p \\ -\bar{p} & \hat{p} \end{pmatrix}. \tag{3.4}$$

If p is null, then $p\bar{p} = \check{p}\hat{p}$ and this matrix factorises as $(p \cdot \bar{\sigma})_{\alpha\dot{\alpha}} = \lambda_\alpha \tilde{\lambda}_{\dot{\alpha}}$, where we can choose

$$\lambda_\alpha = 2^{1/4} \begin{pmatrix} -p/\sqrt{\hat{p}} \\ \sqrt{\hat{p}} \end{pmatrix} \quad \text{and} \quad \tilde{\lambda}_{\dot{\alpha}} = 2^{1/4} \begin{pmatrix} -\bar{p}/\sqrt{\hat{p}} \\ \sqrt{\hat{p}} \end{pmatrix}. \tag{3.5}$$

Hence the spinor brackets can be expressed as

$$\langle 1\,2\rangle = \epsilon^{\alpha\beta}\lambda_{1\alpha}\lambda_{2\beta} = \sqrt{2}\frac{(1\,2)}{\sqrt{\hat{1}\hat{2}}} \quad \text{and} \quad [1\,2] = \epsilon^{\dot{\alpha}\dot{\beta}}\lambda_{1\dot{\alpha}}\lambda_{2\dot{\beta}} = \sqrt{2}\frac{\{1\,2\}}{\sqrt{\hat{1}\hat{2}}}. \tag{3.6}$$

3.1.2 Gauge-fixing the action

Mansfield's programme for the construction of the Canonical MHV Lagrangian begins with light-cone gauge Yang–Mills theory, which we will derive in this section. We start

with non-gauge-fixed Yang–Mills action

$$S = \frac{1}{2g^2}\int d^4x \ \mathrm{tr}\, \mathcal{F}^{\mu\nu}\mathcal{F}_{\mu\nu}, \tag{3.7}$$

where d^4x is the usual Minkowski 4-volume element, and our field strength tensor, covariant derivative and gauge potential are defined according to

$$\mathcal{F}_{\mu\nu} = [\mathcal{D}_\mu, \mathcal{D}_\nu], \quad \mathcal{D}_\mu = \partial_\mu + \mathcal{A}_\mu, \quad \mathcal{A}_\mu = -\frac{ig}{\sqrt{2}}A^a_\mu T^a. \tag{3.8}$$

Note that here, and throughout, the $\mathrm{SU}(N_\mathrm{C})$ generators T^a are normalised as in chapter 2, *i.e.*

$$[T^a, T^b] = i\sqrt{2}f^{abc}T^c, \quad \mathrm{tr}(T^aT^b) = \delta^{ab}. \tag{3.9}$$

We will quantise the theory on a null 3-surface Σ of constant x^0. This has a normal vector $\mu = (1,0,0,1)/\sqrt{2}$ in Minkowski co-ordinates. Light-cone gauge imposes the condition $\mu\cdot\mathcal{A} \equiv \hat{\mathcal{A}} = 0$ for which the Faddeev–Popov ghosts decouple (contributing an overall infinite constant factor to the path integral, which we discard). Now, with this condition in force, we find that (3.7) becomes

$$S = \frac{1}{2g^2}\int d^4x \ \mathrm{tr}(\mathcal{L}_2 + \mathcal{L}_3 + \mathcal{L}_4) \tag{3.10}$$

where (after integrating by parts)

$$\mathcal{L}_2 = 2(\mathcal{A}[\check{\partial}\hat{\partial} - \partial\bar{\partial}]\bar{\mathcal{A}} + \check{\mathcal{A}}\,\hat{\partial}^2\check{\mathcal{A}} - \mathcal{A}\,\hat{\partial}\bar{\partial}\check{\mathcal{A}} - 2\bar{\mathcal{A}}\,\hat{\partial}\partial\check{\mathcal{A}} + \mathcal{A}\,\bar{\partial}^2\mathcal{A} + \bar{\mathcal{A}}\,\partial^2\bar{\mathcal{A}} + \mathcal{A}\,\partial\bar{\partial}\bar{\mathcal{A}}), \tag{3.11}$$

$$\mathcal{L}_3 = 4(\partial\bar{\mathcal{A}}[\bar{\mathcal{A}}, \mathcal{A}] + \bar{\partial}\mathcal{A}[\mathcal{A}, \bar{\mathcal{A}}] - \hat{\partial}\mathcal{A}[\check{\mathcal{A}}, \bar{\mathcal{A}}] - \hat{\partial}\bar{\mathcal{A}}[\check{\mathcal{A}}, \mathcal{A}]), \tag{3.12}$$

$$\mathcal{L}_4 = 2([\mathcal{A}, \bar{\mathcal{A}}][\bar{\mathcal{A}}, \mathcal{A}]). \tag{3.13}$$

Importantly, we notice here that the lagrangian density (3.11)–(3.13) is quadratic in $\check{\mathcal{A}}$. Furthermore, it is non-dynamical with respect to light-cone time (*i.e.* it there are no $\check{\partial}$ operators acting on it). Therefore we will integrate it out of the action.

To see how this is done, consider briefly a toy model field theory with a hermitian, algebra-valued field ϕ, and a set of other independent fields which we will label Ψ_i. Let $K(\Psi)$ be a hermitian, algebra-valued function of the Ψ_i. We can write this theory's partition function as

$$\int \mathcal{D}\phi\,\mathcal{D}\Psi \exp\int d^4x\, ik\left\{\mathrm{tr}[\tfrac{1}{2}\phi\Delta^{-1}\phi + K(\Psi)\phi] + L(\Psi)\right\}, \tag{3.14}$$

where k is a constant, Δ^{-1} is a differential operator, and $L(\Psi)$ is a real function of the Ψ_i only. Now make the following change of variables:

$$\phi \to \phi' = \phi + \Delta K(\Psi), \tag{3.15}$$

where we assume a regularisation prescription that allows Δ to exist. Since this is a shift, its jacobian is unity and the path integral becomes

$$\int \mathcal{D}\phi' \, \mathcal{D}\Psi \exp \int d^4x \, ik \left\{ \mathrm{tr}[\tfrac{1}{2}\phi' \Delta^{-1} \phi' - \tfrac{1}{2} K(\Psi) \Delta K(\Psi)] + L(\Psi) \right\}. \tag{3.16}$$

The first term above calculates $\det(-k\Delta^{-1})^{-1/2}$. In the case that Δ^{-1} is field-independent, this is a divergent but physically irrelevant factor in the path integral. We may therefore discard the ϕ' terms in the action of (3.16).

Now for (3.13), the analogue of $K(\Psi)$ is the coefficient of $\check{A}$ found the trace therein, specifically

$$K_{\mathrm{YM}} = 4([\hat{\partial}\mathcal{A}, \bar{\mathcal{A}}] + [\hat{\partial}\bar{\mathcal{A}}, \mathcal{A}] - \partial\hat{\partial}\bar{\mathcal{A}} - \bar{\partial}\hat{\partial}\mathcal{A}). \tag{3.17}$$

The operator $\frac{1}{2}\Delta^{-1} = 2\hat{\partial}^2$, and so by (3.16), we drop all terms in (3.10) that contain $\check{A}$ and replace them with

$$-\frac{1}{2g^2} \int d^4x \ \mathrm{tr} \, \tfrac{1}{8} K_{\mathrm{YM}} \hat{\partial}^{-2} K_{\mathrm{YM}}. \tag{3.18}$$

We plug (3.17) into (3.18) and after some algebra (where we take derivatives and inverse derivatives to commute) and integration by parts, we arrive at the light-cone Yang–Mills action:

$$S_{\mathrm{LCYM}} = \frac{4}{g^2} \int dx^0 (L^{-+} + L^{-++} + L^{--+} + L^{--++}) \tag{3.19}$$

where

$$L^{-+} = \ \mathrm{tr} \int_\Sigma d^3\mathbf{x} \, \bar{\mathcal{A}} (\check{\partial}\hat{\partial} - \partial\bar{\partial}) \mathcal{A}, \tag{3.20}$$

$$L^{-++} = -\mathrm{tr} \int_\Sigma d^3\mathbf{x} \, (\bar{\partial}\hat{\partial}^{-1}\mathcal{A}) \, [\mathcal{A}, \hat{\partial}\bar{\mathcal{A}}], \tag{3.21}$$

$$L^{--+} = -\mathrm{tr} \int_\Sigma d^3\mathbf{x} \, [\bar{\mathcal{A}}, \hat{\partial}\mathcal{A}] \, (\partial\hat{\partial}^{-1}\bar{\mathcal{A}}), \tag{3.22}$$

$$L^{--++} = -\mathrm{tr} \int_\Sigma d^3\mathbf{x} \, [\bar{\mathcal{A}}, \hat{\partial}\mathcal{A}] \, \hat{\partial}^{-2} \, [\mathcal{A}, \hat{\partial}\bar{\mathcal{A}}]. \tag{3.23}$$

The result, as seen above, is a relatively simple form for the Yang–Mills action in terms of the physical degrees of freedom alone.[1] This is the motivation behind this choice, not least because it allows us to identify $\mathcal{A}$ and $\bar{\mathcal{A}}$ with positive and negative helicity, respectively. To see this, consider the standard polarisation vectors (2.10) for a massless on-shell vector boson of momentum $p = \lambda\tilde{\lambda}$, which we reprint here:

$$(E_+)_{\alpha\dot{\alpha}} = \sqrt{2}\frac{\nu_\alpha \tilde{\lambda}_{\dot{\alpha}}}{\langle \nu \, \lambda \rangle} \quad \text{and} \quad (E_-)_{\alpha\dot{\alpha}} = \sqrt{2}\frac{\lambda_\alpha \tilde{\nu}_{\dot{\alpha}}}{[\nu \, \lambda]}.$$

[1] We note here that there is still some residual gauge freedom left over in (3.19), something to which we will turn our attention later.

Let us choose the reference vector to be $\nu\tilde{\nu} = \mu$, the null vector normal to the quantisation surface Σ. Since (3.5) is singular for μ, instead we choose

$$\nu_\alpha = \tilde{\nu}_{\dot{\alpha}} = 2^{1/4} \begin{pmatrix} 1 \\ 0 \end{pmatrix}. \tag{3.24}$$

Substituting into (2.10) and comparing the bispinor components with (3.4), we find that the polarisation vectors' non-zero components are $E_+ = \bar{E}_- = -1$ and $\check{E}_\pm$. Scattering amplitudes are formed by the application of LSZ reduction to correlation functions of the $\mathcal{A}$ fields. Schematically, for outgoing momenta $\{p_i\}$ and helicities $\{h_i\}$,

$$\langle p_1^{h_1}, \ldots, p_n^{h_n} | S | 0 \rangle = (-i)^n \lim_{p_i^2 \to 0} p_1^2 \cdots p_n^2 \, \langle E_{h_1}^{\mu_1} \mathcal{A}_{\mu_1} \cdots E_{h_n}^{\mu_n} \mathcal{A}_{\mu_n} \rangle. \tag{3.25}$$

(up to normalisation). By considering the invariant (3.2), we see that each + (−) external state gluon on the LHS above is associated with an insertion of $\bar{\mathcal{A}}$ ($\mathcal{A}$) in the correlation function on the RHS. The $\check{E}_\pm$ component couples to $\hat{\mathcal{A}}$, which vanishes by gauge choice. The scalar propagator of (3.20) connects $\mathcal{A}$ to $\bar{\mathcal{A}}$ and *vice versa*, so when the LSZ procedure 'amputates' these propagators, we come to identify the $\mathcal{A}$ and $\bar{\mathcal{A}}$ as the positive and negative helicity fields, respectively.

3.2 Structure of the MHV lagrangian

Let us now begin to construct and explore the field transformation that takes us from (3.19) to a lagrangian that makes manifest the CSW construction.

3.2.1 Form of the transformation and lagrangian

In [46], Mansfield defines the field transformation that gives the new gauge fields $\mathcal{B}$ and $\bar{\mathcal{B}}$ as

$$L^{-+}[\mathcal{A}, \bar{\mathcal{A}}] + L^{-++}[\mathcal{A}, \bar{\mathcal{A}}] = L^{-+}[\mathcal{B}, \bar{\mathcal{B}}]. \tag{3.26}$$

This transformation is to be performed entirely in the quantisation surface Σ, so that all the fields involved have the same x^0 'time' dependence (which we will henceforth suppress unless clarity dictates otherwise). At first, it might seem rather odd to absorb the interacting part of one field theory into the kinetic term of another. However, we recognise the LHS of (3.26) as the Chalmers–Siegel self-dual truncation of Yang–Mills theory [96]; this is a classically free theory[2] [60] which we are mapping onto another free theory.

The momentum conjugate to $\mathcal{A}^a(x)$ is

$$\Pi^a(x) = \frac{\delta L^{-+}}{\delta \check{\partial} \mathcal{A}^a(x)} = -\hat{\partial} \mathcal{A}^a(x),$$

[2]Inasmuch as all of its tree-level amplitudes are of the form $(-+\cdots+)$ and therefore vanish on shell.

and as such the path integral measure

$$\mathcal{D}\mathcal{A}\mathcal{D}\bar{\mathcal{A}} \equiv \prod_{x,a} \mathcal{A}^a(x)\bar{\mathcal{A}}^a(x)$$

is proportional to the phase space measure. In the interest of simplicity, we would like this measure to be preserved, and this will be so if the field transformation is *canonical* (in the sense of Hamiltonian mechanics). Section 3.A explains canonical transformations and their properties in more detail, but what we need to know here is that we can construct one by starting with a transformation of the canonical co-ordinates alone — in the case here by postulating that $\mathcal{A}$ be a functional of just $\mathcal{B}$. One important outcome of this choice is (3.70), which links the new and old momenta, and since (3.26) is defined on a surface of constant x^0 and preserves the form of the kinetic part, $-\hat{\partial}\mathcal{B}^a(x)$ is the momentum conjugate to $\mathcal{B}^a(x)$ so

$$\hat{\partial}\bar{\mathcal{B}}^a(\mathbf{y}) = \int_\Sigma d^3\mathbf{x}\, \frac{\delta\mathcal{A}^b(\mathbf{x})}{\delta\mathcal{B}^a(\mathbf{y})}\hat{\partial}\bar{\mathcal{A}}^b(\mathbf{x}). \tag{3.27}$$

Let us write out (3.26) explicitly:

$$\mathrm{tr}\int_\Sigma d^3\mathbf{x}\{\check{\partial}\mathcal{A}\hat{\partial}\bar{\mathcal{A}} - \omega\mathcal{A}\hat{\partial}\bar{\mathcal{A}} + [\zeta\mathcal{A},\mathcal{A}]\hat{\partial}\bar{\mathcal{A}}\} = \mathrm{tr}\int_\Sigma d^3\mathbf{x}\{\check{\partial}\mathcal{B}\hat{\partial}\bar{\mathcal{B}} - \omega\mathcal{B}\hat{\partial}\bar{\mathcal{B}}\} \tag{3.28}$$

where we have introduced the differential operators $\omega := \partial\bar{\partial}/\hat{\partial}$ and $\zeta := \bar{\partial}/\hat{\partial}$. Substituting with (3.27) into its LHS, we can eliminate the leading terms on either side and obtain

$$\mathrm{tr}\int_\Sigma d^3\mathbf{x}\{\omega\mathcal{A}\hat{\partial}\bar{\mathcal{A}} - [\zeta\mathcal{A},\mathcal{A}]\hat{\partial}\bar{\mathcal{A}}\} = \mathrm{tr}\int_\Sigma d^3\mathbf{x}\,\omega\mathcal{B}\hat{\partial}\bar{\mathcal{B}}. \tag{3.29}$$

We can again use (3.27) to eliminate $\hat{\partial}\bar{\mathcal{B}}$ in favour of $\hat{\partial}\bar{\mathcal{A}}$, and noting that $\bar{\mathcal{A}}$ is arbitrary here, it follows that $\mathcal{A}$ has a power series expansion in $\mathcal{B}$ of the form

$$\mathcal{A} = \mathcal{B} + \mathcal{O}(\mathcal{B}^2), \tag{3.30}$$

and from (3.27) that $\bar{\mathcal{A}}$ has an expansion in $\mathcal{B}$ and a single power of $\bar{\mathcal{B}}$ in each term, *i.e.* of the form

$$\bar{\mathcal{A}} = \bar{\mathcal{B}} + \mathcal{O}(\mathcal{B}\bar{\mathcal{B}}). \tag{3.31}$$

The remaining part of the Yang–Mills lagrangian is $L^{--+} + L^{--++}$, and it follows from (3.30) and (3.31) that upon substitution for $\mathcal{A}$ and $\bar{\mathcal{A}}$ in terms of $\mathcal{B}$ and $\bar{\mathcal{B}}$ that this will generate an infinite series of terms with the helicity content required to be identified as a MHV lagrangian: terms with an increasing number $n_+ \geq 1$ of $\mathcal{B}$ fields, but only ever two $\bar{\mathcal{B}}$ fields. These interaction terms, together with the $\mathcal{B}$ kinetic term, form what we refer to as the Canonical MHV Lagrangian. In more detail, inspection of (3.22) and (3.23) shows that the fields are within traces and all possible helicity arrangements thereunder occur. If we now work in momentum space on the quantisation surface, we

can write the general n-gluon term of the MHV lagrangian as

$$L^{--\overbrace{+\cdots+}^{n-2}} = \frac{1}{2}\sum_{s=2}^{n}\int_{1\cdots n} V^s_{1\cdots n}\,\mathrm{tr}(\bar{\mathcal{B}}_{\bar{1}}\mathcal{B}_{\bar{2}}\cdots\bar{\mathcal{B}}_{\bar{s}}\cdots\mathcal{B}_{\bar{n}}). \tag{3.32}$$

Note that by the cyclicity of the trace, we can always arrange for the first field in (3.32) to be a $\bar{\mathcal{B}}$. We have introduced a number of new notations here: the subscripts are the 3-momentum arguments, with a bar denoting negation, *e.g.* $\mathcal{B}_{\bar{1}} = \mathcal{B}(-\mathbf{p}_1)$, and the momentum integral short-hand is defined via

$$\int_{1\cdots n} \equiv \prod_{k=1}^{n}\int_{\Sigma}\frac{d\hat{k}\,dk\,d\bar{k}}{(2\pi)^3} \tag{3.33}$$

Now since (3.32) must conserve momentum, it will often be convenient to factor off the implicit δ^3 function as

$$V^s_{1\cdots n} = (2\pi)^2\delta^3(\textstyle\sum_{i=1}^{n}\mathbf{p}_i)\;V^s(1\cdots n). \tag{3.34}$$

The presence of the δ^3 function above should be taken as an indication that the vertices V^s are only defined when the sum of their arguments is zero. (We could have restricted the upper limit of the sum in (3.32) to $\lfloor n/2+1\rfloor$ and obtained all possible helicity arrangements, but by writing it this way we get the same thing except for in the $s = n/2+1$ term when n is even, which is is accompanied by a factor of $\frac{1}{2}$. We will defer discussing the significance of this momentarily.)

3.2.2 Amplitudes, vertices and the CSW rules

Let us show that this construction coincides with the CSW rules [15], as described in section 2.4. First, inspection of (3.26) tells us that the propagator associated with the new fields is

$$\langle\mathcal{B}\bar{\mathcal{B}}\rangle = -\frac{ig^2}{2p^2} \quad\Leftrightarrow\quad \langle B\bar{B}\rangle = \frac{i}{p^2} \tag{3.35}$$

using (3.8), *i.e.* a scalar propagator.

We must next show that the vertices of the Canonical MHV Lagrangian constructed in this manner coincide with the Parke–Taylor amplitudes and that we recover the CSW off-shell prescription. First, let us address the off-shell continuation of the Weyl spinors. The choice (3.5) depend only on three of the four momentum components, and makes sense even for off-shell momenta. For λ and $\tilde{\lambda}$ obtained from a 4-momentum p, their product corresponds to the null vector given by

$$(p_{\mathrm{null}})_{\alpha\dot{\alpha}} = \lambda_\alpha\tilde{\lambda}_{\dot{\alpha}} = \sqrt{2}\begin{pmatrix} p\bar{p}/\hat{p} & -p \\ -\bar{p} & \hat{p}\end{pmatrix}. \tag{3.36}$$

It is easy to see, *e.g.* by subtracting (3.36) from (3.4) that $p_{\text{null}} = p + a\mu$ where $a = p\bar{p}/\hat{p} - \check{p} = -p^2/2\mu \cdot p$ and $\mu = \nu\tilde{\nu}$ is the null vector normal to the quantisation surface, its spinors given by (3.24). But this is just the CSW prescription of (2.39), coinciding with (3.5) by choosing the arbitrary spinor $\tilde{\eta} \propto \tilde{\nu}$.

Turning to the vertices themselves, we first note that the Canonical MHV Lagrangian is defined in terms of the new $\mathcal{B}$ fields. We would expect to formulate S-matrix elements by applying the LSZ theorem to correlation function in $\mathcal{A}$ and $\bar{\mathcal{A}}$ as in (3.25), but by the equivalence theorem (explained in section 3.B), at tree level for generic momenta we can equally well use $\mathcal{B}$ and $\bar{\mathcal{B}}$ in their places when we attach external lines to the interaction vertices in the Feynman graphs. This is because higher order terms in the expansion of $\mathcal{A}$ (and likewise $\bar{\mathcal{A}}$) introduce products of multiple $\mathcal{B}$ fields, whose momenta must sum to that of the original $\mathcal{A}$. Generically, their propagators cannot generate the poles required for such terms to survive as the LSZ procedure takes the external momenta on shell[3]. Now consider formulating an on-shell partial amplitude using (3.32): since such an object is defined as the term in an S-matrix element that multiplies a given colour trace, it is therefore clear that to extract a colour-ordered MHV amplitude using (3.32), one simply contracts the external momentum and gauge indices into the trace as appropriate and multiplies by the relevant polarisation and quantum mechanical factors. Thus contracting an external MHV state into the MHV lagrangian to obtain a partial amplitude amounts to pulling out the term with the relevant helicity content and colour ordering and replacing

$$\mathcal{B}(x^0, \mathbf{p}_j), \bar{\mathcal{B}}(x^0, \mathbf{p}_j) \to -1 \times -\frac{ig}{\sqrt{2}} \exp(i\check{p}_j x^0)\, T^{a_j}$$

in (3.32) and symmetrising as appropriate. (The significance of the factor of $\frac{1}{2}$ for the $s = n/2 + 1$ term in (3.32) when n is even is now apparent: this term has a symmetry under the index shift $i \mapsto i + n/2 \mod n$, and in such a circumstance there are two ways to contract the external state into it for a given colour order. The factor of $\frac{1}{2}$ absorbs this, assuming V^s is symmetrised accordingly.)

Given what we know about tree-level gluon scattering, we can equate this with the known Parke–Taylor form of the MHV amplitude to put

$$\begin{aligned}\frac{4}{g^2} \int dx^0\, V^s_{1\cdots n} \left(\frac{ig}{\sqrt{2}}\right)^n \exp\{i(\check{1} + \cdots \check{n})x^0\} \operatorname{tr}(T^{a_1} \cdots T^{a_n}) \\ = ig^{n-2}(2\pi)^2 \delta^4(p_1 + \cdots + p_n) \frac{\langle 1\, s\rangle^4}{\langle 1\, 2\rangle \cdots \langle n-1, n\rangle \langle n\, 1\rangle} \operatorname{tr}(T^{a_1} \cdots T^{a_n}). \quad (3.37)\end{aligned}$$

[3]This is assuming that the transformation does not generate a pole as an external momentum is taken on shell in such a way that higher-order terms survive the LSZ reduction. We note here that there exist certain conditions within the context of the MHV lagrangian where the equivalence theorem is evaded. Specifically, these include when off-shell at tree-level, in certain non-physical on-shell situations, and at loop-level. However, this is outside the sequence in which the topic was developed and is addressed in more detail in chapter 4.

Of course, this just tells us that the vertex is the MHV amplitude on-shell, specifically that

$$\begin{aligned} V^s(1\cdots n) &= (-i\sqrt{2})^{n-4}\frac{\langle 1\, s\rangle^4}{\langle 1\,2\rangle\cdots\langle n-1,n\rangle\langle n\,1\rangle} \\ &= (-i)^n\frac{\hat{2}\cdots\hat{n}\,(1\,s)^4}{\hat{1}\hat{s}^2(1\,2)\cdots(n-1,n)(n\,1)}, \end{aligned} \tag{3.38}$$

using (3.6). It remains for us to show that this is also true off-shell as per the CSW prescription, and to do so we follow the argument given by Mansfield in [46]. Now since we constructed $V^s_{1\cdots n}$ to be independent of x^0, carrying out the integration on the LHS above gives

$$\begin{aligned} &(2\pi)\delta(\check{1}+\cdots+\check{n})(-i\sqrt{2})^{4-n}V^s_{1\cdots n} = \\ &\qquad (2\pi)\delta(\check{1}+\cdots+\check{n})\,(2\pi)^3\delta^3(\mathbf{p}_1+\cdots+\mathbf{p}_n)\frac{\langle 1\, s\rangle^4}{\langle 1\,2\rangle\cdots\langle n-1,n\rangle\langle n\,1\rangle}. \end{aligned} \tag{3.39}$$

We would like to simply cancel the $\delta(\check{1}+\cdots+\check{n})$ on either side here and claim (3.38) applies off-shell, but we cannot do this: we must demonstrate the absence of terms in the action that vanish on the support of the δ function if such a claim is to have any merit.

This will be so if the vertices are holomorphic, in the sense that they contain no $\bar{\partial}$ derivatives (or equivalently $\bar{p}$ momentum factors). First, for $n > 3$, any term that vanishes on the support of this δ function must depend on a subset of the $\bar{p}_i$ when all the momenta are on shell, since $\check{p} = p\bar{p}/\hat{p}$. The $n = 3$ case is exceptional, since

$$\check{1}+\check{2}+\check{3} = \frac{|(1\,2)|^2}{\hat{1}\hat{2}(\hat{1}+\hat{2})}.$$

As we are dealing with real momenta, $(1\,2)$ must vanish on the support of the δ function, even though it is independent of any $\bar{p}_i$. Nevertheless, we can (and will) check by computing the relevant terms using the explicit form of the transformation that (3.38) still holds off shell for the case of $n = 3$.

Now, we will show that the terms of the MHV lagrangian are holomorphic explicitly in section 3.3 when we solve the transformation, but it is worthwhile noting here that Mansfield showed that this was so in a rather elegant manner by considering the action of the homogeneous part of gauge transformation

$$\delta\mathcal{A} = [\mathcal{A}, \theta(\bar{z})], \quad \delta\bar{\mathcal{A}} = [\bar{\mathcal{A}}, \theta(\bar{z})] \tag{3.40}$$

for an infinitesimal algebra-valued function θ of $\bar{z}$ *alone* on the canonical transformation (3.26): under the above shift, its LHS transforms as

$$\delta(L^{-+} + L^{--++}) = \int_\Sigma d^3\mathbf{x}\,[\mathcal{A}, \bar{\partial}\theta(\bar{z})](\partial\bar{\mathcal{A}} + \hat{\partial}^{-1}[\mathcal{A}, \hat{\partial}\bar{\mathcal{A}}]).$$

However, the same shift in $L^{-+} + L^{-++}$ can be achieved by just shifting $\bar{\partial}\mathcal{A}$ by

$$\delta\bar{\partial}\mathcal{A} = [\mathcal{A}, \bar{\partial}\theta(\bar{z})]$$

and changing nothing else, so varying $\bar{\partial}\mathcal{A}$ has the same effect on the canonical transformation as (3.40). However, the vertices of the MHV lagrangian are generated by $L^{--+} + L^{--++}$ and this is invariant under (3.40). Thus the MHV lagrangian can contain no $\bar{\partial}$ dependence, and hence for $n > 3$ the vertices contain no terms that generically vanish on mass shell.

We will test this for up to five gluons in section 3.4 by explicitly computing the relevant terms of the MHV lagrangian.

3.3 Explicit form of the transformation

In this section, we will solve for the power series expansions of $\mathcal{A}$ and $\bar{\mathcal{A}}$ to all orders in $\mathcal{B}$ and $\bar{\mathcal{B}}$. To do this, we derive recurrence relations from the definition of the transformation (3.26) and (3.27), which follows from it being canonical.

3.3.1 $\mathcal{A}$ series to all orders

Taking (3.29), we eliminate $\hat{\partial}\bar{\mathcal{B}}$ using (3.27) and, dropping the $\hat{\partial}\bar{\mathcal{A}}$ factor, arrive at the following momentum space equation:

$$\omega_1\mathcal{A}_1 + i\int_{23}\zeta_3[\mathcal{A}_2,\mathcal{A}_3]\delta(\mathbf{p}_1-\mathbf{p}_2-\mathbf{p}_3) = \int_{\mathbf{p}}\omega_{\mathbf{p}}\mathcal{B}^b_{\mathbf{p}}\frac{\delta\mathcal{A}_1}{\delta\mathcal{B}^b_{\mathbf{p}}}. \tag{3.41}$$

Here, we use the momentum-space analogues of the ω and ζ operators, defined as

$$\omega_{\mathbf{p}} := \frac{p\bar{p}}{\hat{p}} \quad \text{and} \quad \zeta_{\mathbf{p}} := \frac{\bar{p}}{\hat{p}}.$$

As noted earlier, we postulate a solution for $\mathcal{A}$ as a power series in $\mathcal{B}$. In momentum space, we write this in the form

$$\mathcal{A}_1 = \sum_{n=2}^{\infty}\int_{2\cdots n}\Upsilon(12\cdots n)\mathcal{B}_2\cdots\mathcal{B}_n(2\pi)^3\delta(\textstyle\sum_{i=1}^n\mathbf{p}_i). \tag{3.42}$$

Our task now is to obtain the Υ coefficients. Note that we have absorbed the various arrangements of $\mathcal{B}$ strings in the terms of (3.42) into Υ coefficient. Indeed, brief inspection of (3.41) shows the the various strings that emerge this way may be expressed as nested commutators of the $\mathcal{B}_i$, thereby ensuring the tracelessness of both sides of (3.42). By cyclicity of the trace, this condition leads us to the result that

$$\Upsilon(123\cdots n) + \Upsilon(134\cdots n2) + \cdots + \Upsilon(1,n,2,\ldots,n-2,n-1) = 0, \tag{3.43}$$

i.e. an off-shell dual Ward identity.

At the lowest order, one can inspect (3.41) and conclude that for non-vanishing momenta, $\mathcal{A}_1 = \mathcal{B}_1$ (*i.e.* $\Upsilon(12) = 1$). To do this we had to cancel ω_1 on either side of (3.41), so we cannot rule out $\mathcal{A}$ also having terms with $\delta(p)$ and/or $\delta(\bar{p})$ support. To deal this, we notice that there is some residual gauge freedom left in the light-cone Yang–Mills action (3.19), which we obtained by gauge-fixing $\hat{\mathcal{A}} = 0$ and integrating out $\check{\mathcal{A}}$. Thus, gauge motions of the form $\delta\mathcal{A} = [\mathcal{D}, \theta]$ where θ does *not* depend on $x^{\bar{0}}$ are not fixed by this. (Should θ depend on x^0, the form of the transformation would be complicated when we integrate out $\check{\mathcal{A}}$.) Let us study the case where θ is a function of just z, *i.e.* holomorphic gauge transformations, under which the terms of (3.19) transform as

$$\delta L^{-+} = \operatorname{tr}\int_\Sigma d^3\mathbf{x}\, \bar{\mathcal{A}}[\partial\theta, \bar{\partial}\mathcal{A}], \tag{3.44}$$

$$\delta L^{-++} = \operatorname{tr}\int_\Sigma d^3\mathbf{x}\, \bar{\mathcal{A}}[\bar{\partial}\mathcal{A}, \partial\theta], \tag{3.45}$$

$$\delta L^{--+} = -\operatorname{tr}\int_\Sigma d^3\mathbf{x}\, \{[\bar{\mathcal{A}}, \hat{\partial}\mathcal{A}]\partial\hat{\partial}^{-1}[\bar{\mathcal{A}}, \theta] - [[\hat{\partial}\mathcal{A}, \bar{\mathcal{A}}], \theta]\partial\hat{\partial}^{-1}\bar{\mathcal{A}}\} \tag{3.46}$$

$$\begin{aligned}\delta L^{--++} = -\operatorname{tr}\int_\Sigma d^3\mathbf{x}\, \{&[\bar{\mathcal{A}}, \hat{\partial}\mathcal{A}]\hat{\partial}^{-2}[\partial\theta, \hat{\partial}\bar{\mathcal{A}}] \\ &- [[\hat{\partial}\mathcal{A}, \bar{\mathcal{A}}], \theta]\hat{\partial}^{-2}[\mathcal{A}, \hat{\partial}\bar{\mathcal{A}}] - [[\hat{\partial}\bar{\mathcal{A}}, \mathcal{A}], \theta]\hat{\partial}^{-2}[\bar{\mathcal{A}}, \hat{\partial}\mathcal{A}]\}\end{aligned} \tag{3.47}$$

(Notice that this requires us to interpret $\bar{\partial}\hat{\partial}^{-1}\theta(z) = \hat{\partial}^{-1}\bar{\partial}\theta(z) = 0$, in line with the Mandelstam–Leibbrandt prescription [97, 98]. Similarly, it follows that the lagrangian is also invariant when θ is a function of just $\bar{z}$.) Significantly, we notice from the above that the LHS of (3.26) is invariant under holomorphic gauge transformations; this would imply that $\mathcal{B}$ and $\bar{\mathcal{B}}$ are also invariant. Now under such a transformation $\mathcal{A} \to \mathcal{A} + \partial\theta(z) + [\mathcal{A}, \theta(z)]$. If we apply this to the leading order term of (3.42) and take the Fourier transform, we obtain

$$\mathcal{A}(p, \bar{p}) - ip\,\theta(p)\,(2\pi)\delta(\bar{p}) + \int \frac{dk}{2\pi}\,[\mathcal{A}(p-k, \bar{p}), \theta(k)] = \mathcal{B}(p, \bar{p}).$$

Thus we will interpret the form of (3.42) as tantamount to further gauge fixing.

That aside, we substitute (3.42) into (3.41), remove the momentum-conserving δ functions and carefully relabel to yield the recurrence relation

$$\Upsilon(1\cdots n) = \frac{-i}{\omega_1 + \cdots + \omega_n}\sum_{j=2}^{n-1}(\zeta_{j+1,n} - \zeta_{2j})\,\Upsilon(-, 2, \cdots, j)\Upsilon(-, j+1, \cdots, n). \tag{3.48}$$

Here, we have made use of the following new notation: first, an argument "$-$" in Υ (and in other related coefficients that we will encounter later in this work) stands for minus the sum of the remaining arguments, as per conservation of momentum. Secondly, we have $\zeta_{jk} := \zeta(P_{jk})$ where $P_{jk} := \sum_{i=j}^{k}\mathbf{p}_i$. We will use a similar short-hand for ω below.

By iterating (3.48), we obtain the following coefficients:

$$\Upsilon(123) = -i\frac{\zeta_3 - \zeta_2}{\omega_1 + \omega_2 + \omega_3}, \tag{3.49}$$

$$\Upsilon(1234) = \frac{1}{\omega_1 + \omega_2 + \omega_3 + \omega_4}\left[\frac{(\zeta_4 - \zeta_3)(\zeta_{34} - \zeta_2)}{\omega_{34} - \omega_3 - \omega_4} + \frac{(\zeta_4 - \zeta_{23})(\zeta_3 - \zeta_2)}{\omega_{23} - \omega_2 - \omega_3}\right] \tag{3.50}$$

At first glance, these seem to not be holomorphic. However, if we use conservation of momentum to express these in terms of independent momenta and simplify, we obtain the following very compact expressions:

$$\Upsilon(123) = i\frac{\hat{1}}{(2\,3)},$$
$$\Upsilon(1234) = \frac{\hat{1}\hat{3}}{(2\,3)(3\,4)},$$
$$\Upsilon(12345) = -i\frac{\hat{1}\hat{3}\hat{4}}{(2\,3)(3\,4)(4\,5)},$$

whence we conjecture

$$\Upsilon(1\cdots n) = (-i)^n\frac{\hat{1}\hat{3}\hat{4}\cdots\widehat{n-1}}{(2\,3)(3\,4)\cdots(n-1,n)}, \tag{3.51}$$

for $n > 3$.

We prove this by induction on n. Clearly, the above expressions for the lower order coefficients provide the initial step. For the inductive step, we substitute (3.51) into the RHS of (3.48) and pull out as many j independent factors as possible to obtain

$$-\frac{\Upsilon(1\cdots n)}{\hat{1}(\omega_1 + \cdots + \omega_n)}\sum_{j=2}^{n-1}\frac{(j, j+1)}{\hat{j}\,\widehat{j+1}}\{P_{2j}\,P_{j+1,n}\}$$

To evaluate this sum, we expand $(j, j+1)$ so the sum becomes

$$\sum_{j=3}^{n}\frac{\tilde{j}}{\hat{j}}\{P_{2,j-1}\,P_{jn}\} - \sum_{j=2}^{n-1}\frac{\tilde{j}}{\hat{j}}\{P_{2j}\,P_{j+1,n}\} = \sum_{j=2}^{n}\frac{\tilde{j}}{\hat{j}}(\{P_{2,j-1}\,P_{jn}\} - \{P_{2j}\,P_{j+1,n}\})$$

where the end cases are dealt with by defining $P_{ij} := \mathbf{p}_i + \cdots + \mathbf{p}_n + \mathbf{p}_1 + \cdots + \mathbf{p}_j$ when $j < i$, hence $P_{i,i-1} = 0$. Upon substituting $P_{jn} = -\mathbf{p}_1 - P_{2,j-1}$ and similarly for $P_{j+1,n}$, the sum collapses to $-\hat{1}(\omega_1 + \cdots + \omega_n)$, and the claim (3.51) is proved.

3.3.2 $\bar{A}$ expansion to all orders

Differentiating (3.42) with respect to $\mathcal{B}$ and substituting the inverse into (3.27) implies a Σ momentum space expansion for $\bar{\mathcal{A}}$ of the form

$$\bar{\mathcal{A}}_{\bar{1}} = \sum_{m=2}^{\infty}\sum_{s=2}^{m}\int_{2\cdots m}\frac{\hat{s}}{\hat{1}}\Xi^{s-1}(\bar{1}2\cdots m)\,\mathcal{B}_{\bar{2}}\cdots\mathcal{B}_{\overline{s-1}}\tilde{\mathcal{B}}_{\bar{s}}\mathcal{B}_{\overline{s+1}}\cdots\mathcal{B}_{\bar{m}}\,(2\pi)^3\delta(\mathbf{p}_1-\textstyle\sum_{i=2}^{m}\mathbf{p}_i) \tag{3.52}$$

where the superscript on Ξ indicates the relative position of $\bar{\mathcal{B}}$ in the string, not the momentum argument. To extract a recurrence relation, we use the fact that

$$\mathrm{tr}\int_{\Sigma} d^3\mathbf{x}\,\check{\partial}\mathcal{A}\hat{\partial}\bar{\mathcal{A}} = \mathrm{tr}\int_{\Sigma} d^3\mathbf{x}\,\check{\partial}\mathcal{B}\hat{\partial}\bar{\mathcal{B}}, \tag{3.53}$$

which follows from the properties of a canonical transform, specifically (3.71). Since all the fields have the same x^0 dependence, and none of the Υ coefficients depend on x^0,

$$\check{\partial}\mathcal{A}_1 = \sum_{n=2}^{\infty}\sum_{r=2}^{n}\int_{2\cdots m}\Upsilon(1\cdots n)\mathcal{B}_{\bar{2}}\cdots\check{\partial}\mathcal{B}_{\bar{r}}\cdots\mathcal{B}_{\bar{n}}\,(2\pi)^3\delta^3(\textstyle\sum_{i=1}^{m}\mathbf{p}_i), \tag{3.54}$$

which we substitute into the LHS of (3.53) along with (3.52). By considering each order in powers of $\mathcal{B}$, using the cyclic property of the trace to move $\check{\partial}\mathcal{B}$ to the front of each string, matching up the position of $\bar{\mathcal{B}}$ in the strings on both sides, and then carefully relabelling the momentum arguments, we arrive at

$$\Xi^{l}(1\cdots n) = -\sum_{r=2}^{n+1-l}\sum_{m=\max(r,3)}^{r+l-1}\Upsilon(\overbrace{-,n-r+3,\cdots,m-r+1}^{(m)})\times \Xi^{l+r-m}(\underbrace{-,m-r+2,\cdots,n-r+2}_{(n-m+2)}) \tag{3.55}$$

(the braces' labels indicate the number of arguments they enclose). The momentum indices on the RHS should be interpreted cyclically (*i.e.* modulo n). Note that in the case where the upper limit of the inner sum is less than the lower limit, the sum should be taken as zero (specifically, this happens when $r=2$ and $l=1$).

To obtain concrete expressions for the Ξ coefficients from (3.55), we begin by noting that $\Xi(12)=1$, as required by the fact that the leading term in the expansion of $\bar{\mathcal{A}}$ is $\bar{\mathcal{B}}$. We can now iterate (3.55) directly to compute the first few non-trivial coefficients:

$$\Xi^1(123) = -\Upsilon(231) = -\frac{\hat{2}}{\hat{1}}\Upsilon(123), \tag{3.56}$$

$$\Xi^2(123) = -\Upsilon(312) = -\frac{\hat{3}}{\hat{1}}\Upsilon(123). \tag{3.57}$$

Continuing, we have

$$\begin{aligned}\Xi^1(1234) &= -\Upsilon(2+3,4,1)\Xi^1(1+4,2,3) - \Upsilon(2341)\\ &= -\frac{\hat{2}(\hat{2}+\hat{3})}{(4\,1)(2\,3)} - \frac{\hat{2}\hat{4}}{(3\,4)(4\,1)}\\ &= -\frac{\hat{2}(\hat{2}+\hat{3})(3\,4)+\hat{2}\hat{4}(2\,3)}{(4\,1)(2\,3)(3\,4)}\\ &= -\frac{\hat{2}\hat{3}}{(2\,3)(3\,4)} = -\frac{\hat{2}}{\hat{1}}\Upsilon(1234)\end{aligned}$$

for which we have used the Bianchi-like identity (4.76), and similarly,

$$\begin{aligned}\Xi^2(1234) &= -\Upsilon(3{+}4,1,2)\,\Xi^1(1{+}2,3,4) - \Upsilon(2{+}3,4,1)\,\Xi^2(1{+}4,2,3) - \Upsilon(3412)\\ &= -\frac{\hat{3}}{\hat{1}}\Upsilon(1234),\\ \Xi^3(1234) &= -\Upsilon(3{+}4,1,2)\,\Xi^2(1{+}2,3,4) - \Upsilon(4123)\\ &= -\frac{\hat{4}}{\hat{1}}\Upsilon(1234).\end{aligned}$$

From this, we claim that

$$\Xi^{s-1}(1\cdots n) = -\frac{\hat{s}}{\hat{1}}\Upsilon(1\cdots n) \tag{3.58}$$

for $n \geq 2$ and $2 \leq s \leq n$.

The proof of this claim follows by induction on n. The low-order coefficients above clearly supply the initial step. The inductive part can be proved by substituting (3.58) into the RHS of (3.55). We pull out the r and m independent factors to obtain

$$(-i)^n\,\widehat{l+1}\,\frac{\hat{1}\cdots\hat{n}}{(1\,2)\cdots(n{-}1,n)(n\,1)}\times \sum_{r=2}^{n+1-l}\sum_{m=\max(r,3)}^{r+l-1}\frac{(m{-}r{+}1,m{-}r{+}2)(n{-}r{+}2,n{-}r{+}3)\,\hat{P}_{n-r+3,m-r+1}}{\widehat{m-r+1}\quad\widehat{m-r+2}\quad\widehat{n-r+2}\quad\widehat{n-r+3}},$$

so the proof follows if we can show that the nested sum here equals

$$-\frac{(1\,2)(n\,1)}{\hat{1}\hat{2}\hat{n}} \tag{3.59}$$

and so the RHS equals the LHS as given by (3.58). First, we evaluate the inner sum. By performing the change of variables $j = m - r + 1$, this becomes one of the form

$$\sum_{j=a}^{b}\hat{P}_{ij}\left(\frac{\widetilde{j+1}}{\widehat{j+1}} - \frac{\tilde{j}}{\hat{j}}\right) = \hat{P}_{ib}\frac{\widetilde{b+1}}{\widehat{b+1}} - \hat{P}_{ia}\frac{\tilde{a}}{\hat{a}} - \tilde{P}_{a+1,b}, \tag{3.60}$$

so we are left with

$$\sum_{r=2}^{n+1-l} \frac{(n-r+2, n-r+3)}{\widehat{n-r+2}\ \ \widehat{n-r+3}} \left\{ -\tilde{P}_{q+2,l} + \frac{\widetilde{l+1}}{\widehat{l+1}} \hat{P}_{n-r+3,l} - \frac{\widetilde{q+1}}{\widehat{q+1}} \hat{P}_{n-r+3,q+1} \right\} \tag{3.61}$$

where $q = 1$ if $r = 2$, otherwise $q = 0$. We note that the expression in the braces vanishes when $r = 2$ and $l = 1$ given the wrap-around interpretation of P_{ij}. This is consistent with our statement earlier that this quantity is taken to vanish the lower limit of the inner sum exceeds the upper limit.

We now evaluate the remaining sum (3.61). First, we will treat the end case $l = n-1$ separately: here, the sum has only one term, $r = 2$, and (3.61) becomes

$$\frac{(n\,1)}{\hat{n}\hat{1}} \left\{ -\tilde{P}_{3,n-1} + \frac{\tilde{n}}{\hat{n}} \hat{P}_{1,n-1} - \frac{\tilde{2}}{\hat{2}} \hat{P}_{12} \right\} = \frac{(n\,1)}{\hat{n}\hat{1}} \left\{ \tilde{1} + \tilde{2} - \frac{\tilde{2}}{\hat{2}} (\hat{1} + \hat{2}) \right\}$$

which is clearly equal to (3.59). For the remaining $l < n-1$, we obtain a telescoping sum from the first term plus two sums of the form (3.60) from the remaining terms (treating the $r = 2$ term separately as necessary) to obtain

$$\tilde{P}_{1,l+1} \left(\frac{\tilde{1}}{\hat{1}} - \frac{\widetilde{l+1}}{\widehat{l+1}} \right) + \frac{\tilde{n}}{\hat{n}} \left(\frac{\hat{1}\tilde{2}}{\hat{2}} - \tilde{1} \right) + \frac{\tilde{1}}{\hat{1}} \left(-\tilde{P}_{3l} + \frac{\widetilde{l+1}}{\widehat{l+1}} \hat{P}_{1l} - \tilde{2} - \frac{\hat{1}\tilde{2}}{\hat{2}} \right) + \frac{\widetilde{l+1}}{\widehat{l+1}} \left(\tilde{P}_{2l} + \widetilde{l+1} + \frac{\tilde{1}}{\hat{1}} \hat{P}_{l+2,1} \right).$$

Applying conservation of momentum, this collapses to

$$\frac{\tilde{1}^2}{\hat{1}} + \frac{\tilde{n}}{\hat{n}} \left(\frac{\hat{1}\tilde{2}}{\hat{2}} - \tilde{1} \right) - \frac{\tilde{1}\tilde{2}}{\hat{2}} = -\frac{(n\,1)(1\,2)}{\hat{1}\hat{2}\hat{n}},$$

and thus the assertion of (3.58) is proved.

We note here that we have proved explicitly that Υ and Ξ, and hence the vertices formed by substituting their parent series (3.42) and (3.52) into (3.22) and (3.23) are holomorphic, in line with Mansfield's analytical argument. If follows that these vertices give the CSW continuation of the Parke–Taylor MHV amplitudes when taken off-shell.

3.4 Examples

Let us now verify that the field transformation as described above results in vertices proportional to the Parke–Taylor amplitudes. We will do this by computing the interaction terms in the MHV lagrangian for up to five gluons.

3.4.1 Three-gluon vertex

Since $\mathcal{A}$ ($\bar{\mathcal{A}}$) is $\mathcal{B}$ ($\bar{\mathcal{B}}$) to the lowest order, the three-gluon vertex is simply the vertex (3.22):

$$V^2(123) = i\frac{\hat{3}}{\hat{1}\hat{2}}(1\,2).$$

Conversely, (3.38) says it is

$$i\frac{\hat{3}}{\hat{1}\hat{2}}\frac{(1\,2)^3}{(2\,3)(3\,1)}$$

and conservation of momentum implies that $(1\,2) = (2\,3) = (3\,1)$, so the two expressions are equal and V^2 is of the Parke–Taylor form.

3.4.2 Four-gluon vertices

The four-gluon MHV vertices are the first to receive contributions from the next-to-leading order terms in (3.42) and (3.52), and so are more interesting tests of the technique. Both receive contributions from L^{--+} of (3.22), and (3.23), which is

$$L^{--++} = \int_{1234}\Big\{W^2(1234)\,\mathrm{tr}(\bar{\mathcal{A}}_{\bar{1}}\bar{\mathcal{A}}_{\bar{2}}\mathcal{A}_{\bar{3}}\mathcal{A}_{\bar{4}}) + \frac{1}{2}W^3(1234)\,\mathrm{tr}(\bar{\mathcal{A}}_{\bar{1}}\mathcal{A}_{\bar{2}}\bar{\mathcal{A}}_{\bar{3}}\mathcal{A}_{\bar{4}})\Big\}\,(2\pi)^3\delta^3(\textstyle\sum_{i=1}^4 \mathbf{p}_i), \quad (3.62)$$

written in Σ momentum space, where the coefficients

$$W^2(1234) = -\frac{\hat{1}\hat{3}+\hat{2}\hat{4}}{(\hat{1}+\hat{4})^2} \quad \text{and} \quad W^3(1234) = \frac{\hat{1}\hat{4}+\hat{2}\hat{3}}{(\hat{1}+\hat{2})^2} + \frac{\hat{1}\hat{2}+\hat{3}\hat{4}}{(\hat{1}+\hat{4})^2}$$

after symmetrization.

First, consider $A(1^-2^-3^+4^+)$, which is proportional to $V^2(1234)$ by (3.38). It comprises four terms in turn from substituting for:

1. the first $\bar{\mathcal{A}}$ in (3.22) with the $\mathcal{O}(\mathcal{B}\bar{\mathcal{B}})$ term in (3.52);
2. the second $\bar{\mathcal{A}}$ in (3.22) with the $\mathcal{O}(\bar{\mathcal{B}}\mathcal{B})$ term in (3.52);
3. the $\mathcal{A}$ in (3.22) with the $\mathcal{O}(\mathcal{B}^2)$ term in (3.42); and
4. the fields in (3.62) at the trivial leading order.

This gives

$$V^2(1234) = \frac{\hat{1}}{\bar{5}}V^2(523)\Xi^2(\bar{5}41) + \frac{\hat{2}}{\bar{5}}V^2(154)\Xi^1(\bar{5}23) + V^2(125)\Upsilon(\bar{5}34) + W^2(1234), \quad (3.63)$$

where $\mathbf{p}_5$ is determined by momentum conservation in each term (thus *e.g.* in the first term $\mathbf{p}_5 = \mathbf{p}_1 + \mathbf{p}_4$). To compare this formula to the expected result (3.38), we must write both as unique functions of independent momenta. We eliminate $\mathbf{p}_4$ using conservation

of momentum, and simplifying by partial fractions with the help of computer algebra, both (3.38) and (3.63) give:

$$\frac{(\hat{1}+\hat{2})^2(\hat{1}\tilde{2}-\hat{2}\tilde{1})}{\hat{1}\hat{2}\,[(\hat{1}+\hat{2})\tilde{3}-\hat{3}\tilde{1}-\hat{3}\tilde{2}]}-\frac{\hat{2}(\hat{1}+\hat{2}+\hat{3})(\hat{1}\tilde{2}-\hat{2}\tilde{1})}{\hat{1}(\hat{2}+\hat{3})(\hat{2}\tilde{3}-\hat{3}\tilde{2})}-\frac{\hat{1}\hat{3}(\hat{1}\tilde{2}-\hat{2}\tilde{1})}{\hat{2}(\hat{2}+\hat{3})(\hat{1}\tilde{2}+\hat{1}\tilde{3}-\hat{2}\tilde{1}-\hat{3}\tilde{1})}.$$

Thus we conclude that

$$V^2(1234)=\frac{\langle 1\,2\rangle^3}{\langle 2\,3\rangle\langle 3\,4\rangle\langle 4\,1\rangle}.$$

We treat $A(1^-2^+3^-4^+)$ similarly, and after symmetrization,

$$\begin{aligned}V^3(1234)=&\frac{\hat{1}}{\hat{5}}\,V^2(352)\Xi^2(\bar{5}41)+\frac{\hat{3}}{\hat{5}}\,V^2(512)\Xi^1(\bar{5}34)\\&+\frac{\hat{3}}{\hat{5}}\,V^2(154)\,\Xi^2(\bar{5}23)+\frac{\hat{1}}{\hat{5}}\,V^2(534)\Xi^1(\bar{5}12)+W^3(1234),\end{aligned}\quad(3.64)$$

and it is straightforward to confirm as above that this agrees with (3.38):

$$V^3(1234)=\frac{\hat{2}\hat{4}}{\hat{1}\hat{3}}\frac{(1\,3)^4}{(1\,2)(2\,3)(3\,4)(4\,1)}.$$

3.4.3 Five-gluon vertices

Finally, we calculate the coefficients of the five-gluon terms in the MHV lagrangian, $V^2(12345)$ and $V^3(12345)$. This calculation involves substituting up to the first three terms in the expansions (3.42) and (3.52) into both original vertices (3.22) and (3.23). We find that

$$\begin{aligned}V^2(12345)=&\frac{\hat{3}}{\hat{6}}\,V^2(612)\,\Xi^1(\bar{6}345)+\frac{\hat{1}}{\hat{7}}\,V^2(726)\Upsilon(\bar{6}34)\,\Xi^2(\bar{7}51)+V^2(126)\Upsilon(\bar{6}345)\\&+\frac{\hat{2}}{\hat{6}}\frac{\hat{1}}{\hat{7}}\,V^2(764)\,\Xi^1(\bar{6}23)\,\Xi^2(\bar{7}51)+\frac{\hat{2}}{\hat{6}}\,V^2(167)\,\Xi^1(\bar{6}23)\Upsilon(\bar{7}45)\\&+\frac{\hat{2}}{\hat{6}}\,V^2(165)\,\Xi^1(\bar{6}234)+W^2(1236)\Upsilon(\bar{6}45)+W^2(1265)\Upsilon(\bar{6}34)\\&+\frac{\hat{2}}{\hat{6}}\,W^2(1645)\,\Xi^1(\bar{6}23)+\frac{\hat{1}}{\hat{6}}\,W^2(6234)\,\Xi^2(\bar{6}51),\\V^3(12345)=&\frac{\hat{3}}{\hat{6}}\,V^2(612)\,\Xi^1(\bar{6}345)+\frac{\hat{1}}{\hat{6}}\,V^2(634)\,\Xi^2(\bar{6}512)+\frac{\hat{1}}{\hat{6}}\,V^2(637)\,\Xi^1(\bar{6}12)\Upsilon(\bar{7}45)\\&+\frac{\hat{1}}{\hat{6}}\frac{\hat{3}}{\hat{7}}\,V^2(675)\,\Xi^1(\bar{6}12)\,\Xi^1(\bar{7}34)+\frac{\hat{1}}{\hat{7}}\frac{\hat{3}}{\hat{6}}\,V^2(672)\,\Xi^1(\bar{6}34)\,\Xi^2(\bar{7}51)\\&+\frac{\hat{1}}{\hat{6}}\frac{\hat{3}}{\hat{7}}\,V^2(674)\,\Xi^2(\bar{6}51)\,\Xi^2(\bar{7}23)+\frac{\hat{3}}{\hat{6}}\,V^2(167)\,\Xi^2(\bar{6}23)\Upsilon(\bar{7}45)\\&+\frac{\hat{3}}{\hat{6}}\,V^2(165)\,\Xi^2(\bar{6}234)+\frac{\hat{1}}{\hat{6}}\,V^2(362)\,\Xi^3(\bar{6}451)+\frac{\hat{3}}{\hat{6}}\,W^2(1645)\,\Xi^2(\bar{6}23)\\&+\frac{\hat{1}}{\hat{6}}\,W^2(6345)\,\Xi^1(\bar{6}12)+\frac{\hat{3}}{\hat{6}}\,W^3(1265)\,\Xi^2(\bar{6}34)+\frac{\hat{1}}{\hat{6}}\,W^3(3462)\,\Xi^2(\bar{6}51)\\&+W^3(1236)\Upsilon(\bar{6}45)\end{aligned}$$

(where, like before, indices 6 and 7 label momenta that are uniquely determined in terms of the first five by momentum conservation). Again, we eliminate $\mathbf{p}_5$ in favour of the first four momenta and doing likewise for the corresponding right hand sides of (3.38), we find the expressions agree, and thus confirm that

$$V^2(12345) = -i\sqrt{2}\frac{\langle 1\,2\rangle^3}{\langle 2\,3\rangle\langle 3\,4\rangle\langle 4\,5\rangle\langle 5\,1\rangle},$$
$$V^3(12345) = -i\sqrt{2}\frac{\langle 1\,3\rangle^4}{\langle 1\,2\rangle\langle 2\,3\rangle\langle 3\,4\rangle\langle 4\,5\rangle\langle 5\,1\rangle}.$$

3.5 Summary and discussion

In this chapter, we have reviewed the construction of ref. [46] in which a lagrangian that produces the CSW rules of ref. [15] at tree-level is obtained by means of a canonical transformation of the gauge field variables $\mathcal{A}$ and $\bar{\mathcal{A}}$ of light-cone gauge Yang–Mills theory. This transformation absorbs the kinetic term and $\overline{\text{MHV}}$ vertex into the kinetic term of the theory in terms of the new variables $\mathcal{B}$ and $\bar{\mathcal{B}}$ according to

$$L^{-+}[\mathcal{A},\bar{\mathcal{A}}] + L^{-++}[\mathcal{A},\bar{\mathcal{A}}] = L^{-+}[\mathcal{B},\bar{\mathcal{B}}],$$

and the interaction part of the MHV lagrangian comes from expressing $L^{--+} + L^{--++}$ in terms of $\mathcal{B}$ and $\bar{\mathcal{B}}$.

We then solved for the explicit form of $\mathcal{A}$ and $\bar{\mathcal{A}}$ as power series in $\mathcal{B}$ and $\bar{\mathcal{B}}$ and found that the coefficients take a particularly simple form. We summarise these results below:

$$\mathcal{A}_1 = \sum_{n=2}^{\infty}\int_{2\cdots n}\Upsilon(1\cdots n)\mathcal{B}_{\bar{2}}\cdots\mathcal{B}_{\bar{n}}\,(2\pi)^3\delta^3(\textstyle\sum_{i=1}^n \mathbf{p}_i),$$
$$\bar{\mathcal{A}}_1 = \sum_{m=2}^{\infty}\sum_{s=2}^{m}\int_{2\cdots m}\frac{\hat{s}^2}{\hat{1}^2}\Upsilon(1\cdots m)\mathcal{B}_{\bar{2}}\cdots\bar{\mathcal{B}}_{\bar{s}}\cdots\mathcal{B}_{\bar{m}}\,(2\pi)^3\delta(\textstyle\sum_{i=1}^m \mathbf{p}_i),$$

where the coefficient

$$\Upsilon(1\cdots n) = (-i)^n\frac{\widehat{\hat{1}\hat{3}\cdots n-1}}{(2\,3)\cdots(n-1,n)}.$$

We note that this transformation is local in light-cone time, but non-local in the quantisation surface. The validity of this was tested by computing the terms of the MHV lagrangian for up to five gluons and showing that the vertices are the Parke–Taylor MHV amplitudes, continued off-shell by the CSW prescription. Essential to this is the holomorphic nature of the transformation, and hence the vertices, which is demonstrated explicitly. The algebraic manipulations used in this process were greatly aided by the use of (3.6) to express the spinor invariants in terms of light-cone co-ordinates.

The significance of this work lies in the field-theoretic understanding it gives to the CSW construction, which here is seen to be underpinned by light-cone quantisation. Furthermore, since they have now been shown to have a Lagrangian formulation, we can proceed to apply well understood quantum field theory techniques. Of particular

relevance to the phenomenological programme is the calculation of quantum corrections, and hence the regularisation of the MHV lagrangian: we simply take our favourite regulator, and observe the consequences unfold as we apply the transformation This will be considered further in the next chapter, where we will perform such an analysis for dimensional regularisation; unfortunately, we will see that this comes at the expense of the simplicity of formalism that we have in four dimensions.

3.5.1 The Case of the Missing Amplitudes

We hinted at the end of section 2.8 the CSW rules were in a sense 'incomplete', in that it was impossible using vertices with an MHV helicity content alone to construct loop amplitudes with up to one gluon of negative helicity and an arbitrary number of positive helicity. This is a particular annoyance since in pure Yang–Mills, amplitudes like (++++) at one loop are non-vanishing *viz.* (2.62). Even more fundamentally, the $\overline{\text{MHV}}$ amplitude is also missing. This takes the value

$$A(1^-, 2^+, 3^+) = ig\frac{[2\,3]^3}{[3\,1][1\,2]}. \tag{3.65}$$

For this to be non-vanishing in the on-shell limit, we need to work with complex momenta or a space-time with a $(2,2)$ signature metric; in either circumstance, $\tilde{\lambda}$ is not necessarily the complex conjugate of λ, so $[i\,j]$ does not have to vanish as $p_i \cdot p_j \propto \langle i\,j\rangle[i\,j] \to 0$.

But all is not lost: the next chapter addresses this issue by showing that under certain circumstances the transformation 'evades' the S-matrix equivalence theorem, bringing in contributions that allow us to recover precisely these missing pieces.

3.A Canonical transformations

The aim of this appendix is not to give a complete treatment of the subject of canonical transformations (which may be found in the literature, *e.g.* [99]), but rather develop the points and results relevant to the main text.

A canonical transformation is a map from one set of phase space co-ordinates $\mathbf{q} = (q^1, \ldots, q^n)$ and $\mathbf{p} = (p_1, \ldots, p_n)$ (the conjugate momenta) for a system with hamiltonian H onto another set $\mathbf{Q}$, $\mathbf{P}$ with hamiltonian K such that this map preserves the *form* of Hamilton's equations of motion, *i.e.*

$$\begin{pmatrix}\dot{\mathbf{q}}\\ \dot{\mathbf{p}}\end{pmatrix} = \begin{pmatrix}0 & +1\\ -1 & 0\end{pmatrix}\begin{pmatrix}\partial H/\partial\mathbf{q}\\ \partial H/\partial\mathbf{p}\end{pmatrix} \quad\longleftrightarrow\quad \begin{pmatrix}\dot{\mathbf{Q}}\\ \dot{\mathbf{P}}\end{pmatrix} = \begin{pmatrix}0 & +1\\ -1 & 0\end{pmatrix}\begin{pmatrix}\partial K/\partial\mathbf{Q}\\ \partial K/\partial\mathbf{P}\end{pmatrix}. \tag{3.66}$$

There are a number of equivalent ways to approach the analysis of canonical transformations. First, let us consider the generating function approach. Hamilton's equations of motion (3.66) may be obtained from the variational principle: under an arbitrary variation δ of the phase space co-ordinates, the action in both variables must be stationary,

i.e.

$$\delta \int_a^b (\dot{q}^i p_i - H)\, dt = 0,$$
$$\delta \int_a^b (\dot{Q}^i P_i - K)\, dt = 0.$$

where a dot denotes a total derivative with respect to time, t. Now in order that both of these are satisfied, we must have

$$\lambda(\dot{q}^i p_i - H) = \dot{Q}^i P_i - K + \frac{dF}{dt}. \tag{3.67}$$

Here, F may depend on t and any of the phase space co-ordinates (in which it must have continuous second derivatives). We can add a total time derivative of it on the RHS above since the variation is taken to vanish at $t = a$ and $t = b$, and so it does not affect the variational integrals. We can then obtain expressions relating the two sets of phase space co-ordinates in terms of partial derivatives of F, hence it is referred to as the *generating function.*

Let us study the particular case where

$$F(\mathbf{q}, \mathbf{P}) = f^i(\mathbf{q}) P_i - Q^i P_i, \tag{3.68}$$

where the Q^i on the RHS may be regarded as functions of $\mathbf{q}$ and $\mathbf{P}$.[4] Then

$$\frac{dF}{dt} = \dot{q}^i \frac{\partial f^j}{\partial q^i} P_j + f^i(\mathbf{q}) \dot{P}_i - \dot{Q}^i P_i - Q^i \dot{P}_i,$$

which we plug into the RHS of (3.67) (setting $\lambda = 1$ by scaling the co-ordinates in a straightforward manner if necessary). Since we may regard $\mathbf{q}$ and $\mathbf{P}$ as independent variables, this equation is only satisfied if

$$H = K,$$
$$Q^i = f^i(\mathbf{q}), \tag{3.69}$$
$$p_i = \frac{\partial f^j}{\partial q^i} P_j = \frac{\partial Q^j}{\partial q^i} P_j. \tag{3.70}$$

Under these conditions, $\dot{F}$ vanishes and one immediate consequence from (3.67) is that

$$\dot{q}^i p_i = \dot{Q}^i P_i. \tag{3.71}$$

Let us now generalise to *contact transformations*, time-independent transformations of the phase space co-ordinates (both co-ordinates and momenta); clearly, the transformation described above is an example of this. The hamiltonian is invariant under such a transformation, *i.e.* $H = K$, which can be shown by extending the generating function

[4] This is a particular case of the 'Type 2' canonical transform in chapter 9 of [99].

approach to other forms of F using Legendre transforms, or alternatively by considering the hamiltonian as a scalar function on the phase space manifold. Taking this geometric viewpoint, we can deduce some important conditions that canonical transformations must satisfy in general. If we apply the chain rule to the first equation of (3.66), we have

$$\begin{aligned}\begin{pmatrix}\dot{\mathbf{q}}\\ \dot{\mathbf{p}}\end{pmatrix} &= \frac{\partial(\mathbf{Q},\mathbf{P})}{\partial(\mathbf{q},\mathbf{p})}\begin{pmatrix}\dot{\mathbf{Q}}\\ \dot{\mathbf{P}}\end{pmatrix}\\ &= \frac{\partial(\mathbf{Q},\mathbf{P})}{\partial(\mathbf{q},\mathbf{p})}\begin{pmatrix} & +1\\ -1 & \end{pmatrix}\begin{pmatrix}\partial K/\partial\mathbf{Q}\\ \partial K/\partial\mathbf{P}\end{pmatrix}\\ &= \frac{\partial(\mathbf{Q},\mathbf{P})}{\partial(\mathbf{q},\mathbf{p})}\begin{pmatrix} & +1\\ -1 & \end{pmatrix}\frac{\partial(\mathbf{Q},\mathbf{P})}{\partial(\mathbf{q},\mathbf{p})}^{\mathrm{T}}\begin{pmatrix}\partial H/\partial\mathbf{q}\\ \partial H/\partial\mathbf{p}\end{pmatrix},\end{aligned}$$

where the Jacobian matrix

$$\frac{\partial(\mathbf{Q},\mathbf{P})}{\partial(\mathbf{q},\mathbf{p})} \equiv \begin{pmatrix}\partial\mathbf{Q}/\partial\mathbf{q} & \partial\mathbf{Q}/\partial\mathbf{p}\\ \partial\mathbf{P}/\partial\mathbf{q} & \partial\mathbf{P}/\partial\mathbf{p}\end{pmatrix}.$$

Comparing with the first equation in (3.66), we infer that a canonical transform must satisfy

$$\begin{pmatrix} & +1\\ -1 & \end{pmatrix} = \frac{\partial(\mathbf{Q},\mathbf{P})}{\partial(\mathbf{q},\mathbf{p})}\begin{pmatrix} & +1\\ -1 & \end{pmatrix}\frac{\partial(\mathbf{Q},\mathbf{P})}{\partial(\mathbf{q},\mathbf{p})}^{\mathrm{T}}. \tag{3.72}$$

This leads us immediately to an important result for canonical transformations: a theorem, due to Liouville, that states the phase space volume element is invariant under a canonical transformation. In particular,

$$d\mathbf{Q}\wedge d\mathbf{P} = \left|\det\frac{\partial(\mathbf{Q},\mathbf{P})}{\partial(\mathbf{q},\mathbf{p})}\right| d\mathbf{q}\wedge d\mathbf{p},$$

but taking the determinant of both sides of (3.72) tells us that

$$\det\frac{\partial(\mathbf{Q},\mathbf{P})}{\partial(\mathbf{q},\mathbf{p})} = \pm 1,$$

and thus the claim is proved.

The important point of this appendix is that we have shown that an arbitrary change of the canonical co-ordinates given by (3.69) induces a canonical transformation given that the momenta transform as (3.70), and that this transformation preserves the kinetic term (3.71) and the phase space measure. It should be noted here that these results hold also for mixtures of c-number and Grassman-valued dynamical variables, provided the order of the factors is preserved. When generalising to field theory, of course the partial derivatives are promoted to functional derivatives, and the sums over co-ordinate indices to integrals.

3.B The S-matrix equivalence theorem

The S-matrix equivalence theorem [100] states that while an invertible change of field variables modifies correlation functions, it does not affect the S-matrix elements derived thereof, up to a wavefunction renormalisation.

Let us illustrate this concretely using a toy scalar model. We compute correlation functions from the model's partition function

$$\mathcal{Z}[j] = \int \mathcal{D}\phi \, \exp i \left\{ I[\phi] + \int d^4x \, j\phi \right\} \tag{3.73}$$

for some action $I[\phi]$ by taking functional derivatives with respect to $j(x)$ at $j = 0$. Then the LSZ theorem gives us the S-matrix elements as

$$\begin{aligned} \langle \mathbf{q}_1 \cdots \mathbf{q}_m | S | \mathbf{p}_1 \cdots \mathbf{p}_n \rangle = Z_2^{-(m+n)/2} \prod_{i=1}^{m} \int d^4x_i \, e^{-ip_i \cdot x_i} \Delta^{-1}(x_i) \frac{\delta}{i\delta j(x_i)} \\ \times \prod_{j=1}^{n} \int d^4y_j \, e^{+iq_j \cdot y_j} \Delta^{-1}(y_j) \frac{\delta}{i\delta j(y_j)} \left. \frac{\mathcal{Z}[j]}{\mathcal{Z}_0} \right|_{j=0} \end{aligned} \tag{3.74}$$

where Δ^{-1} is the kinetic operator, Z_2 is the field strength renormalisation, and $\mathcal{Z}_0$ is the free partition function.

Now let us write the action in terms of a new field variable ϕ' given implicitly by the invertible transformation $\phi = \phi' + F[\phi', \partial_\mu \phi', \partial_\mu \partial_\nu \phi', \dots]$, where F is a *regular* function(al) of ϕ' and its derivatives. (If this change of variables has a non-unit jacobian, we can ignore it for the purposes of this discussion.) Then (3.73) becomes

$$\mathcal{Z}[j] = \int \mathcal{D}\phi' \, \exp i \left\{ I[\phi' + F] + \int d^4x \, j(\phi' + F) \right\}. \tag{3.75}$$

If we define a new action

$$I'[\phi'] := I[\phi' + F]$$

then the equivalence theorem tells us that we can just as well use

$$\mathcal{Z}'[j] = \int \mathcal{D}\phi' \, \exp i \left\{ I'[\phi'] + \int d^4x \, j\phi' \right\} \tag{3.76}$$

in (3.74) as the original $\mathcal{Z}[j]$.

Upon taking functional derivatives with respect to j, we see that additional terms of ϕ'^2 and higher powers hidden in F are pulled down from the exponential: an insertion of $\phi'^n(x)$ will connect to n propagators, whose momenta sum to that associated with x by the Fourier transform. Unlike when $n = 1$, these propagators will not, in general, cancel the inverse propagator from LSZ reduction and thus vanish in the on-shell limit. Hence, we can truncate the source term in (3.75) to $\int d^4x j\phi'$. At the quantum level, self-energy-like terms can be made from insertions of $\phi'^n(x)$, but these will alter scattering amplitudes by at most a wavefunction renormalisation.

Chapter 4

Equivalence Theorem Evasion and Dimensional Regularisation

In the previous chapter, we saw that by applying a canonical change of variables to light-cone Yang–Mills theory, we obtained the Canonical MHV Lagrangian: one with Parke–Taylor MHV vertices and Feynman rules that follow the CSW rules. In our closing comments in section 3.5, we noted a number of shortcomings. First, there are the so-called 'missing' amplitudes: using the vertex content alone, it is impossible to construct certain non-vanishing objects, significantly the one-loop amplitudes with at most one negative-helicity gluon (something we also mentioned in our review in section 2.8). It was also noted that the $\overline{\text{MHV}}$ amplitude at tree-level, which does not vanish for complex momenta or in $(2,2)$-signature space-times, does not appear in the theory. Secondly, we note that the CSW rules don't appear to suggest in a natural manner how one should go about imposing a regularisation structure, which would be required for a complete treatment of the theory at the quantum level. Can our lagrangian formulation be extended to provide this? In this chapter, we will begin to address these issues.

This chapter may be considered to be divided into two segments. The first, in section 4.1, introduces the notion of *completion vertices*: contributions to the S-matrix that arise from the canonical transformation itself. We use these to recover the tree-level $(-{+}{+})$ amplitude by a mechanism that evades S-matrix equivalence theorem. We then consider their role in tree-level amplitudes in general.

The second segment (sections 4.3 and 4.4) works towards understanding the construction of the missing one-loop all-$+$ amplitudes in pure Yang–Mills. We begin by applying the canonical transformation to a light-cone Yang–Mills theory which has been extended to D dimensions in a particular manner, which we use to derive D-dimensional completion coefficients and associated completion vertices. Equivalence theorem evading contributions are used to construct the one-loop $(+{+}{+}{+})$ amplitude, and we analyse their cuts to demonstrate that the quadruple cut of the propagators coincides with that of the known one-loop $(+{+}{+}{+})$ amplitude. Then we demonstrate that [for a particular momentum routing topology] that the equivalence theorem evading contributions

sum up precisely to the amplitude one would have obtained using light-cone Yang–Mills theory.

Finally, we draw our conclusions on this chapter in section 4.5.

This work was published in [49].

4.1 MHV completion vertices and evading the equivalence theorem

Let us re-visit (3.26), which defined the canonical transformation by absorbing the $\overline{\text{MHV}}$ vertex into the kinetic part of the theory in terms of $\mathcal{B}$ and $\bar{\mathcal{B}}$. Written in quantisation surface momentum space, the $\overline{\text{MHV}}$ vertex is

$$L^{-++} = \text{tr} \int_{123} \bar{V}^2(123)\, \mathcal{A}_{\bar{1}} \mathcal{A}_{\bar{2}} \bar{\mathcal{A}}_{\bar{3}}\, (2\pi)^3 \delta^3(\mathbf{p}_1 + \mathbf{p}_2 + \mathbf{p}_3) \tag{4.1}$$

where

$$\bar{V}^2(123) = i \frac{\hat{3}}{\hat{1}\hat{2}} \{1\, 2\}. \tag{4.2}$$

Now had we written (3.41) retaining $\bar{V}^2$ rather than writing it out explicitly, we would have arrived at the following recurrence relation for Υ:

$$\Upsilon(1 \cdots n) = -\frac{1}{\hat{1}(\sum_{i=1}^n \omega_i)} \sum_{j=2}^{n-1} \bar{V}^2(P_{2j}, P_{j+1,n}, 1) \Upsilon(-, 2, \ldots, j) \Upsilon(-, j+1, \ldots, n), \tag{4.3}$$

whence

$$\Upsilon(123) = -\frac{\bar{V}^2(231)}{\hat{1}(\omega_1 + \omega_2 + \omega_3)} = \frac{2\bar{V}^2(231)}{\hat{1}(P_1 + P_2 + P_3)}. \tag{4.4}$$

Here, $P_i := p_i^2/\hat{\imath}$, and the second line follows using (4.78).

Now clearly this can be performed for any choice of $\bar{V}^2$. Furthermore, the derivation of the series for $\bar{\mathcal{A}}$ in section 3.3.2 does not involve $\bar{V}^2$, so the recurrence relation (3.55) still holds and taken together with (4.3), we have a recipe for computing the series expansions of $\mathcal{A}$ and $\bar{\mathcal{A}}$. This is an important indicator as to how amplitudes involving the 'missing' $\overline{\text{MHV}}$ vertex $\bar{V}^2$ are recovered, and to demonstrate that the recovery mechanism is generic in any theory where a canonical transformation is used to absorb a three-point vertex into a kinetic term.

4.1.1 Defining completion vertices

At the end of section 3.1.2, we commented on how scattering amplitudes can be formed by applying the LSZ reduction to correlation functions of $\mathcal{A}$ and $\bar{\mathcal{A}}$ fields. Let us write such a (momentum space) correlation function somewhat schematically as

$$\langle \cdots \mathcal{A}(p) \cdots \bar{\mathcal{A}}(q) \cdots \rangle.$$

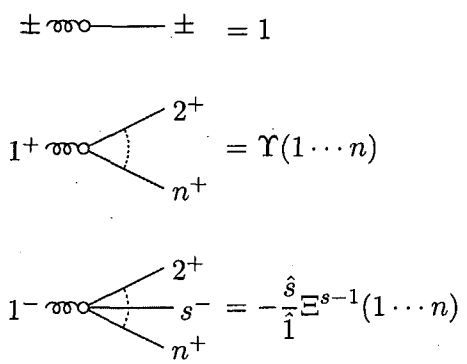

FIGURE 4.1: The MHV completion vertices: graphical representations of the Υ and Ξ coefficients of the series expansion of $\mathcal{A}$ and $\bar{\mathcal{A}}$. The wavy lines with a $+(-)$ denote insertions of $\mathcal{A}(\bar{\mathcal{A}})$ operators in correlation functions; $\mathcal{B}$ and $\bar{\mathcal{B}}$ attach to the straight lines. All momenta are outgoing.

However, it is now the $\mathcal{B}$ fields which propagate in the theory. Therefore, we must regard $\mathcal{A}$ and $\bar{\mathcal{A}}$ above as functions of $\mathcal{B}$ and $\bar{\mathcal{B}}$ and make the replacements from the series; again, schematically we can write this as (neglecting the field normalisation factors and integral symbols for clarity)

$$\langle \cdots \left(\sum_n \Upsilon_{p2\cdots n} \mathcal{B}_{\bar{2}} \cdots \mathcal{B}_{\bar{n}} \right) \cdots \left(- \sum_{n,s} \frac{\hat{\hat{s}}}{\hat{q}} \Xi^{s-1}_{q2\cdots n} \mathcal{B}_{\bar{2}} \cdots \bar{\mathcal{B}}_{\bar{s}} \cdots \mathcal{B}_{\bar{n}} \right) \cdots \rangle. \tag{4.5}$$

Order-by-order, we take Wick contractions between the $\mathcal{B}$ field's operators using its propagator. This naturally lends itself to a Feynman graph representation where we have vertices for the coefficients of the series (3.42) and (3.52), and they are shown in fig. 4.1. We refer to these vertices as 'MHV completion vertices' and graphs built from them as 'MHV completion graphs' since they allow the construction of amplitudes otherwise absent from the theory. Each vertex, which we have drawn here with an empty circle, corresponds to the insertion of an $\mathcal{A}$ or $\bar{\mathcal{A}}$ operator, labelled diagrammatically by the sign on the curly line. Of course, $\mathcal{B}$ propagators attach only to the straight lines.

Note that the figure shows the vertices appropriate for $\mathcal{A}$, $\mathcal{B}$, etc. so that the normalisation factors of (3.8) can be omitted for clarity. If one wishes to work with canonical normalisation, as we will do in the rest of this chapter, we make the replacements

$$\frac{4i}{g^2} V^s(1 \cdots n) \to \frac{4i}{g^2} \left(-\frac{ig}{\sqrt{2}} \right)^n V^s(1 \cdots n), \tag{4.6}$$

$$\Upsilon(1 \cdots n) \to \left(-\frac{ig}{\sqrt{2}} \right)^{n-2} \Upsilon(1 \cdots n), \tag{4.7}$$

$$\Xi^s(1 \cdots n) \to \left(-\frac{ig}{\sqrt{2}} \right)^{n-2} \Xi^s(1 \cdots n), \tag{4.8}$$

which for V^s also includes the normalisation of the action.

4.1.2 Equivalence theorem evasion: the tree-level $(-++)$ amplitude

Let us now use the completion vertices to recover the tree-level $(-++)$ amplitude. By (3.25), this is obtained by amputating the $\langle A\bar{A}\bar{A}\rangle$ correlation function. The diagrams for this are shown in fig. 4.2, from which we see we need to take the limit as $p_1^2, p_2^2, p_3^2 \to 0$ of

$$\begin{aligned} &-ip_1^2p_2^2p_3^2 \times \left(-\frac{ig}{\sqrt{2}}\right) \times (-1)^3 \times \left\{\frac{1}{p_2^2}\frac{1}{p_3^2}\Upsilon(123) - \frac{1}{p_3^2}\frac{1}{p_1^2}\frac{\hat{1}}{\hat{2}}\Xi^2(231) - \frac{1}{p_1^2}\frac{1}{p_2^2}\frac{\hat{1}}{\hat{3}}\Xi^1(312)\right\} \\ &= \frac{ig}{\sqrt{2}}\frac{\hat{1}^2}{(2\,3)}\left(\frac{p_1^2}{\hat{1}} + \frac{p_2^2}{\hat{2}} + \frac{p_3^2}{\hat{3}}\right). \end{aligned} \tag{4.9}$$

In the first line, the leading factor of $-i$ comes from an un-cancelled inverse propagator, the second from the restoration of the canonical normalisation using (3.8), and the third is the gluon polarisation factor. Three-particle kinematics mean that this does not vanish in the null limit: using (4.77) cancels the factor of $(2\,3)$ in the denominator but leaves a $\{1\,3\} = -\{2\,3\}$ in the numerator, giving the $\overline{\text{MHV}}$ amplitude. However, we can see this in a more direct manner if we use the first equalities of (3.56) and (3.57) to substitute for Ξ^1 and Ξ^2 in favour of Υ,[1] then use (4.4) and notice that for (4.2)

$$\bar{V}^2(231) = \frac{\hat{1}^2}{\hat{2}^2}\bar{V}^2(312) = \frac{\hat{1}^2}{\hat{3}^2}\bar{V}^2(123),$$

the first line of (4.9) simplifies immediately to

$$g\sqrt{2}\bar{V}^2(231),$$

which is precisely the $\overline{\text{MHV}}$ amplitude we sought. Notice that this occurred *before* taking the on-shell limit, and without any reference to the specific form of $\bar{V}^2$. Evaluating $\bar{V}^2$ and using (3.6), we arrive at the result

$$A(1^-, 2^+, 3^+) = g\sqrt{2}\bar{V}^2(231) = ig\sqrt{2}\frac{\hat{1}}{\hat{2}\hat{3}}\{2\,3\} = ig\frac{[2\,3]^3}{[3\,1][1\,2]}, \tag{4.10}$$

which is precisely the Parke–Taylor $\overline{\text{MHV}}$ amplitude given in (3.65)

The origin of equivalence theorem evasion

It would appear here that the S-matrix equivalence theorem, as described in section 3.B has been violated, since recovering a non-vanishing amplitude from a theory in which it is ostensibly absent is certainly not a wave-function renormalisation. Clearly, what has

[1] We note here that in (3.56) and (3.57), and the following three formulae for the four-point Ξ coefficients, the first equality in each is derived directly from the recurrence relation (3.55), and as such is independent of the exact form of $\bar{V}^2$. The subsequent equalities depend on knowing the form of Υ and hence $\bar{V}^2$.

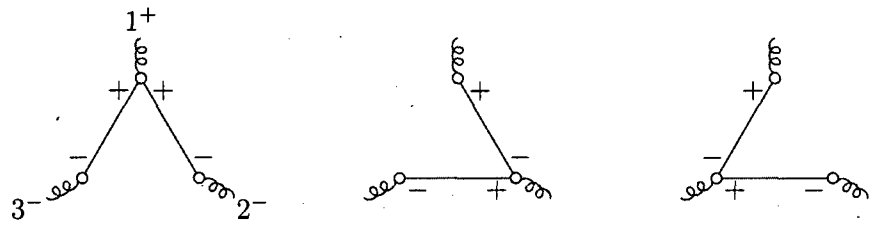

FIGURE 4.2: Contributions to the tree-level $(--++)$ amplitude, before applying LSZ reduction.

happened is that the transformation itself does not completely satisfy the hypothesis of the theorem, in particular regarding locality.

The presence of momenta in the denominators of Υ, or equivalently inverse derivatives, shows that the transformation is non-local on the quantisation surface. However, it is local in light-cone time; moreover, it contains no x^0 dependence, hence the absence of any terms in $\check{p}$. As such, one would not expect it to generate the factor of $1/p^2$ required to cancel the inverse propagator from the LSZ reduction to allow the graph to survive the on-shell limit. It is therefore somewhat remarkable that there exist conditions under which the theorem is circumvented: what we have seen here is the terms in the first factor of the recurrence relation (4.3) collecting together so that the factor $\sum_j p_j^2/\hat{j}$ is formed (by (4.78)) despite such terms being independent of $\check{p}$.

4.2 Higher order tree-level amplitudes

The proof given in section 3.2.2 that the vertices of the Canonical MHV Lagrangian were the Parke–Taylor amplitudes continued off shell by the CSW prescription relied on the tree-level amplitudes and vertices agreeing (up to polarisation) when on shell. One might begin to worry at this point that the presence of these completion vertices could contribute to MHV amplitudes and spoil this. Indeed, it is possible to construct tree diagrams involving completion vertices that contribute to MHV (and higher) helicity configurations. For example, fig. 4.3 shows the completion vertex contributions to $A(1^-2^-3^+4^+)$. Consider the first, fig. 4.3(a): the contribution of this graph is proportional to

$$\hat{1}P_4\Xi^1(4,1,2+3)\frac{1}{(p_1+p_4)^2}V^2(4+1,2,3)$$
$$= -\hat{1}P_4\frac{2\bar{V}^2(2+3,4,1)}{\hat{1}(P_1+P_{2+3}+P_4)}\frac{1}{(p_1+p_4)^2}V^2(4+1,2,3),$$

For generic momenta, the momentum p_1+p_4 which runs through the gluon propagator will not be null, and as such the expression above cannot produce the $1/p_4^2$ pole required for it to survive the on-shell limit. By considering the other diagrams similarly, we see that they also make no contribution in the on-shell limit.

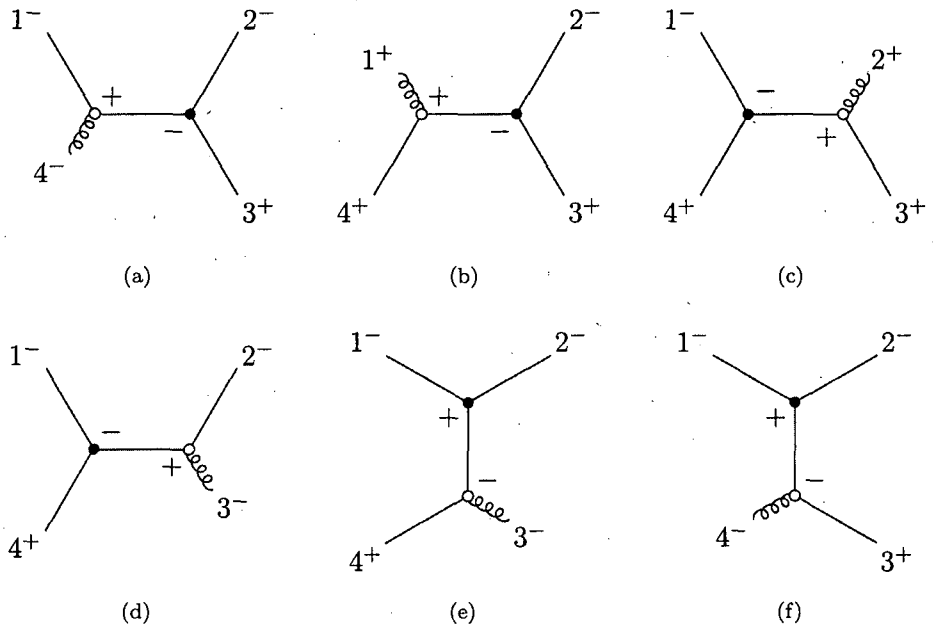

FIGURE 4.3: Graphs containing completion vertices that contribute to the amplitude $A(1^-2^-3^+4^+)$. These annihilated in the on-shell limit of the LSZ reduction since the momentum in the propagator is generically off-shell, and the completion vertices cannot provide the $1/p_i^2$ pole required.

More generally this happens because the helicity content of MHV and N^{r}MHV ($r \geq 1$) amplitudes require that any completion vertex/vertices is/are attached to a propagator(s) which at tree-level will carry non-null momenta. By considering the explicit form of Υ, or moreover by inspecting (4.3), it is clear that the completion vertices cannot generate the required poles to ensure their survival of the LSZ reduction. Thus, MHV completion vertices make no contribution to the non-vanishing tree-level on-shell amplitudes for four or more gluons, and the proof at the end of section 3.2 still holds.

What of the $A(1^-2^+\cdots n^+)$ tree-level amplitude for $n \geq 4$? Its helicity configuration permits contributions of the form of a *single* completion vertex connected to no internal propagators, which we might expect to survive. The completion vertex contribution to this amplitude is proportional to the on-shell limit of

$$\hat{1}P_1\Upsilon(1\cdots n) - \hat{1}\sum_{j=2}^{n} P_j\Xi^{n-j+1}(j,\ldots,n,1,\ldots,j-1).$$

Now we can see from (3.55) that all terms but one in a Ξ, namely a lone Υ with the same number of arguments as the Ξ, consist of products of Υs with generically off-shell momentum arguments. We therefore discard these terms for the same reasons as above (they cannot generate the poles required for survival of LSZ), and make the replacement $\Xi^r(1\cdots n) \to \Upsilon(r+1,\ldots,n,1,\ldots,r)$ to obtain

$$\hat{1}(P_1+\cdots+P_n)\,\Upsilon(1\cdots n). \tag{4.11}$$

However, for $n \geq 4$ we know that all other contributions to this amplitude vanish, as does the amplitude itself, so (4.11)·must also vanishes on shell. It is easy to see that it does simply by inspection using the explicit form of $\Upsilon(1234\cdots n)$ in (3.51), which has only co-linear singularities.

4.2.1 Tree-level off-shell reconstruction

Although completion vertices have no contribution to on-shell tree-level amplitudes, we expect them to contribute off shell to recover the underlying light-cone Yang–Mills theory. That this is so is strongly hinted at by the recurrence relations (4.3) and (3.55) which express the Υ and Ξ vertices as sums of terms proportional to $\bar{V}^2$ vertices in a manner that consistently matches up the external helicities (after amputation). So, although the individual graphs of fig. 4.3 do not correspond to LCYM graphs due to the denominator in the leading factor on the RHS of (4.3), we might expect that when summed and added to the contributions from the graphs constructed with MHV vertices, the inverse propagators supplied by the LSZ reduction cancel the denominators to leave the LCYM graphs, before taking the on-shell limit.

An example: tree-level $A(1^-2^-3^+4^+)$

Let us demonstrate this in the case of $A(1^-2^-3^+4^+)$. By a fairly straightforward calculation, we can see that by taking the sum of the graphs of fig. 4.3, multiplying by the inverse propagators, and then adding the contribution from $V^2(1234)$ (the $(--++)$ vertex from the Canonical MHV Lagrangian shown in (3.63)), we reconstruct *algebraically* the off-shell amplitude as computed with LCYM Feynman rules. It is instructive to illustrate at least in part how this works, and since the topology of the momentum routing between the vertices on the MHV lagrangian side must match that of the LCYM graphs we seek to recover, we can consider just the $(1,2)$ channel, *i.e.* the contribution from figs. 4.3(e) and 4.3(f) and from the third term in (3.63) (its first two terms clearly have the topology of the $(1,4)$ channel, and the last term is just the $(--++)$ vertex from light-cone Yang–Mills theory). Restoring the normalisation of A, these terms are, respectively

$$
\begin{aligned}
& ig^2V^2(1,2,3+4)\Upsilon(1+2,3,4) \\
& + ig^2V^2(1,2,3+4)\frac{1}{(p_1+p_2)^2}\left(-\frac{\hat{1}+\hat{2}}{\hat{3}}\right)\Xi^2(3,4,1+2)\,\hat{3}P_3 \\
& + ig^2V^2(1,2,3+4)\frac{1}{(p_1+p_2)^2}\left(-\frac{\hat{1}+\hat{2}}{\hat{4}}\right)\Xi^1(4,1+2,3)\,\hat{4}P_4 \\
& = 2ig^2\frac{1}{(p_1+p_2)^2}V^2(1,2,3+4)\bar{V}^2(3,4,1+2)\left\{\frac{P_{1+2}}{P_{1+2}+P_3+P_4}\right. \\
& \quad \left. + \frac{P_3}{P_{1+2}+P_3+P_4} + \frac{P_4}{P_{1+2}+P_3+P_4}\right\},
\end{aligned}
$$

where we have used the first equality of (3.56) and (3.57) to evaluate Ξ^1 and Ξ^2. This is of course trivially equal to

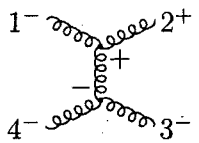

$$= 2g^2 V^2(1,2,3+4)\frac{i}{(p_1+p_2)^2}\bar{V}^2(3,4,1+2).$$

We shall see in section 4.4 that the same features are responsible for the recovery of the all-+ one-loop amplitudes.

4.3 The D-Dimensional Canonical MHV Lagrangian

The treatment of quantum corrections to amplitudes in the canonical MHV lagrangian formalism will require that the theory be regulated, and we will do so by dimensional regularisation. It turns out that we can then apply the canonical transformation procedure essentially as before, save for the fact that pieces outside four dimensions result in much richer structure and hence more complicated MHV rules.

4.3.1 Light-cone Yang-Mills in D dimensions

We write the co-ordinates in $D = 4 - 2\epsilon$ dimensions as:

$$x^0 = \tfrac{1}{\sqrt{2}}(t - x^{D-1}), \qquad z^I = \tfrac{1}{\sqrt{2}}(x^{2I-1} + ix^{2I}),$$
$$x^{\bar{0}} = \tfrac{1}{\sqrt{2}}(t + x^{D-1}), \qquad \bar{z}^I = \tfrac{1}{\sqrt{2}}(x^{2I-1} - ix^{2I}),$$

where the index I runs over the $\frac{1}{2}(2-2\epsilon)$ pairs of transverse directions. In these co-ordinates, the metric takes block diagonal form with non-zero components $g_{0\bar{0}} = g_{\bar{0}0} = 1$, $g_{z^I\bar{z}^J} = g_{\bar{z}^I z^J} = -\delta_{IJ}$. Again, we introduce a more compact notation for the components of 1-forms and momenta, for which we write $(p_0, p_{\bar{0}}, p_{z^I}, p_{\bar{z}^J}) \equiv (\check{p}, \hat{p}, p_I, \bar{p}_I)$, with $(\check{n}, \hat{n}, n_I, \bar{n}_I)$ for momenta labelled by a number.

The reason we make this choice of basis is that it will lead us again to a lagrangian with an MHV structure and thus inherit some of the simplicity of MHV rules in four space-time dimensions, for example the tree-level properties that the first non-vanishing vertices are MHV vertices, that NMHV amplitudes are constructed by joining precisely two such vertices together by the propagator and so on.

In these co-ordinates, the invariant becomes

$$A \cdot B = \check{A}\hat{B} + \hat{A}\check{B} - A_I\bar{B}_I - \bar{A}_I B_I, \tag{4.12}$$

where we have assumed the summation convention that a repeated capital Roman index in a product is summed over $1, \ldots, 1-\epsilon$. The bilinears of (3.3) become

$$(1\,2)_I := \hat{1}2_I - \hat{2}1_I, \quad \{1\,2\}_I := \hat{1}\bar{2}_I - \hat{2}\bar{1}_I. \tag{4.13}$$

They amount to our D dimensional generalisation of the familiar spinor brackets (3.6). Scalar products between these will often be shortened to

$$(1\,2)\cdot\{1\,2\} \equiv (1\,2)_I\{1\,2\}_I,$$

where the dot is obviously redundant when the bilinears are purely four-dimensional.

The Yang-Mills action is written as before in Minkowski co-ordinates as

$$S = \frac{1}{2g^2}\int d^D x \ \mathrm{tr}\, \mathcal{F}^{\mu\nu}\mathcal{F}_{\mu\nu}. \tag{4.14}$$

The field-strength tensor and group generators are defined as before in (3.8). The quantisation procedure is similar to that in four dimensions. It takes place on surfaces Σ with normal $\mu = (1,0,\ldots,0,1)/\sqrt{2}$ (*i.e.* of constant x^0) in Minkowski co-ordinates, subject to the axial gauge condition $\mu \cdot \mathcal{A} = \hat{\mathcal{A}} = 0$. We apply the gauge condition and integrate $\check{\mathcal{A}}$ out of the lagrangian by the same procedure as in section 3.1, extended to accommodate the additional degrees of freedom, and are left with a D-dimensional light-cone action in the form (3.19), where now

$$L^{-+} = \ \mathrm{tr}\int_\Sigma d^{D-1}\mathbf{x}\, \mathcal{A}_I(\check{\partial}\hat{\partial} - \partial_J\bar{\partial}_J)\bar{\mathcal{A}}_I, \tag{4.15}$$

$$L^{-++} = -\,\mathrm{tr}\int_\Sigma d^{D-1}\mathbf{x}\, (\bar{\partial}_I\mathcal{A}_J[\hat{\partial}^{-1}\mathcal{A}_I, \hat{\partial}\bar{\mathcal{A}}_J] + \bar{\partial}_I\bar{\mathcal{A}}_J[\hat{\partial}^{-1}\mathcal{A}_I, \hat{\partial}\mathcal{A}_J]), \tag{4.16}$$

$$L^{--+} = -\,\mathrm{tr}\int_\Sigma d^{D-1}\mathbf{x}\, (\partial_I\mathcal{A}_J[\hat{\partial}^{-1}\bar{\mathcal{A}}_I, \hat{\partial}\bar{\mathcal{A}}_J] + \partial_I\bar{\mathcal{A}}_J[\hat{\partial}^{-1}\bar{\mathcal{A}}_I, \hat{\partial}\mathcal{A}_J]), \tag{4.17}$$

$$\begin{aligned} L^{--++} = -\,\mathrm{tr}\int_\Sigma d^{D-1}\mathbf{x}\, \Big(& \tfrac{1}{4}[\hat{\partial}\mathcal{A}_I, \bar{\mathcal{A}}_I]\,\hat{\partial}^{-2}\,[\hat{\partial}\mathcal{A}_J, \bar{\mathcal{A}}_J] \\ & + \tfrac{1}{2}[\hat{\partial}\mathcal{A}_I, \bar{\mathcal{A}}_I]\,\hat{\partial}^{-2}\,[\hat{\partial}\bar{\mathcal{A}}_J, \mathcal{A}_J] \\ & - \tfrac{1}{4}[\hat{\partial}\bar{\mathcal{A}}_I, \mathcal{A}_I]\,\hat{\partial}^{-2}\,[\hat{\partial}\bar{\mathcal{A}}_J, \mathcal{A}_J] \\ & - \tfrac{1}{4}[\mathcal{A}_I, \mathcal{A}_J][\bar{\mathcal{A}}_I, \bar{\mathcal{A}}_J] - \tfrac{1}{4}[\mathcal{A}_I, \bar{\mathcal{A}}_J][\bar{\mathcal{A}}_I, \mathcal{A}_J]\Big). \end{aligned} \tag{4.18}$$

It may be shown with integration by parts that these expressions reduce in four dimensions to (3.20)–(3.23).

4.3.2 The transformation

We will now specify the change of field variables from $\mathcal{A}$ and $\bar{\mathcal{A}}$ to $\mathcal{B}$ and $\bar{\mathcal{B}}$. From (4.15), we see that the momentum conjugate to $\mathcal{A}_I$ is $\Pi_I(x) = -\hat{\partial}\bar{\mathcal{A}}_I(x)$, and as such

$$\mathcal{D}\mathcal{A}\,\mathcal{D}\Pi \equiv \prod_{x,I} d\mathcal{A}_I(x)\, d\Pi_I(x) \tag{4.19}$$

is proportional (up to a constant) to the path integral measure $\mathcal{D}\mathcal{A}\,\mathcal{D}\bar{\mathcal{A}}$; therefore under a canonical field transformation the jacobian will be unity. Again we choose $\mathcal{A}$ to be a

functional of $\mathcal{B}$ alone, and by (3.70) and (3.71),

$$\hat{\partial}\bar{\mathcal{A}}^a_I(x^0,\mathbf{x}) = \int_\Sigma d^{D-1}\mathbf{y}\,\frac{\delta\mathcal{B}^b_J(x^0,\mathbf{y})}{\delta\mathcal{A}^a_I(x^0,\mathbf{x})}\hat{\partial}\bar{\mathcal{B}}^b_J(x^0,\mathbf{y}), \tag{4.20}$$

$$\mathrm{tr}\int_\Sigma d^{D-1}\mathbf{x}\,\check{\partial}\mathcal{A}_I\,\hat{\partial}\bar{\mathcal{A}}_I = \mathrm{tr}\int_\Sigma d^{D-1}\mathbf{x}\,\check{\partial}\mathcal{B}_I\,\hat{\partial}\bar{\mathcal{B}}_I. \tag{4.21}$$

Again, working in momentum space on the quantisation surface, we express $\mathcal{A}$ as a series in $\mathcal{B}$, but this time the series coefficients carry extra indices for the new transverse directions:

$$\mathcal{A}_{I_1}(\mathbf{p}_1) = \sum_{n=2}^{\infty}\int_{2\cdots n}\Upsilon_{I_1\cdots I_n}(1\cdots n)\,\mathcal{B}_{I_2}(-\mathbf{p}_2)\cdots\mathcal{B}_{I_n}(-\mathbf{p}_n) \tag{4.22}$$

where $\Upsilon_{IJ}(12) = \delta(\mathbf{p}_1+\mathbf{p}_2)\delta_{IJ}$. The integral short-hand used here is

$$\int_{1\cdots n} = \prod_{k=1}^{n}\frac{1}{(2\pi)^{3-2\epsilon}}\int d\hat{k}\prod_{I=1}^{1-\epsilon}dk_I d\bar{k}_I$$

and for later use we introduce the δ-function stripped form of a coefficient, given (as the first factor on the right-hand side) by

$$\Upsilon_{I_1\cdots I_n}(1\cdots n) = \Upsilon(1^{I_1}\cdots n^{I_n})\,(2\pi)^{3-2\epsilon}\delta^{3-2\epsilon}(\mathbf{p}_1+\cdots+\mathbf{p}_n) \tag{4.23}$$

and similarly for the other vertices Ξ, V and W, defined below. They should only be considered to be defined when the sum of their momentum arguments is 0. Repeated transverse indices in the superscripts are also subject to the summation convention. For convenience, we will often also subsume the index into the momentum label when the association is obvious (e.g. $\Upsilon(1^{I_1}\cdots n^{I_n}) \to \Upsilon(1\cdots n)$ above).

The canonical transformation removes the $(-{+}{+})$ terms from the lagrangian by absorbing them into the kinetic term for $\mathcal{B}$:

$$L^{-+}[\mathcal{A},\bar{\mathcal{A}}] + L^{-++}[\mathcal{A},\bar{\mathcal{A}}] = L^{-+}[\mathcal{B},\bar{\mathcal{B}}]. \tag{4.24}$$

Briefly delving into momentum space on the quantisation surface, it is seen that the term on the right-hand side of (4.24) supplies the tree-level propagator

$$\langle\mathcal{B}_I\bar{\mathcal{B}}_J\rangle = -\frac{ig^2}{2p^2}\delta_{IJ}. \tag{4.25}$$

Similarly, from the quantisation surface Fourier transform of (4.16), expanding the commutator and re-labelling leads us to

$$L^{-++} = \mathrm{tr}\int_{123}\bar{V}^2_{IJK}(123)\,\mathcal{A}_I(\bar{1})\mathcal{A}_J(\bar{2})\bar{\mathcal{A}}_K(\bar{3}) \tag{4.26}$$

where

$$\bar{V}^2(1^I2^J3^K) = -i\left(\frac{\{3\,1\}_J\delta_{KI}}{\hat{2}} + \frac{\{2\,3\}_I\delta_{JK}}{\hat{1}}\right). \tag{4.27}$$

It obviously follows from (4.24) and the light-cone lagrangian that this is the D dimensional equivalent of the $(++-)$ $\overline{\text{MHV}}$ vertex for the $\mathcal{A}$ field, and this is reflected in our choice of notation.

The remaining pieces of the lagrangian, (4.17) and (4.18), form MHV vertices in $4-2\epsilon$ dimensions, as explained in the next section. To obtain the Υ coefficients, we take the explicit expression of (4.24) and use (4.20) and (4.21), as before, to further reduce it to

$$\left\{\frac{\partial\cdot\bar{\partial}}{\hat{\partial}}\mathcal{A}_I - [\bar{\partial}_J\mathcal{A}_I, \hat{\partial}^{-1}\mathcal{A}_J] - \frac{\bar{\partial}_J}{\hat{\partial}}[\hat{\partial}^{-1}\mathcal{A}_J, \hat{\partial}\mathcal{A}_I]\right\}(\mathbf{x}) = \int_\Sigma d^3\mathbf{y}\,\frac{\delta\mathcal{A}_I(\mathbf{x})}{\delta\mathcal{B}^b_J(\mathbf{y})}\left(\frac{\partial\cdot\bar{\partial}}{\hat{\partial}}\right)_{\mathbf{y}}\mathcal{B}^b_J(\mathbf{y}). \tag{4.28}$$

By again transforming to momentum space and substituting the series expansion for $\mathcal{A}$ into both sides of (4.28) above, carefully rearranging the fields, and comparing terms order-by-order in $\mathcal{B}$, we extract successive Υ coefficients. At $\mathcal{O}(\mathcal{B}^2)$, one finds

$$\Upsilon(1^I 2^J 3^K) = \frac{i}{(2\,3)\cdot\{2\,3\}}(\hat{2}\{2\,3\}_K\delta_{IJ} + \hat{3}\{2\,3\}_J\delta_{KI}) \tag{4.29}$$

$$= -\frac{1}{\hat{1}}\frac{\bar{V}^2(2^J 3^K 1^I)}{(\Omega_1+\Omega_2+\Omega_3)}$$

$$= \frac{2}{\hat{1}}\frac{\bar{V}^2(2^J 3^K 1^I)}{p_1^2/\hat{1}+p_2^2/\hat{2}+p_3^2/\hat{3}} \tag{4.30}$$

and for compactness we have defined

$$\Omega_p := \frac{p_I\bar{p}_I}{\hat{p}}.$$

Again, substituting the series ansatze for $\mathcal{A}$ in the definition of the transformation and working order-by-order in $\mathcal{B}$ leads to the recurrence relation

$$\Upsilon(1\cdots n) = -\frac{1}{\hat{1}\sum_{i=1}^n\Omega_i}\sum_{j=2}^{n-1}\bar{V}^2(P^A_{2j}, P^B_{j+1,n}, 1)\Upsilon(-^A, 2, \ldots, j)\Upsilon(-^B, j+1, \ldots, n), \tag{4.31}$$

a particularly useful case of which is

$$\Upsilon(1234) = \frac{1}{\hat{1}\sum_{i=1}^4\Omega_i}\left\{\bar{V}^2(2,\bar{5}^A,1)\frac{1}{\hat{5}(\Omega_5+\Omega_3+\Omega_4)}\bar{V}^2(3,4,5^A)\right.$$
$$\left.+\bar{V}^2(\bar{5}^A,4,1)\frac{1}{\hat{5}(\Omega_5+\Omega_2+\Omega_3)}\bar{V}^2(2,3,5^A)\right\}. \tag{4.32}$$

Note that here (and throughout) $\mathbf{p}_5$ is a dummy momentum with scope limited to each term, and that its value should be taken to be the negative of the sum of the other arguments that accompany it in each term.

Differentiating (4.22) with respect to $\mathcal{B}$ and inserting the inverse into (4.20) suggests a series expansion for $\bar{\mathcal{A}}$ of the form

$$\bar{\mathcal{A}}_{I_1}(-\mathbf{p}_1) = \sum_{n=2}^{\infty}\sum_{s=2}^{n}\int_{2\cdots n}\frac{\hat{s}}{\hat{1}}\Xi^{s-1}_{I_1\cdots I_n}(\bar{1}2\cdots n)\,\mathcal{B}_{I_2}(-\mathbf{p}_2)\cdots\bar{\mathcal{B}}_{I_s}(-\mathbf{p}_s)\cdots\mathcal{B}_{I_n}(-\mathbf{p}_n). \quad (4.33)$$

Now, inserting (4.22) and (4.33) into (4.21), and then comparing coefficients order-by-order in $\mathcal{B}$, we may obtain expressions for the Ξ coefficients in terms of other Ξs and Υs of lower order. The results

$$\Xi^1(1^I2^J3^K) = -\Upsilon(2^J3^K1^I) \quad \text{and} \quad \Xi^2(1^I2^J3^K) = -\Upsilon(3^K1^I2^J) \quad (4.34)$$

will be of particular relevance to the forthcoming. By careful examination of the expansion of (4.21) at the $(n-1)^{\text{th}}$ order in $\mathcal{B}$, one finds that this recursion relation

$$\begin{aligned}\Xi^s(1\cdots n) = -\sum_{r=\max(2,4-s)}^{n+1-s}\sum_{m=\max(r,3)}^{r+s-1}&\Upsilon(-^A,3-r,\ldots,m+1-r)\\ &\times\Xi^{r+s-m}(-^A,m+2-r,\ldots,2-r).\end{aligned} \quad (4.35)$$

holds, given that $\Xi(1^I2^J) = \delta_{IJ}$.

As in section 4.1.1, we introduce a diagrammatic representation of Υ and Ξ in the form of D-dimensional MHV completion vertices, the first few of which are shown in fig. 4.1. We note that the process of deriving Υ and Ξ in $4-2\epsilon$ dimensions differs only from that in four dimensions by the presence of extra transverse indices, which are seen to each ride alongside (and can therefore be built into) a momentum index. It is therefore not surprising that the relationship between Υ and Ξ is, from this point of view, identical to that in four dimensions.

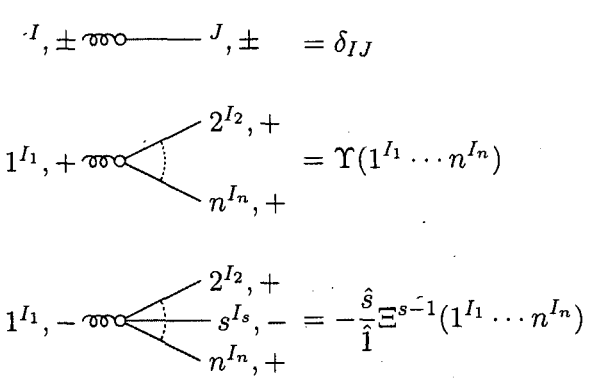

FIGURE 4.4: Completion vertices for the D-dimensional Canonical MHV Lagrangian.

4.3.3 $4-2\epsilon$-dimensional MHV vertices

We will now extract the $4-2\epsilon$-dimensional generalisations of the three and four gluon MHV vertices. The interaction part of the lagrangian takes the same form as (3.32) except that the vertices carry polarisation indices to contract into the corresponding $\mathcal{B}$s and $\bar{\mathcal{B}}$s:

$$\frac{1}{2}\sum_{s=2}^{n}\int_{1\cdots n} V^{s}_{I_1\cdots I_n}(1\cdots n)\,\mathrm{tr}[\bar{\mathcal{B}}_{I_1}(-\mathbf{p}_1)\mathcal{B}_{I_2}(-\mathbf{p}_2)\cdots\bar{\mathcal{B}}_{I_s}(-\mathbf{p}_s)\cdots\mathcal{B}_{I_n}(-\mathbf{p}_n)]$$

The Feynman rule for a particular $\mathcal{B}$ vertex is thus $4iV^s(1^{I_1}\cdots n^{I_n})/g^2$ ((4.6) applies in the canonical normalisation), and this follows from its definition as the sum of all contractions of external lines into the term in the action with the matching colour factor, while accounting for the cyclic symmetry of the trace.

The three-point MHV vertex follows trivially from L^{--+} using the leading order terms in the series for $\mathcal{A}$ and $\bar{\mathcal{A}}$. In quantisation surface momentum space, (4.17) reads

$$L^{--+} = \mathrm{tr}\int_{123} V^2_{IJK}(123)\,\bar{\mathcal{A}}_I(\bar{1})\bar{\mathcal{A}}_J(\bar{2})\mathcal{A}_K(\bar{3}) \tag{4.36}$$

where

$$V^2(1^I2^J3^K) = -i\left(\frac{(3\,1)_J\delta_{KI}}{\hat{2}} + \frac{(2\,3)_I\delta_{JK}}{\hat{1}}\right). \tag{4.37}$$

Since $\mathcal{A}=\mathcal{B}$ and $\bar{\mathcal{A}}=\bar{\mathcal{B}}$ to leading order, upon substituting (4.22) and (4.33) into (4.36), we immediately see that $V^2(1^I2^J3^K)$ is the $\bar{\mathcal{B}}_I(1)\bar{\mathcal{B}}_J(2)\mathcal{B}_K(3)$ colour-ordered vertex.

We note that the $\bar{\mathcal{B}}\bar{\mathcal{B}}\mathcal{B}\mathcal{B}$ and $\bar{\mathcal{B}}\mathcal{B}\bar{\mathcal{B}}\mathcal{B}$ colour-ordered vertices receive contributions from $L^{--+}[\mathcal{A}]$ and $L^{--++}[\mathcal{A}]$. Upon writing the latter in momentum-space, we have

$$\begin{aligned} L^{--++} = \mathrm{tr}\int_{1234}\{&W^2_{IJKL}(1234)\,\bar{\mathcal{A}}_I(\bar{1})\bar{\mathcal{A}}_J(\bar{2})\mathcal{A}_K(\bar{3})\mathcal{A}_L(\bar{4}) \\ &+ W^3_{IJKL}(1234)\,\bar{\mathcal{A}}_I(\bar{1})\mathcal{A}_J(\bar{2})\bar{\mathcal{A}}_K(\bar{3})\mathcal{A}_L(\bar{4})\} \end{aligned} \tag{4.38}$$

where

$$W^2(1^I2^J3^K4^L) = \delta_{IK}\delta_{JL} + \delta_{IL}\delta_{JK}\frac{\hat{1}\hat{2}+\hat{3}\hat{4}}{(\hat{1}+\hat{4})^2}, \tag{4.39}$$

$$W^3(1^I2^J3^K4^L) = \frac{1}{2}\left(\delta_{IL}\delta_{JK}\frac{\hat{1}\hat{2}+\hat{3}\hat{4}}{(\hat{1}+\hat{4})^2} + \delta_{IJ}\delta_{KL}\frac{\hat{1}\hat{4}+\hat{2}\hat{3}}{(\hat{1}+\hat{2})^2}\right). \tag{4.40}$$

We substitute (4.22) and (4.33) into $L^{--+}[\mathcal{A}]+L^{--++}[\mathcal{A}]$, and collect the terms of each colour (trace) order of $\mathcal{O}(\mathcal{B}^4)$. Contracting external lines in a colour-ordered manner into these terms, we have

$$\begin{aligned} V^2(1234) = \;&\frac{\hat{1}}{\hat{5}}V^2(5^A23)\Xi^2(\bar{5}^A41) + \frac{\hat{2}}{\hat{5}}V^2(15^A4)\Xi^1(\bar{5}^A23) \\ &+V^2(125^A)\Upsilon(\bar{5}^A34) + W^2(1234) \end{aligned} \tag{4.41}$$

for the $\bar{\mathcal{B}}_I(1)\bar{\mathcal{B}}_J(2)\mathcal{B}_K(3)\mathcal{B}_L(4)$ vertex, and

$$\begin{aligned} V^3(1234) = & \frac{\hat{1}}{\hat{5}}V^2(5^A34)\Xi^1(\bar{5}^A12) + \frac{\hat{3}}{\hat{5}}V^2(15^A4)\Xi^2(\bar{5}^A23) \\ & + \frac{\hat{3}}{\hat{5}}V^2(5^A12)\Xi^2(\bar{5}^A34) + \frac{\hat{1}}{\hat{5}}V^2(35^A2)\Xi^1(\bar{5}^A41) \\ & + 2W^3(1234) \end{aligned} \tag{4.42}$$

for the $\bar{\mathcal{B}}_I(1)\mathcal{B}_J(2)\bar{\mathcal{B}}_K(3)\mathcal{B}_L(4)$ vertex.

That these expressions reduce in four dimensions should be obvious by comparing the forms of (4.41) and (4.42) to their four-dimensional analogs in section 3.4.2 and noting the reduction of the individual factors.

It is worthwhile noting here that unlike in the four-dimensional case, the vertices (4.41) and (4.42) contain terms which vanish on shell. Furthermore, the transformation coefficients and the resulting vertices are no longer holomorphic (owing to the scalar product in the denominator of (4.29) preventing cancellation of the antiholomorphic bilinear, something possible in four dimensions) or have a simple form. The CSW rules are an inherently four-dimensional construction, and nor do we have any known D-dimensional generalisation of the Parke–Taylor amplitudes with which to compare. As such, we simply take (4.41), (4.42), and higher vertices computed using this programme as the definitions of the D-dimensional MHV vertices.

4.4 The one-loop (++++) amplitude

It is not possible to construct a one-loop (++++) amplitude using only the $\mathcal{B}$ vertices of the canonical MHV lagrangian. Nevertheless, we know it is non-vanishing and given by (2.62). We will see that it arises (as it indeed must) from equivalence theorem evading pieces, constructed from the MHV completion vertices of fig. 4.4. In all, we can construct four classes of graphs for this contribution: boxes, triangles, two classes of bubbles (corresponding to the two possible arrangements of external lines on either side of the loop), and the tadpoles.

In the next three subsections, we will consider the quadruple cut of these diagrams. We will restrict ourselves to analysing the cuts that arise from the singularities provided by the propagators, which we refer to as *standard* cuts. From general considerations [33] we expect other *non-standard* cuts arising from the singular denominators in the vertices. This is true both of the D dimensional version we have here and the four dimensional Parke–Taylor forms (2.22), but from the earlier derivation it is clear that this singular behaviour is restricted to the quantisation surface (they have no dependence on $\check{p}$). These cuts therefore depend on the orientation of the quantisation surface, *i.e.* μ, and are thus gauge artifacts which should all cancel out in any complete on-shell amplitude.

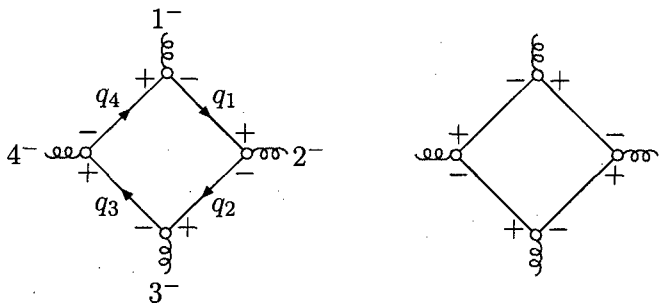

FIGURE 4.5: Box contributions to the one-loop (++++) amplitude. All external momenta are taken as outgoing.

4.4.1 Off-shell quadruple cut

The (++++) amplitude is obtained by amputating $\langle \bar{A}\bar{A}\bar{A}\bar{A}\rangle$, the box diagram for which is shown in fig. 4.5. This gives a contribution of

$$A^{\text{box}}(1^+,2^+,3^+,4^+) = \lim_{p_1^2,p_2^2,p_3^2,p_4^2\to 0} \frac{1}{4} g^4 \frac{p_1^2 p_2^2 p_3^2 p_4^2}{\hat{1}\hat{2}\hat{3}\hat{4}} \int \frac{d^D q}{(2\pi)^D} \frac{16}{q_1^2 q_2^2 q_3^2 q_4^2} \frac{1}{\Sigma_1\Sigma_2\Sigma_3\Sigma_4} \times$$
$$\{\bar{V}^2(-q_4^D,1,q_1^A)\bar{V}^2(-q_1^A,2,q_2^B)\bar{V}^2(-q_2^B,3,q_3^C)\bar{V}^2(-q_3^C,4,q_4^D)$$
$$+\bar{V}^2(1,q_1^A,-q_4^D)\bar{V}^2(2,q_2^B,-q_1^A)\bar{V}^2(3,q_3^C,-q_2^B)\bar{V}^2(4,q_4^D,-q_3^C)\}, \tag{4.43}$$

where we have already used (4.30) and (4.34), the internal momenta are defined as $q_i = q - P_{1i}$, and we define the short-hand

$$\Sigma_j := \frac{q_j^2}{\hat{q}_j} - \frac{q_{j-1}^2}{\hat{q}_{j-1}} + \frac{p_j^2}{\hat{p}_j} \tag{4.44}$$

(indices interpreted cyclically). Note that the external momenta $p_1,\ldots,p_4$ are in four dimensions and thus their transverse indices have all been set to one.

Before going on to compute the quadruple standard cut of the box, as an aside we will show that its double and triple standard cuts vanish for on-shell external momenta. Consider cutting any three internal lines of fig. 4.5, keeping the remaining internal line strictly off-shell. Without loss of generality, we choose these internal lines to be q_1, q_2 and q_3. In order that the amplitude survives LSZ reduction, the correlator must generate a singularity in $p_1^2p_2^2p_3^2p_4^2$. Clearly, the Σ_2 and Σ_3 denominators provide a singularity $p_2^2p_3^2$ once the internal lines are cut. We now claim that the triple cut vanishes as follows: the required singularity in $p_1^2p_4^2$ must come from the denominators in the remaining tree graph connecting p_1 and p_4. The relevant factors from (4.43) are the q_4 propagator, and the Σ_1 and Σ_4 denominators, *i.e.*

$$\frac{1}{q_4^2}\left(\frac{q_1^2}{\hat{q}_1} - \frac{q_4^2}{\hat{q}_4} + \frac{p_1^2}{\hat{p}_1}\right)^{-1}\left(\frac{q_4^2}{\hat{q}_4} - \frac{q_3^2}{\hat{q}_3} + \frac{p_4^2}{\hat{p}_4}\right)^{-1}.$$

Upon setting q_1^2 and q_3^2 to zero and discarding (the non-vanishing) factors of momenta that appear on the numerator, we arrive at

$$\frac{1}{q_4^2}\frac{1}{\hat{q}_4\, p_1^2 - \hat{1}\, q_4^2}\frac{1}{\hat{4}\, q_4^2 + \hat{q}_4\, p_4^2}.$$

The above factors clearly cannot cancel $p_1^2 p_4^2$ so long as $q_4^2 \neq 0$. Hence this cut vanishes as we take all the external momenta on shell. By similar consideration, one can also see that both possible double cuts of this graph also vanish.

Now, we will compute the standard quadruple cut. This is obtained by putting all four internal lines on shell [33, 35, 36]. The external momenta are kept off shell momentarily. We see that the Σ_i reduce to $p_i^2/\hat{i}$ factors upon cutting, producing poles which thus cancel the factors of p_i^2 from LSZ reduction and the $1/\hat{i}$ factors. The remaining terms have a finite non-vanishing[2] on-shell limit and it is already clear that they are exactly what we obtain from the four-cut box contribution using the light cone Yang–Mills action (3.19).

For the purposes of demonstrating that precisely this contribution arises from the four-cut MHV completion box graph within the present formalism we do not need to go any further. However, let us show how this contribution can be straightforwardly computed within the formalism we have developed here.

4.4.2 Explicit evaluation of box quadruple cut

We begin with (4.43), and substitute for $\bar{V}^2$ using (4.27). For the moment, the external momenta p_i are four-dimensional and off-shell, whereas the loop momentum $q \equiv q_4$ in the integral is D-dimensional. To compute the cut, we replace the four propagators with

$$\delta^{+4}(q_1)\delta^{+4}(q_2)\delta^{+4}(q_3)\delta^{+4}(q_4),$$

and by splitting the integral over momentum space as in section 2.6.1, these δ functions enforce the four constraints $q_i^2 = 0$. This in turn fixes the four-dimensional part of q to a discrete set of solutions (in fact two) in term of the remaining, orthogonal -2ϵ components ν. It is now safe to take the p_i on-shell and, assuming solution to the constraints exist, we are left with

$$8g^4(1-\epsilon)\frac{1}{\hat{1}\hat{2}\hat{3}\hat{4}}\int \frac{d\nu^{-2\epsilon}}{(2\pi)^{-2\epsilon}}\{q\,1\}\{q-1,2\}\{q+4,3\}\{q\,4\}. \tag{4.45}$$

Some comments are in order here. First, note that the $\{\cdots\}$ bilinears above have their index set to 1, but this has been dropped for clarity. Now by their q dependence, the bilinears above are functions of ν, but we can say more: since q can only contract with either itself or the four-dimensional external momenta, we see that these solutions can in fact only depend on

$$\nu^2 = 2(q_I \bar{q}_I - \tilde{q}\bar{q}). \tag{4.46}$$

[2]Recall that four-cut solutions are non-vanishing because they use complex external and internal momenta [33, 35, 36].

We would also like to point out the factor of $(1-\epsilon)$ comes from dimensional regularisation of the gauge field degrees of freedom (*cf.* the four-dimensional helicity scheme [101], which extends only the loop momentum to D dimensions and therefore lacks this factor).

What remains is to obtain expressions for the bilinears in terms of ν^2. In the following, since the momenta are complex, $\{q\,1\}$ is not related by complex conjugation to $(q\,1)$. First, consider $(q\,1)\cdot\{q\,1\}$. Since, $q_1^2 = q^2 = p_1^2 = 0$, (4.75), or (4.77), implies that this vanishes. Splitting away the four-dimensional part and using (4.46) gives

$$(q\,1)\{q\,1\} + \hat{1}^2\nu^2/2 = 0, \tag{4.47}$$

and similarly

$$(q-1,2)\{q-1,2\} + \hat{2}^2\nu^2/2 = 0 \quad \text{and} \tag{4.48}$$

$$(q\,4)\{q\,4\} + \hat{4}^2\nu^2/2 = 0. \tag{4.49}$$

We eliminate ν^2 between (4.47), and (4.49), and then use (4.76) to eliminate $(q\,4)$ and its conjugate. This gives

$$\hat{q} + \hat{4}\frac{(q\,1)}{(1\,4)} + \hat{4}\frac{\{q\,1\}}{\{1\,4\}} = 0.$$

Similarly, eliminating ν^2 between (4.47) and (4.48) leads to

$$\hat{q} - \hat{1} + \hat{2}\frac{(q\,1)}{(1\,2)} + \hat{2}\frac{\{q\,1\}}{\{1\,2\}} = 0. \tag{4.50}$$

Subtracting, and using (4.47) to eliminate $\{q\,1\}$ yields the quadratic equation

$$\alpha(q\,1)^2 + \hat{1}(q\,1) - \bar{\alpha}\frac{\hat{1}^2\nu^2}{2} = 0 \tag{4.51}$$

where

$$\alpha = \frac{\hat{4}}{(1\,4)} - \frac{\hat{2}}{(1\,2)}, \quad \bar{\alpha} = \frac{\hat{4}}{\{1\,4\}} - \frac{\hat{2}}{\{1\,2\}}. \tag{4.52}$$

This has solutions

$$(q\,1) = -\frac{\hat{1}}{2\alpha}(1 \pm \beta), \quad \{q\,1\} = -\frac{\hat{1}}{2\bar{\alpha}}(1 \mp \beta), \quad \beta = \sqrt{1 + 2\alpha\bar{\alpha}\nu^2}. \tag{4.53}$$

Next, the Bianchi-like identity (4.76) gives

$$\hat{1}\{q-1,2\} = \hat{2}\{q\,1\} + (\hat{q} - \hat{1})\{1\,2\}. \tag{4.54}$$

Using (4.50) and (4.53) gives

$$\{q-1,2\} = \frac{\hat{2}}{2\alpha}\frac{\{1\,2\}}{(1\,2)}(1 \pm \beta). \tag{4.55}$$

Similarly, we find

$$\{q\,4\} = \frac{\hat{4}}{2\alpha}\frac{\{1\,4\}}{(1\,4)}(1 \pm \beta). \tag{4.56}$$

To obtain the final bilinear $\{q+4,3\}$, we use (4.76) twice to obtain it in terms of $\{q\,1\}$ and $\{q\,4\}$. (4.77) is then applied to eliminate a quotient of $(\cdots)$ bilinears present in one of the terms in favour of conjugate bilinears, giving

$$\{q+4,3\} = \frac{1}{2}\frac{\{2\,3\}\{3\,4\}}{\{2\,4\}}(1 \pm \beta). \tag{4.57}$$

Assembling the product of the $\{\cdots\}$ bilinears from (4.53), (4.55), (4.56) and (4.57), we have

$$\{q\,1\}\{q-1,2\}\{q+4,3\}\{q\,4\} = -\tfrac{1}{4}\hat{1}^2\hat{2}\hat{4}\,\nu^4\,\frac{\{2\,3\}\{3\,4\}}{(1\,2)(4\,1)} = -\tfrac{1}{4}\hat{1}\hat{2}\hat{3}\hat{4}\,\nu^4\,\frac{\{1\,2\}\{3\,4\}}{(1\,2)(3\,4)} \tag{4.58}$$

for either of the solutions (4.53), where in the second assertion we have used the fact that the right-hand side of (4.77) is zero for null p_j. Using this in (4.45) and reinstating the propagators, we arrive at

$$2(1-\epsilon)g^4\frac{\{1\,2\}\{3\,4\}}{(1\,2)(3\,4)}\int\frac{d^4q\,d^{-2\epsilon}\nu}{(2\pi)^D}\frac{\nu^4}{q_1^2q_2^2q_3^2q_4^2}. \tag{4.59}$$

Thus we conclude that (4.43) has precisely the quadruple cut of the $4-2\epsilon$-dimensional box function K_4, as expected of this amplitude [77, 87, 92, 102, 103].

4.4.3 Triangle, bubble and tadpole contributions

Typical triangle, bubble and tadpole contributions to the one-loop (++++) amplitude with internal helicities running from $-$ to $+$ in a clockwise sense[3] are shown in figs. 4.6, 4.7 and 4.8.

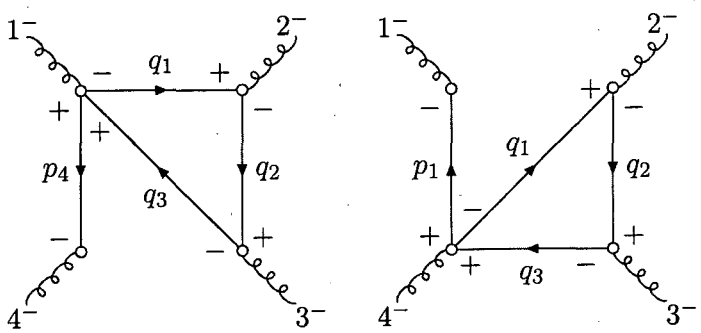

FIGURE 4.6: One-loop MHV completion triangle graphs for the (++++) amplitude. Note that the propagator carrying an external momentum is attached to the Ξ vertex differently in each case.

Despite appearances, these diagrams do have quadruple cuts as a result of the singularities in the vertices. We therefore have to consider also cutting the vertices. Let us

[3]The "sense" of internal helicity orientation is always defined here as propagating from $-$ to $+$.

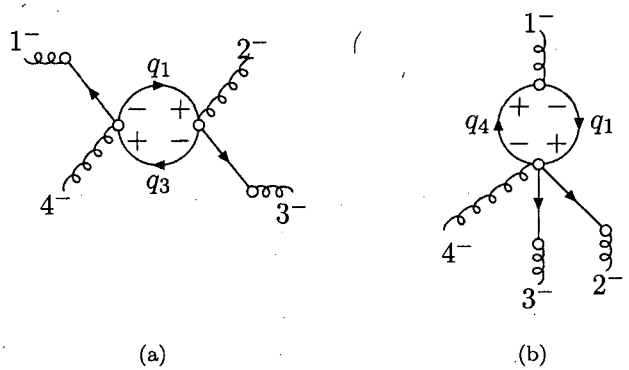

FIGURE 4.7: MHV completion bubble graphs. In (a) we show a 2|2 bubble. There are three other graphs like it (up to shifting the external momentum labels once by $i \to i+1$) obtained by swapping the external momentum propagators between gluons 1 and 4, and between gluons 2 with 3. The 3|1 bubble is shown in (b); there are two additional graphs (up to rotations of the labels), in this case obtained by associating the curly line attached to the five-point Ξ with gluon 2 or 3 instead of 4.

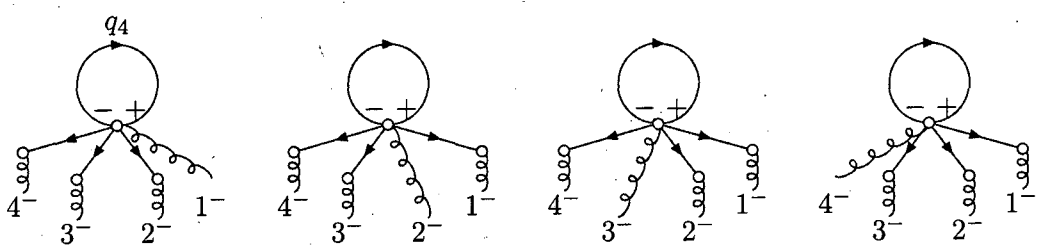

FIGURE 4.8: Tadpole MHV completion graphs. Notice that the coupling of the six-point Ξ to the $\bar{A}$ field (denoted by the curly line) is associated with a different gluon in each case.

first consider the quadruple cut of the triangle graph. We can restrict our analysis to the graphs fig. 4.6. Their contribution to the (++++) amplitude is

$$\lim_{p_1^2,p_2^2,p_3^2,p_4^2\to 0} \frac{1}{4}g^4 \frac{p_1^2p_2^2p_3^2p_4^2}{\hat{1}\hat{2}\hat{3}\hat{4}} \int \frac{d^Dq}{(2\pi)^D} \frac{\hat{q}_1\hat{q}_2\hat{q}_3}{q_1^2q_2^2q_3^2} \times \left\{ -\Xi^1(1,q_1^A,-q_3^C,4)\Xi^1(2,q_2^B,-q_1^A)\Xi^1(3,q_3^C,-q_2^B)\frac{\hat{4}}{p_4^2} - \Xi^2(4,1,q_1^A,-q_3^C)\Xi^2(2,q_2^B,-q_1^A)\Xi^2(3,q_3^C,-q_2^B)\frac{\hat{1}}{p_1^2} \right\}. \tag{4.60}$$

Using the recurrence relations (4.31) and (4.35) to evaluate the Ξs, we can re-write this as

$$\lim_{p_1^2,p_2^2,p_3^2,p_4^2\to 0} \frac{1}{4}g^4 \frac{p_1^2p_2^2p_3^2p_4^2}{\hat{1}\hat{2}\hat{3}\hat{4}} \int \frac{d^Dq}{(2\pi)^D} \frac{16}{q_1^2q_2^2q_3^2} \left\{ \frac{X}{\hat{q}_4\Sigma_1\Sigma_2\Sigma_3\Sigma_4(\Sigma_1+\Sigma_4)} \left(\frac{\Sigma_1\hat{4}}{p_4^2} - \frac{\Sigma_4\hat{1}}{p_1^2} \right) + \frac{Y}{(\hat{1}+\hat{4})\Sigma'_{1+4}\Sigma_2\Sigma_3} \left(\frac{1}{\Sigma_{1+4}} - \frac{1}{\Sigma_1+\Sigma_4} \right) \left(\frac{\hat{1}}{p_1^2} + \frac{\hat{4}}{p_4^2} \right) \right\} \tag{4.61}$$

with

$$X = \bar{V}^2(-q_4^D, 1, q_1^A)\bar{V}^2(-q_1^A, 2, q_2^B)\bar{V}^2(-q_2^B, 3, q_3^C)\bar{V}^2(-q_3^C, 4, q_4^D), \tag{4.62}$$

$$Y = \bar{V}^2(4, 1, 2 + 3^D)\bar{V}^2(-q_3^C, 1 + 4^D, q_1^A)\bar{V}^2(-q_1^A, 2, q_2^B)\bar{V}^2(-q_2^B, 3, q_3^C), \tag{4.63}$$

$q_4 := q_3 - p_4$ flowing "through" the vertex attached to p_1 (or p_4) as part of a box-like momentum-flow topology (see section 4.4.4 below for a further investigation of this), and we define the following extensions of Σ_i as

$$\Sigma_{1+4} := \frac{q_1^2}{\hat{q}_1} - \frac{q_3^2}{\hat{q}_3} + \frac{(p_1 + p_4)^2}{\hat{1} + \hat{4}}, \tag{4.64}$$

$$\Sigma'_{1+4} := \frac{p_1^2}{\hat{1}} + \frac{p_4^2}{\hat{4}} - \frac{(p_1 + p_4)^2}{\hat{1} + \hat{4}}. \tag{4.65}$$

Note that one can write down expressions for the analogues of X and Y from graphs with internal helicities of an anti-clockwise sense. (It is easy to check for the case at hand (where $\bar{V}^2$ is the three-point $\overline{\text{MHV}}$ vertex), that these are the same as in the clockwise scenario.)

Now, recall that we are only studying the standard cuts. We will extract such a quadruple cut contribution here, by keeping the external momenta off the mass shell, and look for any terms containing $1/q_4^2$ in addition to the three propagators already appearing in (4.61). Clearly, by inspection of the Σ_i factors in (4.61), no such $1/q_4^2$ are generated. Indeed it is impossible to generate such terms from the vertices since the singularity in $1/q_4^2$ is not restricted to the quantisation surface. Although the inverse Σ_is and Σ_{1+4} appear in (4.44) and above to yield singularities that look superficially similar to those from propagators, by (4.78) these terms do not contain $\tilde{q}$ components and thus their singularities lie entirely within the quantisation surface.

A similar analysis of the graphs of figs. 4.7 and 4.8 leads one quickly to the same conclusion: they have no contribution to the quadruple cut for off-shell external momenta, because in this region none of the denominators from their Ξ vertices form the necessary propagators. Hence, we see that for the one-loop (++++) amplitude in the Canonical MHV Lagrangian's formalism, if we keep the external momenta off shell until after the cuts, only the box graph of fig. 4.5 contributes to the quadruple cut.

4.4.4 Light-cone Yang–Mills reconstructions

As with section 4.2.1, expressions (4.43), (4.62) and (4.63) expose the relationship between between the MHV completion graphs of figs. 4.5–4.8 and the Feynman graphs one would use to compute the same amplitude in conventional perturbative LCYM. We already see parallels of the latter in the topology of the linking amongst $\bar{V}^2$ $\overline{\text{MHV}}$ vertices.[4]

[4]Recall that these are the same as the ++− vertices in light-cone Yang–Mills.

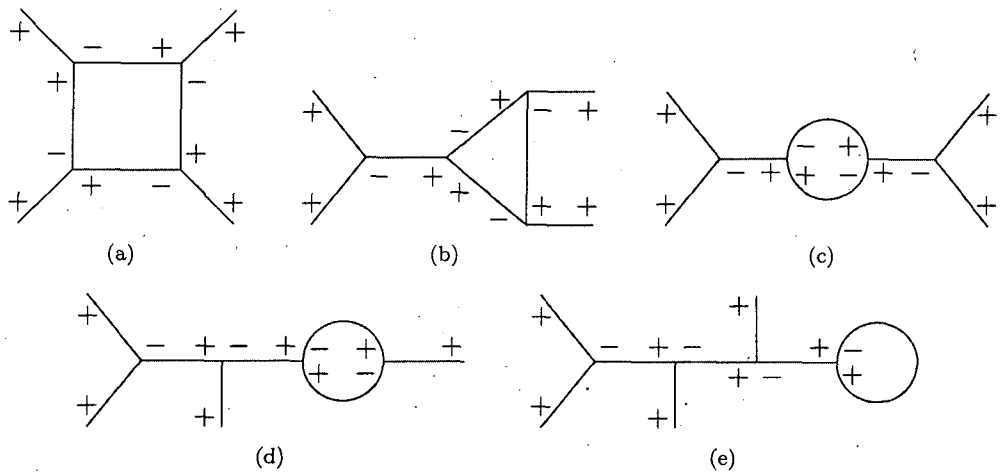

FIGURE 4.9: Typical LCYM Feynman graphs that contribute to the (++++) amplitude. Shown topologies are the (a) box, (b) triangle, (c) bubble, (d) typical external leg correction, and (e) one of the tadpoles (there is another tadpole not shown here with the loop attached to the central leg of the tree instead).

Starting with expression (4.43) for the box graph, it is immediately apparent that the momentum routing through the $\bar{V}^2$s yields the two box-like topologies in LCYM: one with the internal helicities arranged in a clockwise sense (from the first term in the curly braces, shown in fig. 4.9(a)), and another with an anticlockwise arrangement.

The triangle MHV completion graphs of fig. 4.6 reveal a mixture of topologies in the momentum routing. Naturally, one would expect the triangle diagram of fig. 4.9(b), and indeed this arises from the factor Y in (4.61). The MHV completion triangle graph also has terms with factors of X, which we know is nothing but one of the vertex configurations found in (4.43) of box topology, *i.e.* fig. 4.9(a). (As we have seen however, in this case the fourth propagator is missing.)

The bubble and tadpole graphs can be processed in a similar manner: the graph of fig. 4.7(a) contains the topology of, and therefore contributes to the reconstruction of, the LCYM self-energy correction graph in fig. 4.9(c); similarly fig. 4.7(b) contributes to the reconstruction of the external leg corrections (an example of which is seen in fig. 4.9(d)). The MHV completion tadpole graphs in fig. 4.8 contain terms of topology of the LCYM tadpoles of fig. 4.9(e) (these are ill-defined but we can take them to vanish in dimensional regularisation just as we would for the LCYM tadpole), as well as contributing pieces with the self-energy and external leg correction topologies. Additionally, both MHV completion bubbles and tadpoles contribute to the reconstruction of box and triangle LCYM graphs.

Full reconstruction of the light-cone Yang–Mills box contribution

We saw in section 4.2.1 for the case of the (−−++) tree-level amplitude that although individual completion vertex graphs are identical to LCYM graphs, the *sum* of all completion and MHV graphs with a given momentum-routing topology did recover the off-shell LCYM graphs of that topology. In this section, we will demonstrate this at the

loop level for the (++++) amplitude. Again, rather than do this for all graphs displayed in fig. 4.9, we will concentrate on the diagrams of box topology with the internal helicity configuration as displayed in fig. 4.9(a) (note the sense of the signs on the internal lines). This corresponds to terms containing the factor X of (4.62).

The MHV completion box graph of fig. 4.5 provides a contribution to the amplitude, given in (4.43) of

$$4g^4 \int \frac{d^D q}{(2\pi)^D} \frac{XC}{q_1^2 q_2^2 q_3^2 q_4^2} \tag{4.66}$$

This is clearly of the box momentum-routing topology, as we remind the reader that X is simply the product of $\overline{\text{MHV}}$ vertices in a box configuration. The factor C is

$$C_{\text{box}} = \frac{P_1 P_2 P_3 P_4}{\Sigma_1 \Sigma_2 \Sigma_3 \Sigma_4}. \tag{4.67}$$

We can repeat this analysis for the two triangle configurations in fig. 4.6, whose contribution is given in (4.61). We multiply the integrand by q_4^2/q_4^2 and extract the relevant C factor to obtain

$$C_{\text{triangle}} = \frac{P_2 P_3}{\Sigma_2 \Sigma_3} \frac{Q_4}{\Sigma_4 + \Sigma_1} \left(\frac{P_1}{\Sigma_4} - \frac{P_4}{\Sigma_1} \right), \tag{4.68}$$

where we have introduced the short-hand $Q_i := q_i^2/\hat{q}_i$. By a similar procedure, the C factors for the bubble and tadpole graphs are obtained. The algebra for this is fairly straightforward, and we simply state the results. For the four possible bubble configurations of fig. 4.7(a) (see the caption for the description of these configurations),

$$C_{2|2} = \frac{Q_2}{\Sigma_2 + \Sigma_3} \left(\frac{P_3}{\Sigma_2} - \frac{P_2}{\Sigma_3} \right) \frac{Q_4}{\Sigma_4 + \Sigma_1} \left(\frac{P_1}{\Sigma_4} - \frac{P_4}{\Sigma_1} \right). \tag{4.69}$$

The three bubble configurations of fig. 4.7(b) have

$$C_{3|1} = \frac{P_1}{\Sigma_1} \frac{Q_2 Q_3}{\Sigma_2} \left\{ \frac{P_2}{(\Sigma_3 + \Sigma_4)\Sigma_4} - \frac{P_2 + P_3}{(\Sigma_2 + \Sigma_3)\Sigma_4} + \frac{P_2 + P_3 + P_4}{(\Sigma_2 + \Sigma_3)(\Sigma_2 + \Sigma_3 + \Sigma_4)} \right\}, \tag{4.70}$$

and finally the tadpoles of fig. 4.8 yield

$$C_{\text{tadpole}} = \frac{Q_1 Q_2 Q_3}{\Sigma_1} \left\{ \frac{1}{(\Sigma_1 + \Sigma_2)(\Sigma_1 + \Sigma_2 + \Sigma_3)} - \frac{P_1}{(\Sigma_2 + \Sigma_3 + \Sigma_4)(\Sigma_3 + \Sigma_4)\Sigma_4} + \frac{P_1 + P_2}{(\Sigma_1 + \Sigma_2)(\Sigma_3 + \Sigma_4)\Sigma_4} - \frac{P_1 + P_2 + P_3}{(\Sigma_1 + \Sigma_2)(\Sigma_1 + \Sigma_2 + \Sigma_3)\Sigma_4} \right\} \tag{4.71}$$

We must now account for additional contributions that arise from the images of the graphs under cyclic permutations of the external momenta. These permutations can be effected in the expressions (4.67)–(4.71) by permuting *all* the momentum labels. Now, the box graph is invariant under these cycles so provides only one contribution; the triangles, 3|1 bubbles and tadpole graphs all provide three extra contributions obtained

from the three label shifts $i \to i+1$ in (4.68), (4.70) and (4.71); the 2|2 bubbles provide one extra contribution from the shift $i \to i+2$ acting on (4.69).

Adding these contributions and simplifying leads to, after some considerable but straightforward algebra, the satisfying result that $C = 1$, *i.e.* the sum of all the MHV completion graphs contributing to the box topology is nothing other than what we would have obtained using LCYM Feynman rules. Note that this happened *before* taking on-shell limits or performing any integration; recovering the missing amplitude is a purely algebraic processes.

Taking the external momenta on-shell first

In section 4.4.1, we reproduced the correct standard quadruple cut contribution to the one-loop (++++) amplitude by starting with off-shell external momenta, then cutting the internal lines, and finally taking the external momenta on shell. Now it follows that if the cut is well-defined (and it should be, given the correspondence between MHV completion and LCYM graphs is algebraic), it should not matter in which order we take these limits.

Inspecting (4.67) and (4.69)–(4.71), it is clear that the order in which these limits are taken will 'switch off' different contributions. For instance, it is clear to see that upon cutting all the internal lines by letting q_i^2 and hence $Q_i \to 0$, only the box (4.67) will survive. Conversely, we see that when we take the external momenta on shell first, $P_i \to 0$ so only the tadpole contribution

$$C'_{\text{tadpole}} = \frac{Q_1Q_2Q_3}{\Sigma_1} \frac{1}{(\Sigma_1+\Sigma_2)(\Sigma_1+\Sigma_2+\Sigma_3)} = \frac{Q_1Q_2Q_3}{(Q_1-Q_4)(Q_2-Q_4)(Q_3-Q_4)}. \tag{4.72}$$

and its three cyclic permutations survive. When one sums over these permutations, one finds that $C = 1$ so the correct quadruple cut is again obtained. Choosing other, more mixed limits would produce more complicated combinations of terms surviving from the various C coefficients.

As an interesting aside, the reason that the tadpole is the sole survivor in this limit may be understood from the structure of the Υ vertices: the tadpole provides the only configuration in which the correct poles are generated to cancel the inverse propagators from the LSZ reduction. Consider the tadpole graphs shown in fig. 4.8: their contribution is

$$\frac{1}{4}g^4 \int \frac{d^Dq_4}{(2\pi)^D} \frac{\hat{q}_4}{q_4^2} \Big\{ -P_1\Xi^4(1,2,3,4,q_4^A,-q_4^A) - P_2\Xi^3(2,3,4,q_4^A,-q_4^A,1) \\ - P_3\Xi^2(3,4,q_4^A,-q_4^A,1,2) - P_4\Xi^1(4,q_4^A,-q_4^A,1,2,3) \Big\}. \tag{4.73}$$

Inspecting (4.35), we see that they all contain the term $-\Upsilon(q_4^A,-q_4^A,1,2,3,4)$. Since we are concerned only with the box topology, we can ignore the other terms in (4.35)

since they correspond to the topologies of tree decorations to triangles, bubbles and tadpoles. A similar argument simplifies the extraction of the box topology terms from Υ: to extract the terms in $\Upsilon(q_n^A, -q^A, 1, \ldots, n)$, where $q_n = q$, with an n-gonal topology, we keep only the terms in (4.31) with q in each term, so in this situation we can make the replacement

$$\Upsilon(q_n^A, -q^A, 1, \ldots, n) \to -\frac{\bar{V}^2(-q_{n-1}^B, n, q_n^A)\Upsilon(q_{n-1}^B, -q^A, 1, \ldots, n-1)}{\hat{q}_n(\Omega_{q_n} - \Omega_q + \sum_{i=1}^n \Omega_i)}.$$

Iterating this for $n = 4$ gives

$$\begin{aligned}\Upsilon(q_4^A, -q^A, 1, 2, 3, 4) &= -\frac{\bar{V}^2(-q_3^B, 4, q^A)\Upsilon(q_3^B, -q^A, 1, 2, 3)}{\hat{q}_4 \sum_{i=1}^4 \Omega_i} \\ &= \cdots \\ &= \frac{16X}{\hat{q}_1\hat{q}_2\hat{q}_3\hat{q}_4} \frac{1}{\sum_{i=1}^4 P_i} \frac{1}{\sum_{i=1}^4 P_i + Q_3 - Q_4} \\ &\qquad \times \frac{1}{\sum_{i=1}^4 P_i + Q_2 - Q_4} \frac{1}{\sum_{i=1}^4 P_i + Q_1 - Q_4}.\end{aligned}$$

using (4.78).

Making these replacements in (4.73), reinstating the propagators by multiplying the integrand by q_i^2/q_i^2 $(i = 1, 2, 3)$ and taking the limit $P_i \to 0$, it is easy to see that (4.72) and hence (4.71) are recovered directly.

4.5 Conclusion

In this chapter, we have seen that the amplitudes that cannot be built from the CSW rules arise in the Canonical MHV Lagrangian framework as a result of terms in the field transformation that evade the S-matrix equivalence theorem in the LSZ reduction. In detail, we found that the series coefficients of the field transformation, Υ and Ξ, furnish a set of 'completion vertices' that supplant insertions of A and $\bar{A}$, respectively, in correlation functions with products of B and $\bar{B}$ fields.

To demonstrate this, we recovered the three-gluon $\overline{\text{MHV}}$ amplitude (which is non-vanishing in $(2,2)$ signature or for complex momenta), computed in light-cone Yang–Mills theory using the $\bar{V}^2$ vertex eliminated from the lagrangian by the transformation. This is constructed by the LSZ reduction of the correlation function $\langle A\bar{A}\bar{A}\rangle$. Now not only does this have the correct pole structure to survive the on-shell limit, it recovers the off-shell $\overline{\text{MHV}}$ vertex $\bar{V}^2$ algebraically.

For the treatment of amplitudes at the quantum level, we applied dimensional regularisation to the light-cone Yang–Mills lagrangian and used the field transformation to obtain D-dimensional versions of the MHV and completion vertices. We augmented the light-cone co-ordinates in such a way that the ideas of positive and negative 'helicity' are preserved (exact in the four-dimensional limit). It also allows a clean separation of the

two 'helicities' into canonical co-ordinates and momenta, as before. The result is clearly an MHV lagrangian, insomuch as its vertices contain just two fields of negative 'helicity' and one or more positive, joined together with a helicity-flipping propagator. The field transformation that results has a similar structure to the four-dimensional case, but unlike it lacks the simple, holomorphic expressions for the vertices and transformation coefficients.

Using this technology, we to constructed the one-loop $(++++)$ amplitude, whose corresponding correlation function consists only of completion vertices. We first studied its generalised unitarity cuts, finding that when the external momenta are kept off-shell, only the box graphs of fig. 4.5 contribute to the cut. Furthermore, only the quadruple cut of this MHV completion graph is non-vanishing, and we computed it directly and demonstrated that it reproduces precisely the quadruple cut of the D-dimensional massless box function K_4.

It was then seen that, like at the tree-level, the sum of the MHV completion diagrams reduces to the LCYM expression for the amplitude, even before integrating the loop momentum or taking any on-shell limits. That the loop amplitude is recovered in such a straightforward way is evidence contrary to the twistor-space inspired suggestion in [29] that the $(++++)$ and $(-+++)$ amplitudes come from new local vertices.

The precise circumstances under which the completion vertices must be used is a subject for further investigation. We have seen that they are not required for on-shell tree amplitudes. We presume that they may also not be required for amplitudes where only certain legs are off shell. Nevertheless, they are required for the complete construction of off-shell tree amplitudes, and on shell at the loop level due to the existence of regions of propagator phase space that give rise to poles that cancel inverse propagators from the LSZ reduction.

In keeping with the field theory spirit which motivated this work, one might also consider the possibility of directly evaluating individual MHV completion graphs. However, defining the integrals poses a technical challenge when it comes to dealing with the unusual, gauge-dependent singularity structures hidden in the completion vertices. Conversely, given that we have seen that off-shell LCYM is recovered algebraically before any integration takes place, one might question the wisdom of this; again, without knowing the conditions under which completion vertices must be used, it is hard to see whether this would provide any computational advantage over LCYM.

4.A Light-cone vector identities

The appendix gives some of the identities particular to vectors in D-dimensional light-cone co-ordinates. Some of these appear in a different form in [104]. First, for any two D-vectors p and q,

$$(p\,q)\cdot\{p\,q\} = -\tfrac{1}{2}(\hat{p}\,q - \hat{q}\,p)^2 \tag{4.74}$$

from which it is clear that for null p, q,

$$(p\,q)\cdot\{p\,q\} = \hat{p}\,\hat{q}\,p\cdot q. \tag{4.75}$$

The Bianchi-like identity

$$\hat{i}(j\,k) + \hat{j}(k\,i) + \hat{k}(i\,j) = 0 \tag{4.76}$$

holds also under replacement of the hat with any transverse component i_I or $\bar{i}_I$, and replacement of the bilinear with its adjoint.

For a set of momenta $\{p_j\}$ that sum to zero,

$$\sum_j \frac{(p\,j)\cdot\{j\,q\}}{\hat{j}} = \frac{\hat{p}\,\hat{q}}{2}\sum_j \frac{p_j^2}{\hat{j}} \tag{4.77}$$

for any p and q. This is the D-dimensional, off-shell generalisation of the spinor identity $\sum_j \langle p\ j\rangle[j\ q] = \langle p|(\sum_j |j\rangle[j|)|q] = 0$. In four dimensions the above identity looks the same except that the dot product is simply multiplication. Also,

$$\sum_j \Omega_j = -\frac{1}{2}\sum_j \frac{p_j^2}{\hat{j}}. \tag{4.78}$$

(In four dimensions the left hand side has ω_j in place of Ω_j.)

Chapter 5

The Canonical MHV Lagrangian for Massless QCD

In this chapter, we will extend the work of chapter 3 and develop the ideas sketched by Mansfield in section 3 of [46] to construct an MHV lagrangian for massless QCD. The structure of this chapter is as follows. In section 5.1, we start with the manifestly Lorentz-covariant action for massless QCD, and then fix it to the light-cone gauge, and integrate out the non-dynamical degrees of freedom. Then, in section 5.2, we specify the field transformation that eliminates the $\overline{\text{MHV}}$-like vertices from the action. We establish what form this transformation will take, and argue that the lagrangian that results will have an infinite series of terms with MHV helicity content, and that these continue off-shell by the CSW prescription as in [28]. We solve explicitly for this transformation as a perturbative series. Next, in section 5.3, we demonstrate explicitly that this lagrangian does indeed contain vertices corresponding to the known expressions for MHV amplitudes containing quarks for the cases of: two quarks and two gluons, four quarks, and two quarks and three gluons in the $(1_q^+ 2^+ 3^- 4^+ 5_{\bar{q}}^-)$ configuration. Finally, we draw conclusions on this chapter in section 5.4.

This work was published in [50].

5.1 The light-cone action for massless QCD

Let us begin with the action for a massless QCD theory with $\mathrm{SU}(N_C)$ gauge symmetry. Its action is

$$S_{\text{QCD}} = \frac{1}{2g^2}\int d^4x\, 2ig^2\, \bar{\psi}\, \not{\mathcal{D}}\, \psi + \frac{1}{2g^2}\int d^4x\ \mathrm{tr}\, \mathcal{F}^{\mu\nu}\mathcal{F}_{\mu\nu}. \tag{5.1}$$

Here, we will use the chiral Weyl representation of the Dirac matrices

$$\gamma^\mu = \begin{pmatrix} 0 & \sigma^\mu \\ \bar{\sigma}^\mu & 0 \end{pmatrix},$$

and the spinors

$$\psi = (\alpha^+, \beta^+, \beta^-, \alpha^-)^{\mathrm{T}} \quad \text{and} \quad \bar{\psi} = (\bar{\beta}^+, \bar{\alpha}^+, \bar{\alpha}^-, \bar{\beta}^-)$$

are the quark field and its conjugate. They have the canonical normalisation and are in the fundamental representation of $\mathrm{SU}(N_{\mathrm{C}})$. Note that the superscripts $\pm$ in the components denote the physical helicity for *outgoing* particles, as we shall later see; that $\bar{\alpha}^+ = (\alpha^-)^*$ should be understood, and similarly for β. $\mathcal{A}$, $\mathcal{D}$, $\mathcal{F}_{\mu\nu}$ and the gauge group generator matrices are defined as in the pure Yang-Mills case of chapter 3, given in (3.8).

As before, we quantise the theory on surfaces Σ of constant x^0, *i.e.* those with normal $\mu = (1,0,0,1)/\sqrt{2}$ in Minkowski co-ordinates, and fix to the same axial gauge $\mu \cdot \mathcal{A} = \hat{\mathcal{A}} = 0$, for which the Faddeev-Popov ghosts are completely decoupled. We can set this gauge condition immediately (and discard the infinite, field-independent factor the Faddeev-Popov procedure produces). With this condition in force, the Dirac term in (5.1) may be expressed as

$$\begin{aligned}\frac{1}{2g^2}\int 2g^2\, i\{\bar{\varphi}\,(\partial\cdot\sigma - \mathcal{A}\bar{\sigma} - \bar{\mathcal{A}}\sigma)\,\varphi + \omega\,(\partial\cdot\bar{\sigma} + \mathcal{A}\sigma + \bar{\mathcal{A}}\bar{\sigma})\bar{\omega}\} \\ + \mathrm{tr}\,\{2g^2\, i(\bar{\varphi}\,T^a\hat{\sigma}\,\varphi + \omega\,T^a\check{\sigma}\bar{\omega})T^a\,\check{\mathcal{A}}\},\end{aligned}$$

where for compactness we have split ψ, $\bar{\psi}$ into Weyl spinors:

$$\begin{aligned}\bar{\omega}^{\dot{\alpha}} &= \begin{pmatrix}\alpha^+\\ \beta^+\end{pmatrix}, \\ \varphi_\alpha &= \begin{pmatrix}\beta^-\\ \alpha^-\end{pmatrix}, \\ \omega^\alpha &= (\bar{\alpha}^-, \bar{\beta}^-), \\ \bar{\varphi}_{\dot{\alpha}} &= (\bar{\beta}^+, \bar{\alpha}^+).\end{aligned}$$

(Note that the meaning of σ and $\bar{\sigma}$ as either a 4-vector, or light-cone co-ordinate component thereof, should be clear from the context.) That done, the lagrangian is quadratic in $\check{\mathcal{A}}$ and we can integrate it out. In section 3.1, we did this by finding the coefficient of $\check{\mathcal{A}}$ under the trace in (3.10), calling it K_{YM}, and replaced all terms in the action containing $\check{\mathcal{A}}$ with

$$-\frac{1}{2g^2}\int \mathrm{tr}\,\tfrac{1}{8}K_{\mathrm{YM}}\hat{\partial}^{-2}K_{\mathrm{YM}}.$$

This time, we must put $K_{\mathrm{YM}} \to K_{\mathrm{YM}} + K_\psi$, where

$$K_\psi = 2g^2\, i(\bar{\varphi}\,T^a\hat{\sigma}\,\varphi + \omega\,T^a\check{\sigma}\bar{\omega})T^a$$

is the coefficient of the Dirac term linear in $\check{\mathcal{A}}$ under the $\frac{1}{2}g^{-2}\int \mathrm{tr}$. Hence, all terms in (5.1) containing $\check{\mathcal{A}}$ should be replaced with

$$\frac{1}{2g^2}\int \mathrm{tr}\,\{-\tfrac{1}{8}K_\psi\hat{\partial}^{-2}K_\psi - \tfrac{1}{4}K_\psi\hat{\partial}^{-2}K_{\mathrm{YM}} - \tfrac{1}{8}K_{\mathrm{YM}}\hat{\partial}^{-2}K_{\mathrm{YM}}\}. \tag{5.2}$$

The first term here is a four-fermion effective vertex arising from the integrated-out gauge degree of freedom; similarly, the second term accounts for the interaction with unphysical gluon states. The last term produces contributions that result in the same gluonic terms as before (*cf.* (3.21)–(3.23)). If we evaluate (5.2), integrating by parts as necessary, and use it to substitute for the $\check{\mathcal{A}}$ terms in (5.1), we arrive at the action

$$\begin{aligned} S_{\mathrm{LCQCD}} = \int \frac{4}{g^2}(\mathcal{L}^{-+} + \mathcal{L}^{-++} + \mathcal{L}^{--+} + \mathcal{L}^{--++}) \\ + \mathcal{L}_{\bar{\psi}\psi} + \mathcal{L}_{\bar{\psi}\mathcal{A}\psi} + \mathcal{L}_{\bar{\psi}\bar{\mathcal{A}}\psi} + \mathcal{L}_{\bar{\psi}\mathcal{A}\bar{\mathcal{A}}\psi} + \mathcal{L}_{\bar{\psi}\psi\bar{\psi}\psi} \end{aligned} \tag{5.3}$$

where

$$\begin{aligned} \mathcal{L}_{\bar{\psi}\psi} &= i\,\{\bar{\varphi}\,\partial\cdot\sigma\,\varphi + \omega\,\partial\cdot\bar{\sigma}\,\bar{\omega}\}\,, \\ \mathcal{L}_{\bar{\psi}\mathcal{A}\psi} &= i\left\{\bar{\varphi}\left[(\hat{\sigma}\bar{\partial}\hat{\partial}^{-1} - \bar{\sigma})\mathcal{A}\right]\varphi + \omega\left[(\check{\sigma}\bar{\partial}\hat{\partial}^{-1} + \bar{\sigma})\mathcal{A}\right]\bar{\omega}\right\}, \\ \mathcal{L}_{\bar{\psi}\bar{\mathcal{A}}\psi} &= i\left\{\bar{\varphi}\left[(\hat{\sigma}\partial\hat{\partial}^{-1} - \sigma)\bar{\mathcal{A}}\right]\varphi + \omega\left[(\check{\sigma}\bar{\partial}\hat{\partial}^{-1} + \sigma)\bar{\mathcal{A}}\right]\bar{\omega}\right\}, \\ \mathcal{L}_{\bar{\psi}\mathcal{A}\bar{\mathcal{A}}\psi} &= i\left\{\bar{\varphi}\,\hat{\partial}^{-2}([\hat{\partial}\mathcal{A},\bar{\mathcal{A}}] + [\hat{\partial}\bar{\mathcal{A}},\mathcal{A}])\hat{\sigma}\,\varphi + \omega\,\hat{\partial}^{-2}([\hat{\partial}\mathcal{A},\bar{\mathcal{A}}] + [\hat{\partial}\bar{\mathcal{A}},\mathcal{A}])\check{\sigma}\,\bar{\omega}\right\}, \\ \mathcal{L}_{\bar{\psi}\psi\bar{\psi}\psi} &= \tfrac{1}{2}g^2 j^a\hat{\partial}^{-2}j^a, \quad j^a = \bar{\varphi}\,T^a\hat{\sigma}\,\varphi + \omega\,T^a\check{\sigma}\,\bar{\omega}. \end{aligned} \tag{5.4}$$

Let us study the quark kinetic terms (5.4) above. Written out, they are

$$\begin{aligned} \mathcal{L}_{\bar{\psi}\psi} = i\sqrt{2}\{\bar{\beta}^+\hat{\partial}\beta^- + \bar{\beta}^+\partial\alpha^- + \bar{\alpha}^+\bar{\partial}\beta^- + \bar{\alpha}^+\check{\partial}\alpha^- \\ + \bar{\alpha}^-\check{\partial}\alpha^+ - \bar{\alpha}^-\partial\beta^+ - \bar{\beta}^-\bar{\partial}\alpha^+ + \bar{\beta}^-\hat{\partial}\beta^+\} \end{aligned}$$

from which it is clear that $\beta^\pm$ and $\bar{\beta}^\pm$ are non-dynamical with respect to $\check{\partial}$. Since the terms in (5.3) that couple only non-dynamical fields contain no other fields, evaluating their path integral amounts to computing the determinant of a non-field-dependent object (specifically $\hat{\partial}$). Therefore this integration can be carried out just as well by replacing the non-dynamical fields according to their classical equations of motion. These are

$$\begin{aligned} \hat{\partial}\beta^- &= -\mathcal{D}\alpha^-, \\ \hat{\partial}\bar{\beta}^+ &= \bar{\alpha}^+\bar{\mathcal{A}} - \bar{\partial}\bar{\alpha}^+, \\ \hat{\partial}\beta^+ &= \bar{\mathcal{D}}\alpha^+, \\ \hat{\partial}\bar{\beta}^- &= \partial\bar{\alpha}^- - \bar{\alpha}^-\mathcal{A}. \end{aligned}$$

Substituting back into (5.3), we finally arrive at the following gauge-fixed action that features only dynamical components:

$$S_{\text{LCQCD}} = \frac{4}{g^2}\int dx^0 (L^{-+} + L^{-++} + L^{--+} + L^{--++} + L^{\bar\psi\psi} + L^{\bar\psi+\psi} + L^{\bar\psi-\psi} + L^{\bar\psi+-\psi} + L^{\bar\psi\psi\bar\psi\psi}), \tag{5.5}$$

where L^{-+}, L^{-++}, L^{--+} and L^{--++} form the same Yang-Mills sector of the theory from chapter 3, set out in eqs. (3.21)–(3.23), and the new terms involving the fermions are

$$L^{\bar\psi\psi} = \frac{ig^2}{\sqrt{8}}\int_\Sigma d^3\mathbf{x}\left\{\bar\alpha^+(\check\partial-\omega)\alpha^- + \bar\alpha^-(\check\partial-\omega)\alpha^+\right\}, \tag{5.6}$$

$$L^{\bar\psi+\psi} = -\frac{ig^2}{\sqrt{8}}\int_\Sigma d^3\mathbf{x}\left\{\bar\alpha^+\,\bar\partial\hat\partial^{-1}(\mathcal{A}\,\alpha^-) + \bar\alpha^-\mathcal{A}\,\bar\partial\hat\partial^{-1}\alpha^+ - \bar\alpha^+(\bar\partial\hat\partial^{-1}\mathcal{A})\alpha^- - \bar\alpha^-(\bar\partial\hat\partial^{-1}\mathcal{A})\alpha^+\right\}, \tag{5.7}$$

$$L^{\bar\psi-\psi} = -\frac{ig^2}{\sqrt{8}}\int_\Sigma d^3\mathbf{x}\left\{\bar\alpha^+\bar{\mathcal{A}}\,\partial\hat\partial^{-1}\alpha^- + \bar\alpha^-\partial\hat\partial^{-1}(\bar{\mathcal{A}}\,\alpha^+) - \bar\alpha^+(\partial\hat\partial^{-1}\bar{\mathcal{A}})\alpha^- - \bar\alpha^-(\partial\hat\partial^{-1}\bar{\mathcal{A}})\alpha^+\right\}, \tag{5.8}$$

$$L^{\bar\psi+-\psi} = -\frac{ig^2}{\sqrt{8}}\int_\Sigma d^3\mathbf{x}\left\{\bar\alpha^+\bar{\mathcal{A}}\hat\partial^{-1}(\mathcal{A}\alpha^-) + \bar\alpha^-\mathcal{A}\hat\partial^{-1}(\bar{\mathcal{A}}\alpha^+) + \bar\alpha^+\hat\partial^{-2}(\hat\partial\mathcal{A}\bar{\mathcal{A}} - \mathcal{A}\hat\partial\bar{\mathcal{A}})\alpha^- + \bar\alpha^+\hat\partial^{-2}(\hat\partial\bar{\mathcal{A}}\mathcal{A} - \bar{\mathcal{A}}\hat\partial\mathcal{A})\alpha^- + \bar\alpha^-\hat\partial^{-2}(\hat\partial\mathcal{A}\bar{\mathcal{A}} - \mathcal{A}\hat\partial\bar{\mathcal{A}})\alpha^+ + \bar\alpha^-\hat\partial^{-2}(\hat\partial\bar{\mathcal{A}}\mathcal{A} - \bar{\mathcal{A}}\hat\partial\mathcal{A})\alpha^+\right\}, \tag{5.9}$$

$$L^{\bar\psi\psi\bar\psi\psi} = \frac{g^4}{16}\int_\Sigma d^3\mathbf{x}\, j^a\hat\partial^{-2}j^a, \quad j^a = \sqrt{2}(\bar\alpha^+T^a\alpha^- + \bar\alpha^-T^a\alpha^+). \tag{5.10}$$

5.2 The MHV QCD field transformation

Let us now construct the field transformation that results in a MHV lagrangian for massless QCD. We label the new algebra-valued gauge fields $\mathcal{B}$ and $\bar{\mathcal{B}}$ as before, and the new fundamental representation fermions ξ^+, $\bar\xi^-$, ξ^- and $\bar\xi^+$; their Lorentz transformation properties are the same as those of the old fields with similar embellishments. We remove terms in the light-cone lagrangian with a $(-++)$ helicity structure by absorbing them into the kinetic terms of the new fields as follows:

$$L^{-+}[\mathcal{A},\bar{\mathcal{A}}] + L^{-++}[\mathcal{A},\bar{\mathcal{A}}] + L^{\bar\psi\psi}[\alpha^\pm,\bar\alpha^\pm] + L^{\bar\psi+\psi}[\mathcal{A},\alpha^\pm,\bar\alpha^\pm] = L^{-+}[\mathcal{B},\bar{\mathcal{B}}] + L^{\bar\psi\psi}[\xi^\pm,\bar\xi^\pm]. \tag{5.11}$$

We remark that this appears sensible, since the theory formed by the truncation on the LHS of (5.11) is classically free. The remaining terms in the lagrangian, (3.22), (3.23) and (5.8)–(5.10) form the MHV vertices, as we will show in the next section.

5.2.1 Form of the transformation and MHV lagrangian

First, let us establish the general form of the field transformation and the resulting lagrangian. We note that the canonical (co-ordinate, momentum) pairs of the system (5.5) are

$$(\mathcal{A}, -\hat{\partial}\bar{\mathcal{A}}), \quad \left(\alpha^+, -\frac{ig^2}{\sqrt{8}}\bar{\alpha}^-\right) \quad \text{and} \quad \left(\alpha^-, -\frac{ig^2}{\sqrt{8}}\bar{\alpha}^+\right),$$

and likewise for the new fields (by replacing $\mathcal{A} \to \mathcal{B}$ and $\alpha \to \xi$ above). We have defined the momenta with respect to the lagrangian *under the integral* in (5.5). The path integral measure

$$\mathcal{D}\mathcal{A}\mathcal{D}\bar{\mathcal{A}}\,\mathcal{D}\alpha^+\mathcal{D}\bar{\alpha}^-\,\mathcal{D}\alpha^-\mathcal{D}\bar{\alpha}^+,$$

is therefore the phase-space measure (up to an irrelevant constant), and it will be preserved if the transformation is canonical. This, and our demands on the helicity content of the resulting lagrangian, restrict the form of the transformation as follows.

Again, we choose a canonical transformation of the form generated by (3.68), $\mathcal{A}$ will be a functional of $\mathcal{B}$ alone. Since the transformation takes place entirely on Σ (*i.e.* no explicit x^0 dependence), and preserves the form of the kinetic part of the lagrangian, the new (co-ordinate, momentum) pairs are

$$(\mathcal{B}, -\hat{\partial}\bar{\mathcal{B}}), \quad \left(\xi^+, -\frac{ig^2}{\sqrt{8}}\bar{\xi}^-\right) \quad \text{and} \quad \left(\xi^-, -\frac{ig^2}{\sqrt{8}}\bar{\xi}^+\right).$$

We remind the reader that they satisfy (3.70), which in this case implies that

$$\hat{\partial}\bar{\mathcal{A}}^a(\mathbf{x}) = \int_\Sigma d^3\mathbf{y}\left\{\frac{\delta\mathcal{B}^b(\mathbf{y})}{\delta\mathcal{A}^a(\mathbf{x})}\hat{\partial}\bar{\mathcal{B}}^b(\mathbf{y}) - \frac{ig^2}{\sqrt{8}}\left(\bar{\xi}^-(\mathbf{y})\frac{\delta\xi^+(\mathbf{y})}{\delta\mathcal{A}^a(\mathbf{x})} + \bar{\xi}^+(\mathbf{y})\frac{\delta\xi^-(\mathbf{y})}{\delta\mathcal{A}^a(\mathbf{x})}\right)\right\}. \quad (5.12)$$

(Note that we take all derivatives with respect to Grassman variables as acting from the left. Also the order of the fermion co-ordinate and momentum factors above is the opposite of that of (3.70), and as such these terms pick up an extra factor of -1.)

By charge conservation, and the requirement that this will be a canonical transformation that results in a lagrangian whose vertices have MHV helicity content, tells us that the fermion co-ordinate transformation takes the form

$$\xi^\pm(\mathbf{x}) = \int_\Sigma d^3\mathbf{y}\; R^\mp[\mathcal{A}](\mathbf{x},\mathbf{y})\;\alpha^\pm(\mathbf{y}). \quad (5.13)$$

The superscript of $R^\pm$ refers to the *chirality* of the Weyl spinor from which the field components originate: $+$ for right-handed, $-$ for left-handed. $R^\pm$ is a matrix-valued functional of $\mathcal{A}$. Putting additional factors of $\bar{\mathcal{A}}$ into the RHS of (5.13) would result in terms in the resulting lagrangian with more than two fields of negative helicity; likewise with extra quark fields, since charge conservation requires these to be added in $(+-)$

helicity pairs. Conversely, the behaviour of the canonical momenta must be

$$\bar{\alpha}^{\pm}(\mathbf{x}) = \int_{\Sigma} d^3\mathbf{y}\, \bar{\xi}^{\pm}(\mathbf{y})\, R^{\pm}[\mathcal{A}](\mathbf{y},\mathbf{x}), \tag{5.14}$$

It will also be useful to define the inverse transformations

$$\alpha^{\pm}(\mathbf{x}) = \int_{\Sigma} d^3\mathbf{y}\, S^{\mp}[\mathcal{A}](\mathbf{x},\mathbf{y})\, \xi^{\pm}(\mathbf{y}) \tag{5.15}$$

as well.

At this point we can immediately read off the propagators for the new fields from (5.11) as

$$\langle \mathcal{B}\bar{\mathcal{B}} \rangle = -\frac{ig^2}{2p^2} \quad \text{and} \quad \langle \xi^-\bar{\xi}^+ \rangle = \langle \xi^+\bar{\xi}^- \rangle = i\sqrt{2}\frac{\hat{p}}{p^2}. \tag{5.16}$$

By using (3.8), one obtains the canonically normalised propagator $\langle B\bar{B} \rangle = i/p^2$, and indeed in practical calculations with the MHV lagrangian it is often more convenient to absorb powers of this factor into the lagrangian's vertices and transformation series coefficients, as was done in chapter 4. For the purposes of this chapter, however, we will account for these factors at the end of the calculations we present in the next section.

If we now assume solutions for R and S as infinite series in $\mathcal{A}$, it is not hard to see that, upon substitution into the remaining terms of the light-cone QCD lagrangian, this choice of transformation gives a set of terms with no more than two fields of negative helicity ($\bar{\mathcal{B}}$, ξ^- and $\bar{\xi}^-$) in each, but an increasing number of $\mathcal{B}$ fields as shown in table 5.1. (The number of positive-helicity quark fields present is, of course, strictly constrained by charge conservation.) The sum of these terms has precisely the helicity and colour structure required to be identified as the interaction part of a MHV lagrangian, and we claim here that the Feynman rules of its tree-level perturbation theory follow the CSW rules. We will address the proof of this in section 5.2.3.

LCQCD term	**New field content**
L^{--+}	$\bar{\mathcal{B}}\bar{\mathcal{B}}\mathcal{B}\cdots$, $\bar{\xi}\xi\bar{\mathcal{B}}\mathcal{B}\cdots$, $\bar{\xi}\xi\bar{\xi}\xi\mathcal{B}\cdots$
L^{--++}	$\bar{\mathcal{B}}\bar{\mathcal{B}}\mathcal{B}\mathcal{B}\cdots$, $\bar{\xi}\xi\bar{\mathcal{B}}\mathcal{B}\cdots$, $\bar{\xi}\xi\bar{\xi}\xi\mathcal{B}\mathcal{B}\cdots$
$L^{\bar{\psi}-\psi}$	$\bar{\xi}\xi\bar{\mathcal{B}}$, $\bar{\xi}\xi\bar{\mathcal{B}}\mathcal{B}\cdots$, $\bar{\xi}\xi\bar{\xi}\xi\mathcal{B}\cdots$
$L^{\bar{\psi}+-\psi}$	$\bar{\xi}\xi\bar{\mathcal{B}}\mathcal{B}\cdots$, $\bar{\xi}\xi\bar{\xi}\xi\mathcal{B}\cdots$
$L^{\bar{\psi}\psi\bar{\psi}\psi}$	$\bar{\xi}\xi\bar{\xi}\xi$, $\bar{\xi}\xi\bar{\xi}\xi\mathcal{B}\cdots$

TABLE 5.1: The contents of the new vertices provided by our choice of field transformation. The new fermion fields, ξ, always occur in bilinear pairs and as such $\bar{\xi}\xi$ is the sum of a term containing exactly one $-$ helicity quark, and another term with one $-$ helicity antiquark. An ellipsis $\cdots$ denotes an infinite series wherein the field to its immediate left is repeated.

We can deduce from the forms of the light-cone Yang–Mills lagrangian (5.6)–(5.10) and the transformation that terms containing a single quark-antiquark pair are of the

form

$$\int_{1\cdots n} \sum_{n=3}^{\infty} \sum_{j=2}^{n-1} \sum_{\pm} \bar{\xi}_{\bar{1}}^{\pm} \mathcal{B}_{\bar{2}} \cdots \mathcal{B}_{\bar{j}} \cdots \mathcal{B}_{\overline{n-1}} \xi_{\bar{n}}^{\mp} \, V_{2\mathrm{q}\,1\cdots n}^{j;\pm}. \tag{5.17}$$

Clearly this is coincident with the colour structure of (2.16). Similarly, for two quark-antiquark pairs, we expect a contribution to the lagrangian of the form

$$\begin{aligned}\int_{1\cdots n} \sum_{n=4}^{\infty} \sum_{j=3}^{n-1} \sum_{(h_1,h_j)\in\mathcal{H}} \Big\{ & \bar{\xi}_{\bar{1}}^{h_1} \mathcal{B}_{\bar{2}} \cdots \mathcal{B}_{\overline{j-2}} \xi_{\overline{j-1}}^{-h_j} \bar{\xi}_{\bar{j}}^{h_j} \mathcal{B}_{\overline{j+1}} \cdots \mathcal{B}_{\overline{n-1}} \xi_{\bar{n}}^{-h_1} \, V_{4\mathrm{q}\,1\cdots n}^{j;h_1h_j} \\ & + \frac{1}{N_\mathrm{C}} \bar{\xi}_{\bar{1}}^{h_1} \mathcal{B}_{\bar{2}} \cdots \mathcal{B}_{\overline{j-2}} \xi_{\bar{n}}^{-h_1} \bar{\xi}_{\bar{j}}^{h_j} \mathcal{B}_{\overline{j+1}} \cdots \mathcal{B}_{\overline{n-1}} \xi_{\overline{j-1}}^{-h_j} \, V_{4\mathrm{q}(1)\,1\cdots n}^{j;h_1h_j} \Big\} \mathcal{S}(h_1,h_j). \end{aligned} \tag{5.18}$$

Here, $\mathcal{H} = \{(+,+),(+,-),(-,-)\}$, and

$$\mathcal{S}(h_1,h_j) = \begin{cases} 1/2 & (h_1 = h_j) \\ 1 & (\text{otherwise}) \end{cases}$$

is a symmetry factor whose function is similar to the factor of 1/2 in (3.32) (*i.e.* it absorbs potential over-counting issues due to two possible external contractions leading to the same colour structure). We interpret any $\mathcal{B}$-string to be the identity above when it exceeds the bounds at either end of the ellipsis. This clearly corresponds to the structure of (2.18).[1] Both terms have the same relative sign due to the swapping of the fermion fields induced by the SU(N_C) Fierz rearrangement.

We will refer to these forms later in section 5.3 when we construct explicit examples of $V_{2\mathrm{q}}$ and $V_{4\mathrm{q}}$ for a few low-order cases. Note that we will also use the same notation as (3.34) to factor out δ functions.

5.2.2 Solution to the transformation

Extracting explicit solutions proceeds much like in the pure gluon case. We will obtain the old field variables as perturbative series expansions in the gauge field $\mathcal{B}$.

$\mathcal{A}$ and quark transformation $R^{\pm}$

Let us begin with (5.11). We write it out explicitly, making use of (5.12), (5.13) and (5.14) to substitute for $\hat{\partial}\bar{\mathcal{A}}$, $\bar{\alpha}^{\pm}$ and $\xi^{\pm}$ respectively. For clarity, we show below only the

[1] Since much of the literature works with U(N_C) gauge symmetry, many of the two-quark-pair amplitudes given there only correspond to the $\mathcal{O}({N_\mathrm{C}}^0)$ piece, *i.e.* partial amplitudes distilled from $\widetilde{V}_{4\mathrm{q}\,1\cdots n}^{j;h_1h_j}$.

left-handed chiral fermion components:

$$\int_{\mathbf{xy}} \{\omega\mathcal{A} + [\mathcal{A}, \zeta\mathcal{A}]\}^a(\mathbf{x}) \frac{\delta\mathcal{B}^b(\mathbf{y})}{\delta\mathcal{A}^a(\mathbf{x})} \hat{\partial}\bar{\mathcal{B}}^b(\mathbf{y}) - \frac{ig^2}{\sqrt{8}} \int_{\mathbf{xyz}} \{\omega\mathcal{A} + [\mathcal{A}, \zeta\mathcal{A}]\}^a(\mathbf{z}) \times$$
$$\left\{ \bar{\xi}^-(\mathbf{x}) \frac{\delta R^-(\mathbf{x},\mathbf{y})}{\delta\mathcal{A}^a(\mathbf{z})} \alpha^+(\mathbf{y}) + \text{r.h.} \right\} + \frac{ig^2}{\sqrt{8}} \int_{\mathbf{xy}} \Big[\bar{\xi}^-(\mathbf{x}) \{ R^-(\mathbf{x},\mathbf{y})[\zeta\mathcal{A}(\mathbf{y})]$$
$$+ \omega_y R^-(\mathbf{x},\mathbf{y}) - \zeta_y[R^-(\mathbf{x},\mathbf{y})\mathcal{A}(\mathbf{y})] \} \alpha^+(\mathbf{y}) + \text{r.h.} \Big]$$
$$= \int_{\mathbf{x}} \omega\mathcal{B}^a \hat{\partial}\bar{\mathcal{B}}^a - \frac{ig^2}{\sqrt{8}} \int_{\mathbf{xy}} \{ \bar{\xi}^-(\mathbf{x}) \omega_x R^-(\mathbf{x},\mathbf{y}) \alpha^+(\mathbf{y}) + \text{r.h.} \}. \quad (5.19)$$

We have adopted the convenient short-hand $\int_{\mathbf{xy}\ldots} := \int_\Sigma d^3\mathbf{x}\, d^3\mathbf{y} \cdots$, and defined the differential operator $\zeta = \bar{\partial}/\hat{\partial}$. Now recall from chapter 3 we expressed $\mathcal{A}$ as a series in $\mathcal{B}$, given in eqs. (3.42) and (3.51). This was obtained by solving (3.41), reproduced here in configuration space:

$$\int_{\mathbf{x}} \{\omega\mathcal{A} + [\mathcal{A}, \zeta\mathcal{A}]\}^a(\mathbf{x}) \frac{\delta\mathcal{B}^b(\mathbf{y})}{\delta\mathcal{A}^a(\mathbf{x})} = \omega\mathcal{B}^b(\mathbf{y}),$$

so by substituting for $\mathcal{A}$ with (3.42), we can eliminate the first terms from either side of (5.19). Furthermore, we can use (3.41) on the LHS of (5.19) to trade the $\delta R^-/\delta\mathcal{A}$ for $\delta R^-/\delta\mathcal{B}$, and we arrive at

$$\int_{\mathbf{xyz}} \bar{\xi}^-(\mathbf{x}) \left\{ (\omega_x + \omega_y) R^-(\mathbf{x},\mathbf{y}) - [\omega\mathcal{B}^a(\mathbf{z})] \frac{\delta R^-(\mathbf{x},\mathbf{y})}{\delta\mathcal{B}^a(\mathbf{z})} \right\} \alpha^+(\mathbf{y})$$
$$= \int_{\mathbf{xyz}} \bar{\xi}^-(\mathbf{x}) \left\{ \zeta_y[R^-(\mathbf{x},\mathbf{y})\mathcal{A}(\mathbf{y})] - R^-(\mathbf{x},\mathbf{y})[\zeta\mathcal{A}(\mathbf{y})] \right\} \alpha^+(\mathbf{y}). \quad (5.20)$$

The same procedure yields a similar equation for the right-handed sector:

$$\int_{\mathbf{xyz}} \bar{\xi}^+(\mathbf{x}) \left\{ (\omega_x + \omega_y) R^+(\mathbf{x},\mathbf{y}) - [\omega\mathcal{B}^a(\mathbf{z})] \frac{\delta R^+(\mathbf{x},\mathbf{y})}{\delta\mathcal{B}^a(\mathbf{z})} \right\} \alpha^-(\mathbf{y})$$
$$= \int_{\mathbf{xyz}} \bar{\xi}^+(\mathbf{x}) \left\{ [\zeta_y R^+(\mathbf{x},\mathbf{y})]\mathcal{A}(\mathbf{y}) - R^+(\mathbf{x},\mathbf{y})[\zeta\mathcal{A}(\mathbf{y})] \right\} \alpha^-(\mathbf{y}). \quad (5.21)$$

As the quark fields are arbitrary, equations (5.20) and (5.21) determine the solutions for $R^\pm$ in terms of $\mathcal{B}$. We switch to momentum space on Σ, and postulate a series solution of the form

$$R^\pm(12) = (2\pi)^3\delta^3(\mathbf{p}_1 + \mathbf{p}_2) + \sum_{n=3}^{\infty} \int_{3\cdots n} R^\pm(12;3\cdots n)\mathcal{B}_{\bar{3}} \cdots \mathcal{B}_{\bar{n}}\, (2\pi)^3\delta^3(\textstyle\sum_{i=1}^n \mathbf{p}_i)$$

Here, momenta $\mathbf{p}_1$ and $\mathbf{p}_2$ are associated with the Fourier transforms of $\mathbf{x}$ and $\mathbf{y}$, respectively, in (5.13). For future purposes, it will often be convenient to absorb the first term above into the sum by defining $R^\pm(12;) = 1$. As the quark fields are arbitrary, we can drop them and the integrals over $\mathbf{x}$ and $\mathbf{y}$ in (5.20) and (5.21) and what is left

determines the solutions for $R^{\pm}$ in terms of $\mathcal{B}$.

Writing equations (5.20) and (5.21) in momentum space and using (3.42) to substitute for $\mathcal{A}$ leads to the following two recurrence relations:

$$R^{-}(12;3\cdots n) = \frac{-i}{\omega_1+\cdots+\omega_n}\sum_{j=2}^{n-1}\frac{\{2,P_{j+1,n}\}}{\hat{2}\,\hat{P}_{j+1,n}}\,R^{-}(1,2{+}P_{j+1,n};3\ldots j)\Upsilon(-,j{+}1,\cdots,n) \quad (5.22)$$

and

$$R^{+}(12;3\cdots n) = \frac{-i}{\omega_1+\cdots+\omega_n}\sum_{j=2}^{n-1}\frac{\{2,P_{j+1,n}\}}{(\hat{2}{+}\hat{P}_{j+1,n})\,\hat{P}_{j+1,n}}\,R^{+}(1,2{+}P_{j+1,n};3\ldots j)\Upsilon(-,j{+}1,\cdots,n), \quad (5.23)$$

where, as before, we define the momentum space analogue of the ω operator as $\omega_p := p\bar{p}/\hat{p}$, $P_{ij} := \sum_{k=i}^{j} p_k$, and $-$ as a momentum argument denotes the negative of the sum of the other arguments. We notice immediately from the above that if we put

$$R^{-}(12;3\cdots n) = -\frac{\hat{1}}{\hat{2}}R^{+}(12;3\cdots n) \quad (5.24)$$

into (5.22), we recover (5.23); note that this only fixes the numerator $\hat{1}$ above, whereas the sign and the denominator follow by noting that the lowest-order coefficients $R^{\pm}(12;\,) = 1$ are defined for conserved momentum (*i.e.* at $\mathbf{p}_1 = -\mathbf{p}_2$). Thus, we need only solve for R^{+}.

Now one could obtain (and prove) a form for the R^{+} coefficients by direct iteration of (5.23) and induction on n, but in fact it turns out that the recurrence relation (5.23) is nothing other than a re-labelling of the Υ recurrence relation (3.48), reproduced below:

$$\Upsilon(1\cdots n) = \frac{-i}{\omega_1+\cdots+\omega_n}\sum_{j=2}^{n-1}\left(\frac{\bar{P}_{j+1,n}}{\hat{P}_{j+1,n}}-\frac{\bar{P}_{2j}}{\hat{P}_{2j}}\right)\Upsilon(-,2,\cdots,j)\Upsilon(-,j{+}1,\cdots,n).$$

The solution to this was proved to be (3.51), so if we now put

$$R^{+}(12;3\cdots n) = \Upsilon(213\cdots n) = (-i)^n\frac{\widehat{\hat{2}\hat{3}\cdots n-1}}{(1\,3)(3\,4)\cdots(n-1,n)} \quad (5.25)$$

into (5.23) (and swap momenta 1 and 2), we arrive at (3.48), and (5.25) is thereby proved.

Quark inverse transformation $S^{\pm}$

The inverse fermion transformation, $S^{\pm}$, may be obtained from $R^{\pm}$ in an order-by-order manner. Let us begin by writing it as

$$S^{\pm}(12) = \sum_{n=2}^{\infty} \int_{3\cdots n} S^{\pm}(12;3\cdots n)\mathcal{B}_{\bar{3}}\cdots\mathcal{B}_{\bar{n}}\,(2\pi)^3\delta^3(\textstyle\sum_{i=1}^{n}\mathbf{p}_i),$$

where momenta $\mathbf{p}_1$ and $\mathbf{p}_2$ correspond to the Fourier transforms of $\mathbf{x}$ and $\mathbf{y}$ in (5.15), and we have absorbed the $\mathcal{O}(\mathcal{B}^0)$ (*i.e.* $n=2$) term into the sum by defining $S^{\pm}(12;)=1$. The $S^{\pm}$ coefficients satisfy the recurrence relations

$$S^{\pm}(12;3\cdots n) = -\sum_{j=2}^{n-1} S^{\pm}(1,-;3\ldots j)R^{\pm}(-,2;j{+}1,\cdots,n). \tag{5.26}$$

Now it is clear from (5.24) that

$$S^{+}(12;3\cdots n) = -\frac{\hat{2}}{\hat{1}}S^{-}(12;3\cdots n) \tag{5.27}$$

where again the overall normalisation is fixed by the lowest order coefficient.

Direct iteration of (5.26) gives the first few non-trivial S^{-}:

$$S^{-}(12;3) = i\frac{\hat{1}}{(3\,2)}, \tag{5.28}$$

$$S^{-}(12;34) = \frac{\hat{1}\hat{4}}{(3\,4)(4\,2)}, \tag{5.29}$$

and so-on, from which we claim that

$$S^{-}(12;3\cdots n) = (-i)^n\frac{\hat{1}\hat{4}\cdots\hat{n}}{(3\,4)\cdots(n-1,n)(n\,2)} = \Upsilon(13\cdots n2) \tag{5.30}$$

where in the case of $S^{-}(12;3)$ only the first factor in the numerator and the last factor in the denominator are retained. The proof is by induction on n. Expressions (5.28) and (5.29) provide the initial steps. For the inductive step, we use (5.30) to substitute for S^{-}, so the RHS of (5.26) becomes

$$\begin{aligned}&(-i)^n\frac{\hat{1}\hat{4}\cdots\widehat{n-1}}{(3\,4)\cdots(n{-}1,n)}\left\{\frac{\hat{3}}{(3,2{+}P_{3n})}+\sum_{j=3}^{n-1}\frac{(j,j{+}1)}{(j,2{+}P_{j,n})}\frac{\hat{2}+\hat{P}_{j+1,n}}{(j{+}1,2{+}P_{j+1,n})}\right\}\\ &=(-i)^n\frac{\hat{1}\hat{4}\cdots\widehat{n-1}}{(3\,4)\cdots(n{-}1,n)}\left(x_3+\sum_{j=3}^{n-1}y_j\right)\end{aligned}$$

where

$$y_j = \frac{(j,j{+}1)}{(j,2{+}P_{jn})}\frac{\hat{2}+\hat{P}_{j+1,n}}{(j{+}1,2{+}P_{j+1,n})} \quad\text{and}\quad x_j = \frac{\hat{j}}{(j,2{+}P_{jn})}.$$

Now notice that $x_j + y_j = x_{j+1}$, so the sum on the RHS of (5.26) collapses to

$$(-i)^n \frac{\hat{1}\hat{4}\cdots\widehat{n-1}}{(3\,4)\cdots(n-1,n)} x_n = S^-(12;3\cdots n),$$

and the proof is complete.[2]

Let us now summarise the quark field transformations we have found here:

$$\bar{\alpha}_1^{\pm} = \bar{\xi}_1^{\pm} + \sum_{n=3}^{\infty} \int_{2\cdots n} \begin{Bmatrix} 1 \\ -\hat{1}/\hat{2} \end{Bmatrix} \Upsilon(1\cdots n)\, \bar{\xi}_{\bar{2}}^{\pm} \mathcal{B}_{\bar{3}} \cdots \mathcal{B}_{\bar{n}}\, (2\pi)^3 \delta^3(\textstyle\sum_{i=1}^n \mathbf{p}_i), \tag{5.31}$$

$$\alpha_1^{\pm} = \xi_1^{\pm} + \sum_{n=3}^{\infty} \int_{2\cdots n} \begin{Bmatrix} 1 \\ -\hat{2}/\hat{1} \end{Bmatrix} \Upsilon(1\cdots n)\, \mathcal{B}_{\bar{2}} \cdots \mathcal{B}_{\overline{n-1}} \xi_{\bar{n}}^{\pm}\, (2\pi)^3 \delta^3(\textstyle\sum_{i=1}^n \mathbf{p}_i), \tag{5.32}$$

where the stacked expressions in braces take their value in accordance with the upper or lower choice of sign.

$\bar{A}$ transformation

Finally, we obtain an expression for $\bar{\mathcal{A}}$. Owing to the form of the canonical transformation, condition (3.71) still holds and gives

$$\begin{aligned} \int_{\mathbf{x}} \left\{ \operatorname{tr} \check{\partial}\mathcal{A}\hat{\partial}\bar{\mathcal{A}} - \frac{ig^2}{\sqrt{8}} \int d^3\mathbf{x} (\bar{\alpha}^- \check{\partial}\alpha^+ + \bar{\alpha}^+ \check{\partial}\alpha^-) \right\} \\ = \int_{\mathbf{x}} \left\{ \operatorname{tr} \check{\partial}\mathcal{B}\hat{\partial}\bar{\mathcal{B}} - \frac{ig^2}{\sqrt{8}} \int d^3\mathbf{x} (\bar{\xi}^- \check{\partial}\xi^+ + \bar{\xi}^+ \check{\partial}\xi^-) \right\}. \end{aligned} \tag{5.33}$$

Now consider the functional form of $\hat{\partial}\bar{\mathcal{A}}$ as given by (5.12). We can split into two pieces,

$$\hat{\partial}\bar{\mathcal{A}} = \hat{\partial}\bar{\mathcal{A}}^0 + \hat{\partial}\bar{\mathcal{A}}^{\mathrm{F}}, \tag{5.34}$$

where the first term depends only on $\mathcal{B}$ and $\bar{\mathcal{B}}$, and the second contains the fermion dependence. If we substitute this into (5.33), we find the terms

$$\operatorname{tr} \int_{\mathbf{x}} \check{\partial}\mathcal{A}\hat{\partial}\bar{\mathcal{A}}^0 \quad \text{and} \quad \operatorname{tr} \int_{\mathbf{x}} \check{\partial}\mathcal{B}\hat{\partial}\bar{\mathcal{B}}. \tag{5.35}$$

on the left- and right-hand sides, respectively. Now, these are the left- and right-hand side respectively of (3.53), which we solved in chapter 3 to obtain $\bar{\mathcal{A}}$ in the pure Yang–Mills case. Thus, we can consistently identify $\hat{\partial}\bar{\mathcal{A}}^0$ with the first term in (5.12) and eliminate (5.35) from (5.33) by using the same solution, but this time for $\bar{\mathcal{A}}^0$. In quantisation surface momentum space,

$$\bar{\mathcal{A}}_{\bar{1}}^0 = \sum_{m=2}^{\infty} \sum_{s=2}^{m} \int_{2\cdots m} \frac{\hat{s}^2}{\hat{1}^2} \Upsilon(\bar{1}2\cdots m)\, \mathcal{B}_{\bar{2}} \cdots \bar{\mathcal{B}}_{\bar{s}} \cdots \mathcal{B}_{\bar{m}}\, (2\pi)^3 \delta^3(\mathbf{p}_1 - \textstyle\sum_{i=2}^m \mathbf{p}_i). \tag{5.36}$$

[2] We could, of course, have obtained $S^{\pm}$ in a manner similar to $R^{\pm}$ by deriving an explicit recurrence relation and then mapping it to that for Υ, but we believe this to be a quicker route.

From this, we immediately see that the pure-gauge MHV lagrangian of chapter 3 is recovered via the terms that $\bar{\mathcal{A}}^0$ contributes to $\bar{\mathcal{A}}$ when used in L^{--+} and L^{--++}.

Next, we turn to $\mathcal{A}^{\mathrm{F}}$. From (5.12) and (5.34), we know that in momentum-space $\bar{\mathcal{A}}^{\mathrm{F}}$ is given by

$$\hat{1}\bar{\mathcal{A}}^{\mathrm{F}}_{\bar{1}} = -\frac{g^2}{\sqrt{8}}(F^-_{\bar{1}} + F^+_{\bar{1}}), \quad F^{\pm}_{\bar{1}} = \int_{\alpha\beta\gamma} \bar{\xi}^{\pm}_{\bar{\alpha}} \frac{\delta R^{\pm}(\boldsymbol{\alpha\gamma})}{\delta \mathcal{A}^a_1} S^{\pm}(\bar{\boldsymbol{\gamma}}\boldsymbol{\beta}) \xi^{\mp}_{\bar{\beta}}\, T^a, \tag{5.37}$$

where we have substituted with (5.13) and then (5.15). We could, in principle, use the known expressions for $R^{\pm}$ and $S^{\pm}$ to evaluate this, but this is a laborious process. Instead, we will solve for it outright, as follows.

First, let us study the series expansion for $F^{\pm}$. Consider the *form* of the objects between $\bar{\xi}$ and ξ in (5.37): since $\mathcal{A}$ depends only on $\mathcal{B}$, we see that it must be expressable in the form

$$\sum_{n=2}^{\infty}\sum_{j=1}^{n}\int_{2\cdots n} (\mathrm{coeff})_{\bar{1}2\cdots n} \times \mathcal{B}_{\bar{2}}\cdots\mathcal{B}_{\overline{j-1}}\,\delta^3(\mathbf{p}_1+\mathbf{p}_j)T^a\,\mathcal{B}_{\overline{j+1}}\cdots\mathcal{B}_{\bar{n}}. \tag{5.38}$$

Thus,

$$\begin{aligned} F^{\pm}_{\bar{1}} = -\sum_{n=3}^{\infty}\sum_{s=2}^{n-1}\int_{2\cdots n} \Delta^{\pm(s)}(\bar{1}2\cdots n)\Big\{ & \mathcal{B}_{\bar{2}}\cdots\mathcal{B}_{\overline{s-1}}\xi^{\mp}_{\bar{s}}\bar{\xi}^{\pm}_{\overline{s+1}}\mathcal{B}_{\overline{s+2}}\cdots\mathcal{B}_{\bar{n}} \\ & + \frac{1}{N_{\mathrm{C}}}(\bar{\xi}^{\pm}_{\overline{s+1}}\mathcal{B}_{\overline{s+2}}\cdots\mathcal{B}_{\bar{n}}\mathcal{B}_{\bar{2}}\cdots\mathcal{B}_{\overline{s-1}}\xi^{\mp}_{\bar{s}})\Big\}(2\pi)^3\delta^3(\mathbf{p}_1 - \textstyle\sum_{i=2}^{n}\mathbf{p}_i) \end{aligned} \tag{5.39}$$

where we have used the $\mathrm{SU}(N_{\mathrm{C}})$ Fierz identity (2.15) to evaluate the sum over the gauge generators. Note the sign change due to the Grassman nature of $\xi^{\pm}$ and $\bar{\xi}^{\pm}$, and that the $\mathcal{O}(1/N_{\mathrm{C}})$ term is proportional to the identity matrix. Our goal now is to compute $\Delta^{\pm(s)}(1\cdots n)$, where $n \geq 3$ and $2 \leq s \leq n-1$.

Next, we return to (5.33). With (5.35) eliminated, its momentum-space representation is left with

$$-\operatorname{tr}\int_1 \check{\partial}\mathcal{A}_1\hat{1}\bar{\mathcal{A}}^{\mathrm{F}}_{\bar{1}} + \frac{g^2}{\sqrt{8}}\int_1(\bar{\alpha}^-_{\bar{1}}\check{\partial}\alpha^+_{\bar{1}} + \bar{\alpha}^+_{\bar{1}}\check{\partial}\alpha^-_{\bar{1}}) = \frac{g^2}{\sqrt{8}}\int_1(\bar{\xi}^-_{\bar{1}}\check{\partial}\xi^+_{\bar{1}} + \bar{\xi}^+_{\bar{1}}\check{\partial}\xi^-_{\bar{1}}).$$

We substitute for $\alpha^{\pm}$ and $\bar{\alpha}^{\pm}$ using the momentum-space representations of (5.15) and (5.14), and this becomes

$$\operatorname{tr}\int_1 \check{\partial}\mathcal{A}_1(F^-_{\bar{1}} + F^+_{\bar{1}}) = -\int_{\alpha\beta\gamma}\{\bar{\xi}^-_{\bar{\alpha}}R^-(\boldsymbol{\alpha\gamma})(\check{\partial}S^-(\bar{\boldsymbol{\gamma}}\boldsymbol{\beta}))\xi^+_{\bar{\beta}} + \bar{\xi}^+_{\bar{\alpha}}R^+(\boldsymbol{\alpha\gamma})(\check{\partial}S^+(\bar{\boldsymbol{\gamma}}\boldsymbol{\beta}))\xi^-_{\bar{\beta}}\}. \tag{5.40}$$

We can split this into left- and right-handed chiral pieces and solve for F^+ and F^- separately. Let us first study the terms on the RHS of (5.40).

$$\begin{aligned}
&-\int_{\alpha\beta\gamma} \bar{\xi}^{\pm}_{\bar{\alpha}} R^{\pm}(\boldsymbol{\alpha\gamma})[\check{\partial} S^{\pm}(\bar{\boldsymbol{\gamma}}\bar{\boldsymbol{\beta}})]\xi^{\mp}_{\bar{\beta}} \\
&= \mathrm{tr}\int_{\alpha\beta\gamma} \xi^{\mp}_{\bar{\beta}}\bar{\xi}^{\pm}_{\bar{\alpha}} R^{\pm}(\boldsymbol{\alpha\gamma})[\check{\partial} S^{\pm}(\bar{\boldsymbol{\gamma}}\bar{\boldsymbol{\beta}})] \\
&= \mathrm{tr}\sum_{n=3}^{\infty}\sum_{s=2}^{n-1}\sum_{l=s+1}^{n}\int_{1\cdots n} R^{\pm}(s{+}1,-;s{+}2,\ldots,l)S^{\pm}(-,s;l{+}1,\ldots,n,1,\ldots,s{-}1)\times \\
&\qquad\qquad (\mathcal{B})_{n,s}\times(2\pi)^3\delta(\textstyle\sum_{i=1}^{n}\mathbf{p}_i),
\end{aligned} \tag{5.41}$$

where we use the short-hand

$$(\mathcal{B})_{n,s} \equiv \check{\partial}\mathcal{B}_{\bar{1}}\mathcal{B}_{\bar{2}}\cdots\mathcal{B}_{\overline{s-1}}\xi^{\mp}_{\bar{s}}\bar{\xi}^{\pm}_{\overline{s+1}}\mathcal{B}_{\overline{s+2}}\cdots\mathcal{B}_{\bar{n}}.$$

The LHS of (5.40) is

$$\begin{aligned}
\mathrm{tr}\int_1 \check{\partial}\mathcal{A}_1 F^{\pm}_{\bar{1}} = -\,\mathrm{tr}\int_1\sum_{i=2}^{\infty}\sum_{j=2}^{i}\sum_{k=3}^{\infty}\sum_{l=2}^{k-1}\int_{2\cdots i}\int_{2'\cdots k'}\Upsilon(12\cdots i)\Delta^{\pm(s)}(\bar{1}2'\cdots k') \\
\times\check{\partial}\mathcal{B}_{\bar{j}}\cdots\mathcal{B}_{\bar{i}}\mathcal{B}_{\bar{2}'}\cdots\mathcal{B}_{\overline{l-1}'}\xi^{\mp}_{\bar{l}'}\bar{\xi}^{\pm}_{\overline{l+1}'}\mathcal{B}_{\overline{l+2}'}\cdots\mathcal{B}_{\bar{k}'}\mathcal{B}_{\bar{2}}\cdots\mathcal{B}_{\overline{j-1}} \\
\times(2\pi)^6\delta(\textstyle\sum_{m=1}^{i}\mathbf{p}_m)\delta(\mathbf{p}_1-\sum_{n=2}^{k}\mathbf{p}_n),
\end{aligned}$$

summed over the $\pm$ superscript. Notice that the $\mathcal{O}(1/N_{\mathrm{C}})$ piece has vanished since it is proportional to the identity matrix, and $\check{\partial}\mathcal{A}$ is traceless. After carefully relabelling the momenta, starting with $j\to 1$, this becomes

$$\begin{aligned}
-\,\mathrm{tr}\sum_{n=3}^{\infty}\sum_{s=2}^{n-1}\sum_{m=2}^{n-1}\sum_{p=\max(0,m-s)}^{\min(m-2,n-s-1)}\Upsilon(-,n-p+1,\ldots,n,1,\ldots,m-p-1) \\
\times\Delta^{\pm(s+p-m+2)}(-,m-p,\ldots,n-p)(\mathcal{B})_{n,s}.
\end{aligned}$$

Now fix n and s above. The following change of variables

$$q=n-p,\quad r=m-p-1$$

allows us to write the coefficient of $(\mathcal{B})_{n,s}$ as

$$\begin{aligned}
&-\Delta^{\pm(s)}(1\cdots n)-\sum_{r=2}^{s-1}\Upsilon(-,1,\ldots,r)\Delta^{\pm(s-r+1)}(-,r+1,\ldots,n) \\
&\qquad-\sum_{q=s+1}^{n-1}\sum_{r=1}^{s-1}\Upsilon(-,q+1,\ldots,n,1,\ldots,r)\Delta^{\pm(s-r+1)}(-,r+1,\ldots,q).
\end{aligned} \tag{5.42}$$

We can now equate the coefficients of $(\mathcal{B})_{n,s}$ from (5.41) and (5.42) to obtain the following recurrence relation for $\Delta^{\pm}$ [3]:

$$\begin{aligned}\Delta^{\pm(s)}(1\cdots n) = &-\sum_{q=s+1}^{n} R^{\pm}(s+1,-;\underbrace{s+2,\ldots,q}_{(q-s-1)})S^{\pm}(-,s;\underbrace{q+1,\ldots,n,1,\ldots,s-1}_{(n+s-q+1)})\\ &-\sum_{r=2}^{s-1}\Upsilon(\underbrace{-,1,\ldots,r}_{(r+1)})\Delta^{\pm(s-r+1)}(\underbrace{-,r+1,\ldots,n}_{(n-r+1)})\\ &-\sum_{q=s+1}^{n-1}\sum_{r=1}^{s-1}\Upsilon(\underbrace{-,q+1,\ldots,n,1,\ldots,r}_{(n-q+r+1)})\Delta^{\pm(s-r+1)}(\underbrace{-,r+1,\ldots,q}_{(q-r+1)}).\end{aligned} \tag{5.43}$$

The numbers below the underbraces denote the number of arguments they enclose. In cases where the upper limit of a sum is less than the lower limit — such as when $s = 2$ in the sum over r in the second term, or when $s = n-1$ in the sum over q in the third — the sum is taken to vanish.

Now if we notice that, using (5.24) and (5.27),

$$\begin{aligned}&R^{+}(s+1,-;s+2,\ldots,q)S^{+}(-,s;q+1,\ldots,n,1,\ldots,s-1)\\ &=\left(-\frac{\hat{P}_{s+1,q}}{\widehat{s+1}}\right)\left(-\frac{\hat{s}}{\hat{P}_{q+1,n}+\hat{P}_{1s}}\right)\\ &\quad\times R^{-}(s+1,-;s+2,\ldots,q)S^{-}(-,s;q+1,\ldots,n,1,\ldots,s-1)\\ &=-\frac{\hat{s}}{\widehat{s+1}}R^{-}(s+1,-;s+2,\ldots,q)S^{-}(-,s;q+1,\ldots,n,1,\ldots,s-1).\end{aligned}$$

(since $P_{1s}+P_{q+1,n}=-P_{s+1,q}$ on account of conservation of momentum) and place this into (5.43) for Δ^{+}, it is easy to see that putting

$$\Delta^{+(s)}(1\cdots n) = -\frac{\hat{s}}{\widehat{s+1}}\Delta^{-(s)}(1\cdots n) \tag{5.44}$$

leads back to (5.43) for Δ^{-}. Hence, we will solve for just Δ^{-} and use the above relationship to obtain Δ^{+}.

Let us compute by hand first few Δ^{-} coefficients. First,

$$\Delta^{-(2)}(123) = -S^{-}(32;1) = -i\frac{\hat{3}}{(2\,3)}.$$

[3]Note that in the interest of clarity concerning the origin of certain terms in the forthcoming, we have *not* substituted for $R^{\pm}$ and $S^{\pm}$ in terms of Υ.

Next,

$$\begin{aligned}\Delta^{-(2)}(1234) &= -\Upsilon(-,4,1)\Delta^{-(2)}(-,2,3) - S^{-}(32;41) - R^{-}(3,-;4)S^{-}(-,2;1)\\ &= -\frac{\hat{3}^2}{(2\,3)(3\,4)}.\end{aligned}$$

Similarly, we can obtain next few coefficients:

$$\begin{aligned}\Delta^{-(3)}(1234) &= -\frac{\hat{3}\hat{4}}{(2\,3)(3\,4)},\\ \Delta^{-(2)}(12345) &= i\frac{\hat{3}^2\hat{4}}{(2\,3)(3\,4)(4\,5)},\\ \Delta^{-(3)}(12345) &= i\frac{\hat{3}\hat{4}^2}{(2\,3)(3\,4)(4\,5)},\\ \Delta^{-(4)}(12345) &= i\frac{\hat{3}\hat{4}\hat{5}}{(2\,3)(3\,4)(4\,5)},\end{aligned}$$

from which we conjecture

$$\Delta^{-(s)}(1\cdots n) = -(-i)^n\frac{\widehat{s+1}\,\hat{3}\hat{4}\cdots\widehat{n-1}}{(2\,3)(3\,4)\cdots(n-1,n)} = -\frac{\widehat{s+1}}{\hat{1}}\Upsilon(1\cdots n) \tag{5.45}$$

This can be proved by induction on n. The foregoing calculations of the lowest-order coefficients obviously furnish the initial step. For the inductive part, we substitute (5.45) into the recurrence relation. For each term on the RHS of (5.43), we can pull out a factor of

$$\frac{\hat{1}\cdots\hat{n}}{(1\,2)\cdots(n\,1)}$$

leaving telescoping sums of the form (3.60). (In the second term of (5.43), two such sums are nested.) One might worry about the cases discussed below (5.43) where certain terms are taken to vanish. It turns out that we can handle these cases consistently by understanding the sum $P_{ij} = p_i + p_{i+1} + \cdots + p_n + p_1 + \cdots + p_j$ when $j < i$. When this is so and we evaluate the sums using (3.60), we find that they vanish in these particular conditions because of terms of the form $P_{i,i-1} = 0$. To complete the proof, one simply evaluates the sums and does the algebra while applying the conservation of momentum. This results in an expression on the RHS of (5.43) equal to the given for $\Delta^{-(s)}(1\cdots n)$ in (5.45).

To finish this section, we state the series expansion of $\bar{\mathcal{A}}$, assembled from (5.34), (5.36) and (5.39), and using (5.44) and (5.45):

$$\begin{aligned}\bar{\mathcal{A}}_1 = &\sum_{m=2}^{\infty}\sum_{s=2}^{m}\int_{2\cdots m}\frac{\hat{s}^2}{\hat{1}^2}\Upsilon(1\cdots m)\mathcal{B}_{\bar{2}}\cdots\bar{\mathcal{B}}_{\bar{s}}\cdots\mathcal{B}_{\bar{m}}\,(2\pi)^3\delta(\textstyle\sum_{i=1}^{m}\mathbf{p}_i)\\ &+\frac{g^2}{\hat{1}^2\sqrt{8}}\sum_{\pm}\sum_{n=3}^{\infty}\sum_{s=2}^{n-1}\int_{2\cdots n}\left\{\begin{matrix}-\hat{s}\\ \widehat{s+1}\end{matrix}\right\}\Upsilon(1\cdots n)\Big\{\mathcal{B}_{\bar{2}}\cdots\mathcal{B}_{\overline{s-1}}\xi^{\mp}_{\bar{s}}\bar{\xi}^{\pm}_{\overline{s+1}}\mathcal{B}_{\overline{s+2}}\cdots\mathcal{B}_{\bar{n}}+\\ &\qquad\frac{1}{N_{\mathrm{C}}}\bar{\xi}^{\pm}_{\overline{s+1}}\mathcal{B}_{\overline{s+2}}\cdots\mathcal{B}_{\bar{n}}\mathcal{B}_{\bar{2}}\cdots\mathcal{B}_{\overline{s-1}}\xi^{\mp}_{\bar{s}}\Big\}\times(2\pi)^3\delta^3(\textstyle\sum_{i=1}^{n}\mathbf{p}_i).\end{aligned}$$

But there is one further simplification we can apply: if we relabel the fields in the $\mathcal{O}(1/N_{\mathrm{C}})$ terms, we can use the dual Ward identity (3.43) to evaluate the sum over s in this term to leave

$$\begin{aligned}\bar{\mathcal{A}}_1 = &\sum_{m=2}^{\infty}\sum_{s=2}^{m}\int_{2\cdots m}\frac{\hat{s}^2}{\hat{1}^2}\Upsilon(1\cdots m)\mathcal{B}_{\bar{2}}\cdots\bar{\mathcal{B}}_{\bar{s}}\cdots\mathcal{B}_{\bar{m}}\,(2\pi)^3\delta(\textstyle\sum_{i=1}^{m}\mathbf{p}_i)\\ &+\frac{g^2}{\hat{1}^2\sqrt{8}}\sum_{\pm}\sum_{n=3}^{\infty}\int_{2\cdots n}\Upsilon(1\cdots n)\Bigg[\sum_{s=2}^{n-1}\left\{\begin{matrix}-\hat{s}\\ \widehat{s+1}\end{matrix}\right\}\mathcal{B}_{\bar{2}}\cdots\mathcal{B}_{\overline{s-1}}\xi^{\mp}_{\bar{s}}\bar{\xi}^{\pm}_{\overline{s+1}}\mathcal{B}_{\overline{s+2}}\cdots\mathcal{B}_{\bar{n}}\\ &\qquad+\frac{1}{N_{\mathrm{C}}}\left\{\begin{matrix}\hat{n}\\ -\hat{2}\end{matrix}\right\}\bar{\xi}^{\pm}_{\bar{2}}\mathcal{B}_{\bar{3}}\cdots\mathcal{B}_{\overline{n-1}}\xi^{\mp}_{\bar{n}}\Bigg]\times(2\pi)^3\delta^3(\textstyle\sum_{i=1}^{n}\mathbf{p}_i).\end{aligned}\tag{5.46}$$

Completion vertices

Naturally, one can define completion vertices for massless QCD by the same protocol as used in the pure-gauge scenario. From (5.31), (5.32) and (5.46), we can write down the rules for the completion vertices, and the non-trivial ones are shown in fig. 5.1. These augment those from the pure-gauge theory, shown in fig. 4.1. (Note that the figure shows the vertices as appropriate for the normalisation of $\mathcal{A}$, $\mathcal{B}$, *etc.* so that the normalisation factors from (3.8) can be omitted for clarity.) For an example of these vertices in action, see section 5.3.5, where they are used to reconstruct the 'missing' $A(1^+_{\mathrm{q}}2^+3^-_{\bar{\mathrm{q}}})$ partial amplitude.

5.2.3 An indirect proof of MHV vertices

We now return to the discussion started at the end of section 5.2.1. There we claimed that the vertices of the transformed lagrangian are proportional to the MHV amplitudes continued off-shell by the CSW prescription (in this case by using the choice (3.5) for the Weyl spinors). To prove this, let us first review the proof from the pure gauge case. First, for each vertex in the Canonical MHV Lagrangian, its unique helicity and colour structure means that it is the sole contributor to the corresponding tree-level MHV amplitude *on shell*. This was first stated in section 3.2.2, and later in section 4.2 we plugged a possible hole in this claim by showing that for on-shell tree-level amplitudes, diagrams constructed using completion vertices were annihilated in the LSZ reduction

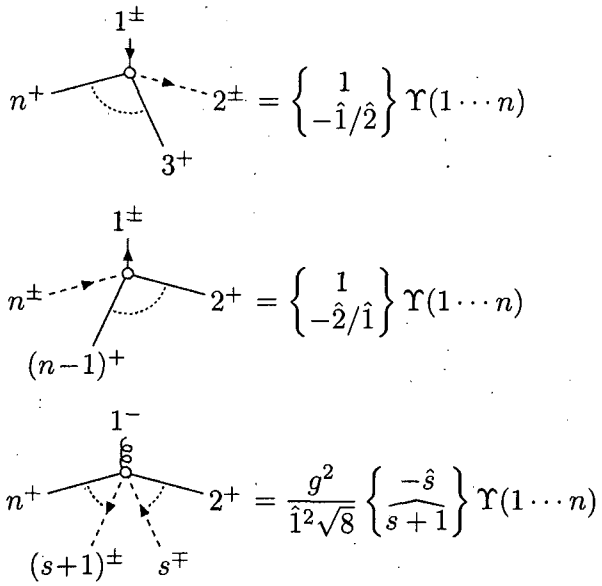

FIGURE 5.1: The non-trivial MHV completion vertices for massless QCD. Curly and solid, arrowless lines are as in fig. 4.1. Solid lines with arrows represent correlation function insertions of $\alpha^{\pm}$ ($\bar{\alpha}^{\pm}$) when the arrow points outwards (inwards), and $\xi^{\pm}$ ($\bar{\xi}^{\pm}$) attach to the dotted lines with the arrows pointing inwards (outwards). The direction of the arrow shows charge flow in both cases, and the missing lines are for +-helicity gluons. (Stacked expressions in braces take their value in accordance with the upper or lower choice of sign for the fermion helicities.)

procedure, and so did not contribute. Then to show that the vertex was also valid off shell, we argued that due to the holomorphicity of the vertices, they could contain no terms vanishing on the support of the on-shell condition.

It is straightforward to extend this argument to the QCD theory studied in this chapter. First, it is quite clear that the vertex coupling a −-helicity gluon to a quark-antiquark pair in the MHV lagrangian is the same as that of light-cone gauge QCD, *i.e.* (5.8). The helicity configuration precludes any contribution from completion vertices. For higher order vertices, we can see again from the form of the completion vertices shown fig. 5.1 that the diagrams through which they contribute terms in MHV amplitudes do not survive LSZ reduction for generic momenta (for the same reason as in the pure-gauge case; notice that they are all proportional to Υ). Finally, that there are no terms that vanish on-shell follows since the transformation is performed on a surface of equal light-cone time and has no x^0 dependence, and transformed lagrangian is manifestly holomorphic (*cf.* (5.9), (5.10), (5.31), (5.32) and (5.46)). This completes the proof that the vertices of the transformed lagrangian are indeed MHV vertices.

5.3 Example vertices

We now have all-orders expressions for the 'old' fields $\mathcal{A}$, $\bar{\mathcal{A}}$, $\alpha^{\pm}$ and $\bar{\alpha}^{\pm}$ in terms of their new counterparts $\mathcal{B}$, $\bar{\mathcal{B}}$, $\xi^{\pm}$ and $\bar{\xi}^{\pm}$. Let us now verify explicitly that the vertices obtained by substituting for the old fields in remaining terms of the LCYM lagrangian, (3.22) and (3.23), are proportional off-shell to the known tree-level MHV amplitudes.

5.3.1 On external states, vertices and amplitudes

As in section 3.4, a partial MHV amplitude is obtained from the MHV lagrangian by contracting an external state into the vertex with the relevant helicity and charge content, and summing if there is more than once contraction which picks out the desired colour structure.

We must define the polarisation vectors and spinors. As before, the relevant components of the gluon polarisation vectors are given by (2.10) of section 3.4. In co-ordinates, $E_+ = \bar{E}_- = -1$ so again by the LSZ theorem, when an external $+$ $(-)$ polarisation state is contracted into a $\mathcal{A}$ $(\bar{\mathcal{A}})$ vertex from the lagrangian, it contributes a factor of

$$-1 \times -\frac{ig}{\sqrt{2}},$$

where the second factor accounts restores the canonical normalisation of the gauge field from (3.8). For the polarisation spinors for the massless quarks, we must solve the Dirac equation $\not{p}\psi = 0$. This has the following positive-energy solutions for ψ:

$$\bar{u}^+(p) \equiv (\bar{\varphi}(p), 0) \quad \text{and} \quad \bar{u}^-(p) \equiv (0, \omega(p)).$$

For the purposes of the LSZ theorem (or, more simply as polarisation spinors contracted into γ matrices for external lines in Feynman diagrams), these correspond to positive- and negative-helicity *outgoing* quarks, respectively. Similarly, the negative-energy solutions are

$$v^+(p) \equiv \begin{pmatrix} \bar{\omega}(p) \\ 0 \end{pmatrix} \quad \text{and} \quad v^-(p) \equiv \begin{pmatrix} 0 \\ \varphi(p) \end{pmatrix}$$

for *outgoing* antiquarks, where again the sign in the superscript denotes physical helicity. Here we have used the following definitions for the Weyl spinors:

$$\varphi(p) = 2^{1/4} \begin{pmatrix} -p/\sqrt{\hat{p}} \\ \sqrt{\hat{p}} \end{pmatrix}, \tag{5.47}$$

$$\bar{\omega}(p) = 2^{1/4} \begin{pmatrix} \sqrt{\hat{p}} \\ \bar{p}/\sqrt{\hat{p}} \end{pmatrix}, \tag{5.48}$$

$$\bar{\varphi}(p) = 2^{1/4}(-\bar{p}/\sqrt{\hat{p}}, \sqrt{\hat{p}}), \tag{5.49}$$

$$\omega(p) = 2^{1/4}(\sqrt{\hat{p}}, p/\sqrt{\hat{p}}), \tag{5.50}$$

These are such that the Dirac spinors have the conventional phenomenologists' normalisation of $u^\dagger(p)u(p) = 2p^t$.

Let us consider the LSZ reduction *before* we remove the non-dynamical fermionic degrees of freedom. For example, in this context, an outgoing + helicity quark with momentum p produces a term

$$\bar{u}^+(p)(-i\not{p})\langle\cdots\psi\cdots\rangle = \bar{\varphi}(p)_{\dot{\alpha}}(-ip\cdot\sigma)^{\dot{\alpha}\beta}\langle\cdots\begin{pmatrix}\beta^-\\ \alpha^-\end{pmatrix}_\beta\cdots\rangle,$$

where $-ip\cdot\sigma$ is the inverse of the propagator obtained from (5.6). We can now compute the correlation function using the partition function generated by the MHV lagrangian. Since $\varphi_1 \equiv \beta^-$ is replaced by its equation of motion, one might expect this non-propagating component to complicate things. Fortunately,

$$\bar{\varphi}(p)(-ip\cdot\sigma) = -\frac{i}{2^{1/4}\sqrt{\hat{p}}}(0, p^2), \tag{5.51}$$

so it does not arise in the computation. We proceed to replace $\varphi_2 \equiv \alpha^-$ with its expression in terms of the new variables, and note that momentum conservation implies only the leading order term ξ^- survives the on-shell limit for generic momenta at tree-level. The propagator $\langle\xi^-\bar{\xi}^+\rangle$ of (5.16) cancels factors in (5.51) to leave a polarisation factor

$$2^{1/4}\sqrt{\hat{p}}.$$

One may show similarly that the same expression applies for the − helicity state, and for the anti-quarks. In summary, we state the polarisation spinors and the fields in the lagrangian associated with each outgoing state in table 5.2.

State		**Polarisation**	**Field**
particle	+	$\bar{\varphi}(p)$	$\bar{\xi}^+$
	−	$\omega(p)$	$\bar{\xi}^-$
antiparticle	+	$\bar{\omega}(p)$	ξ^+
	−	$\varphi(p)$	ξ^-

TABLE 5.2: The polarisation spinor and lagrangian field associated with each outgoing quark state.

Let us now frame this in the context of the lagrangian vertices V_{2q} and V_{4q}, used to express the general form of the quark-gluon interaction terms in (5.17) and (5.18). As we noted before, these contain the only terms in the MHV QCD lagrangian that contribute to tree-level MHV quark-gluon amplitudes, and as in the pure-gluon case of section 3.2 we extract partial amplitudes by contracting external states into these terms in a manner that picks out the desired colour order. As with the purely gluonic case, our outgoing states are constructed by having annihilation operators act to the right on the 'out' vacuum state $\langle 0|$. We note that when dealing with fermions, we must take

extra care with statistics, which essentially comes down to a choice of sign convention, or equivalently annihilation operator ordering. Now in section 2.3.1, we obtained SUSY partial amplitudes using supersymmetric Ward identities by associating them with S-matrix elements where the order of the annihilation operators placed between the free and physical vacua was the same as that of the arguments of the partial amplitude. Since we wish to compare the output of the MHV lagrangian with SWI-derived amplitudes, we will adopt the same convention when defining the outgoing states.

First, consider the MHV amplitude with one quark-antiquark pair. Its external state is

$$\langle 0|q_1^{\pm} A_2^+ \cdots A_j^- \cdots A_{n-1}^+ \bar{q}_n^{\mp}.$$

This contracts into the vertex in (5.17) multiplied by an external state factor of

$$(-1) \times \frac{4i}{g^2} \times \left(-\frac{ig}{\sqrt{2}}\right)^{n-2} (-1)^{n-2} \times 2^{1/4}\sqrt{\hat{1}} \times 2^{1/4}\sqrt{\hat{n}}.$$

Considering the factors delimited by $\times$ symbols, the first comes from Fermi statistics; the second from the path integral; the third from gluon polarisation and normalisation; and the final two from the external state spinors (see above). Thus, when the partial amplitude is defined as in (2.16),

$$A(1_{\rm q}^{\pm}, 2^+, \ldots, j^-, \ldots, (n-1)^+, n_{\bar{\rm q}}^{\mp}) = 2^{(7-n)/2}\, i^{n+1}\, g^{n-4}\, \sqrt{\hat{1}\hat{n}}\, V_{2{\rm q}}^{j;\pm}(1\cdots n). \qquad (5.52)$$

With two quark-antiquark pairs, we would contract the external state

$$\langle 0|q_1^{h_1} A_2^+ \cdots A_{j-2}^+ \bar{q}_{j-1}^{-h_j}\, q_j^{h_j} A_{j+1}^+ \cdots A_{n-1}^+ \bar{q}_n^{-h_1}$$

into (5.18), taking care with the fermion statistics. By construction $\mathcal{S}(h_1, h_j)$ drops out so we are left with

$$A(1_{\rm q}^{h_1}, 2^+, \ldots, (j-2)^+, (j-1)_{\bar{\rm q}}^{-h_j}; j_{\rm q}^{h_j}, (j+1)^+, \ldots, (n-1)^+, n_{\bar{\rm q}}^{-h_1})$$
$$= 2^{5-n/2} i^{n+1} g^{n-6} \sqrt{\hat{1}\,\hat{j}\,\widehat{j-1}\,\hat{n}}\, V_{4{\rm q}}^{j;h_1h_j}(1\cdots n), \qquad (5.53)$$

and similarly for the sub-leading partial amplitudes

$$A_{(1)}(1_{\rm q}^{h_1}, 2^+, \ldots, (j-2)^+, n_{\bar{\rm q}}^{-h_1}; j_{\rm q}^{h_j}, (j+1)^+, \ldots, (n-1)^+, (j-1)_{\bar{\rm q}}^{-h_j})$$
$$= 2^{5-n/2} i^{n+1} g^{n-6} \sqrt{\hat{1}\,\hat{j}\,\widehat{j-1}\,\hat{n}}\, V_{4{\rm q}(1)}^{j;h_1h_j}(1\cdots n).$$

5.3.2 Two quarks and two gluons

Let us now consider the partial amplitude $A(1_{\rm q}^+ 2^+ 3^- 4_{\bar{\rm q}}^-)$. In the colour structure decomposition of the S-matrix, this arises as the coefficient of $(T^{a_2}T^{a_3})_{i_1}{}^{\bar{\imath}_4}$. This amplitude is

known to be (see (2.43))

$$-ig^2\frac{\langle 1\,3\rangle\langle 4\,3\rangle^2}{\langle 1\,2\rangle\langle 2\,3\rangle\langle 4\,1\rangle} \tag{5.54}$$

(something which can be obtained most easily using supersymmetric Ward identities — see (2.29)). We wish to compare this to the result of (5.52); we just have to compute $V_{2q}^{3+}(1234)$. Note that this amplitude has a single quark-antiquark pair, and as such we may safely discard any $\mathcal{O}(1/N_C)$ terms that arise in the analysis. Were we to retain these terms, we would find they vanish anyway due to antisymmetries in the gluonic coefficients.

Looking table 5.1, we see that, based upon field content, the term we are considering receives contributions from from L^{--+}, $L^{\bar{\psi}+-\psi}$ and $L^{\bar{\psi}-\psi}$ (in (3.22), (5.9) and (5.8) respectively). Let us consider each in turn. Written in momentum space, (3.22) is

$$L^{--+} = i\,\mathrm{tr}\int_{123}\frac{\hat{3}}{\hat{1}\hat{2}}(1\,2)\,\bar{\mathcal{A}}_{\bar{1}}\bar{\mathcal{A}}_{\bar{2}}\mathcal{A}_{\bar{3}}, \tag{5.55}$$

where here and in the foregoing, a momentum-conserving δ function of the sum of all the momenta in the integral measure is omitted for clarity. We start by substituting for $\bar{\mathcal{A}}$: the term in $\bar{\xi}^+_{\bar{1}}\mathcal{B}_{\bar{2}}\bar{\mathcal{B}}_{\bar{3}}\xi^-_{\bar{4}}$ comes from the second $\bar{\mathcal{A}}$ being replaced with the $\bar{\xi}^+\xi^-$ term in (5.46). Relabelling the momenta, the contribution from (5.55) to the vertex is

$$-\frac{g^2}{\sqrt{8}}\int_{1234}\frac{\hat{2}\hat{4}}{\hat{3}(\hat{1}+\hat{4})^2}\frac{(3\,2)}{(4\,1)}\,\bar{\xi}^+_{\bar{1}}\mathcal{B}_{\bar{2}}\bar{\mathcal{B}}_{\bar{3}}\xi^-_{\bar{4}}.$$

Next, consider the contribution from $L^{\bar{\psi}+-\psi}$: here, only the leading order substitutions are needed for the fields involved so we simply extract the relevant term from the momentum-space representation of (5.9), giving

$$\frac{g^2}{\sqrt{8}}\int_{1234}\frac{\hat{3}-\hat{2}}{(\hat{1}+\hat{4})^2}\,\bar{\xi}^+_{\bar{1}}\mathcal{B}_{\bar{2}}\bar{\mathcal{B}}_{\bar{3}}\xi^-_{\bar{4}}.$$

Finally $L^{\bar{\psi}-\psi}$, which in momentum space is

$$L^{\bar{\psi}-\psi} = -\frac{ig^2}{\sqrt{8}}\int_{123}\left\{\left(\frac{\tilde{3}}{\hat{3}}-\frac{\tilde{2}}{\hat{2}}\right)\bar{\alpha}^+_{\bar{1}}\bar{\mathcal{A}}_{\bar{2}}\alpha^-_{\bar{3}}+\left(\frac{\tilde{2}+\tilde{3}}{\hat{2}+\hat{3}}-\frac{\tilde{2}}{\hat{2}}\right)\bar{\alpha}^-_{\bar{1}}\bar{\mathcal{A}}_{\bar{2}}\alpha^+_{\bar{3}}\right\}, \tag{5.56}$$

contributes two terms from the next-to-leading order substitutions for $\bar{\alpha}^+$ and $\bar{\mathcal{A}}$ from (5.15) and (5.46), leading to

$$\frac{g^2}{\sqrt{8}}\int_{1234}\left\{\frac{\hat{1}+\hat{2}}{\hat{3}\hat{4}}\frac{(4\,3)}{(1\,2)}+\frac{\hat{3}^2}{\hat{4}(\hat{1}+\hat{4})^2}\frac{(1\,4)}{(2\,3)}\right\}\bar{\xi}^+_{\bar{1}}\mathcal{B}_{\bar{2}}\bar{\mathcal{B}}_{\bar{3}}\xi^-_{\bar{4}}.$$

This is clearly of the form (5.17).

The sum of these coefficients is, accounting for conservation of momentum, the vertex

$$V_{2q}^{3;+}(1234) = -\frac{g^2}{\sqrt{8}}\frac{\hat{2}}{\hat{3}\hat{4}}\frac{(1\,3)(4\,3)^2}{(1\,2)(2\,3)(4\,1)}.$$

Plugging this into the RHS of (5.52) gives us

$$-ig^2\frac{\sqrt{\hat{1}}\hat{2}}{\hat{3}\sqrt{\hat{4}}}\frac{(1\,3)(4\,3)^2}{(1\,2)(2\,3)(4\,1)},$$

which may be shown to equal (5.54) using (3.6).

One may also show that the remaining three partial amplitudes bearing this colour structure can be obtained in a similar manner by considering the other possible choices of substitutions. We reproduce these amplitudes below:

$$\begin{aligned}
A(1_q^-2^+3^-4_{\bar{q}}^+) &= ig^2\frac{\hat{2}\sqrt{\hat{4}}}{\sqrt{\hat{1}}\hat{3}}\frac{(1\,3)^3}{(1\,2)(2\,3)(4\,1)} = ig^2\frac{\langle 1\,3\rangle^3}{\langle 1\,2\rangle\langle 2\,3\rangle\langle 4\,1\rangle},\\
A(1_q^+2^-3^+4_{\bar{q}}^-) &= -ig^2\frac{\sqrt{\hat{1}}\hat{3}}{\hat{2}\sqrt{\hat{4}}}\frac{(2\,4)^3}{(2\,3)(3\,4)(4\,1)} = -ig^2\frac{\langle 2\,4\rangle^3}{\langle 2\,3\rangle\langle 3\,4\rangle\langle 4\,1\rangle},\\
A(1_q^-2^-3^+4_{\bar{q}}^+) &= ig^2\frac{\hat{3}\sqrt{\hat{4}}}{\sqrt{\hat{1}}\hat{2}}\frac{(1\,2)^2(2\,4)}{(2\,3)(3\,4)(4\,1)} = ig^2\frac{\langle 1\,2\rangle^2\langle 2\,4\rangle}{\langle 2\,3\rangle\langle 3\,4\rangle\langle 4\,1\rangle},
\end{aligned}$$

in agreement with the known expressions.

5.3.3 Four quarks

In amplitudes with two or more quark-antiquark pairs, terms $\mathcal{O}(1/N_C)$ and higher contribute at the tree-level through the sub-leading colour structures. Thus we must keep track of these terms in the analysis.

Let us first compute the terms in the MHV lagrangian containing just two quark-antiquark pairs. To that end, we note they receive contributions from $L^{\bar{\psi}-\psi}$ and $L^{\bar{\psi}\psi\bar{\psi}\psi}$. In momentum space, these are given by (5.56) and

$$\begin{aligned}
L^{\bar{\psi}\psi\bar{\psi}\psi} = \frac{g^4}{8}\int_{1234}\Bigg\{&\left(\frac{1}{(\hat{1}+\hat{4})^2}+\frac{1}{N_C}\frac{1}{(\hat{1}+\hat{2})^2}\right)(\bar{\alpha}_{\bar{1}}^-\alpha_{\bar{2}}^+\bar{\alpha}_{\bar{3}}^-\alpha_{\bar{4}}^+ + \bar{\alpha}_{\bar{1}}^+\alpha_{\bar{2}}^-\bar{\alpha}_{\bar{3}}^+\alpha_{\bar{4}}^-)\\
&+\frac{2}{(\hat{1}+\hat{4})^2}\bar{\alpha}_{\bar{1}}^+\alpha_{\bar{2}}^+\bar{\alpha}_{\bar{3}}^-\alpha_{\bar{4}}^- + \frac{1}{N_C}\frac{1}{(\hat{1}+\hat{2})^2}\bar{\alpha}_{\bar{1}}^-\alpha_{\bar{2}}^+\bar{\alpha}_{\bar{3}}^+\bar{\alpha}_{\bar{4}}^-\Bigg\}.
\end{aligned} \tag{5.57}$$

We substitute for $\bar{\mathcal{A}}$ in (5.56) using the leading order fermion terms in (5.46) and for the fermions in (5.57). Summing and symmetrising over the momentum labels as much

as possible leads to the following terms in the MHV lagrangian:

$$\frac{g^4}{8}\int_{1234}\left\{\frac{1}{2}\frac{(2\,4)^2}{\hat{2}\hat{4}(1\,4)(3\,2)}\left(\bar{\xi}^+_{\bar{1}}\xi^-_{\bar{2}}\bar{\xi}^+_{\bar{3}}\xi^-_{\bar{4}}+\frac{1}{N_C}\bar{\xi}^+_{\bar{1}}\xi^-_{\bar{4}}\bar{\xi}^+_{\bar{3}}\xi^-_{\bar{2}}\right)\right.$$
$$+\frac{1}{2}\frac{(1\,3)^2}{\hat{1}\hat{3}(1\,4)(3\,2)}\left(\bar{\xi}^-_{\bar{1}}\xi^+_{\bar{2}}\bar{\xi}^-_{\bar{3}}\xi^+_{\bar{4}}+\frac{1}{N_C}\bar{\xi}^-_{\bar{1}}\xi^+_{\bar{4}}\bar{\xi}^-_{\bar{3}}\xi^+_{\bar{2}}\right)$$
$$\left.-\frac{(3\,4)^2}{\hat{3}\hat{4}(1\,4)(3\,2)}\left(\bar{\xi}^+_{\bar{1}}\xi^+_{\bar{2}}\bar{\xi}^-_{\bar{3}}\xi^-_{\bar{4}}+\frac{1}{N_C}\bar{\xi}^+_{\bar{1}}\xi^-_{\bar{4}}\bar{\xi}^-_{\bar{3}}\xi^+_{\bar{2}}\right)\right\}. \quad (5.58)$$

The colour structure in each of these terms is $\delta^{\bar{i}_2}_{i_1}\delta^{\bar{i}_4}_{i_3}-\delta^{\bar{i}_4}_{i_1}\delta^{\bar{i}_2}_{i_3}/N_C$. Clearly this conforms to (5.18) with $V^{3;h_1h_3}_{4q(1)}(1234)=V^{3;h_1h_3}_{4q}(1234)$ and

$$V^{3;++}_{4q}(1234)=\frac{g^4}{8}\frac{(2\,4)^2}{\hat{2}\hat{4}(1\,4)(3\,2)}, \quad (5.59)$$

$$V^{3;--}_{4q}(1234)=\frac{g^4}{8}\frac{(1\,3)^2}{\hat{1}\hat{3}(1\,4)(3\,2)}, \quad (5.60)$$

$$V^{3;+-}_{4q}(1234)=-\frac{g^4}{8}\frac{(3\,4)^2}{\hat{3}\hat{4}(1\,4)(3\,2)}. \quad (5.61)$$

We see that there are three independent colour-ordered four-quark partial amplitudes here: $A(1^+_q2^-_{\bar{q}}3^+_q4^-_{\bar{q}})$, $A(1^-_q2^+_{\bar{q}}3^-_q4^+_{\bar{q}})$ and $A(1^-_q2^-_{\bar{q}}3^+_q4^+_{\bar{q}})$. It suffices to check the leading-in-$1/N_C$ amplitudes and we shall check them all in turn. By plugging (5.59) and (5.60) into (5.53), we obtain

$$A(1^+_q2^-_{\bar{q}}3^+_q4^-_{\bar{q}})=ig^2\sqrt{\frac{\hat{1}\hat{3}}{\hat{2}\hat{4}}}\frac{(2\,4)^2}{(1\,4)(3\,2)}=ig^2\frac{\langle 2\,4\rangle^2}{\langle 1\,4\rangle\langle 3\,2\rangle}, \quad (5.62)$$

and

$$A(1^-_q2^+_{\bar{q}}3^-_q4^+_{\bar{q}})=ig^2\sqrt{\frac{\hat{2}\hat{4}}{\hat{1}\hat{3}}}\frac{(1\,3)^2}{(1\,4)(3\,2)}=ig^2\frac{\langle 1\,3\rangle^2}{\langle 1\,4\rangle\langle 3\,2\rangle}, \quad (5.63)$$

respectively. These are readily seen to be the known results (2.44). (They may also be checked against a calculation made *e.g.* using the light-cone QCD Feynman rules obtained from (5.8)–(5.10), discussed in section 5.A. The helicity arrangements here are such that both partial amplitudes lift to the same colour trace on the SUSY side, and so they will both contribute to the SUSY partial amplitude. As such, we cannot obtain these QCD amplitudes from supersymmetric Ward identities.) Finally, putting (5.61) into (5.53) gives

$$A(1^+_q2^+_{\bar{q}}3^-_q4^-_{\bar{q}})=-ig^2\sqrt{\frac{\hat{1}\hat{2}}{\hat{3}\hat{4}}}\frac{(3\,4)^2}{(1\,4)(3\,2)}=-ig^2\frac{\langle 3\,4\rangle^2}{\langle 1\,4\rangle\langle 3\,2\rangle} \quad (5.64)$$

in agreement with the known result in (2.44). (Otherwise it can be quickly checked either by direct computation or by using SWIs to compute the gluino amplitudes with the

same colour structure; we note that unlike the previous case, the helicity arrangements constrain the QCD → SUSY mapping such that it is one-to-one.)

5.3.4 Two quarks and three gluons

Finally, we consider $A(1_q^+2^+3^-4^+5_{\bar{q}}^-)$, which is given by (2.43) as

$$A(1_q^+2^+3^-4^+5_{\bar{q}}^-) = -ig^3\frac{\langle 1\,3\rangle\langle 3\,5\rangle^3}{\langle 1\,2\rangle\langle 2\,3\rangle\langle 3\,4\rangle\langle 4\,5\rangle\langle 5\,1\rangle}. \tag{5.65}$$

This partial amplitude is tied to the $(T^{a_2}T^{a_3}T^{a_4})_{i_1}{}^{\bar{i}_5}$ colour structure. In the MHV lagrangian, the term we seek is $\bar{\xi}_{\bar{1}}^+\mathcal{B}_{\bar{2}}\bar{\mathcal{B}}_{\bar{3}}\mathcal{B}_{\bar{4}}\xi_{\bar{5}}^-\,V_{2q}^{3+}(12345)$ and it receives contributions from L^{--+}, L^{--++}, $L^{\bar{\psi}-\psi}$ and $L^{\bar{\psi}+-\psi}$, so we will write it as[4]

$$\int_{12345}(W^{--+}+W^{--++}+W^{\bar{\psi}-\psi}+W^{\bar{\psi}+-\psi})\,\bar{\xi}_{\bar{1}}^+\mathcal{B}_{\bar{2}}\bar{\mathcal{B}}_{\bar{3}}\mathcal{B}_{\bar{4}}\xi_{\bar{5}}^-. \tag{5.66}$$

Let us consider each of the Ws in turn. First, we observe from (5.55) and the structures of (5.46) that L^{--+} yields four terms with the structure of (5.66) coming from the different possible choices substitution for $\mathcal{A}$. We carry this out and carefully relabel the momenta while accounting for the anticommuting nature of the fermions to obtain

$$\begin{aligned}W^{--+} = -\frac{ig^2}{\sqrt{8}}\Bigg\{&\frac{\hat{2}\hat{3}(2,3+4)}{(\hat{1}+\hat{5})^2(\hat{3}+\hat{4})^2}\frac{\hat{3}}{\hat{3}+\hat{4}}\Upsilon(-,3,4)\Delta^{+(2)}(-,5,1)\\ &+\frac{\hat{3}\hat{4}(2+3,4)}{(\hat{1}+\hat{5})^2(\hat{2}+\hat{3})^2}\frac{\hat{3}}{\hat{2}+\hat{3}}\Upsilon(-,2,3)\Delta^{+(2)}(-,5,1)\\ &+\frac{\hat{4}(3\,4)}{\hat{3}(\hat{3}+\hat{4})^2}\Delta^{+(2)}(-,5,1,2)+\frac{\hat{2}(2\,3)}{\hat{3}(\hat{2}+\hat{3})^2}\Delta^{+(3)}(-,4,5,1)\Bigg\}.\end{aligned} \tag{5.67}$$

We remind the reader here that in the argument lists of Υ, Δ, *etc.*, $-$ is a placeholder whose value should be taken to be the negative of the sum of the other momenta passed to that coefficient.

Next, L^{--++} has terms of the form $\mathrm{tr}(\bar{\mathcal{A}}\mathcal{A}\bar{\mathcal{A}}\mathcal{A})$ and $\mathrm{tr}(\bar{\mathcal{A}}\bar{\mathcal{A}}\mathcal{A}\mathcal{A})$, of which only the former contribute terms to (5.66). In momentum space, this is

$$\mathrm{tr}\int_{1234}\left\{\frac{\hat{2}\hat{3}}{(\hat{3}+\hat{4})^2}+\frac{\hat{3}\hat{4}}{(\hat{2}+\hat{3})^2}\right\}\bar{\mathcal{A}}_{\bar{1}}\mathcal{A}_{\bar{2}}\bar{\mathcal{A}}_{\bar{3}}\mathcal{A}_{\bar{4}}.$$

[4]Note that we will retain $R^{\pm}$, $S^{\pm}$ and $\Delta^{\pm}$ explicitly here and in other forthcoming examples (rather than used their expressions in Υ) to elucidate the origin of each term.

Substituting for each $\bar{A}$ in turn using the lowest-order terms in (5.39) gives

$$W^{--++} = -\frac{g^2}{\sqrt{8}}\Bigg\{\frac{1}{\hat{1}+\hat{5}}\left(\frac{\hat{2}\hat{3}}{(\hat{3}+\hat{4})^2}+\frac{\hat{3}\hat{4}}{(\hat{2}+\hat{3})^2}\right)\Delta^{+(2)}(-,5,1) + \frac{1}{\hat{1}+\hat{5}}\left(\frac{\hat{4}(\hat{1}+\hat{5})}{(\hat{3}+\hat{4})^2}+\frac{\hat{2}(\hat{1}+\hat{5})}{(\hat{2}+\hat{3})^2}\right)\Delta^{+(2)}(-,5,1)\Bigg\}. \quad (5.68)$$

$L^{\bar{\psi}-\psi}$ contributes four terms in the structure of (5.66), owing to the fact that we will now also see terms from the fermion series expansions (5.15) and (5.14) when these are substituted into (5.56). Upon re-arrangement and re-labelling of the momenta, we arrive at the contribution

$$\begin{aligned} W^{\bar{\psi}-\psi} = -\frac{ig^2}{\sqrt{8}}\Bigg\{ & \left(\frac{\tilde{4}+\tilde{5}}{\hat{4}+\hat{5}}-\frac{\tilde{3}}{\hat{3}}\right)R^+(1,-;2)S^+(-,5;4) \\ & +\left(\frac{\hat{3}}{\hat{3}+\hat{4}}\right)^2\left(\frac{\tilde{5}}{\hat{5}}-\frac{\tilde{3}+\tilde{4}}{\hat{3}+\hat{4}}\right)R^+(1,-;2)\Upsilon(-,3,4) \\ & +\left(\frac{\hat{3}}{\hat{2}+\hat{3}+\hat{4}}\right)^2\left(\frac{\tilde{5}}{\hat{5}}-\frac{\tilde{1}+\tilde{5}}{\hat{1}+\hat{5}}\right)\Upsilon(-,2,3,4) \\ & +\left(\frac{\hat{3}}{\hat{2}+\hat{3}}\right)^2\left(\frac{\tilde{4}+\tilde{5}}{\hat{4}+\hat{5}}-\frac{\tilde{2}+\tilde{3}}{\hat{2}+\hat{3}}\right)\Upsilon(-,2,3)S^+(-,5;4)\Bigg\}. \end{aligned} \quad (5.69)$$

Finally, $L^{\bar{\psi}+-\psi}$, which has momentum-space representation

$$L^{\bar{\psi}+-\psi} = -\frac{g^2}{\sqrt{8}}\int_{1234}\Bigg\{\left(\frac{1}{\hat{3}+\hat{4}}+\frac{\hat{2}-\hat{3}}{(\hat{2}+\hat{3})^2}\right)\bar{\alpha}^+_{\bar{1}}\bar{\mathcal{A}}_{\bar{2}}\mathcal{A}_{\bar{3}}\alpha^-_{\bar{4}} + \frac{\hat{2}-\hat{3}}{(\hat{2}+\hat{3})^2}\bar{\alpha}^+_{\bar{1}}\mathcal{A}_{\bar{2}}\bar{\mathcal{A}}_{\bar{3}}\alpha^-_{\bar{4}} + \text{l.h. pieces}\Bigg\},$$

contributes four terms to (5.66) from substitutions for $\bar{A}$ and the fermions:

$$\begin{aligned} W^{\bar{\psi}+-\psi} = -\frac{g^2}{\sqrt{8}}\Bigg\{ & \left(\frac{1}{\hat{4}+\hat{5}}+\frac{\hat{3}-\hat{4}}{(\hat{3}+\hat{4})^2}\right)R^+(1,-;2)+\frac{\hat{2}-\hat{3}}{(\hat{2}+\hat{3})^2}S^+(-,5;4) \\ & +\left(\frac{\hat{3}}{\hat{3}+\hat{4}}\right)^2\frac{\hat{2}-\hat{3}-\hat{4}}{(\hat{2}+\hat{3}+\hat{4})^2}\Upsilon(-,3,4) \\ & +\left(\frac{\hat{3}}{\hat{2}+\hat{3}}\right)^2\left(\frac{1}{\hat{4}+\hat{5}}+\frac{\hat{2}+\hat{3}-\hat{4}}{(\hat{2}+\hat{3}+\hat{4})^2}\right)\Upsilon(-,2,3)\Bigg\}. \end{aligned} \quad (5.70)$$

We take the sum of (5.67), (5.68), (5.69) and (5.70) to be $V_{2\bar{q}}^{3;+}(12345)$ and when plugged into (5.52), its RHS becomes

$$-\frac{ig^3}{\sqrt{2}}\frac{\sqrt{\hat{1}\hat{2}\hat{4}}}{\hat{3}\sqrt{\hat{5}}}\frac{(1\,3)(3\,5)^3}{(1\,2)(2\,3)(3\,4)(4\,5)(5\,1)},$$

which may be shown to equal (5.65) using (3.6).

5.3.5 On missing amplitudes

We learned in chapter 4 that contributions to the S-matrix from completion vertices (arising from the series expansions of the transformations themselves) are required to obtain certain 'missing' amplitudes. In particular, we demonstrated this by calculating $A(1^-2^+3^+)$ at tree-level (which has no vertex in the MHV lagrangian, and is non-vanishing for complex momenta), and by showing that $A(1^+2^+3^+4^+)$ at one-loop matches what would be obtained were one to compute it using light-cone Yang–Mills theory.

The situation with quarks added is no different: quark-gluon amplitudes whose construction requires erstwhile $\overline{\text{MHV}}$-like vertices are recovered through completion vertices found in (5.14), (5.15), (3.42) and (5.46). As an example of this, let us study the partial amplitude $A(1_{\text{q}}^+2^+3_{\bar{\text{q}}}^-)$. Is it easy to evaluate this from either light-cone QCD, and it is given by

$$A(1_{\text{q}}^+2^+3_{\bar{\text{q}}}^-) = ig\frac{[2\,1]^2}{[3\,1]}. \tag{5.71}$$

The LSZ reduction gives this amplitude as

$$A(1_{\text{q}}^+2^+3_{\bar{\text{q}}}^-) = \lim_{p_1^2,p_2^2,p_3^2\to 0} ip_2^2 \times \frac{-ip_1^2}{2^{1/4}\sqrt{1}} \times \frac{-ip_3^2}{2^{1/4}\sqrt{3}} \times \langle \alpha_1^- \bar{A}_2 \bar{\alpha}_3^+ \rangle. \tag{5.72}$$

Here, the first factor contributes the gluon polarisation and inverse propagators; and the second and third factors are (5.51) for the quarks. The correlation function may be computed by substituting for each of the fields involved with their next-to-leading-order expressions from (5.31), (5.32) and (5.46) (in the case of $\bar{A}$ taking the right-handed fermionic part), or equivalently by evaluating the sum of the three diagrams of fig. 5.2, constructed from the vertices of fig. 5.1. Thus, (5.72) becomes (accounting for the normalisation of $\mathcal{A}$, which simply amounts to using (3.8) to substitute for the gauge fields in the series):

$$\begin{aligned} A(1_{\text{q}}^+2^+3_{\bar{\text{q}}}^-) &= -\frac{i}{\sqrt{2}\,\hat{1}\hat{3}}p_1^2p_2^2p_3^2\left\{\frac{\hat{1}}{p_1^2}\frac{\hat{3}}{p_3^2}\frac{ig}{\hat{2}^2}\hat{3}\Upsilon(231) + \frac{\hat{1}}{p_1^2}\frac{1}{p_2^2}\,ig\,\Upsilon(312) + \frac{1}{p_2^2}\frac{\hat{3}}{p_3^2}\,ig\,\frac{\hat{3}}{\hat{1}}\Upsilon(123)\right\} \\ &= \frac{ig}{\sqrt{2}}\sqrt{\hat{1}\hat{3}}\frac{\hat{3}}{(1\,2)}\left(\frac{p_1^2}{\hat{1}} + \frac{p_2^2}{\hat{2}} + \frac{p_3^2}{\hat{3}}\right) \\ &= ig\sqrt{2}\frac{1}{\hat{2}}\sqrt{\frac{\hat{3}}{\hat{1}}}\{3\,1\}. \end{aligned}$$

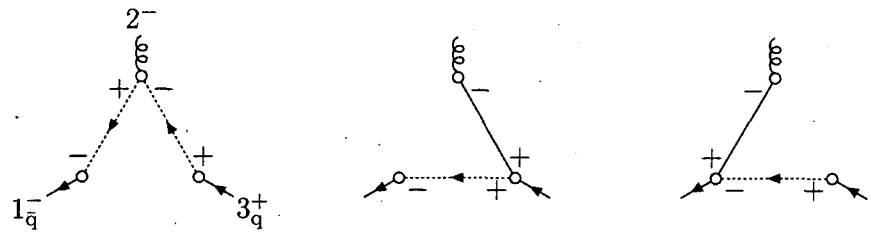

FIGURE 5.2: Contributions to the tree-level $A(1_q^+2^+3_{\bar{q}}^-)$ amplitude, before applying LSZ reduction. All momenta are directed out of the diagrams, arrows indicate colour flow.

Note that the first term on the first line acquires an extra factor of -1 since we need to transpose the quark fields to evaluate the correlation function. This expression may be shown to equal (5.71) using (3.6). (Note that we make use of (4.77) to obtain the final line.)

5.4 Conclusion

In this chapter, we extended the canonical MHV lagrangian formalism of [46] and chapters 3 and 4 to a full massless QCD theory with $\mathrm{SU}(N_C)$ gauge symmetry. We started with massless QCD in the light-cone gauge with the non-dynamical field components integrated out. By applying a canonical transformation to the field variables, we obtain a lagrangian incorporating gluon-gluon and quark-gluon interactions whose vertices are proportional (up to polarisation factors) to the MHV amplitudes in the literature (obtained, for example, by supersymmetry). This has been checked explicitly for amplitudes with two quarks and two gluons, with four quarks, and with two quarks and three gluons in the $(1_q^+2^+3^-4^+5_{\bar{q}}^-)$ configuration. The field transformations for the fermions and $\bar{\mathcal{A}}$ are summarised in (5.31), (5.32) and (5.46).

The MHV QCD lagrangian we have found maintains a certain 'backward compatibility' with the pure-gauge case found in chapter 3. The solution for $\mathcal{A}$ in terms of $\mathcal{B}$ is the same, whereas $\bar{\mathcal{A}}$ acquires new terms in the new fermion fields brought on by the requirement that the transformation is canonical. As in the pure-gauge case, the explicit form of this transformation as a series expansion has coefficients that have simple, holomorphic expressions in the momenta.

As we found out in chapter 4, the S-matrix receives contributions beyond the vertex content of an MHV lagrangian — specifically, the completion vertices that originate in the transformation itself. These allow us to construct otherwise missing amplitudes, notably those eliminated by the choice of field transformation; we demonstrated this for the MHV QCD lagrangian in the simple case of the otherwise missing $(1_q^+2^+3_{\bar{q}}^-)$ partial amplitude. Similarly, we would expect the completion vertices to be important for recovery of the full off-shell theory, and for on-shell loop-level amplitudes.

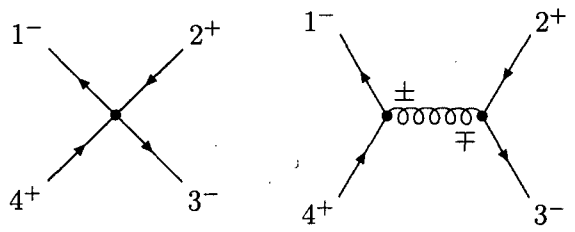

FIGURE 5.3: Feynman graphs from light-cone gauge QCD that contribute to the $\delta_{i_1}^{\bar{i}_2}\delta_{i_3}^{\bar{i}_4} - \delta_{i_1}^{\bar{i}_4}\delta_{i_3}^{\bar{i}_2}/N_C$ term of the $(1_q^-2_{\bar{q}}^+3_q^-4_{\bar{q}}^+)$ amplitude.

5.A On SUSY and $A(1_q^+2_{\bar{q}}^-3_q^+4_{\bar{q}}^-)$ and $A(1_q^-2_{\bar{q}}^+3_q^-4_{\bar{q}}^+)$

In the main text, we compared the the expressions given in (5.62) and (5.63) for the partial amplitudes $A(1_q^+2_{\bar{q}}^-3_q^+4_{\bar{q}}^-)$ and $A(1_q^-2_{\bar{q}}^+3_q^-4_{\bar{q}}^+)$, respectively, with those obtained by directly by light-cone gauge QCD. This is because mapping these results onto the SUSY theory to check that they then satisfy the SWIs requires some care, which we alluded to in section 2.3.1: these helicity arrangements are such that both partial amplitudes lift to the same colour trace on the SUSY side, and so they will both contribute to the SUSY partial amplitude. As such, we cannot obtain these QCD amplitudes from supersymmetric Ward identities.

First, we outline the light-cone QCD calculation used to obtain these amplitudes. For the case of $A(1_q^-2_{\bar{q}}^+3_q^-4_{\bar{q}}^+)$, the contributing diagrams are shown in fig. 5.3. From these, we pull out the terms proportional to $\delta_{i_1}^{\bar{i}_2}\delta_{i_3}^{\bar{i}_4} - \delta_{i_1}^{\bar{i}_4}\delta_{i_3}^{\bar{i}_2}/N_C$. (There are no such terms in the $(1,2)$ channel, hence the absence of these graphs from fig. 5.3.) The coefficient of this colour structure found this way is

$$\frac{2ig^2\sqrt{\hat{1}\hat{2}\hat{3}\hat{4}}}{(\hat{2}+\hat{3})^2}\left\{1+\frac{1}{(p_2+p_3)^2}\left[\frac{\{1\,4\}(2\,3)}{\hat{3}\hat{4}}+\frac{(1\,4)\{3\,2\}}{\hat{1}\hat{2}}\right]\right\},$$

and by putting all momenta on shell and simplifying, this expression can be shown to be equal to (5.63).

Now let us see precisely how the correspondence to the SUSY partial amplitude works in this case. Note that $A(1_q^+2_{\bar{q}}^-3_q^+4_{\bar{q}}^-)$ and $A(4_q^-1_{\bar{q}}^+2_q^-3_{\bar{q}}^+)$ (a re-labelling of (5.63)) have the same helicity arrangement, and suggest comparison with $A(\Lambda_1^+\Lambda_2^-\Lambda_3^+\Lambda_4^-)$; that this mixes quark and antiquark is of no concern here as the SUSY amplitude does not distinguish the two, the gluinos being in the adjoint representation. This particular SUSY partial amplitude contains contributions from gluon exchanges in both the $(1,4)$ and $(1,2)$ channels, and it is associated with the $\mathrm{tr}(T^{a_1}T^{a_2}T^{a_3}T^{a_4})$ colour structure (shown on the right of fig. 2.4). On the QCD side, $A(1_q^+2_{\bar{q}}^-3_q^+4_{\bar{q}}^-)$ is associated with the $\delta_{i_1}^{\bar{i}_2}\delta_{i_3}^{\bar{i}_4}$ leading-order colour structure (see fig. 2.4 left) corresponding to a $(1,4)$ gluon exchange, and $-A(4_q^-1_{\bar{q}}^+2_q^-3_{\bar{q}}^+)$ with $\delta_{i_1}^{\bar{i}_4}\delta_{i_3}^{\bar{i}_2}$ (see fig. 2.4 centre), implying a $(1,2)$ exchange. Since both colour structures lift to $\mathrm{tr}(T^{a_1}T^{a_2}T^{a_3}T^{a_4})$, we would expect that the SUSY

partial amplitude is the sum of the two QCD partial amplitudes, *i.e.*:

$$\begin{aligned} A(\Lambda_1^+\Lambda_2^-\Lambda_3^+\Lambda_4^-) &= A(1_q^+2_{\bar{q}}^-3_q^+4_{\bar{q}}^-) - A(4_q^-1_{\bar{q}}^+2_q^-3_{\bar{q}}^+) \\ &= ig^2\frac{\langle 1\,3\rangle\langle 2\,4\rangle^3}{\langle 1\,2\rangle\langle 2\,3\rangle\langle 3\,4\rangle\langle 4\,1\rangle} \\ &= ig^2\left\{\frac{\langle 2\,4\rangle^2}{\langle 1\,4\rangle\langle 3\,2\rangle} - \frac{\langle 2\,4\rangle^2}{\langle 1\,2\rangle\langle 3\,4\rangle}\right\}, \end{aligned}$$

in agreement with the result from SWIs. The $-$ sign for the second term on the first line above comes from Fermi statistics. Note that we have used the Schouten identity (2.13).

Chapter 6

Discussion

As noted in the introduction, the isolation of New Physics signatures and improved measurements of the QCD coupling constant at the LHC require the theoretical community to have a good understanding of QCD processes, particularly those involving multiple partons, at leading and next-to-leading order [12]. The past two decades have seen considerable advancement in technology for computing amplitudes for multipartonic processes, driven by the observation that gauge theories appear to have structures much simpler than the traditional calculation techniques would imply. The Parke–Taylor formula (2.22) for the tree-level MHV amplitude is a remarkably simple expression in light of the number of Feynman diagrams that would be required to compute it. Subsequent developments have yielded tree-level computational techniques that provide polynomial-in-n time algorithms for n gluon amplitudes. In particular the BCF recursion relations between on-shell amplitudes have been very useful in pushing forward the set of known analytic expressions for tree-level amplitudes (see section 2.5 for background and references to its applications), as have comparable numerical techniques based upon Berends–Giele recursion relations [56]. Taking a more formal approach, the CSW rules (explained in section 2.4) used insight from twistor-string theory to show tree-level amplitudes could be obtained by sewing Parke–Taylor MHV amplitudes together with scalar propagators. This superficially looks like a field theory of a charged scalar with an infinite tower of vertices of ever-increasing valence, and thus grows no faster than n^2, again a significant improvement over Feynman diagrams. The natural question to ask is what field theoretic motivation underpins this, and how this can be extended to quantum corrections.

Developments at the loop level have not been so straightforward, but significant progress has been made using a number of techniques. In particular, the CSW rules have been applied successfully at one loop for supersymmetric theories [43,79,80] and the cut-constructible parts of pure Yang–Mills amplitudes [44, 45] (reviewed in section 2.6.2). Many parts of QCD amplitudes can be obtained by unitarity in four dimensions [34, 58, 89–91] (indeed, *all* of the supersymmetric components are cut-constructible) leading one to promising ideas such as loop-level on-shell recursion relations/bootstrapping [40,

42], unitarity [77] and generalised unitarity [35] outside four dimensions, and direct computation of the rational parts from Feynman diagrams [37–39].

In this thesis, we have seen how one of these modern techniques, the CSW rules, may be understood from the field theory point of view at the action level, both for pure Yang–Mills and massless QCD, and admit the addition of dimensional regularisation structure.

6.1 Summary of work undertaken

This section is intended as an overview of the research described in chapters 3–5. For detailed discussions we refer the reader to the relevant concluding section in each, specifically sections 3.5, 4.5 and 5.4.

The CSW rules are underwritten by field theory, as shown by Mansfield [46] and demonstrated explicitly in chapter 3. In particular, the CSW rules are obtained by a canonical transformation of the fields of light-cone gauge Yang–Mills theory that absorbs the $(--++)$ vertex into the kinetic term of the theory expressed in the new variables. The series solution this entails expresses the remaining pieces of the LCYM lagrangian as an infinite tower of terms with an MHV helicity content, each a Parke–Taylor amplitude continued off shell by the CSW prescription. Of particular utility in this process was moving from the spinor formalism to light-cone co-ordinates.

The precise form of this transformation has series coefficients with a simple, holomorphic form. Chapter 4 showed how these provide additional vertices at the level of correlation functions and hence contribute terms to S-matrix elements via the LSZ reduction. That under certain circumstances these contributions do not vanish is a peculiarity of the non-local nature of the transformation that allows it to evade the equivalence theorem. These vertices 'complete' the CSW rules by recovering the parts of Yang–Mills theory that required the $(--++)$ vertex for their construction, in what (ultimately) turns out to be an algebraic re-arrangement of the contributions arising from this eliminated vertex. In particular we showed this to occur for the one-loop $(++++)$ amplitude.

By exploiting the links we made to Yang–Mills theory, the transformation can be applied to derive MHV vertices in D dimensions and hence indicates how to apply dimensional regularisation to MHV techniques. Unfortunately, the price we pay for this is the destruction of the pleasing holomorphic character of the transformation as well as the simple form of the series coefficients.

In chapter 5, the transformation was extended to include massless quarks in the fundamental representation. This again resulted in an MHV-form lagrangian, with off-shell vertices coincident to on-shell amplitudes and Feynman rules following the CSW prescription as laid out in [28].

6.2 Related developments

Field transformation techniques have since been applied to a variety of theories in order to obtain an MHV lagrangian and/or obtain specific results at the action level. In [105], Feng and Huang use two field transformations (one of which is canonical) to obtain a MHV lagrangian for $\mathcal{N} = 4$ supersymmetric Yang–Mills. In ref. [106], the authors use a field transformation to make manifest the KLT relations [107] for the three- and four-graviton vertices at the action level.

Ref. [82] describes a field transformation that is holomorphic but *not* canonical, giving rise to a non-unit jacobian in the path integral. The authors argue that this jacobian gives rise to one-loop amplitudes with at most one gluon of negative helicity. In ref. [108] a superset of these authors address the issues of the missing amplitudes (and the rational pieces of amplitudes with non-vanishing cuts) by using the transformation associated with the Canonical MHV Lagrangian of chapter 3 in conjunction with a four-dimensional 'light-cone world-sheet friendly' regulator of Qiu, Thorn and Chakrabarti [95, 104, 109]. This regulator violates Lorentz covariance by giving the gluon propagator a non-vanishing $++$ component. This must be removed by a counterterm. By applying the field transformation to the fields in this counterterm, it was demonstrated that one could recover the one-loop $(++++)$ amplitude, and it was argued that he all-$+$ amplitude could be recovered similarly.

Boels *et al.* have been pursuing formal developments complementary to those herein in a series of papers that trace their origins back to the (ambi)twistor Yang–Mills studies of Mason and Skinner [110, 111]. The crux of this idea is that the twistor-space Yang–Mills action has a larger gauge group than that of the usual space-time formulation. By making local, linear gauge transformations on the twistor side that are inaccessible from space-time, the effect on the theory pushed forward to space-time is that it undergoes a non-local, non-linear transformation that recovers the traditional formulation of Yang–Mills, or one which makes the CSW rules manifest [112]. In other words, the MHV lagrangian arises as a result of a choice of gauge fixing in twistor space. Twistor actions that lead to space-time MHV lagrangians have been constructed for pure Yang–Mills, extended to include adjoint scalars and fundamental representation fermions [112], and used in the background gauge to study renormalisability [113]. In [114, 115], CSW rules for a massive scalar are obtained using both the twistor action and space-time field transformation. The research in [116] showed explicitly that these two approaches produce identical field transformations, and initiates a study at the loop-level.

6.3 Future work

It is not yet clear how to decide for a given amplitude and order in perturbation theory when to use the completion vertices. Ideally one would like an algorithmic means of making this decision. We know that by the validity of the CSW construction, completion vertices do not contribute to on-shell tree amplitudes in space-times with a Minkowski

signature. Yet we have seen that they are required for the construction of certain classes of non-vanishing amplitudes. One might also guess that keeping subsets of momenta on shell might eliminate the need for certain subsets of diagrams constructed with completion vertices. The fact that only the tadpole MHV completion graph contributes to the [box topology of the] one-loop (++++) amplitude (when all external momenta are taken on shell from the beginning) has been used as starting point to an attempt to tackle these questions in recent research [117]. It is hoped that a study of how the field transformation behaves under BRST transformation might shed some light on this.

The issue of direct evaluation of *individual* MHV completion diagrams is, at time of writing, an unresolved challenge. It is not completely clear at present what pole prescription is required to correctly define the integrals in the face of the non-standard singularity structure of the completion vertices. Of course, one might question why one would even consider this, given algebraic reconstruction of LCYM before integration — all the more reason to get to grips with the points raised in the previous paragraph.

Whether the MHV lagrangian will lead to a better paradigm for perturbation theory is uncertain at this time. Even if the ideas explored herein do not yield any new computational advantage, we believe it has provided insight into the mechanism underlying methodologies such as the CSW construction and its progeny. More generally, the application of the technology underlying the MHV lagrangian may yet yield insight into possible simplifications hidden in other field theories.

Bibliography

[1] M. E. Peskin and D. V. Schroeder, *"An Introduction to Quantum Field Theory"*. Addison-Wesley, 1995.

[2] T. DeGrand and C. E. Detar, *Lattice methods for quantum chromodynamics.* World Scientific, 2006.

[3] D. J. Gross and F. Wilczek, "Ultraviolet behavior of non-abelian gauge theories," *Phys. Rev. Lett.* **30** (1973) 1343–1346.

[4] H. D. Politzer, "Reliable perturbative results for strong interactions?," *Phys. Rev. Lett.* **30** (1973) 1346–1349.

[5] K. G. Wilson, "Quantum Chromodynamics on a Lattice." Presented at Cargese Summer Inst., Cargese, France, Jul 12–31, 1976.

[6] I. Montvay and G. Munster, *Quantum fields on a lattice.* Cambridge University Press, 1994.

[7] J. M. Maldacena, "The large N limit of superconformal field theories and supergravity," *Adv. Theor. Math. Phys.* **2** (1998) 231–252, `arXiv:hep-th/9711200`.

[8] G. Sterman, "Partons, factorization and resummation," `arXiv:hep-ph/9606312`.

[9] W. K. Tung, "Perturbative QCD and the parton structure of the nucleon," in *At the frontier of particle physics*, M. Shifman, ed., vol. 2, pp. 887–971. 2001.

[10] **Particle Data Group** Collaboration, W. M. Yao *et al.*, "Review of particle physics," *J. Phys.* **G33** (2006) 1–1232.

[11] S. P. Martin, "A supersymmetry primer," `arXiv:hep-ph/9709356`.

[12] C. Buttar *et al.*, "Les Houches physics at TeV colliders 2005, standard model, QCD, EW, and Higgs working group: Summary report," `arXiv:hep-ph/0604120`.

[13] S. J. Parke and T. R. Taylor, "An Amplitude for n Gluon Scattering," *Phys. Rev. Lett.* **56** (1986) 2459.

[14] F. A. Berends and W. T. Giele, "Multiple Soft Gluon Radiation in Parton Processes," *Nucl. Phys.* **B313** (1989) 595.

[15] F. Cachazo, P. Svrcek, and E. Witten, "MHV vertices and tree amplitudes in gauge theory," *JHEP* **09** (2004) 006, arXiv:hep-th/0403047.

[16] K. Risager, "A direct proof of the CSW rules," *JHEP* **12** (2005) 003, arXiv:hep-th/0508206.

[17] R. Britto, F. Cachazo, and B. Feng, "New recursion relations for tree amplitudes of gluons," *Nucl. Phys.* **B715** (2005) 499–522, arXiv:hep-th/0412308.

[18] R. Britto, F. Cachazo, B. Feng, and E. Witten, "Direct proof of tree-level recursion relation in Yang- Mills theory," *Phys. Rev. Lett.* **94** (2005) 181602, arXiv:hep-th/0501052.

[19] K. J. Ozeren and W. J. Stirling, "MHV techniques for QED processes," *JHEP* **11** (2005) 016, arXiv:hep-th/0509063.

[20] M.-x. Luo and C.-k. Wen, "Recursion relations for tree amplitudes in super gauge theories," *JHEP* **03** (2005) 004, arXiv:hep-th/0501121.

[21] K. J. Ozeren and W. J. Stirling, "Scattering amplitudes with massive fermions using BCFW recursion," *Eur. Phys. J.* **C48** (2006) 159–168, arXiv:hep-ph/0603071.

[22] S. D. Badger, E. W. N. Glover, V. V. Khoze, and P. Svrcek, "Recursion relations for gauge theory amplitudes with massive particles," *JHEP* **07** (2005) 025, arXiv:hep-th/0504159.

[23] S. D. Badger, E. W. N. Glover, and V. V. Khoze, "Recursion relations for gauge theory amplitudes with massive vector bosons and fermions," *JHEP* **01** (2006) 066, arXiv:hep-th/0507161.

[24] J. Bedford, A. Brandhuber, B. J. Spence, and G. Travaglini, "A recursion relation for gravity amplitudes," *Nucl. Phys.* **B721** (2005) 98–110, arXiv:hep-th/0502146.

[25] F. Cachazo and P. Svrcek, "Tree level recursion relations in general relativity," arXiv:hep-th/0502160.

[26] P. Benincasa, C. Boucher-Veronneau, and F. Cachazo, "Taming tree amplitudes in general relativity," *JHEP* **11** (2007) 057, arXiv:hep-th/0702032.

[27] G. Georgiou and V. V. Khoze, "Tree amplitudes in gauge theory as scalar MHV diagrams," *JHEP* **05** (2004) 070, arXiv:hep-th/0404072.

[28] J.-B. Wu and C.-J. Zhu, "MHV vertices and fermionic scattering amplitudes in gauge theory with quarks and gluinos," *JHEP* **09** (2004) 063, arXiv:hep-th/0406146.

[29] F. Cachazo, P. Svrcek, and E. Witten, "Twistor space structure of one-loop amplitudes in gauge theory," *JHEP* **10** (2004) 074, arXiv:hep-th/0406177.

[30] F. Cachazo, P. Svrcek, and E. Witten, "Gauge theory amplitudes in twistor space and holomorphic anomaly," *JHEP* **10** (2004) 077, arXiv:hep-th/0409245.

[31] F. Cachazo, "Holomorphic anomaly of unitarity cuts and one-loop gauge theory amplitudes," arXiv:hep-th/0410077.

[32] R. Britto, F. Cachazo, and B. Feng, "Computing one-loop amplitudes from the holomorphic anomaly of unitarity cuts," *Phys. Rev.* **D71** (2005) 025012, arXiv:hep-th/0410179.

[33] R. J. Eden, P. V. Landshoff, D. I. Olive, and J. C. Polkinghorne, *The Analytic S-Matrix*. Cambridge University Press, 1966.

[34] Z. Bern, L. J. Dixon, D. C. Dunbar, and D. A. Kosower, "Fusing gauge theory tree amplitudes into loop amplitudes," *Nucl. Phys.* **B435** (1995) 59–101, arXiv:hep-ph/9409265.

[35] A. Brandhuber, S. McNamara, B. J. Spence, and G. Travaglini, "Loop amplitudes in pure Yang-Mills from generalised unitarity," *JHEP* **10** (2005) 011, arXiv:hep-th/0506068.

[36] R. Britto, F. Cachazo, and B. Feng, "Generalized unitarity and one-loop amplitudes in N = 4 super-Yang-Mills," *Nucl. Phys.* **B725** (2005) 275–305, arXiv:hep-th/0412103.

[37] Z. Xiao, G. Yang, and C.-J. Zhu, "The rational part of QCD amplitude. I: The general formalism," *Nucl. Phys.* **B758** (2006) 1–34, arXiv:hep-ph/0607015.

[38] X. Su, Z. Xiao, G. Yang, and C.-J. Zhu, "The rational part of QCD amplitude. II: The five-gluon," *Nucl. Phys.* **B758** (2006) 35–52, arXiv:hep-ph/0607016.

[39] Z. Xiao, G. Yang, and C.-J. Zhu, "The rational part of QCD amplitude. III: The six-gluon," *Nucl. Phys.* **B758** (2006) 53–89, arXiv:hep-ph/0607017.

[40] Z. Bern, L. J. Dixon, and D. A. Kosower, "On-shell recurrence relations for one-loop QCD amplitudes," *Phys. Rev.* **D71** (2005) 105013, arXiv:hep-th/0501240.

[41] Z. Bern, L. J. Dixon, and D. A. Kosower, "The last of the finite loop amplitudes in QCD," *Phys. Rev.* **D72** (2005) 125003, arXiv:hep-ph/0505055.

[42] Z. Bern, L. J. Dixon, and D. A. Kosower, "Bootstrapping multi-parton loop amplitudes in QCD," *Phys. Rev.* **D73** (2006) 065013, arXiv:hep-ph/0507005.

[43] A. Brandhuber, B. J. Spence, and G. Travaglini, "One-loop gauge theory amplitudes in N = 4 super Yang-Mills from MHV vertices," *Nucl. Phys.* **B706** (2005) 150–180, arXiv:hep-th/0407214.

[44] J. Bedford, A. Brandhuber, B. J. Spence, and G. Travaglini, "Non-supersymmetric loop amplitudes and MHV vertices," *Nucl. Phys.* **B712** (2005) 59–85, arXiv:hep-th/0412108.

[45] A. Brandhuber, B. Spence, and G. Travaglini, "From trees to loops and back," *JHEP* **01** (2006) 142, arXiv:hep-th/0510253.

[46] P. Mansfield, "The Lagrangian origin of MHV rules," *JHEP* **03** (2006) 037, arXiv:hep-th/0511264.

[47] A. Gorsky and A. Rosly, "From Yang-Mills Lagrangian to MHV diagrams," *JHEP* **01** (2006) 101, arXiv:hep-th/0510111.

[48] J. H. Ettle and T. R. Morris, "Structure of the MHV-rules Lagrangian," *JHEP* **08** (2006) 003, arXiv:hep-th/0605121.

[49] J. H. Ettle, C.-H. Fu, J. P. Fudger, P. R. W. Mansfield, and T. R. Morris, "S-Matrix Equivalence Theorem Evasion and Dimensional Regularisation with the Canonical MHV Lagrangian," *JHEP* **05** (2007) 011, arXiv:hep-th/0703286.

[50] J. H. Ettle, T. R. Morris, and Z. Xiao, "The MHV QCD Lagrangian," arXiv:0805.0239 [hep-th].

[51] S. Weinberg, "The quantum theory of fields. Vol. 2: Modern applications,". Cambridge, UK: Univ. Pr. (1996) 489 p.

[52] R. Kleiss and H. Kuijf, "Multi-gluon cross-sections and five jet production at hadron colliders," *Nucl. Phys.* **B312** (1989) 616.

[53] E. Witten, "Perturbative gauge theory as a string theory in twistor space," *Commun. Math. Phys.* **252** (2004) 189–258, arXiv:hep-th/0312171.

[54] M. L. Mangano and S. J. Parke, "Multiparton amplitudes in gauge theories," *Phys. Rept.* **200** (1991) 301–367, arXiv:hep-th/0509223.

[55] G. 't Hooft, "A planar diagram theory for strong interactions," *Nucl. Phys.* **B72** (1974) 461.

[56] F. A. Berends and W. T. Giele, "Recursive Calculations for Processes with n Gluons," *Nucl. Phys.* **B306** (1988) 759.

[57] Z. Bern and D. A. Kosower, "Color decomposition of one loop amplitudes in gauge theories," *Nucl. Phys.* **B362** (1991) 389–448.

[58] Z. Bern, L. J. Dixon, D. C. Dunbar, and D. A. Kosower, "One loop n point gauge theory amplitudes, unitarity and collinear limits," *Nucl. Phys.* **B425** (1994) 217–260, `arXiv:hep-ph/9403226`.

[59] M. T. Grisaru, H. N. Pendleton, and P. van Nieuwenhuizen, "Supergravity and the S Matrix," *Phys. Rev.* **D15** (1977) 996.

[60] L. J. Dixon, "Calculating scattering amplitudes efficiently," `arXiv:hep-ph/9601359`.

[61] M. T. Grisaru and H. N. Pendleton, "Some Properties of Scattering Amplitudes in Supersymmetric Theories," *Nucl. Phys.* **B124** (1977) 81.

[62] C. F. Berger, "Bootstrapping one-loop QCD amplitudes," *AIP Conf. Proc.* **903** (2007) 157–160, `arXiv:hep-ph/0608027`.

[63] L. M. Brown and R. P. Feynman, "Radiative corrections to Compton scattering," *Phys. Rev.* **85** (1952) 231–244.

[64] G. Passarino and M. J. G. Veltman, "One Loop Corrections for e+ e- Annihilation Into mu+ mu- in the Weinberg Model," *Nucl. Phys.* **B160** (1979) 151.

[65] G. 't Hooft and M. J. G. Veltman, "Scalar One Loop Integrals," *Nucl. Phys.* **B153** (1979) 365–401.

[66] R. G. Stuart, "Algebraic reduction of one loop Feynman diagrams to scalar integrals," *Comput. Phys. Commun.* **48** (1988) 367–389.

[67] R. G. Stuart and A. Gongora, "Algebraic reduction of one loop Feynman diagrams to scalar integrals 2," *Comput. Phys. Commun.* **56** (1990) 337–350.

[68] W. L. van Neerven and J. A. M. Vermaseren, "Large loop integrals," *Phys. Lett.* **B137** (1984) 241.

[69] D. B. Melrose, "Reduction of Feynman diagrams," *Nuovo Cim.* **40** (1965) 181–213.

[70] G. J. van Oldenborgh and J. A. M. Vermaseren, "New Algorithms for One Loop Integrals," *Z. Phys.* **C46** (1990) 425–438.

[71] G. J. van Oldenborgh, *One loop calculations with massive particles.* PhD thesis, University of Amsterdam, 1990. RX-1313 (AMSTERDAM).

[72] A. Aeppli. PhD thesis, University of Zurich, 1992.

[73] L. D. Landau, "On analytic properties of vertex parts in quantum field theory," *Nucl. Phys.* **13** (1959) 181–192.

[74] S. Mandelstam, "Analytic properties of transition amplitudes in perturbation theory," *Phys. Rev.* **115** (1959) 1741–1751.

[75] R. E. Cutkosky, "Singularities and discontinuities of Feynman amplitudes," *J. Math. Phys.* **1** (1960) 429–433.

[76] W. L. van Neerven, "Dimensional regularization of mass and infrared singularities in two loop on-shell vertex functions," *Nucl. Phys.* **B268** (1986) 453.

[77] Z. Bern and A. G. Morgan, "Massive Loop Amplitudes from Unitarity," *Nucl. Phys.* **B467** (1996) 479–509, arXiv:hep-ph/9511336.

[78] V. P. Nair, "A current algebra for some gauge theory amplitudes," *Phys. Lett.* **B214** (1988) 215.

[79] C. Quigley and M. Rozali, "One-loop MHV amplitudes in supersymmetric gauge theories," *JHEP* **01** (2005) 053, arXiv:hep-th/0410278.

[80] J. Bedford, A. Brandhuber, B. J. Spence, and G. Travaglini, "A twistor approach to one-loop amplitudes in N = 1 supersymmetric Yang-Mills theory," *Nucl. Phys.* **B706** (2005) 100–126, arXiv:hep-th/0410280.

[81] R. P. Feynman, "Closed loop and tree diagrams,". In *J R Klauder, Magic Without Magic*, San Francisco 1972, 355-375.

[82] A. Brandhuber, B. Spence, and G. Travaglini, "Amplitudes in pure Yang-Mills and MHV diagrams," *JHEP* **02** (2007) 088, arXiv:hep-th/0612007.

[83] M. Dinsdale, M. Ternick, and S. Weinzierl, "A comparison of efficient methods for the computation of Born gluon amplitudes," *JHEP* **03** (2006) 056, arXiv:hep-ph/0602204.

[84] W. T. Giele and G. Zanderighi, "On the Numerical Evaluation of One-Loop Amplitudes: the Gluonic Case," arXiv:0805.2152 [hep-ph].

[85] R. K. Ellis, W. T. Giele, and G. Zanderighi, "The one-loop amplitude for six-gluon scattering," *JHEP* **05** (2006) 027, arXiv:hep-ph/0602185.

[86] W. T. Giele, Z. Kunszt, and K. Melnikov, "Full one-loop amplitudes from tree amplitudes," *JHEP* **04** (2008) 049, arXiv:0801.2237 [hep-ph].

[87] Z. Bern, L. J. Dixon, and D. A. Kosower, "One loop corrections to five gluon amplitudes," *Phys. Rev. Lett.* **70** (1993) 2677–2680, arXiv:hep-ph/9302280.

[88] S. J. Bidder, N. E. J. Bjerrum-Bohr, L. J. Dixon, and D. C. Dunbar, "N = 1 supersymmetric one-loop amplitudes and the holomorphic anomaly of unitarity cuts," *Phys. Lett.* **B606** (2005) 189–201, arXiv:hep-th/0410296.

[89] R. Britto, E. Buchbinder, F. Cachazo, and B. Feng, "One-loop amplitudes of gluons in SQCD," *Phys. Rev.* **D72** (2005) 065012, arXiv:hep-ph/0503132.

[90] R. Britto, B. Feng, and P. Mastrolia, "The cut-constructible part of QCD amplitudes," *Phys. Rev.* **D73** (2006) 105004, arXiv:hep-ph/0602178.

[91] Z. Bern, L. J. Dixon, and D. A. Kosower, "All next-to-maximally helicity-violating one-loop gluon amplitudes in N = 4 super-Yang-Mills theory," *Phys. Rev.* **D72** (2005) 045014, arXiv:hep-th/0412210.

[92] G. Mahlon, "Multi - gluon helicity amplitudes involving a quark loop," *Phys. Rev.* **D49** (1994) 4438–4453, arXiv:hep-ph/9312276.

[93] C. F. Berger, Z. Bern, L. J. Dixon, D. Forde, and D. A. Kosower, "All one-loop maximally helicity violating gluonic amplitudes in QCD," *Phys. Rev.* **D75** (2007) 016006, arXiv:hep-ph/0607014.

[94] C. F. Berger, Z. Bern, L. J. Dixon, D. Forde, and D. A. Kosower, "Bootstrapping one-loop QCD amplitudes with general helicities," *Phys. Rev.* **D74** (2006) 036009, arXiv:hep-ph/0604195.

[95] C. B. Thorn, "Notes on one-loop calculations in light-cone gauge," arXiv:hep-th/0507213.

[96] G. Chalmers and W. Siegel, "The self-dual sector of QCD amplitudes," *Phys. Rev.* **D54** (1996) 7628–7633, arXiv:hep-th/9606061.

[97] S. Mandelstam, "Light Cone Superspace and the Ultraviolet Finiteness of the N=4 Model," *Nucl. Phys.* **B213** (1983) 149–168.

[98] G. Leibbrandt, "The Light Cone Gauge in Yang-Mills Theory," *Phys. Rev.* **D29** (1984) 1699.

[99] Goldstein, Herbet and Poole, Charles and Safko, John, *Classical Mechanics.* Addison-Wesley, third ed., 2002.

[100] C. Itzykson and J. B. Zuber, *Quantum Field Theory.* McGraw-Hill, 1980.

[101] Z. Bern and D. A. Kosower, "The Computation of loop amplitudes in gauge theories," *Nucl. Phys.* **B379** (1992) 451–561.

[102] Z. Bern, L. J. Dixon, and D. A. Kosower, "New QCD results from string theory," arXiv:hep-th/9311026.

[103] Z. Bern, G. Chalmers, L. J. Dixon, and D. A. Kosower, "One loop N gluon amplitudes with maximal helicity violation via collinear limits," *Phys. Rev. Lett.* **72** (1994) 2134–2137, arXiv:hep-ph/9312333.

[104] D. Chakrabarti, J. Qiu, and C. B. Thorn, "Scattering of glue by glue on the light-cone worldsheet. I: Helicity non-conserving amplitudes," *Phys. Rev.* **D72** (2005) 065022, arXiv:hep-th/0507280.

[105] H. Feng and Y.-t. Huang, "MHV lagrangian for N = 4 super Yang-Mills," arXiv:hep-th/0611164.

[106] S. Ananth and S. Theisen, "KLT relations from the Einstein-Hilbert Lagrangian," *Phys. Lett.* **B652** (2007) 128–134, arXiv:0706.1778 [hep-th].

[107] H. Kawai, D. C. Lewellen, and S. H. H. Tye, "A Relation Between Tree Amplitudes of Closed and Open Strings," *Nucl. Phys.* **B269** (1986) 1.

[108] A. Brandhuber, B. Spence, G. Travaglini, and K. Zoubos, "One-loop MHV Rules and Pure Yang-Mills," *JHEP* **07** (2007) 002, arXiv:0704.0245 [hep-th].

[109] D. Chakrabarti, J. Qiu, and C. B. Thorn, "Scattering of glue by glue on the light-cone worldsheet. II: Helicity conserving amplitudes," *Phys. Rev.* **D74** (2006) 045018, arXiv:hep-th/0602026.

[110] L. J. Mason and D. Skinner, "An ambitwistor Yang-Mills Lagrangian," *Phys. Lett.* **B636** (2006) 60–67, arXiv:hep-th/0510262.

[111] R. Boels, L. Mason, and D. Skinner, "Supersymmetric gauge theories in twistor space," *JHEP* **02** (2007) 014, arXiv:hep-th/0604040.

[112] R. Boels, L. Mason, and D. Skinner, "From twistor actions to MHV diagrams," *Phys. Lett.* **B648** (2007) 90–96, arXiv:hep-th/0702035.

[113] R. Boels, "A quantization of twistor Yang-Mills theory through the background field method," *Phys. Rev.* **D76** (2007) 105027, arXiv:hep-th/0703080.

[114] R. Boels and C. Schwinn, "CSW rules for a massive scalar," *Phys. Lett.* **B662** (2008) 80–86, arXiv:0712.3409 [hep-th].

[115] R. Boels, C. Schwinn, and S. Weinzierl, "Recent developments for multi-leg QCD amplitudes with massive particles," arXiv:0712.3506 [hep-ph].

[116] R. Boels and C. Schwinn, "CSW rules for massive matter legs and glue loops," arXiv:0805.4577 [hep-th].

[117] Fudger, Jonathan P. and Morris, Tim R. (in preparation), 2008.